Novel Glycolipids in CD1d-mediated Immunity:

Synthesis of New Agonists of CD1d

by

Justyna Wojno

A thesis submitted to the
University of Birmingham
for the degree of
DOCTOR OF PHILOSOPHY

School of Chemistry
College of Engineering
and Physical Sciences
University of Birmingham
February 2012

For my Family

Abstract

A detailed understanding of the human immune system is crucial for developing novel pharmaceuticals to fight a range of diseases. The glycolipid α-galactosyl ceramide, α-GalCer, has been shown to stimulate the proliferation of murine spleen cells and activate the immune system. Stimulation occurs through binding of the glycolipid to the protein CD1d. Subsequent presentation of the CD1d−glycolipid complex to invariant Natural Killer T cells (iNKT cells) initiates the proliferation of a host of cytokines leading to an immune response. The therapeutic potential of α-GalCer is currently being explored; however the induction of both Th1 *and* Th2 cytokines by this agent is likely to limit its therapeutic application. The crystal structure of human CD1d in complex with α-GalCer reveals a key hydrogen bond between the N-H of the amide group of the glycolipid and the side-chain O-H of Thr 154 located on the α2 helix of the CD1d molecule; however, the carbonyl group of the amide is not directly involved in binding. Carbonyl group replacements should therefore behave similarly but may involve more selective iNKT cell induction as well as improved hydrolytic stability. Significantly, analogues of α-GalCer have been shown to induce iNKT cell-derived cytokines more selectively through a skewed Th1-Th2 response. To date, very few alterations around the amide bond have been explored. To investigate its importance in iNKT cell stimulation, a range of α-GalCer and threitol ceramide (ThrCer) analogues has been synthesised in which the amide functionality in these two leads has been replaced with

different carbonyl functional groups. These compounds have been tested for iNKT cell induction and in particular their Th1/Th2 response, which determined their therapeutic potential. Labelled derivatives of α-GalCer and ThrCer have also been designed and synthesised to find application in lipid trafficking studies.

Declaration

The work recorded in this thesis was carried out in the School of Biosciences at the University of Birmingham, U.K. during the period of November 2007 to March 2011. The work in this thesis is original except where acknowledged by reference.

No portion of this work is being, or has been submitted for a degree, diploma or any other qualification at any other university.

Acknowledgements

I wish to thank my supervisors Dr Liam R. Cox and Prof. Gurdyal S. Besra for offering me a PhD position at University of Birmingham, helping me with my work with patience throughout the time it took me to complete my research and write the thesis. The time I spent working with you has been an extraordinary experience that far exceeded my expectations, strongly shaped my research interests and influenced my future career objectives.

This thesis is dedicated to my family in Poland but also to all members of Besra and Cox groups, who became my colleagues, close friends and everyday companions. It is impossible to fit in one page all your names and precious moments of laughter to/and tears we had together that I shall remember and cherish for a long time to come. Nevertheless, my biggest thanks go to Natacha, Vee, Helen, Luke, Renate, Apoo, Usha, Peter the Russian, Hemza, Yoel, John-Paul, Oona, Cristian, Athina, Becky, Arun, Anaxi, Ting, English Pete, George, Albi, Sara, Mimi, Amrita, Monika, Kiran, Shipra, Liz, Reenette. I could not wish for a better company!

I am very greatful to my Glasgow favourites Dominika, Nick, Sylvain, Julian and Mike for their huge support and making me smile a lot.

Contents

Table of contents

Chapter 1

Chapter 2

Chapter 3

List of Abbreviations

%	percent
°C	degrees centigrade
Å	angstrom
Ac	acyl, acetyl
APC	antigen presenting cell
Ar	aromatic, aryl
Asp	aspartic acid
β_2m	beta 2 microglobulin
Bn	benzyl (CH_2Ph)
BODIPY	boron dipyrromethane difluoride
b.p.	boiling point
Bu	butyl
CD1	cluster of differentiation 1
Cys	cysteine
DC	dendritic cell
DDM	didehydroxymycobactin
DGJ	1-deoxygalactonojirimycin
DMF	*N*,*N*-dimethylformamide
DMSO	dimethylsulfoxide
DN	double negative: CD4-CD8-
DIPEA	diisopropylethylamine
DP	double positive
DTBMP	2,6-di-*tert*-butyl-4-methylpyridine
ELISA	enzyme-linked immunosorbent assay
ER	endoplasmic reticulum
Et	ethyl
FACS	fluorescence-activated cell sorting
FCC	flash column chromatography
g	grammes
GSL	glycosphingolipid

h	hours
hCD1d	human CD1d
HMBC	heteronuclear multiple bond correlation
HSQC	heteronuclear single quantum correlation
IFN	interferon
IL	interleukin
iNKT Cell	invariant natural killer T cell (also referred to as CD1d-restricted T cell)
IR	infrared
K_d	dissociation constant
LTP	lipid transfer protein
M	molar
m	milli
mCD1	mouse CD1
Me	methyl
MFI	mean fluorescent intensity
MHC	major histocompatibility complex
MHz	mega-hertz
min	minute
ml	millilitres
n	nano
NBS	*N*-bromosuccinimide
NIS	*N*-iodosuccinimide
NK	natural killer
NKT	natural killer T
NMR	nuclear magnetic resonance
PE	1-palmitoyl-2-oleoyl-*sn*-glycero-3-phosphoethanolamine
PG	phosphatidylglycerol
Phe	phenylalanine
PI	phosphatidylinositol
p-Ts	*p*ara-toluenesulfonyl
py	pyridine

RT	room temperature
s	second
SPR	surface plasmon resonance
t	time
TBAF	tetrabutylammonium fluoride
TBAI	tetrabutylammonium iodide
TBDPS	tert butyl diphenylsilyl
TCR	T cell receptor
Tf	trifluoromethanesulfonyl
Th	T helper
THF	tetrahydrofuran
Thr	threonine
ThrCer	threitol ceramide
TLC	thin layer chromatography
TMU	tetramethylurea
Tr	trityl
wt	wild type
α-GalCer	alpha-galactosylceramide
α-GlcCer	alpha-glucosylceramide
α-ManCer	alpha-mannosylceramide
μ	micro

Published work associated with this thesis

I. *Synthesis of threitol ceramide and [C-14]threitol ceramide, non-glycosidic analogues of the potent CD1d antigen alpha-galactosyl ceramide;* Garcia Diaz Y. R., Wojno J., Cox L. R., Besra G. S. *Tetrahedron: Asymmetry*, **2009**, *20*, 747-754.

II. *Preparation, characterisation and entrapment of a non-glycosidic threitol ceramide into liposomes for presentation to invariant natural killer T cells;* Kaur R., Chen J., Dawoodji A., Cerundolo V., Garcia Diaz Y. R., Wojno J., Cox L. R., Besra G. S., Moghaddam B., Perrie Y. *J. Pharm. Sci*. **2011**, *100*, 2724-2733.

Chapter 1

Introduction

1. Introduction

1.1. The immune system, an overview

The immune system is a very complex “machinery” that involves many different proteins interacting with each other. In humans first line of defence against invaders such as viruses, bacteria and parasites consists of physical barriers, namely skin and mucous membranes that line our digestive, respiratory and reproductive tracts. The innate immune system serves as a second line of defence, providing a quick response to common invaders.[1] The innate immune system is a universal and ancient form of host defense against infection. Innate immune recognition relies on a limited number of germline-encoded receptors. These receptors have evolved to recognise the conserved products of microbial metabolism, which are produced by microbial pathogens, but not by the host. Recognition of these molecular structures allows the immune system to distinguish infectious non-self from non-infectious self. Toll-like receptors (TLR) play a major role in pathogen recognition and initiation of inflammatory and immune responses.[2] The weapons of the innate immune system include the complement proteins, professional phagocytes, and natural killer (NK) cells.

The adaptive immune system involves great variability and rearrangement of receptor gene segments, and therefore provides specific recognition of foreign antigens, immunological memory of infection, and pathogen-specific adaptor proteins. However, the adaptive immune response is also responsible for allergy, autoimmunity, and the rejection of tissue grafts.

Innate immunity is responsible for most inflammatory responses which are triggered by macrophages, polymorphonuclear leukocytes, and mast cells through their innate immune receptors. Adaptive immunity supports the innate immune system in specific recognition of proteins, carbohydrates, lipids, nucleic acids, and pathogens, using the same activated, but not antigen-specific, effector cells generated by innate immune recognition. Thus the two systems are intimately linked in their use of the same effector cells. The key differences between the innate and adaptive immune systems are summarised in Table 1.1.[2]

Property	**Innate immune system**	**Adaptive immune system**
Receptors	Fixed in genome Rearrangement is not necessary	Encoded in gene segments Rearrangement is necessary
Distribution	Non-clonal, All cells of a class identical	Clonal All cells of a class distinct
Recognition	Conserved molecular patterns (lipopolisaccharides, mannans, glycans)	Details of molecular structure (proteins, peptides, carbohydrates)
Self Non-self discrimination	Perfect: selected over evolutionary time	Imperfect: selected in individual somatic cells
Action time	Immediate activation of effectors	Delayed activation of effectors
Response	Co-stimulatory molecules Cytokines (IL-1β, IL-6) Chemokines (IL-8)	Clonal expansion or anergy IL-2 Effector cytokines: (IL-4, IFNγ)

Table 1.1. Differences between innate and adaptive immunity. Table adapted from ref 2.

1.2. Invariant natural killer T (iNKT) cells

Natural killer T cells (NKT cells) are a major population of innate-like T-lymphocytes. These multifunctional lymphocytes can mediate an immune response to tumours and play an important role in the host's defense mechanism against microbial infections as well as a function in maintaining immune tolerance.[3]

NKT cells possess properties of the natural killer (NK) cells of the innate immune system, and of traditional T cells of the adaptive immune system. They mature in the thymus and co-express the αβ T cell antigen receptor (TCR) and NK receptors NK1.1 or NKR-P1A. In contrast to the αβ receptors of traditional T cells, which are incredibly diverse, the repertoire of receptors expressed by NKT cells is quite limited. Traditional T cells recognise peptides presented by either class I or class II major histocompatibility complex (MHC) molecules, whereas NKT cells recognise lipids and glycolipids presented by CD1 proteins (Figure 1.1).[1]

Four categories of T cell have been referred to as natural killer T cells. Of these, the most abundant and well-studied are so-called type 1 iNKT cells, also referred to as invariant natural killer T cells (iNKT cells) because of their expression of an antigen-specific T-cell receptor (TCR). iNKT cells are unique lymphocytes that bridge the innate and adaptive immune system. The invariant α chain of the iNKT cell TCR consists of a canonical Vα14–Jα18 (V – variable, J – joining region) chain in mice, and a homologous Vα24–Jα18 chain in humans, which is paired with a more variable β chain (Vβ2, Vβ7, Vβ8 in mice, and Vβ11 in humans).[4]

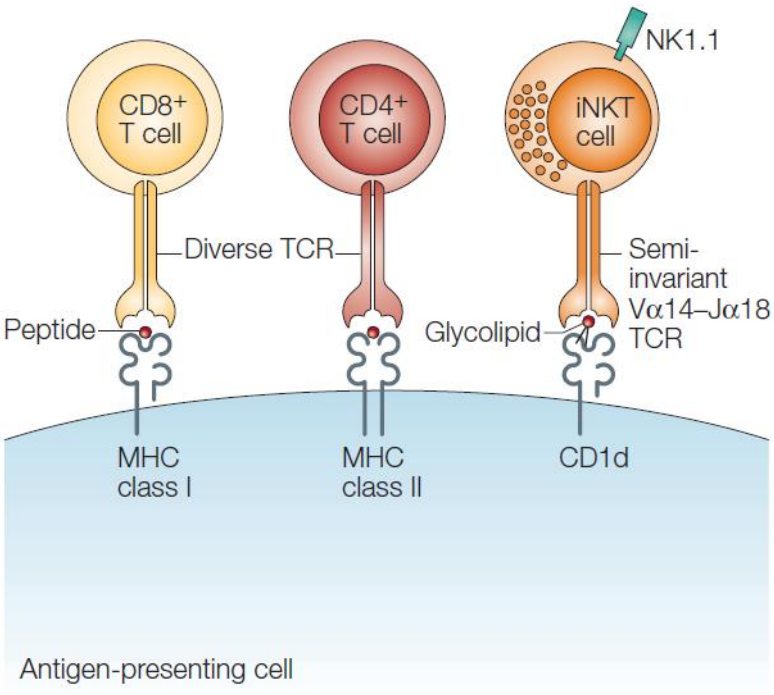

Figure 1.1. **Schematic view of the ligand-specificity of iNKT cells compared with conventional T cells.** Peptide antigens presented by MHC class I molecules are recognised by diverse T-cell receptors (TCRs) expressed by CD8+ T cells, while peptide antigens presented by MHC class II molecules are recognised by diverse TCRs expressed by CD4+ T cells. Semi-invariant Vα14i TCRs expressed by iNKT cells recognise glycolipids presented by CD1 proteins.

Figure adapted from ref. [5] Permission to reproduce figure was obtained from Elsevier through RightsLink® - licence number 2812640815855.

iNKT cells are mainly found in the thymus, liver and bone marrow. They are also present in smaller amounts in the spleen and the peripheral blood, but are rare in the lymph nodes.[6-8] The maturation of iNKT cells begins in the thymus, where an uncommitted precursor thymocyte rearranges and expresses a CD1d-specific Vα14i TCR at the double-positive (DP) stage, and is then positively selected by

CD1d-expressing DP thymocytes (Figure 1.2).[6] Positively selected Vα14i T cells mature into double-negative (DN) and $CD4^+$ T cells, whilst the expression of CD8 cells induces negative selection by increasing the affinity of the TCR for CD1d. After selection, $NK1.1^-$Vα14i T cells are exported to the periphery of the spleen or liver,[7,8] where a hypothetical second signal is required for the acquisition of the mature $NK1.1^+$ phenotype (Figure 1.2).

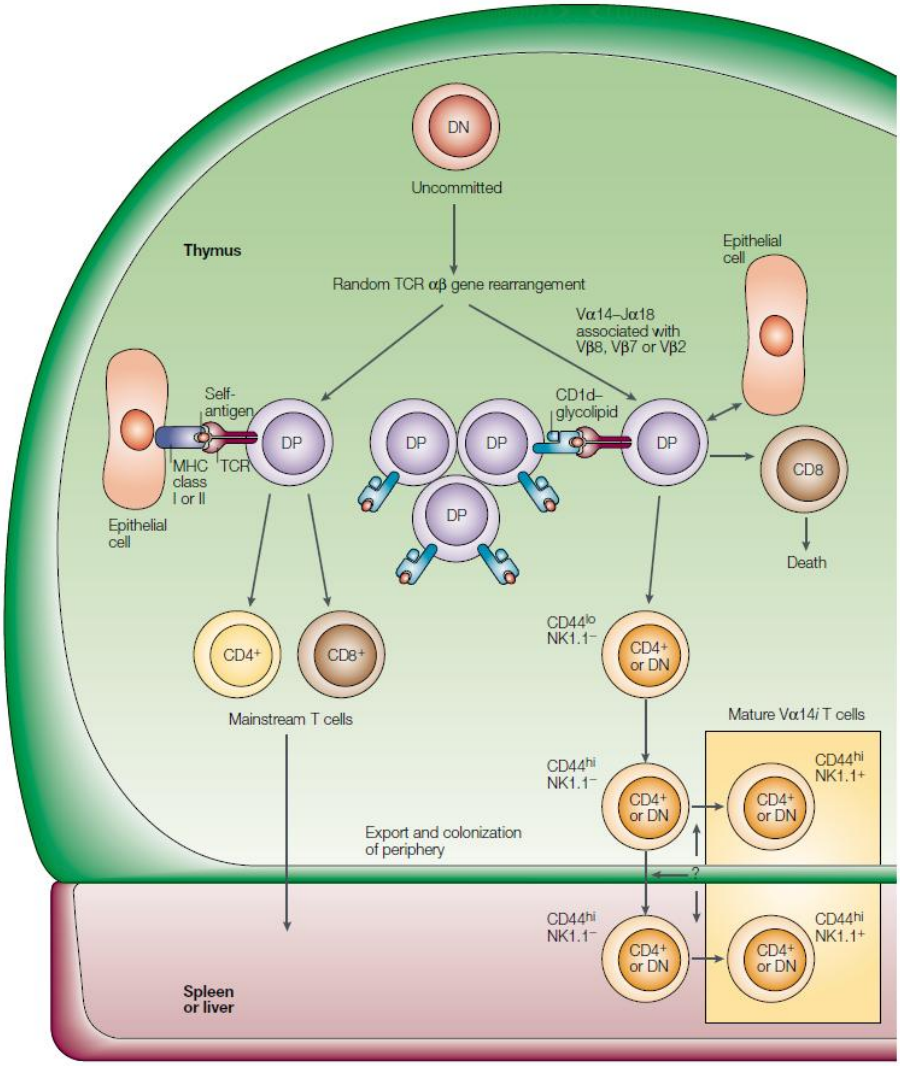

Figure 1.2. **Schematic view of the development of Vα14i T cells in the thymus.** T cell receptor (TCR) with random αβ rearrangement is first expressed by an uncommitted precursor thymocyte at the double-positive (DP) stage. DP cells with CD1d-specific Vα14i α-chain (Vα14–Jα18) are

positively selected by CD1d-expressing DP thymocytes. They mature into double-negative (DN) and CD4+ T cells and are exported to peripheral organs where a hypothetical second signal is required for the expression of mature iNKT cells. Positive selection of T cells with TCRs that are specific for MHC–peptide complexes leads to maturation of mainstream CD4+ and CD8+ T cells.

Figure adapted from ref [9]. Permission to reproduce figure was obtained from *Elsevier* through RightsLink® - licence number 2812641351351.

Mouse Vα14i and human Vα24i T cells have cytolytic activity,[10,11] and they rapidly induce the expression of various cytokines – including IL-4 and interferon-γ (IFNγ) – after TCR stimulation. Vα14i T-cell-derived cytokines can, in turn, activate several other cell types, including NK cells,[12,13] conventional T cells[14], macrophages[15] and B cells,[16] and recruit myeloid dendritic cells (DCs).[17] iNKT cells are able to require T helper 1 (Th1) or Th2 type of cytokine response. The Th1 pattern includes pro-inflammatory cytokines (typified by IFNγ), whereas the Th2 pattern includes regulatory cytokines such as IL-4, IL-5 and IL-13.[9]

1.3. CD1: lipid antigen-presenting molecules

CD1 molecules are a family of highly conserved antigen-presenting proteins that are similar in function to classic MHC molecules. However, whilst classic MHC molecules present peptide antigens to receptors located on T cells, CD1 molecules are able to bind and display a variety of lipids and glycolipids, which they then present to receptors located on CD1-restricted T cells.[18,19] Based on similarities between their nucleotide and amino acid sequences, the five known isoforms of the CD1 family have been divided into two groups, Group I (CD1a, CD1b, CD1c, and CD1e present in humans) and Group II (CD1d present in humans and mice).[20] In humans, one copy of each of the five CD1 molecules is encoded on chromosome 1[21] in the order CD1d, CD1a, CD1c, CD1b, CD1e (Figure 1.3.A). Mice and rats appear to have duplicated CD1d (Figure 1.3.B) and it is postulated that the genes for CD1a, CD1b, CD1c and CD1e have been lost in a chromosomal translocation event.[22]

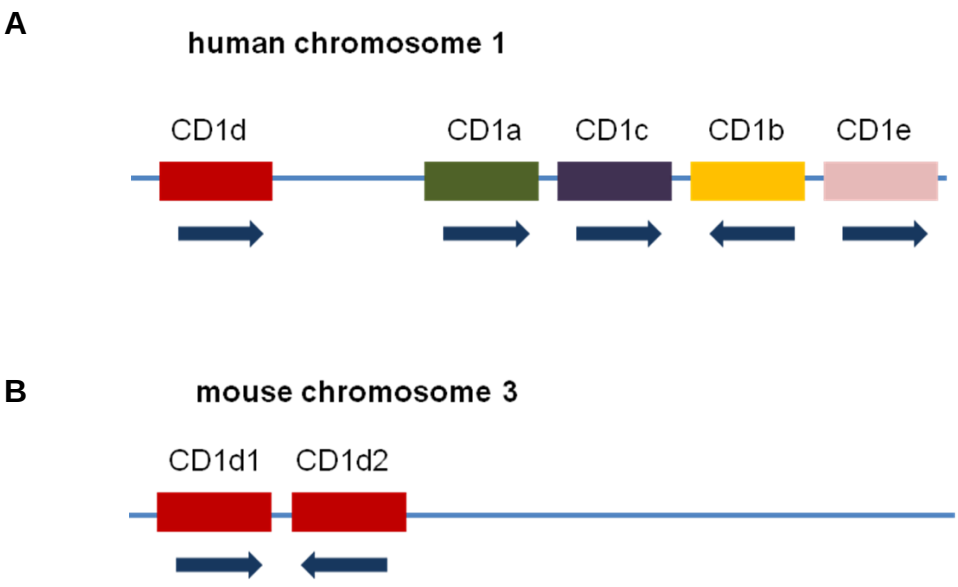

Figure 1.3. (**A**) The order of CD1 proteins encoded on human chromosome 1. (**B**) Duplicated CD1d proteins located on mouse chromosome 3.

CD1 proteins are heterodimers and most closely resemble class I MHC molecules in their overall structure. A transmembrane heavy chain, comprising α1, α2 and α3 domains, is non-covalently associated with β_2-microglobulin (β_2m). The antigen-binding sites of CD1 molecules are deep hydrophobic pockets that accomodate the alkyl chains of lipid antigens, leaving the more polar parts of the antigen accessible at the molecular surface for recognition by T-cell receptors.

Antigens presented by CD1 molecules range from endogenous cellular lipids and foreign lipids derived from intracellular parasites, to extracellular lipids of self or foreign origin.[23,24] CD1a has been found to bind and present glycolipids and mycobacterial lipopeptides such as the sphingolipid sulfatide (**1**, a sulfate ester of β-galactosylceramide)[25] and didehydroxymycobactin (**2**) (DDM).[26] The CD1b isoform is able to bind lipids with very long alkyl chains (*e.g.* C80), such as the mycolic acids, which are important components of mycobacterial cell walls.[26] CD1c has been shown to present mycobacterial isoprenoid lipids (**3**), which contain unusual alkyl chains consisting of repeating branched, saturated units.[27,28] Some lipids, including phospholipids and sphingolipids, have been shown to bind multiple CD1 isoforms including CD1a, CD1b, CD1c and CD1d. The CD1e molecule differs significantly from other CD1 family members. It is the only protein to be converted into a soluble lysosomal form, and in contrast to other CD1 isoforms, is not expressed at the cell surface.[29] However, CD1e remains immunologically relevant and is required for the presentation of the mycobacterial PIM_6 antigen by CD1b to specific T cells and for the *in vitro* conversion of PIM_6 to PIM_2 by α-mannosidase.[30]

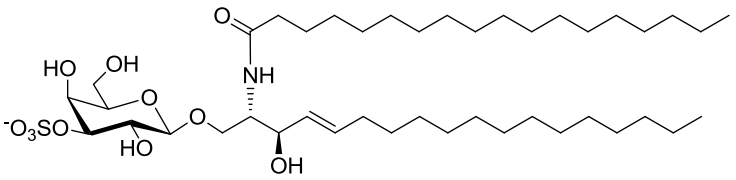

1, 3'-sulfo-galactosylceramide

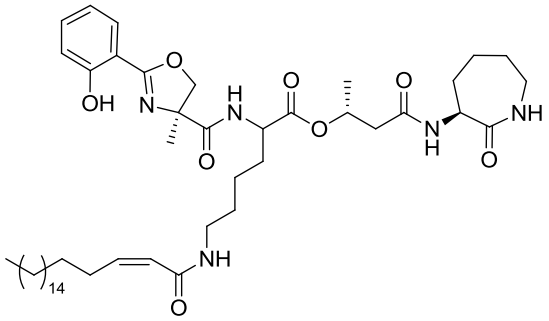

2, dideoxymycobactin (DDM)

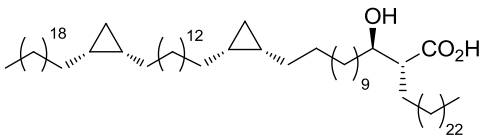

3, mycolic acid

Figure 1.4. Examples of the ligands presented by CD1 molecules.

iNKT cells characteristically express a semi-invariant TCR that specifically recognises the CD1 family member, CD1d. The finding that both mouse and human iNKT cells were autoreactive to cells expressing CD1d, resulted in considerable research in this CD1 subset.[31]

Intracellular trafficking of mouse and human CD1d is depicted in Figure 1.5. CD1d molecules are synthesised in the endoplasmatic reticulum (ER) and are transported through the Golgi and then directly to the plasma membrane *via* the secretory pathway. At the cell surface, nascent CD1d molecules are internalised *via* clathrin-cloated pits – and directed either through the recycling endosomal system or deeper in the endocytic system to lysosomal antigen loading compartments (MIIC), before being re-exported to the cell surface. The route of intracellular trafficking appears to depend largely on the nature of the cytoplasmic tails that bind the adaptor protein (AP)-3, directing their trafficking to sorting endosomes. Murine CD1d contains tyrosine-based motifs and is efficiently directed toward late endosomal MIIC compartments, whereas human CD1d, which cannot bind (AP)-3 is mainly distributed in the early endosomal system.[32] Additionally, a small fraction of human CD1d molecules physically associate with MHC class II molecules during trafficking[33] and are transported through the endosomal system to MIICs prior to their expression on the cell surface (Figure 1.5).

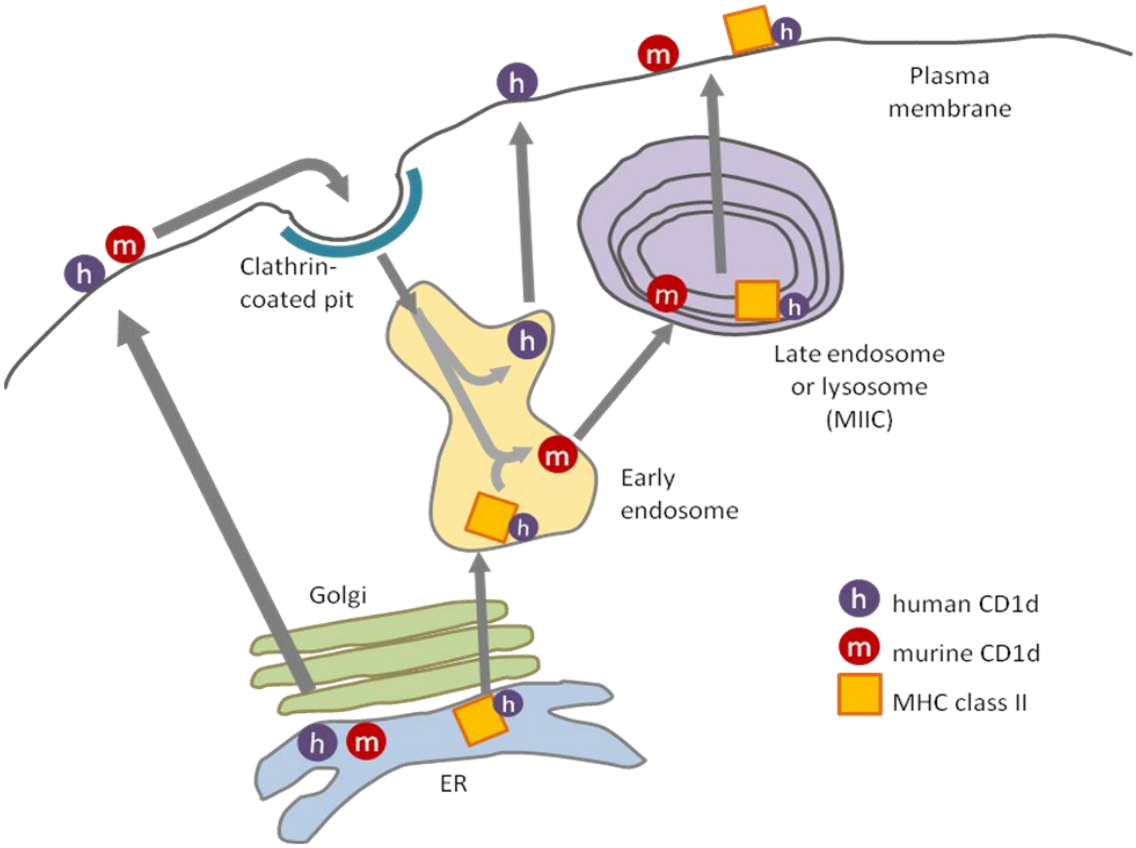

Figure 1.5. **Overview of CD1d intracellular trafficking.** CD1d molecule is synthesised in the endoplasmic reticulum (ER). Both human and mouse CD1d are transported through the Golgi to the cell surface and internalised *via* clathrin-coated pits before being directed into early endosomes. Human CD1d is next re-exported directly to the cell surface, while mouse CD1d and rare human CD1d associated with MHC class II molecule are trafficked deeper into late endosomes or lysosomes (MIIC) before reaching plasma membrain.[32]

1.4. α-Galactosylceramide: the most potent activator of iNKT cells

α-Galactosylceramide (α-GalCer) is one of the most potent agonists of CD1d and the strongest activator of human and mouse iNKT cells. α-GalCer was first discovered by the Kirin Pharmaceutical Research Corporation during a screen for agelasphins (AGLs) that could prevent metastasis of transplanted tumours to the livers of mice. A series of agelasphins was originally isolated from the marine sponge *Agelas mauritianus*, collected in the Okinawa Sea.[34] Although a number of β-galactosylceramides were already known, the AGLs were the first cerebrosides with an α-galactosyl linkage (Figure 1.6). Very interestingly all AGLs showed antitumour activity.

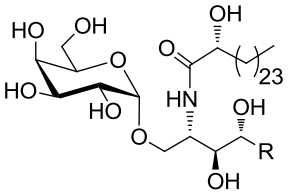

	R =
4, agelasphin-7a	$-(CH_2)_{11}CH_3$
5, agelasphin-9a	$-(CH_2)_{12}CH_3$
6, agelasphin-9b	$-(CH_2)_{11}CH(CH_3)_2$
7, agelasphin-11	$-(CH_2)CH(CH)_3C_2H_5$

Figure 1.6. Agelasphins isolated from the marine sponge *Agelas mauritianus.*

α-GalCer **8** is a synthetic glycolipid (also referred to as KRN7000), and is a derivative of the isolated agelasphin AGL-9b **6**, which was developed for

experimental studies and clinical trials (Figure 1.7). The α-GalCer structure consists of a galactopyranose combined with a ceramide through an α-glycosidic linkage. The ceramide part comprises a phytosphingosine base, which is *N*-acylated with hexacosanoic acid (Figure 1.7).

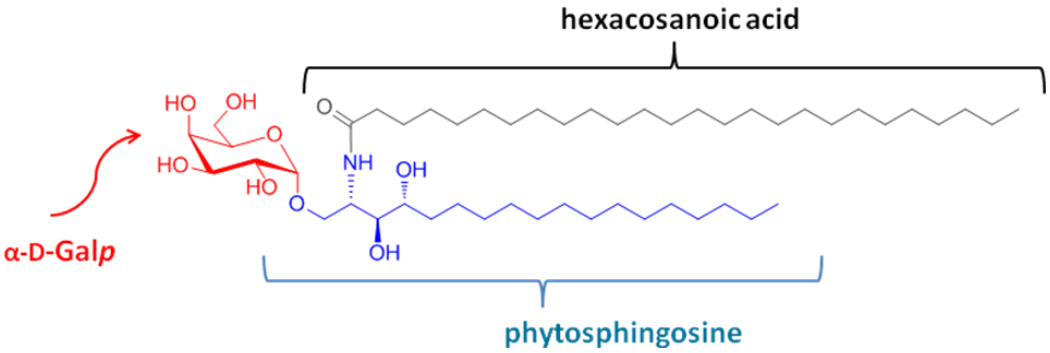

8, α-GalCer

Figure 1.7. Structure of α-galactosylceramide (α-GalCer) **8**.

The affinity of CD1d to α-GalCer was first measured by Naidenko et al. in SPR assay,[35] in which biotinylated α-GalCer was immobilized on a BIAcore chip and CD1d was passed on the lipid, followed by affinity measurements. The dissociation data from this experiment were fitted onto a 2-component dissociation model with the following results (Table 1.2):

CD1 type	Ligand	K_{on} (M^{-1} s^{-1})	K_{off} fast (s^{-1})	K_{off} slow (s^{-1})	Kd (nM) fast	Kd (nM) slow
Mouse	Bio-α-GalCer	6.3×10^{4}	0.1	4×10^{-3}	1587.3	63.5
Human	Bio-α-GalCer	1.0×10^{5}	0.08	4×10^{-3}	800.0	40

Table 1.2. Dissassociation data from SPR assay[35] with human and mouse CD1d protein and biotinylated α-GalCer.

McCarthy *et al*.[36] reported half-life of α-GalCer in CD1d – 593 min measured in SPR half-life assay in which biotinylated human CD1d was refolded with α-GalCer and other antigens (shorter acyl and/or sphingosine chains) and loaded onto a BIAcore chip. The loading was monitored by 9B antibody that recognises the galactose headgroup and CD1d.

Although the expression of α-GalCer in marine sponges could not be linked with any physiologically relevant function, the striking properties of this ligand have provided early support for the hypothesis that the conserved TCRs of NKT cells evolved to recognise conserved lipids. It is widely assumed that α-GalCer is only a mimic of the natural ligand that is recognised by Vα14i and Vα24i T cells, as this lipid is not present in mammals and nearly all natural glycolipids are β-linked glucosylceramides.[37] Nevertheless, α-GalCer very effectively stimulates iNKT cells in a CD1d-dependent manner, resulting in the rapid production of large amounts of

Th1 (IFNγ) and Th2 (IL-4) types of cytokines (Figure 1.8), and the expansion of antigen-specific T- and B cell responses.[12,16,38]

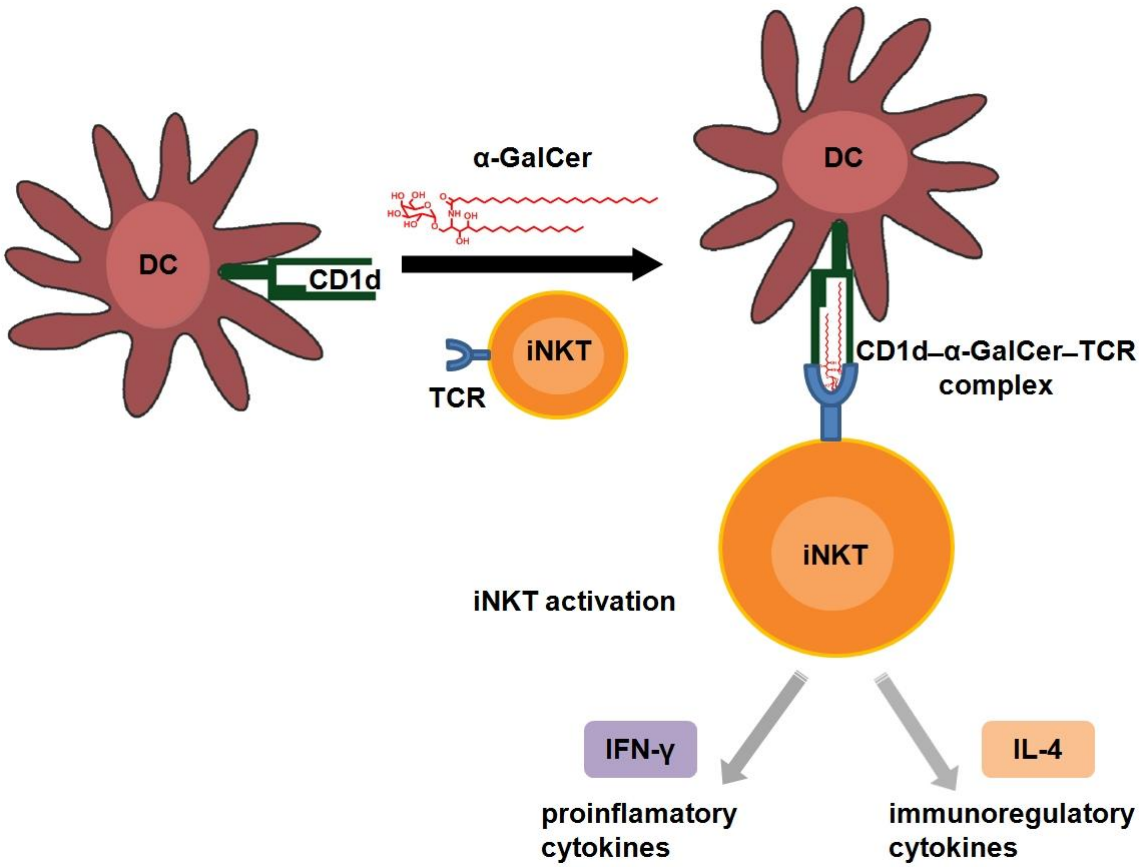

Figure 1.8. Activation of iNKT cells results in the release of large amounts of different cytokines, strongly activating the immune system.

Efficient stimulation of the immune system by α-GalCer made this antigen a promising adjuvant for the generation of optimal therapeutic and vaccination strategies against a range of infectious diseases and cancer. Clinical trials with soluble α-GalCer or α-GalCer-pulsed antigen-presenting cells (APCs) aimed at *in*

vivo reconstitution and activation of human NKT cells have been carried out[39-41] and provided both promising and challenging results. Recent phase I studies on patients with lung cancer,[42] as well as those with recurrent head and neck cancer,[43] demonstrated the safety and effectiveness of α-GalCer-pulsed APCs in anti-tumour therapy.

1.5. Crystal structure of the α-GalCer-CD1d complex

Crystal structures of mouse[44] and human CD1d,[45] with and without α-GalCer, have been determined and show how the glycolipids bind inside the protein (Figure 1.9).

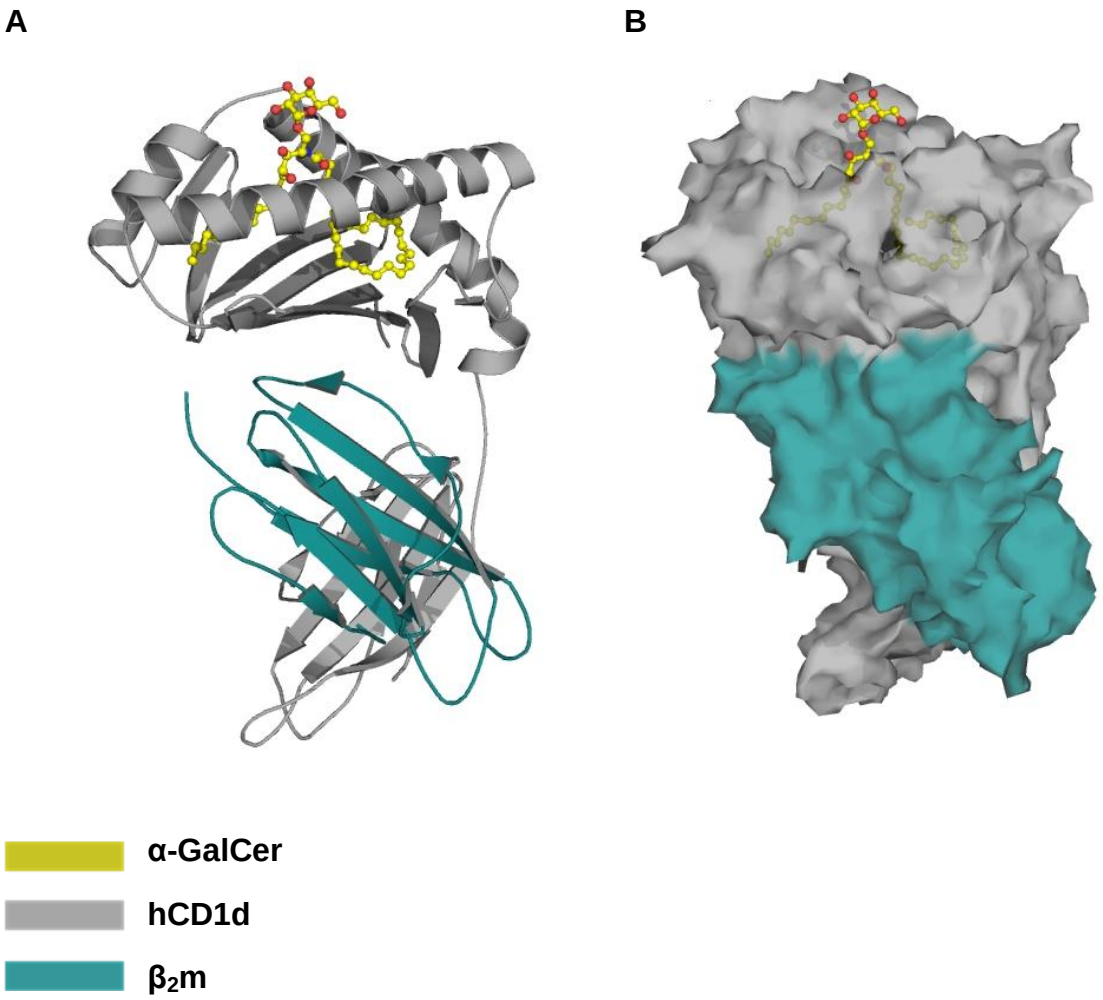

Figure 1.9. Cartoon (**A**) and surface (**B**) representation of the crystal structure of the hCD1d-α-GalCer complex. The galactose head group is exposed for recognition by the iNKT T cell receptor. Figure generated from 1ZT4[45] with Pymol.

The CD1d protein is formed of three domains, namely α1, α2 and α3, comprising the heavy chain, which is non-covalently associated with β_2-microglobulin (β_2m). Both murine and human CD1d molecules contain a large, hydrophobic pocket in the centre of the α1-α2 domain. This antigen-binding groove has two channels that meet at the surface of the protein. Lipid chains of a dialkyl glycolipid are then held inside the CD1d molecule by hydrophobic interactions. The acyl chain (26 carbon atoms) of α-GalCer occupies the longer pocket A', leaving the shorter C18 sphingosine chain to occupy the F' channel. Both lipid tails in α-GalCer terminate at the end of the pockets A' and F' thereby determining the maximum number of atoms in each chain (Figure 1.10). This finding explains why α-GalCer is one of the most potent agonists of CD1d and binds with one of the highest affinities and also why other antigens with longer lipid tails are not suitable since the longer lipid chains cannot fit in the binding pockets. Dialkyl glycolipids with fewer atoms in either of the chains are unable to fully occupy the hydrophobic binding pockets, resulting in an increased rate of lipid dissociation from the CD1d molecule.

The observed mode of glycolipid binding leaves the polar galactopyranose head group exposed over the lipid-binding groove for recognition by the iNKT TCR receptor. Analysis of the crystal structure of the α-GalCer-CD1d complex has identified key hydrogen bonds between the glycolipid and protein (Figure 1.11). The role of these hydrogen bonds is not only to stabilise the glycolipid, but also critically to orient the sugar moiety in such a fashion that it can be recognised by the TCR.

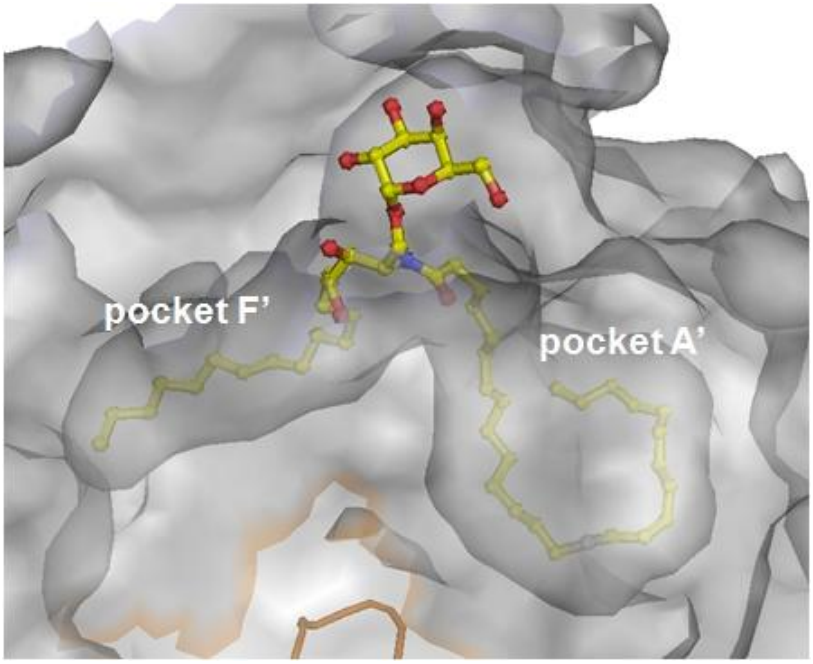

Figure 1.10. The lipid tails of α-GalCer fit tightly in two hydrophobic pockets of CD1d A' and F'.

The oxygen atom 1'-O of the α-GalCer glycosidic forms a hydrogen bond with the side-chain OH of Thr154 (Thr 156 in mouse CD1d), which is located on the α2 helix of the protein. The 2'-OH of the galactose forms a second hydrogen bond to the side-chain of Asp151 (Asp153 in mouse CD1d), which is also located on the α2 helix. The 3-OH hydroxyl group of the phytosphingosine chain is hydrogen-bonded to the α1 helix Asp80 whereas Asp 80 of mouse CD1d binds the 3-OH and 4-OH hydroxyl groups of the phytosphingosine.[44] In combination, these hydrogen bonds anchor the exposed sugar polar head group in a position parallel to the plane of the α helices, which is crucial for the antigenicity of α-GalCer (Figure 1.11).

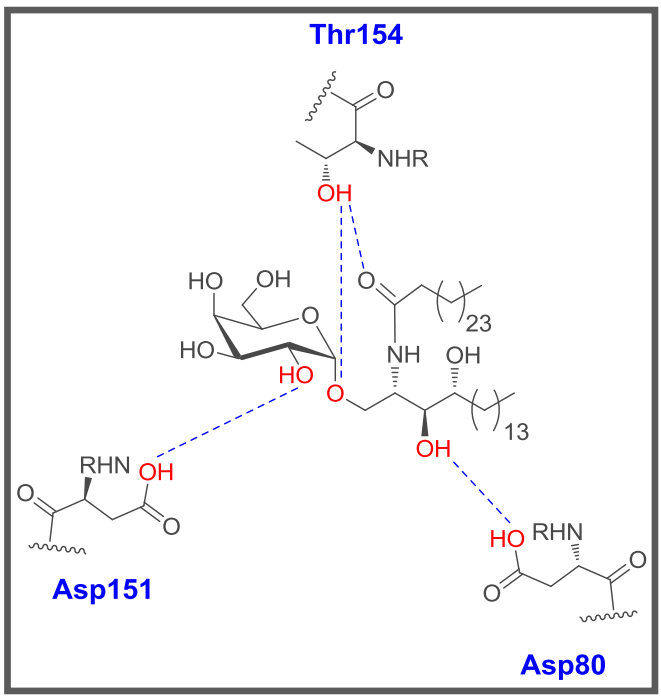

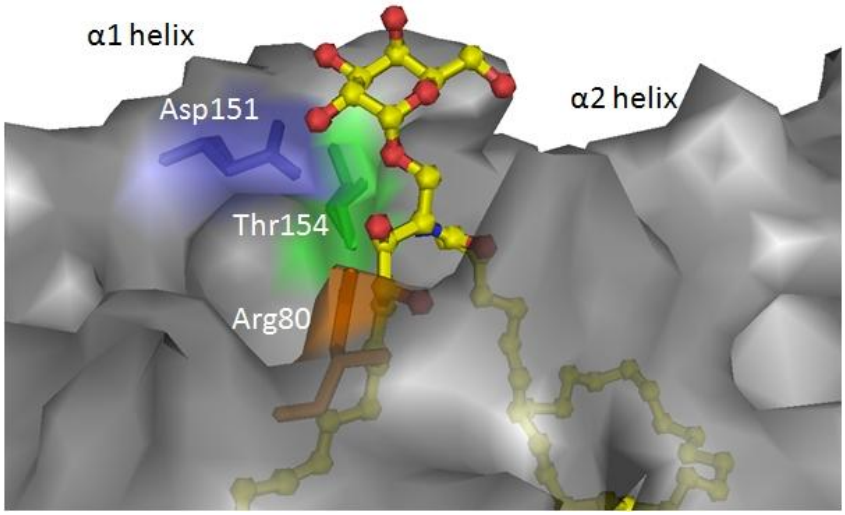

Figure 1.11. Hydrogen bond formation between the amino acid residues of hCD1d and α-GalCer found in the hCD1d-α-GalCer complex. Figure generated from 1ZT4[45] with Pymol.

1.6 Crystal structure of the α-GalCer–CD1d–TCR ternary complex

A co-crystal structure of human CD1d– α-GalCer with the human iNKT T cell receptor (Figure 1.12) has also been described (3.2 Å resolution) and reveals valuable insight into how the TCR recognises the glycolipid-protein complex.[46] The structure shows the T cell receptor locating almost parallel to the long axis of the CD1d–α-GalCer binding cleft and positioned over the extreme end of the CD1d molecule, directly above the F' pocket, which is occupied by the sphingosine chain.

A semi-invariant human NKT cell TCR comprises an invariant α-chain and CDR3α loop (Vα24–Ja18, where V is 'variable' and J is 'joining') and a restricted Vβ11-containing β-chain repertoire (Figure 1.13). The ternary structure shows that the α-chain contributes more interactions with the CD1d-α-GalCer complex than does the β-chain (approximately 82 *versus* 32 contacts, respectively), and also provides more buried surface areas (BSA) (65.5% *versus* 34.5%, respectively).

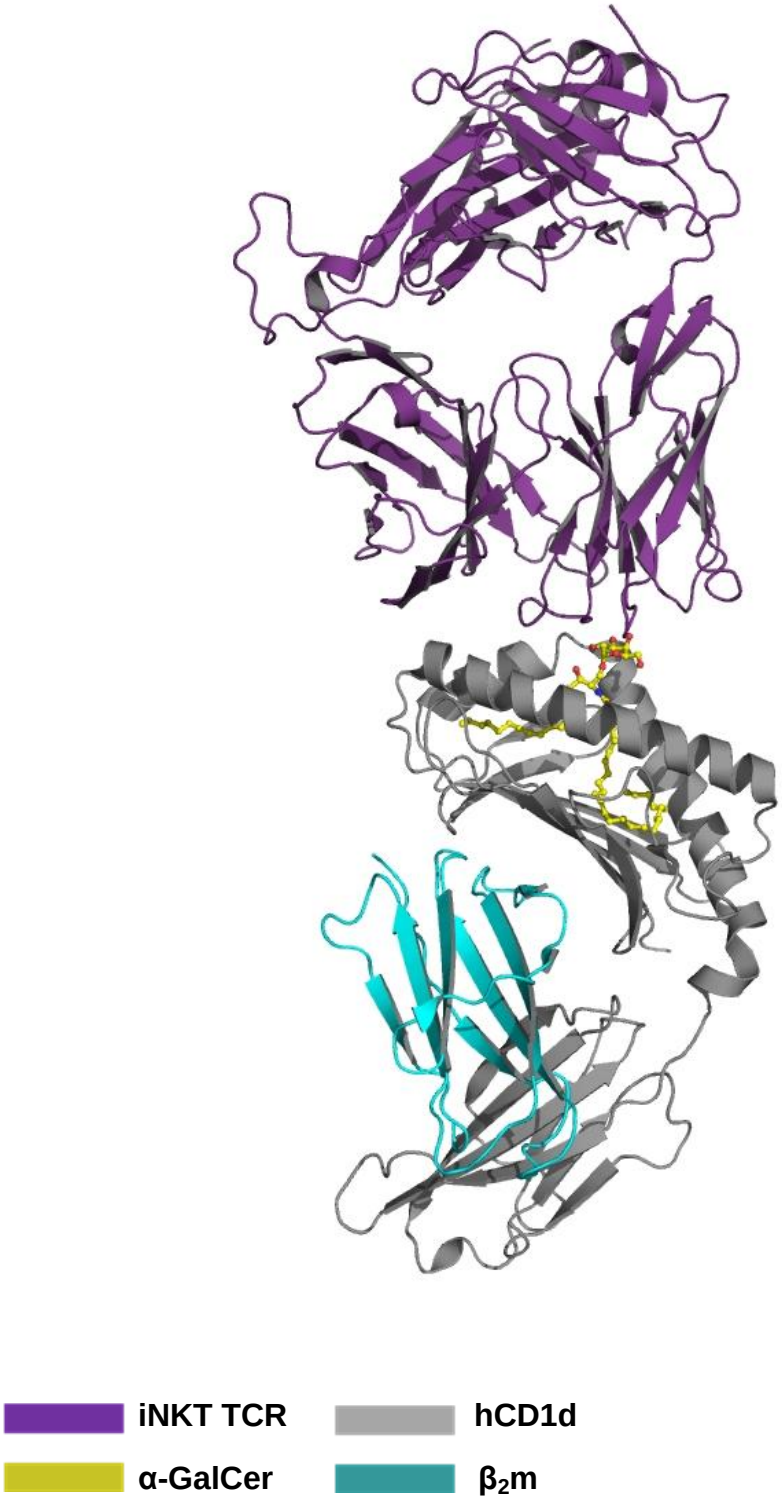

Figure 1.12. Crystal structure of the iNKT TCR–α-GalCer–hCD1d ternary complex. Cartoon representation was obtained with PyMol from 2PO6.[46]

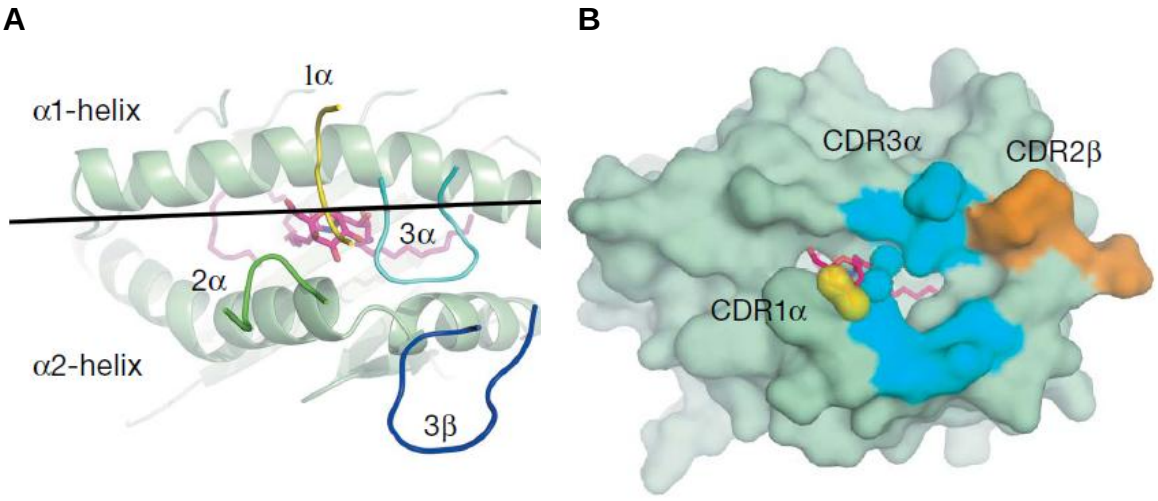

Figure 1.13. **(A)** Parallel docking mode of iNKT TCR CDR loops on to human CD1d-α-GalCer. **(B)** Footprint of the iNKT TCR on the surface of CD1d- α-GalCer.

Figure adapted from ref [46]. Permission to reproduce figure was obtained from *Nature* through RightsLink® - licence number 2822050758022.

Lipid recognition by the T cell receptor occurs through the exposed polar head group of α-GalCer. Contacts with the glycolipid are mediated by the CDR1α and CDR3α loops of the TCR. The invariant TCR α-chain forms three hydrogen bonds with the 2', 3' and 4' hydroxyl groups of the galactose ring: the 2' and 4' hydroxyl groups of the galactose are H-bonded to Gly96 and Phe29, respectively, whilst on the main chain, the 3' hydroxyl forms a hydrogen bond with the side-chain OH in Ser30 (Figure 1.14).

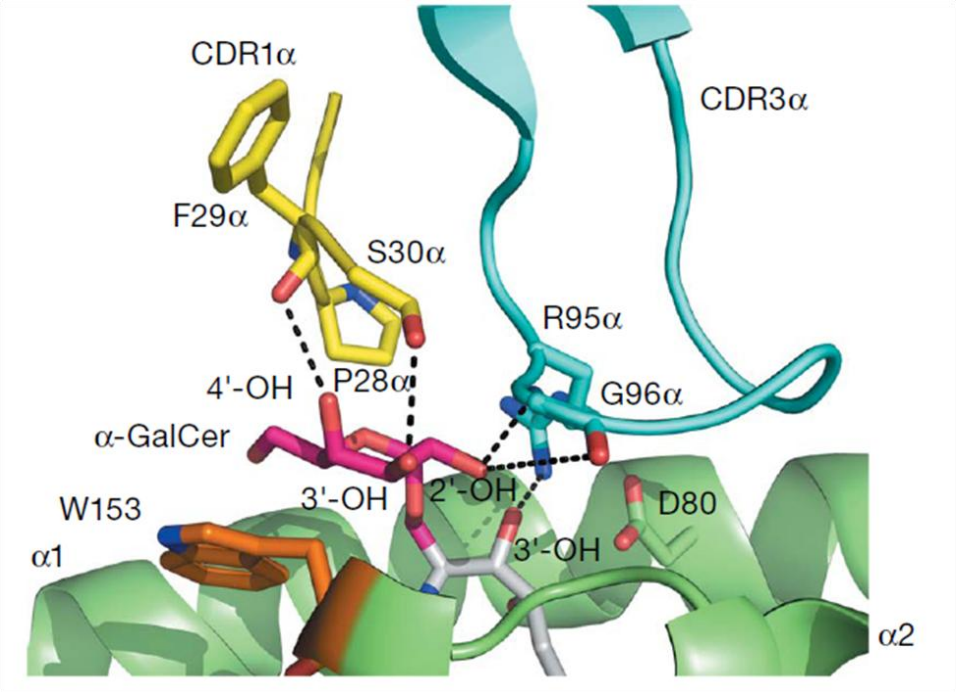

Figure 1.14. α-GalCer-mediated interactions with iNKT T cell receptor.

Figure adapted from ref [46]. Permission to reproduce figure was obtained from *Nature* through RightsLink® - licence number 2812180982041.

The formation of these three hydrogen bonds appears to be important for the recognition of the glycolipid-antigen-presenting complex and activation of iNKT cells. Moreover these observations explain why α-mannosylceramide (α-ManCer) does not activate iNKT cells.[47] The 2' and 4' hydroxyl groups in mannose have a different (2'-axial and 4'-equatorial) orientations when compared with galactose, which results in the loss of two key hydrogen bonds with the TCR. Thus whilst it is

likely that α-ManCer binds to CD1d, the resulting complex is not recognised by the TCR and so does not lead to iNKT cell activation.

The α-glycosidic linkage is also important for TCR recognition. The corresponding β-anomer, β-galactosylceramide, was recently shown to activate iNKT cells *in vivo* and in a CD1d-dependent manner;[48] however it is a siginificantly less potent agonist than α-GalCer. It has been postulated that the β-GalCer binds in a more perpendicular orientation, which disrupts contacts with the α-chain.

1.7 Other agonists of CD1d

Since the discovery of α-GalCer and subsequent detailed evaluation of its biological activity, a large number of natural and other synthetic agonists of CD1d have been examined. It has become clear that the immune responses that these analogues can trigger differ from those elicited by α-GalCer, not only quantitatively but also qualitatively. These observations have had a profound impact on our understanding of the biology of iNKT cells, which is crucial for developing effective iNKT-cell-based therapies.

1.7.1 Natural self-lipids presented by CD1d

A number of CD1d antigens have been found among endogenous self phospholipids and self glycosphingolipids. These are able to activate both mouse and human iNKT cells. Their autoreactivity occurs through the recognition of cellular lipids associated with CD1d proteins within cells.

A representative example of a natural agonist is the glycosphingolipid isoglobotrihexosylceramide **9** (iGb3) (Figure 1.15).[49] iGb3, which is generated in lysosomal compartments, was found to activate human and murine iNKT cells *in vitro*; however when compared with the most potent synthetic CD1d agonist (α-GalCer), it is at least 5 orders of magnitude less active.[49] Recognition of the much

larger trisaccharide head group by the TCR is possible thanks to its peripherally located CDR3β loop, which provides plasticity to accommodate different antigens.[46] Interestingly, it was shown that iNKT cells are not stimulated by Gb3 (the iGb3 analogue with an α1-4-linked terminal galactose), which suggests that the specific orientation of the terminal sugar is crucial for the formation of the CD1d-glycolipid-TCR ternary complex.[46] It remains unclear whether or not iGb3 can serve as a physiologically relevant ligand *in vivo*. To be stimulated, human iNKT cells require lysosomal processing of self antigens.[50,51] Moreover, in contrast to mouse, iGb3 is not found in humans, owing to the lack of functional genes for iGb3 synthase, which is required for its biosynthesis.[52]

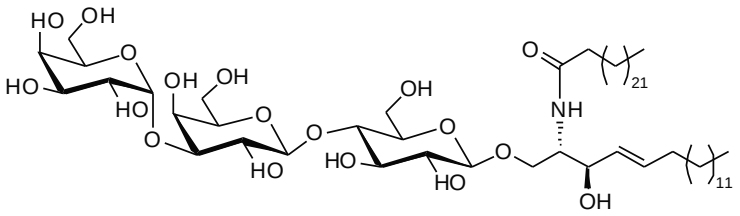

9, iGb3

Figure 1.15. Structure of the natural self-lipid, isoglobotrihexosylceramide (iGB3).

Self phospholipid antigens form another group of natural lipid ligands for CD1d. Among these are phosphatidylinositol (PI), phosphatidylglycerol (PG), phosphatidylethanolamine (PE) and phosphatidylcholine (PC) (Figure 1.16). Whilst these polar lipids were also found to bind murine CD1d, they displayed limited capability to activate murine iNKT hybridoma cells.[53-57] In another study[58] of the cellular ligands of hCD1d such as PE **10**, PC **11** also showed little or no

antigenicity, although it was suggested that lipids found in cell membranes may play an important role in the folding and stabilisation of CD1 molecules and hence modulate the ability of other more antigenic lipids to load on to CD1d molecules.[58]

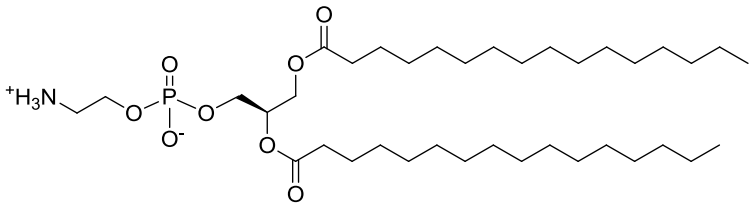

10, PE

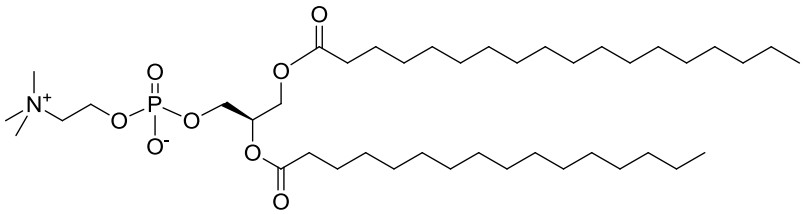

11, PC

Figure 1.16. Structure of natural phospholipids, phosphatidylethanolamine (PE) and phosphatidylcholine (PC).

A recent study of lysophosphatidylcholine (LPC) shows that this monoacyl form of PC also serves as a natural phospholipid ligand for NKT cells. LPC was found among lipids extracted from the plasma of multiple myeloma patients and proved to bind CD1d dimers and activate type II NKT cells ($V\alpha24^{-}V\beta11^{-}$) present in human blood.

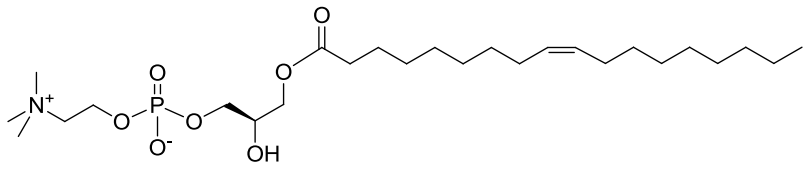

12, LPC (18:1)

Figure 1.17. Structure of monoacyl self-phospholipid, lysophsphatidylcholine (LPC).

This self phospholipid is postulated to be an endogenous signal for cellular stress or damage, as higher levels of LPC are detected in asthma, allergic and autoimmune inflammation and human cancers such as multiple myeloma.[59] LPC has consequently gained an increased interest and a recent study of Fox *et al.*[58] also suggests that NKT cells might be stimulated by physiological lipid signalling pathways to carry out their homeostatic immunoregulatory functions.

1.7.2 Synthetic analogues of α-galactosylceramide

Even though α-GalCer is the most potent agonist of iNKT cells, it may not be an optimal ligand for generating an antitumour or immunomodulatory effect. The iNKT cell activation by α-GalCer leads to the release of both Th1- and Th2-type cytokines. A number of different modifications have been applied to the KRN7000 structure resulting in significant changes in the profiles of cytokine production following iNKT cell activation. Finding the right balance in the Th1 *versus* Th2 cytokine profile is very important as these two types of cytokine result in two different immune responses.

1.7.2.1 Sphingosine base derivatives

Analogues of α-GalCer with modifications in the phytosphingosine base have been extensively studied and provided researchers with a set of useful SAR (structure-activity relationship) information long before the crystal structure of CD1d with bound α-GalCer was disclosed.

Phytosphingosine is structurally similar to naturally occurring sphingosine: both molecules have C18 hydrocarbon chains; however sphingosine lacks the hydroxyl group at C4 and bears a *trans* double bond between C4 and C5 instead of the fully saturated backbone found in phytosphingosine. The importance of the two hydroxyl groups, at C3 and C4 in the phytosphingosine base in α-GalCer structure has been confirmed.[60] Kronenberg and co-workers reported that 4-deoxy α-GalCer binds to murine CD1d but is not recognised by human CD1d.[61] 3,4-Dideoxy-α-GalCer was not antigenic in both mouse and human models.[61] These findings were later rationalised, when it was shown that the 3-OH group forms a hydrogen bond to Asp80 in both mouse and human CD1d, whilst the OH group at the 4 position participates in hydrogen bond formation only in mCD1d.[45]

OCH **13** is an analogue of α-GalCer, which induces a Th2 bias of NKT cells through the predominant production of IL-4 cytokines. In this CD1d agonist, the sphingosine base is truncated from 18 to 9 carbons and the acyl chain is reduced to 24 instead of 26 carbons (Figure 1.18).[62] OCH is five- to tenfold less active in inducing cell proliferation and produces less IFNγ but more IL-4 *in vitro*, when compared with α-GalCer. These observations have been confirmed in experiments

in vivo where IL-4 levels in serum remained unaffected for both agonists, but the amount of IFNγ detected for the OCH analogue was much lower. Even when much lower doses of α-GalCer are administered, the ratios of IL-4 / IFNγ remains almost unchanged, proving that the distinct cytokine polarising effect of OCH cannot be obtained by simply lowering the amount of α-GalCer. Despite being a less active agonist in inducing NKT cell proliferation, OCH displays a different type of activity to α-GalCer. OCH is now commonly used as a control in biological assays for IL-4 production, when compared with new agonists. Other analogues with a truncated phytosphingosine chain ranging from 9 to 15 carbons have been reported and were also found to increase the release of IL-4 in both murine and human iNKT cells.[63] These Th2-biasing analogues may find a future application in the treatment of different autoimmune diseases.

The origin of the Th2 bias for OCH and related analogues remains unclear. However, it has been postulated that the shorter sphingosine length destabilises the CD1d-glycolipid complex. As the release of IFNγ by iNKT cells needs a longer exposure to the CD1d-glycolipid complex (usually measured after 18 hours), lower levels of IFNγ are observed when compared with α-GalCer.

Attaching an aromatic ring to the end of a truncated sphingosine chain has been shown to result in a potent iNKT cell activator that induces a more Th1-biased cytokine response (Figure 1.18).[64] It is suggested that C13 **14** binds to CD1d with higher affinity thanks to the added aromatic substituent in the phytosphingosine

chain, which increases the time that C13 is in contact with CD1d resulting in higher levels of IFNγ upon iNKT cell activation.

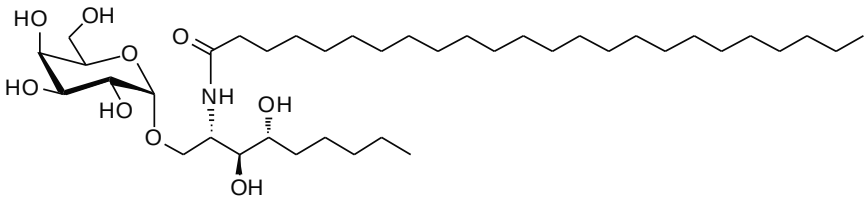

13, OCH

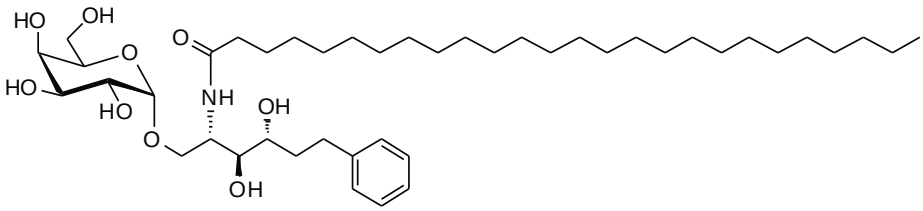

14, C13

Figure 1.18. Structure of OCH **13** and C13, **14** analogues of α-GalCer.

1.7.2.2 *N*-acyl chain derivatives

The length and degree of unsaturation in the *N*-acyl chain of α-GalCer was another point of focus in the search of new agonists of CD1d protein. C10:0 **15** (Figure 1.19) is an analogue with significantly shorter N-acyl chain, bearing 10 instead of 26 carbons in the chain. This modification in the agonist's structure was found to bias Th2 type response and weaken the activation of iNKT cells.[65]

α-GalCer-C20:2 **19** has two double bonds in the acyl chain at carbon 11 and 14 (Figure 1.19) and like compound **15** preferentially induces IL-4 production being another example of Th2 type agonist of CD1d.[66] However, in contrary to α-GalCer, it does not require endosomal localisation of CD1d for efficient loading and presentation.[67]

Other modifications in the *N*-acyl chain involved incorporation of the C20 prostaglandin B1 chain (α-GalCer-PGB1 **16**), aromatic rings (α-GalCer-C11Ph **17**), 4-fluorophenylacetate group (α-GalCer-4FPA **18**) or arachidonic acid (α-GalCer-C20:4 **20**) (Figure 1.19). These analogues also showed Th2-skewing of the cytokine profile generated by iNKT cell activation and are less dependent on endosomal loading for presentation by CD1d when compared with α-GalCer which produces mixed Th1 and Th2 cytokine profile.

It is suggested that the polarised iNKT cell cytokine production biased towards Th2-type response is an effect of direct loading of these agoniststs into CD1d molecules at the cell surface of APC.

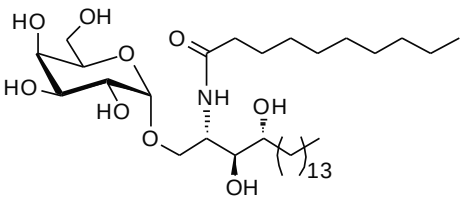

15, C10:0

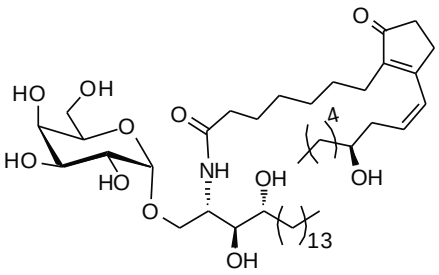

16, PGB1

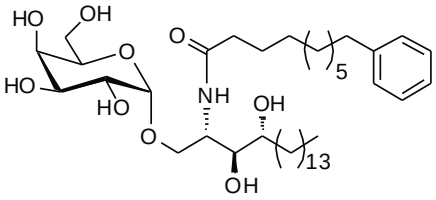

17, C11Ph

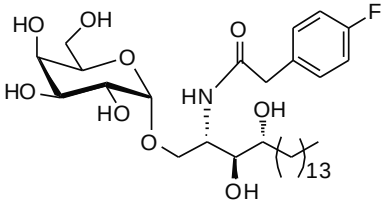

18, 4FPa

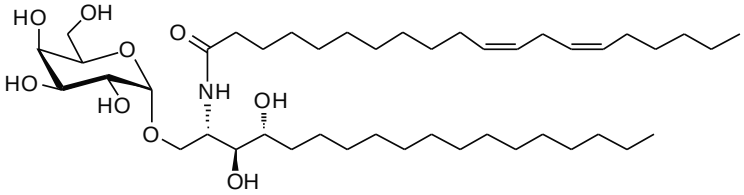

19, C20:2

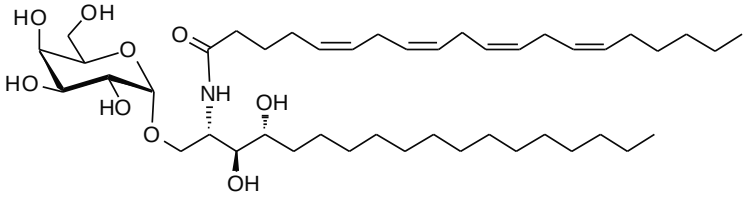

20, C20:4

Figure 1.19. Structures of representative *N*-acyl chain analogues of α-GalCer.

1.7.2.3 Carbohydrate modifications

α-GalCer analogues with modified sugar unit are an important group of new agonists of CD1d. The activity of α-glucosylceramide (α-GlcCer) **21** in mouse spleen iNKT cell activation assay was found to be similar to that of α-GalCer **8** (Figure 1.20). Only configuration of 4-hydroxyl group (equatorial) in α-GlcCer **21** varies from structure of α-GalCer **8** (axial), this indicated that the 4-hydroxyl configuration of the sugar was not essential for bioactivity. However, α-mannosylceramide (α-ManCer) **22** (Figure 1.20) with the 2-hydroxyl group in an axial configuration as compared to an equatorial orientation in α-GalCer **8** or α-GlcCer **21**, was found to be inactive. The configuration of the 2-hydroxyl group on the sugar moiety proved to be crucial to activate iNKT cells.[68] These observations were later explained by determining the crystal structures of mouse and human CD1d-α-GalCer-TCR ternary complexes, which revealed that the equatorial position of the galactose 2'-OH in α-GalCer forms a hydrogen bond with the side-chain of Asp151 in hCD1d (Asp153 in mCD1d) and the resulting adopted orientation of the sugar is crucial for the recognition by the iNKT TCR.

Trappeniers et al. reported few analogues of α-GalCer with modifications at the galactose 6'-position.[69] The crystal structure analysis of human and mouse CD1d-α-GalCer complexes showed that the 6'-hydroxyl group of the galactose in α-GalCer does not take part in a hydrogen bond formation between α-GalCer and CD1d. Analogue **23** (Figure 1.20) in which 1-naphtyl group attached to 6'ureido-6'deoxy-α-GalCer, was found to stimulate a Th1-cytokine biased response with production of IFNγ cytokine similar to α-GalCer.

The threitolceramide ThrCer **24** (Figure 1.20) is a truncated non-glycosidic analogue of α-GalCer. In this compound the labile α-glycosidic linkage is replaced with an ether bond to gain metabolic stability *in vivo*. A galactose ring has been replaced with an acyclic sugar but with retained relative and absolute stereochemistry. ThrCer **24** proved to be a less potent agonist of CD1d when compared with α-GalCer, however it does not cause the lysis of dendritic cells.[70]

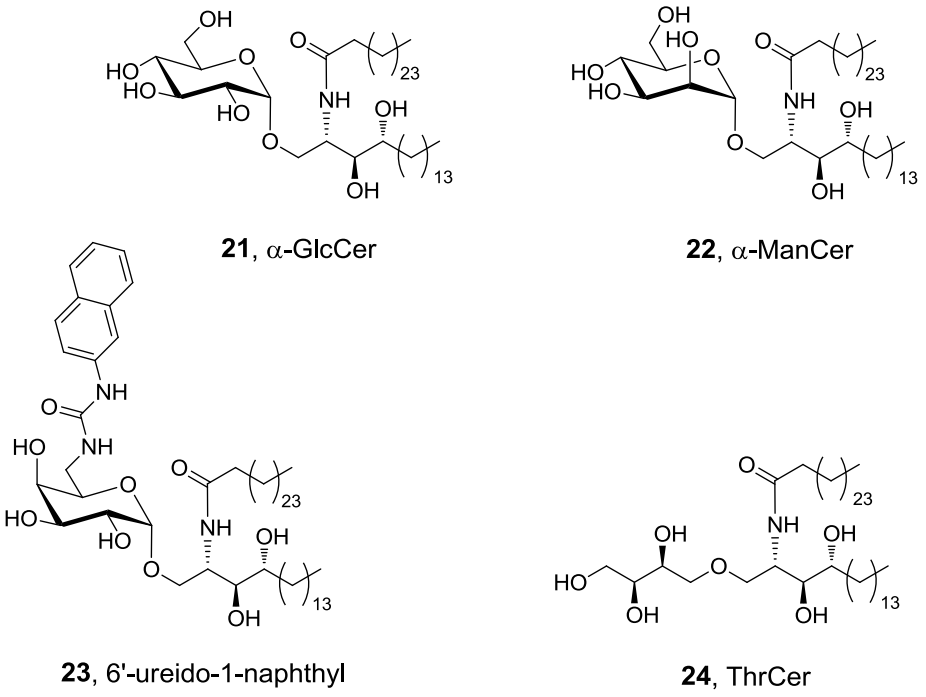

Figure 1.20. Representative carbohydrate derivatives of α-GalCer.

1.7.2.4 Glycosidic bond derivatives

The *C*-glycosyl derivative, α-*C*-GalCer **25** (Figure 1.21), was found to be a more potent agonist than α-GalCer in mouse model of malaria and melastatic melanoma, but also showed induced Th1-biased cytokine production.[71] In this analogue the oxygen atom of the α-GalCer glycosidic bond (a polar hydrogen acceptor) has been replaced with a non-polar CH_2, which cannot participate in hydrogen bonding. This modification has been proposed to cause the glycolipid to sit differently in the CD1d groove thereby changing the structure of the complex and its affinity for the iNKT TCR, and may also allow for free rotation of the "glycoside" bond connecting the galactose and ceramide portions of the molecule.[71,72] Greater levels of IFN-γ production might be also a result of higher stability of this analogue *in vivo*, as *C*-glycosidic linkage has increased resistance to enzymatic degradation.

Recently, the same research group (R. W. Franck and co-workers) reported a series of α-*C*-GalCer analogues and found *E*-alkene-linked *C*-glycoside analogues *e.g.* GK 109 **26** (Figure 1.21) were potent human iNKT-cell stimulants that also induce Th1-biased cytokine production relative to α-GalCer.[73] It was proposed that replacement of the CH_2 glycosidic linkage with the *E*-alkene linker may result in fixed orientation of the polar head group that is beneficial for iNKT cell TCR recognition.[73]

These findings highlight the flexibility of the iNKT cell TCR, which in spite of its relatively limited diversity appears to be capable of different modes of recognition that enable responses to a wide range of CD1d-presented ligands.

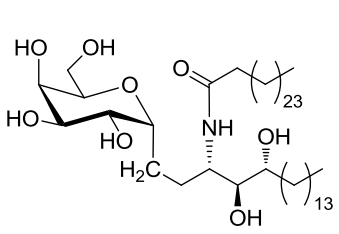

25, α-*C*-GalCer

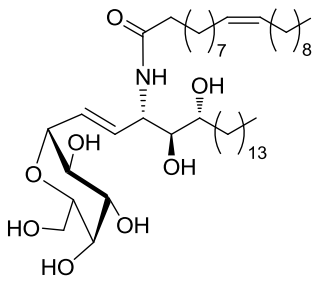

26, GK109

Figure 1.21. Representative glycosidic bond derivatives of α-GalCer.

1.8 Aims and objectives

Recent years have shown a growing interest in understanding the biology of iNKT cells that in turn could translate into successful immune therapies. Numerous α-GalCer analogues have been synthesised and tested in order to find a potent iNKT cell agonist that could selectively induce beneficial cytokine profile.

To date, very few alterations around the amide bond of α-GalCer have been explored. To investigate its importance in iNKT cell stimulation, we decided to synthesise a range of α-GalCer and ThrCer analogues, in which the amide group in our lead has been replaced with different carbonyl functional groups. These compounds would then be tested for iNKT cell induction and in particular their Th1/Th2 response, which in turn would determine their therapeutic potential.

The second part of the project will focus on additional modifications and the synthesis of labelled derivatives, which will find application in intracellular trafficking studies.

Chapter 2

Amide Analogues of α-Galactosylceramide and Threitol Ceramide

2. Amide Analogues of α-Galactosylceramide and Threitol Ceramide

2.1. Interactions between the amide moiety of α-GalCer and amino acid residues of the iNKT TCR and CD1d protein in the human TCR–hCD1d–α-GalCer ternary complex

The first crystal structures of the hCD1d–α-GalCer complex,[45] and the TCR–hCD1d–α-GalCer ternary complex,[46] discussed in the Introduction (Sections 1.5 and 1.6), did not reveal any direct hydrogen bonds between the amide group of α-GalCer and amino acid residues of CD1d or the iNKT cell TCR. Recently however, Pellici *et al*.[74] reported a crystal structure of the human NKT cell TCR–hCD1d–α-GalCer complex at improved (2.5 Å) resolution (Borg *et al*. reported the crystal structure of the NKT cell TCR–hCD1d–α-GalCer complex at 3.2 Å resolution). From this better-resolved structure, the carbonyl group of the amide functionality in α-GalCer was found to form a hydrogen bond with a water molecule, which in turn, formed a hydrogen bond with the backbone carbonyl of isoleucine-69 (Ile69) in the CD1d molecule.

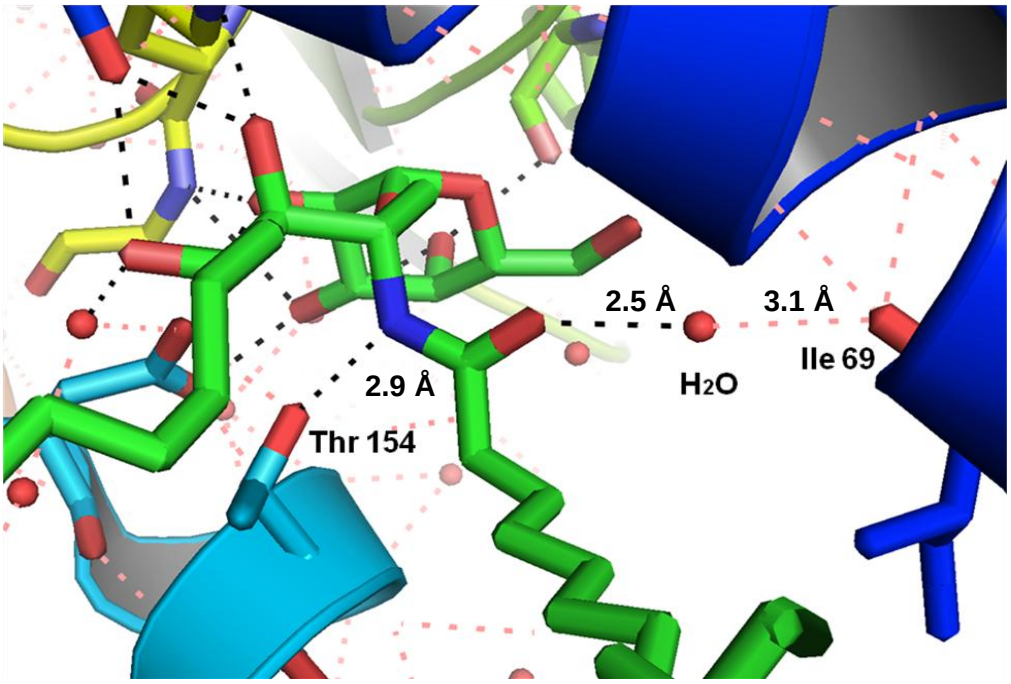

Figure 2.1. Cartoon representation of polar contacts in the iNKT cell TCR–hCD1d–α-GalCer complex (α-GalCer – green sticks, CD1d – blue cartoon). Figure generated from 3HUJ.[74]

The structural analyses made by Pellici *et al*. also identified a direct hydrogen bond between the N-H of the amide group of α-GalCer and the hydroxyl group in the side-chain of the threonine-154 (Thr154) residue located on the α-2 helix of the human CD1d molecule (Thr156 in mouse CD1d). We postulated that this interaction might play an important role in positioning α-GalCer in the right conformation for subsequent recognition by the iNKT cell TCR receptor.

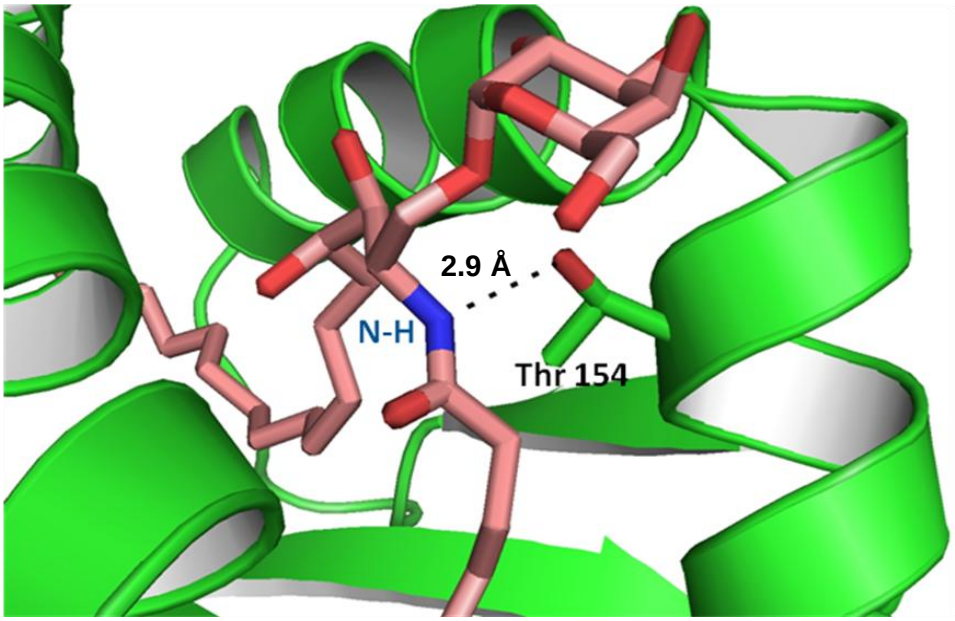

Figure 2.2. Cartoon representation of the hydrogen bond interaction between the –NH of α-GalCer (pink sticks), and the Thr154 residue of hCD1d (green cartoon). Figure generated from 3HUJ.[74]

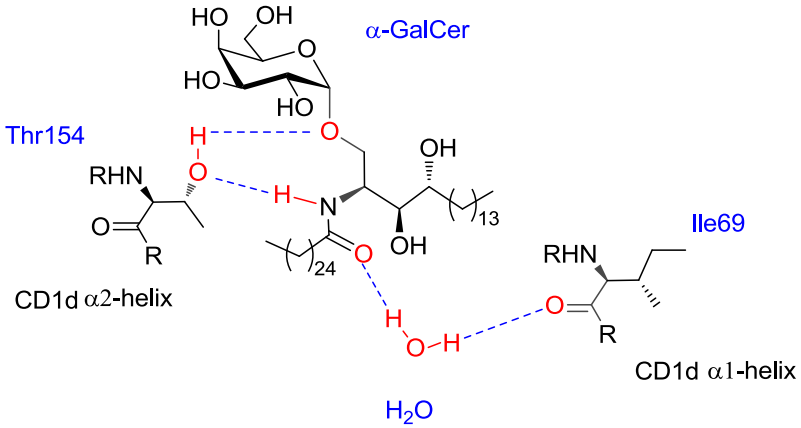

Figure 2.3. Interactions between the amide moiety of α-GalCer and amino acid residues of hCD1d in the iNKT cell TCR–hCD1d–α-GalCer ternary complex revealed by the crystal structure determined at 2.5 Å resolution.[74]

2.2. Reported analogues of α-GalCer with variations around the amide group

To date, only a few analogues of α-GalCer have been synthesised, in which the amide group has been replaced by other functional groups. Lee *et al.*[75] replaced the amide moiety in α-GalCer with a 1,2,3-triazole. They reported a series of analogues containing this heteroaromatic unit and possessing different lengths of the lipid chain ranging from 6 to 26 carbon atoms **27**-**32** (Figure 2.4).

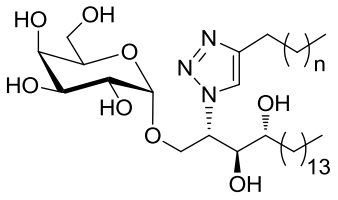

27 n = 4 **28** n = 5 **29** n = 14

30 n = 21 **31** n = 22 **32** n = 23

Figure 2.4. A series of 1,2,3-triazole-containing analogues of α-GalCer **27-32**.

The 1,2,3-triazole functionality exhibits structural similarities to the ubiquitous amide moiety found in natural systems;[76] however in contrast to amides, triazoles are much more stable to hydrolysis, as well as to oxidising and reducing conditions *in vivo.*[77] In a similar fashion to the amide group, a 1,4-disubstituted 1,2,3-triazole can also participate in hydrogen bond formation (Figure 2.5). However, whilst primary and secondary amides can function as hydrogen bond donors *and* acceptors, two of three nitrogen atoms of 1,2,3-triazoles can only ever serve as hydrogen bond acceptors.

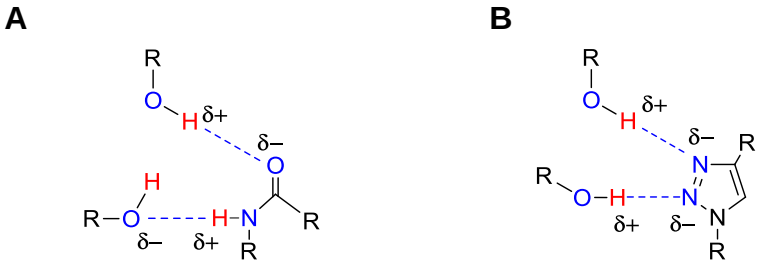

Figure 2.5. Hydrogen bond formation and dipole-dipole interactions between amides (**A**) and 1,2,3-triazoles (**B**) and a hydroxyl group.

The bioisosteric replacement of the amide moiety of α-GalCer with a 1,2,3-triazole unit is potentially interesting as the resulting modified glycolipids should survive a wider range of conditions *in vivo* and therefore last longer. Activation of iNKT cells with the *C*-glycosyl analogue of α-GalCer (discussed in the Introduction in Chapter 1.7.2.4), results in greater production of IFNγ (Th1 - type) and lower amounts of IL-4 (Th2 - type). Since IFNγ requires a longer release time than IL-4, it has been postulated that the longer exposure time of the CD1d-glycolipid complex to iNKT cell TCR might account for this Th1-biased cytokine response.

Biological evaluation of glycolipids **27**-**32** *in vitro* (with the use of mouse splenocytes), however, showed a Th2 bias for all analogues. Analogue **31** in particular, which bears a saturated 24-carbon alkyl chain, produced higher levels of IL-4 and less IFNγ when compared with α-GalCer. Subsequent *in vivo* studies confirmed the *in vitro* observations for triazoles **30**-**32**, which all possess longer alkyl chains (n = 21, 22, 23); however those analogues with short- and medium-chain lengths were unable to stimulate iNKT cells *in vivo*.

Recently, Mori and co-workers investigated the replacement of the amide bond in α-GalCer with ether **33** and ester groups **34**.[78] In both cases, the formation of the hydrogen bond with the Thr154 residue of human CD1d (and Thr156 for mouse CD1d) may still be possible in these analogues with relatively little structural reorganisation; the oxygen atom of the ether or ester group, which replaced the N-H of the amide group of α-GalCer, might now act as a hydrogen bond acceptor to the hydrogen of the hydroxyl group in the side-chain of Thr154.

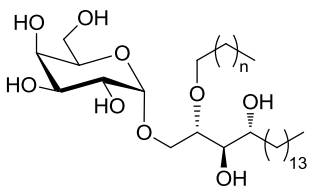

33, n = 24

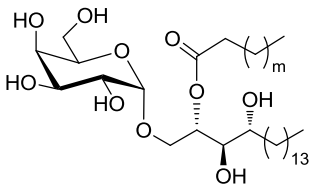

34, m = 23

Figure 2.6. α-GalCer analogues where ether and ester groups have been introduced in place of the amide linkage found in α-GalCer.

The ether analogues, which lacked both the N-H *and* the carbonyl oxygen of the amide in α-GalCer were unable to activate iNKT cells. Glycolipids with an ester group, however, were able to activate iNKT cells although with significantly reduced activity compared to α-GalCer: IFNγ production was 10% of that shown by α-GalCer; IL-4 production was one-third to two-thirds of that shown by α-GalCer. These results further support the importance of the amide N-H in α-GalCer, and its ability to act as a hydrogen bond donor to the Thr154 residue of hCD1d, for iNKT cell activation.

2.3. Target compounds and the rationale for replacing the amide bond

We were also interested in investigating further modifications around the amide bond. In light of the apparent importance of the amide N-H in CD1d binding, and in contrast to other studies, we decided to retain the NH in the structure, and replace the amide moiety with related functional groups, namely a thioamide, urea and carbamate. Our target molecules are shown below in Figure 2.7.

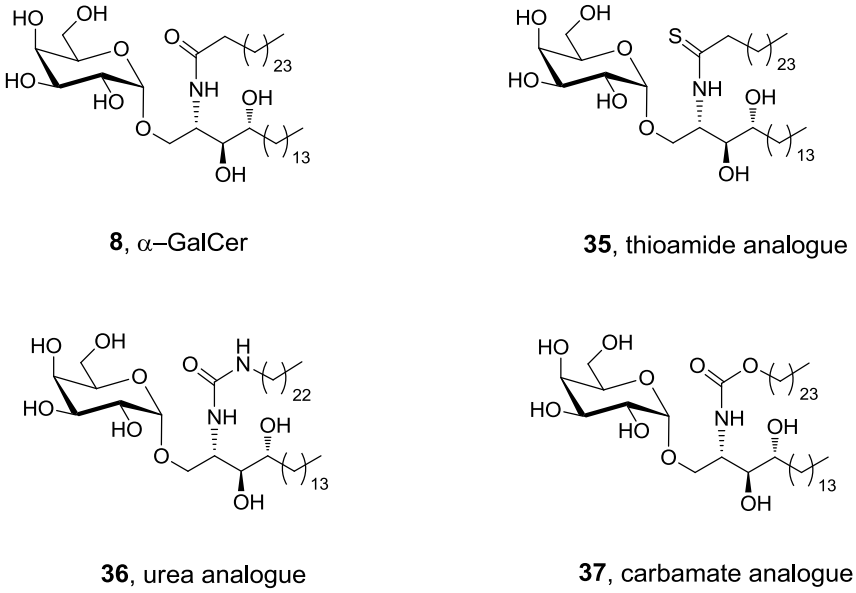

Figure 2.7. Target molecules, α-GalCer and three analogues in which the amide has been replaced with other functional groups.

We also decided to make similar changes to ThrCer, the non-glycosidic analogue of α-GalCer (see Introduction Chapter 1.7.2.3) and the four target molecules based on this scaffold are presented in Figure 2.8.

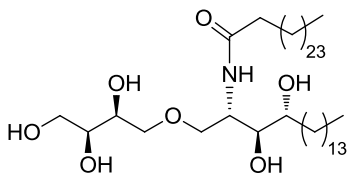

24, ThrCer

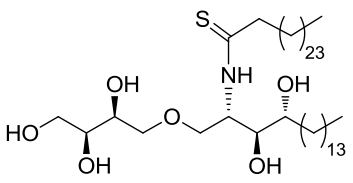

38, thioamide analogue

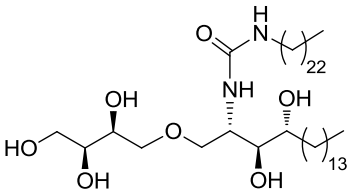

39, urea analogue

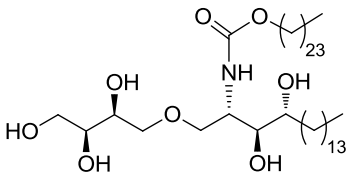

40, carbamate analogue

Figure 2.8. Non-glycosidic glycolipid, ThrCer and thioamide, urea and carbamate analogues.

We postulated that these changes would be interesting for a number of reasons. First, the applied modifications could result in increased metabolic stability, as these functional groups should survive a wider range of conditions *in vivo*, being less prone to enzyme-mediated hydrolysis.[79-81] Second, the introduction of different heteroatoms could alter the hydrogen bonding network. The pK_a values of the N-H in a urea, amide, carbamate and thioamide are summarised in Figure 2.9. The urea has the highest pK_a value and is less acidic than an amide, whereas the N-H in a carbamate and thioamide is more acidic and should be a better hydrogen donor.[82,83]

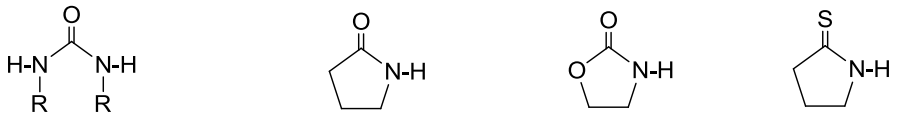

pK_a = 26 - 27 pK_a = 24.2 pK_a = 20.8 pK_a = 13.3

Figure 2.9. Comparison of pK_a values (in DMSO) for amide, carbamate, urea and thioamide.[82,83]

The formation of additional hydrogen bonds is possible for the carbamate analogue, where the additional oxygen atom is a potential hydrogen bond acceptor. Likewise, the urea analogue possesses an additional N-H which could serve as another hydrogen bond donor. In the case of the thioamide analogue, we postulated that the larger[*], lipophilic sulfur atom might also change the rate of glycolipid loading / deloading from CD1d and increase the stability of the CD1d-glycolipid-TCR complex, since this more hydrophobic analogue of α-GalCer, might be buried “deeper” in the hydrophobic binding groove of CD1d, leading to a more stable CD1d-glycolipid-TCR complex.

[*] *The atomic volume of a sulfur atom is 1.66 times larger (24.4/14.7=1.66) than oxygen (van der Waals radius of a sulfur atom r_W = 1.80 Á, for oxygen r_W = 1.52 Á, hydrogen r_W = 1.20 Á)*

A **B**

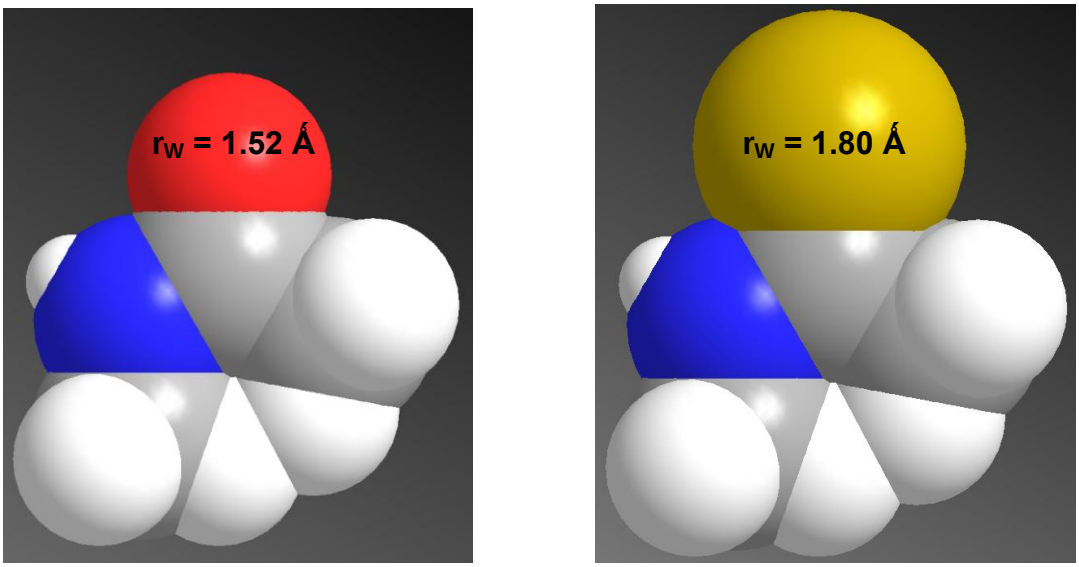

r_W - van der Waals radius

Figure 2.10. Sphere representation of the primary amide *N*-methyl-acetamide (**A**) and *N*-methyl-thioacetamide (**B**), indicating a difference in atomic volume between the carbonyl oxygen and sulfur atoms. (oxygen – red, sulfur – yellow, nitrogen – blue, carbon – grey, hydrogen – white).

These modifications have not been applied to glycosyl ceramide structures, although similar modifications to the amide bond in a ceramide lipid were recently reported[84-87] after this synthetic work had been completed. In this study, De Libero and co-workers prepared a range of sphingolipids and ceramides with different carbonyl functions (Figure 2.11). Compounds **41**-**45** were tested for iNKT cell activation, but none showed significant activity. A competition assay was designed

to test the ability of these ceramides to compete with α-GalCer for binding to CD1d and prevent T cell activation. Only compound **43** bearing a 1,2,3-triazole *and* thioamide function was found to compete with α-GalCer in *in vitro* studies, albeit only at 15-fold molar excess over α-GalCer; the same result was not replicated in *in vivo* assays, even when a large excess of this ceramide was used. In light of the structural differences, principally the absence of a sugar residue, further comparisons of these ceramide analogues with our α-GalCer and ThrCer derivatives are difficult.

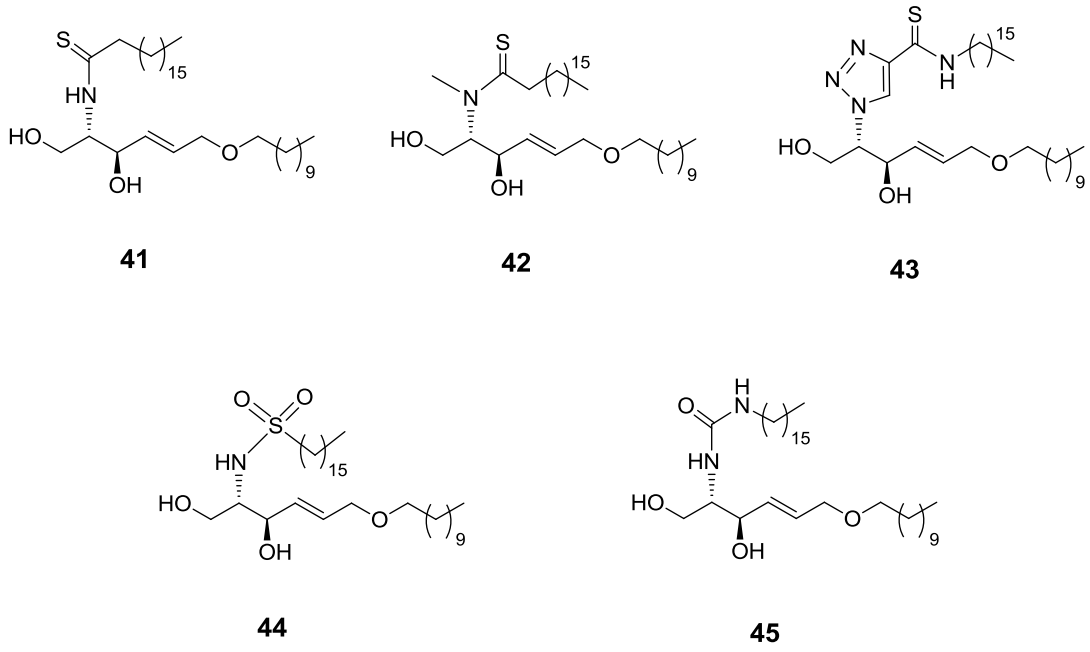

Figure 2.11. Modification of the amide group of 7-oxaceramides.[81]

2.4. Retrosynthetic analysis

The retrosynthesis of α-GalCer **8** and its three analogues **35**, **36** and **37** is outlined in Scheme 2.1. In our approach we wanted to prepare a common precursor, namely amine **46**, which could be functionalised at a late stage of the synthesis with acyl chloride **47**, isocyanate **48** and mixed carbonate **49**, to provide three of our target molecules after deprotection. We identified β-galactose pentaacetate **53** and phytosphingosine **54** as the starting materials for our synthesis; these could be readily converted into the two reacting partners required for the glycosylation reaction, which would unite the two fragments. Galactose **51** would then serve as the glycosyl donor and phytosphingosine **52** as the acceptor. Reduction of the azide in the resulting glycoside product **50** would afford our common precursor, amine **46**.

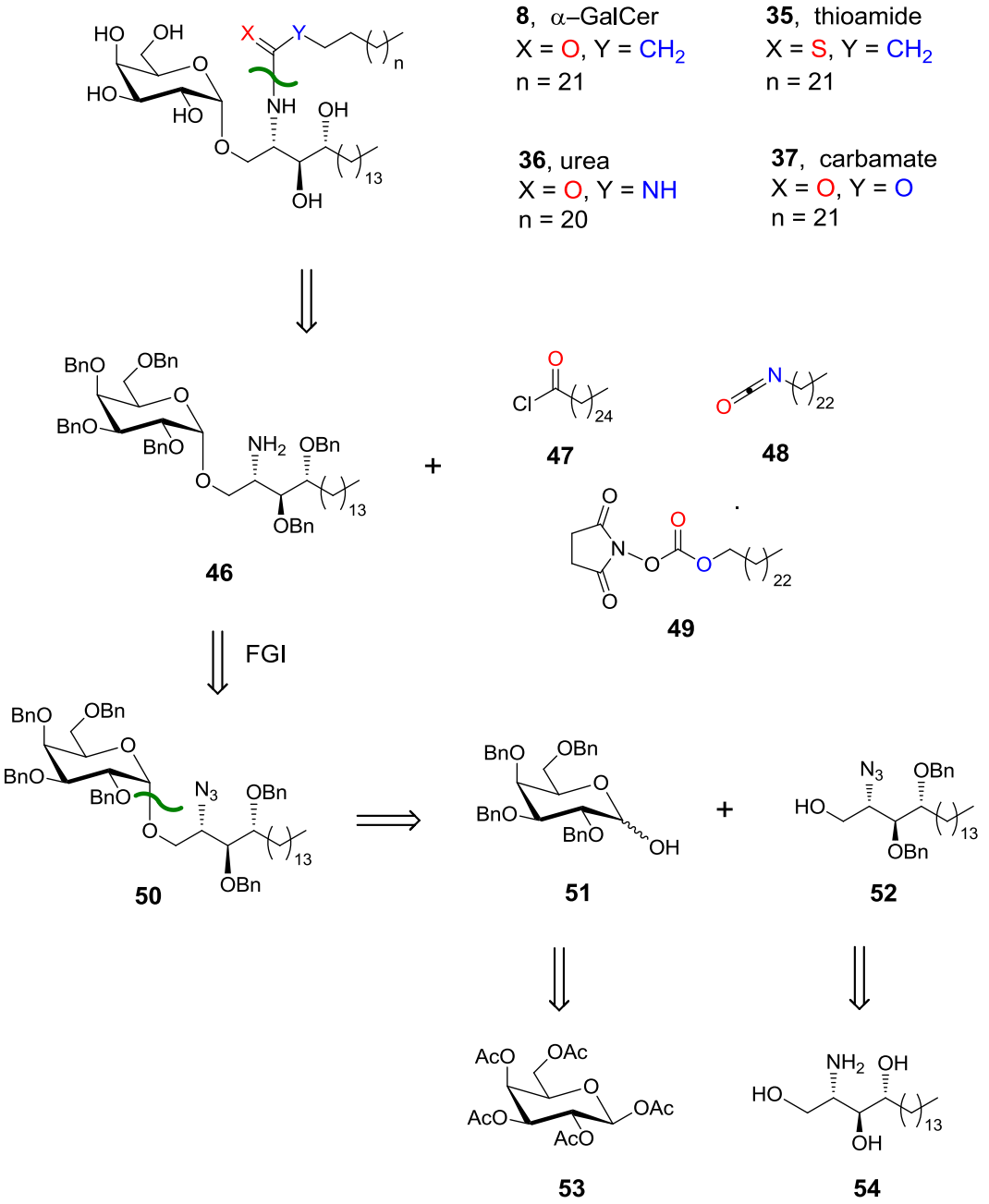

Scheme 2.1. Retrosynthetic analysis of α-GalCer **8** and thioamide **35**, urea **36** and carbamate **37**.

2.5. First-Generation Synthesis of α-GalCer

We first decided to prepare α-GalCer, as this compound would be needed as the control against which our new analogues **35**, **36** and **37** would be compared in the biological assays. Moreover, this first synthesis would help us to identify any limitations (low-yielding reactions, poor choice of reagents and protecting groups) in our planned approach towards advanced intermediate amine **46**, as well as the final deprotection step, before embarking on the synthesis of the new analogues.

The synthesis of 2,3,4,6-tetra-*O*-benzyl-D-galactose **51** began with commercially available β-galactose pentaacetate, which, on activation with $BF_3{\cdot}OEt_2$ at 0 °C in the presence of PhSH, afforded thioglycoside **55** in excellent yield as an inconsequential 1:1 mixture of anomers (Scheme 2.2).[88] The acetate groups in **55** were then removed under Zemplén conditions to afford the fully deprotected thioglycoside **56**. This deprotection method allowed a simple work-up, which consisted of neutralising the reaction mixture with an acidic Dowex ion exchange resin followed by filtration of the resin and removal of the solvent under reduced pressure. The very polar tetraol **56** was collected as a white foam without any need for further purification.[89] Subsequent re-protection of the alcohols in **56** as benzyl ethers provided thioglycoside **57**, which was then hydrolysed with *N*-iodosuccinimide in an acetone/water mixture (10:1) to yield the hemiacetal **51** as our sugar donor precursor as a 1:1 mixture of diastereoisomers.[89] The product was characterised by HRMS, and the 1:1 ratio of diastereoisomers was evidenced

in the ^{1}H NMR spectrum by integrating the OH proton resonances for the two anomers, which appeared at 2.93 ppm and 3.15 ppm. The IR spectrum also showed an OH stretch as further evidence for the thioglycoside hydrolysis.

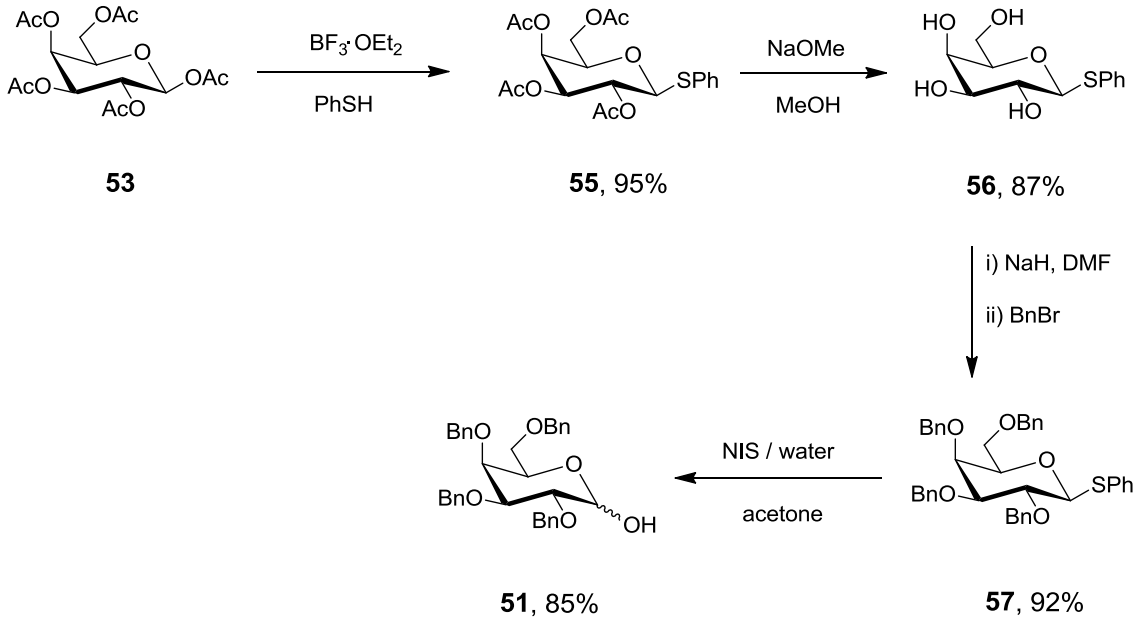

53 **55**, 95% **56**, 87%

51, 85% **57**, 92%

Scheme 2.2. Synthesis of 2,3,4,6-tetra-*O*-benzyl-D-galactose **51**.

Phytosphingosine **54** served as the starting material for the glycosyl acceptor **52** whose synthesis is summarised in Scheme 2.3. This commercially available amine **54** was first converted into the corresponding azide **58** in a diazo transfer reaction.[90] Imidazole-1-sulfonyl azide hydrochloride[90] was used as the "diazo donor" in this copper(II)-catalysed reaction, which proceeded in excellent yield. This reaction had been carried out previously in our group using trifluoromethanesulfonyl azide (TfN_3)[91-93] as the "diazo donor". However, disadvantages of using TfN_3 as a reagent include the explosive nature of neat

TfN_3, and its poor shelf-life, which necessitates its preparation immediately prior to use.[94] Moreover, the preparation of TfN_3 involves the use of expensive trifluoromethanesulfonic anhydride and the removal of trifluoromethanesulfonamide from the reaction mixture, which complicates the work-up procedure.[95] In contrast, imidazole-1-sulfonyl azide hydrochloride is cheap to prepare, more robust, easy to store (in its crystalline form) and provides a much safer alternative to TfN_3.

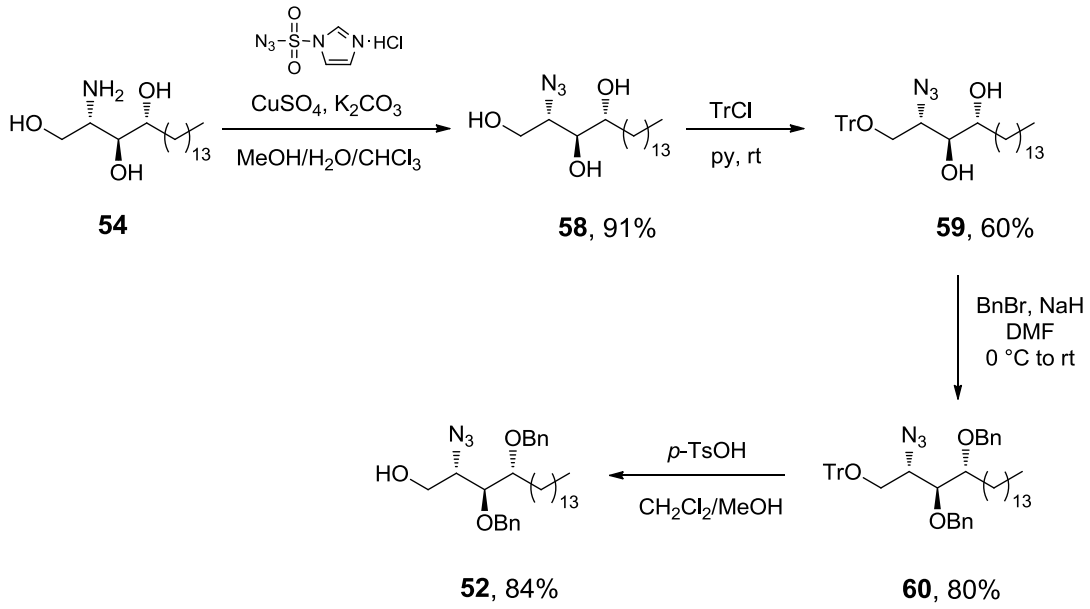

Scheme 2.3. Synthesis of azido alcohol **52**.

Selective tritylation of the less hindered primary alcohol in **58** afforded trityl ether **59** in 60% yield. The low yield of this reaction was a result of by-product formation. MS and NMR spectroscopic analysis of the side-products, isolated from the crude reaction mixture by flash column chromatography, showed that a major side-

product was a di-trityl ether, in which the primary and one of the secondary alcohols had reacted with the trityl chloride. Diol **59** was then treated with sodium hydride to provide the corresponding di-alkoxide, which was reacted with 2.2 equiv of benzyl bromide to give the dibenzylated derivative **60** in 80% yield. The desired glycosyl acceptor **52**[96-98] was finally obtained after selective deprotection of the trityl ether with *p*-TsOH.

A key challenge in our synthesis was the selective formation of the α-glycosidic bond in our target galactosides. To this end, we chose to employ the halide ion-catalysed α-glycosylation methodology developed originally by Lemieux and co-workers,[97-99] and shown to be a useful entry into α-galactosides by Kobayashi and co-workers.[100,101] Scheme 2.4 illustrates the mechanism of this interesting α-glycosylation reaction.

In the first step, a 2-*O*-benzyl-1-hydroxy sugar† reacts with CBr_4 and Ph_3P, the so-called Appel reagents,[102,103] to generate a glycosyl bromide. Under the reaction conditions, and in the presence of an excess of nucleophilic bromide anions (Bu_4NBr) and *N,N*-tetramethyl urea (TMU), the more stable α-glycosyl bromide equilibrates with the highly reactive β-anomer. The acceptor alcohol (R-OH) then reacts preferentially with the more reactive β-glycosyl bromide in an S_N2 fashion to provide the α-glycoside product. TMU and bromide anions play a critical role in the glycosylation, in ensuring the isomerisation of the α- and β-glycosyl bromides is much faster than their reaction with the glycosyl acceptor.

The labile β-glycosyl bromide will also react with adventitious water to generate the starting 2-*O*-benzyl-1-hydroxy sugar. However, CBr_4 and Ph_3P are employed in excess to ensure any hydrolysed donor is recycled. The Appel reagents also capture any adventitious water. Kobayashi and co-workers[100] found that 3 molar equivalents of CBr_4 and Ph_3P were optimal. Under these conditions, *in situ* formation of the glycosyl bromide and glycosylation proceeded without having to

† The key requirement for the glycosyl donor in this α-selective glycosylation is a non-participating protecting group on the C-2 position.

pay special attention to carrying out the reaction under strictly anhydrous conditions.

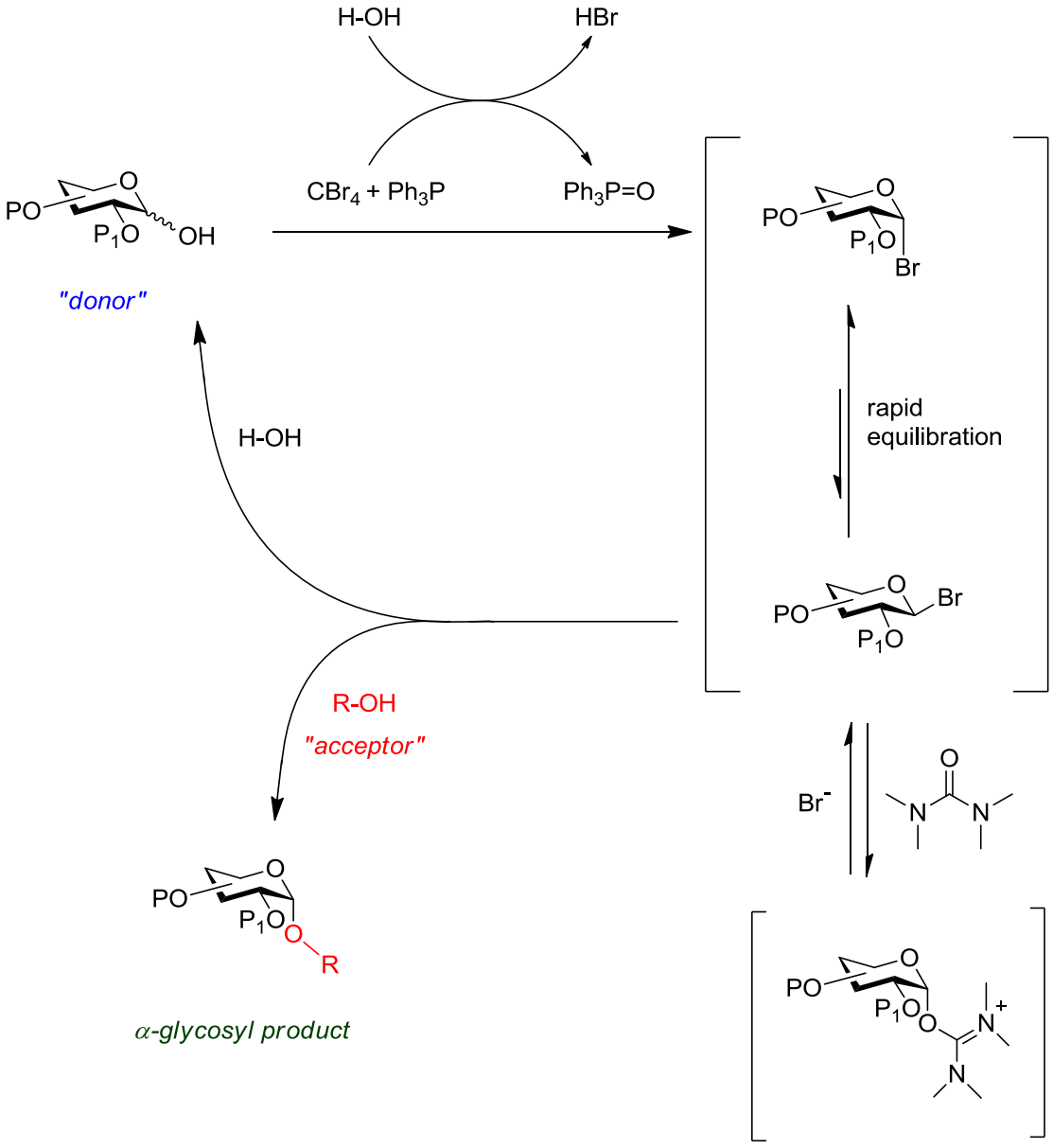

P^1 = non-participating protecting group

Scheme 2.4. Overview of one-pot dehydrative α-glycosylation with Appel agents.

In our hands, when glycosyl donor **51** (2,3,4,6-tetra-*O*-benzyl-D-galactose) was treated with CBr_4 and PPh_3 at r.t., the formation of the glycosyl bromide, as monitored by TLC analysis, was complete within three hours. In the next step, the acceptor **52**, TMU and Bu_4NBr were added to the reaction mixture. Work-up after 72 hours provided the desired α-galactoside **50** as a single anomer.

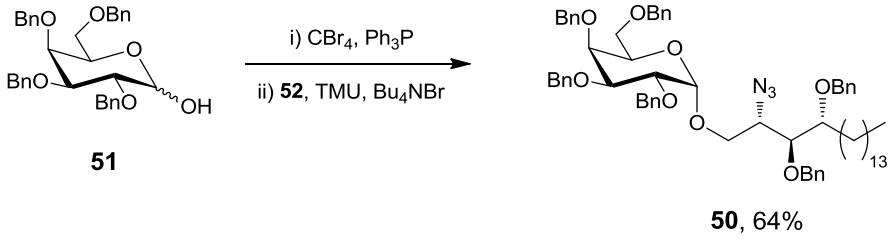

51

50, 64%

Scheme 2.5. Synthesis of α-galactoside **50**.

In our first attempt at glycosylation, the reported procedure was followed closely,[104] with three equivalents of acceptor **52** being employed as directed. However, instead of leaving the reaction for 8 days, the reaction mixture was worked-up after only 3 days, as TLC analysis showed no further consumption of the starting materials after that time. Unfortunately, it proved difficult to separate the α-glycosyl product from the starting materials (bromide of the donor **51** and the acceptor **52**), which compromised the isolated yield (42%) of α-galactoside **50**. Table 2.1 summarises the modifications we applied in order to improve matters.

entry	acceptor **52** [equiv]	scale [mmol of **51**]	3 Å MS used	recovery of **52** [%]	isolated yield of **50** α-glycoside [%]
1	3.0	0.37	no	43	42
2	1.5	0.37	yes	44	64
3	1.5	1.85	yes	45	62
4	1.5	3.50	yes	41	64

Table 2.1. Summary of modifications applied to the literature Kobayashi α-glycosylation.

First, to facilitate the chromatographic separation of the α-glycosyl product **50** from the starting acceptor, we decreased the amount of alcohol **52** from 3.0 to 1.5 equivalents and were pleased to observe that this modification did not result in a lower isolated yield, nor in a longer reaction time. Under these conditions, chromatographic purification of **50** was now possible.[‡] The inclusion of molecular sieves also helped matters. In combination, these changes led to a significantly improved isolated yield (64%) without affecting the reaction time (72 h). Moreover, it was now possible to perform the reaction on larger scale (3.50 mmol) without observing any deleterious effect on either the isolated yield or the stereoselectivity. With these modifications, we were able to access significant quantities of glycoside **50** for further study.

[‡] 45% of the unreacted acceptor **52** was also recovered.

The stereochemistry of the glycosidic linkage was unambiguously assigned by NMR spectroscopic analysis. The easiest signal to find in the ^{13}C NMR spectrum of **50** is the anomeric carbon, which appears at δ 98.6 ppm. From this, the attached H-1' proton was then identified by 2-D chemical shift-correlated spectroscopy (HSQC). Measuring the coupling constant of this anomeric proton from the ^{1}H NMR spectrum [δ 4.91 ppm (1H, d, $J_{1,2}$ 3.5 Hz, H-1')], confirmed the assignment as the α-glycoside. The β-anomer would be expected to show a larger coupling constant in the range 8-12 Hz, associated with *trans* diaxial axial-axial coupling (Figure 2.12). An axial-equatorial coupling constant is much smaller, usually in the range 2-5 Hz.

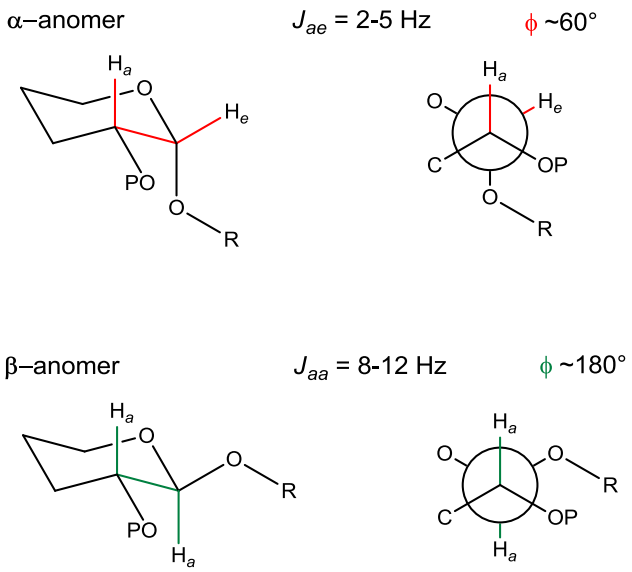

Figure 2.12. $J_{1,2}$ coupling constants for α- and β-glycosyl products.

The azido group in glycoside **50** was next reduced with trimethylphosphine in a Staudinger reaction[105,106] to give amine **46** in 72% yield (Scheme 2.6). In the first step of the proposed mechanism of this Staudinger reaction (Scheme 2.7),[107] a phosphine, usually Ph_3P, reacts with the azide function to form a phosphazide intermediate, which then liberates nitrogen gas in the formation of an iminophosphorane.

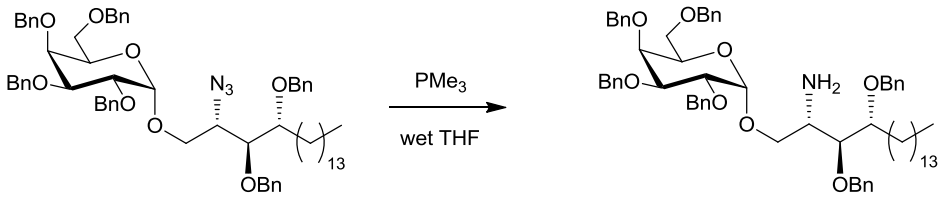

50 **46**, 72%

Scheme 2.6. Synthesis of common precursor amine **46**.

In the presence of water (wet solvent or aqueous work-up) the iminophosphorane is hydrolysed to give the desired amine and a phosphine oxide by-product. Although triphenylphosphine is a stable and easy-to-handle reagent, the resulting by-product, triphenylphosphine oxide, can be difficult to remove in the work-up. We therefore chose to use trimethylphosphine instead as this reacts with azides in the same fashion;[94] however, the trimethylphosphine oxide by-product is a volatile solid, which can be removed from the crude product under reduced pressure.[108]

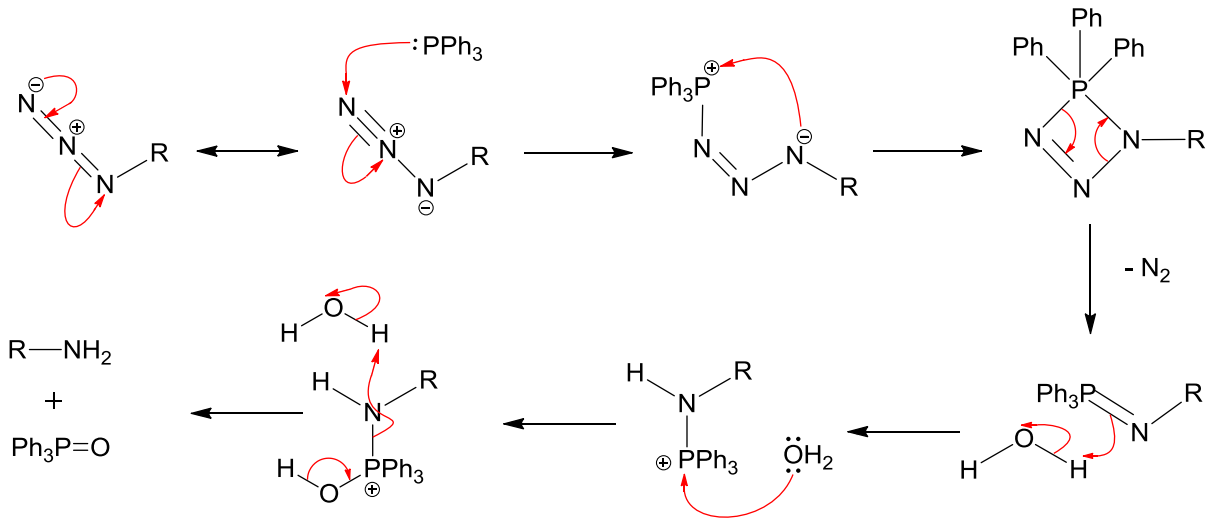

Scheme 2.7. The general mechanism of the Staudinger reaction.

Amine **46** was next reacted with hexacosanoyl chloride **47** in the presence of NEt_3 to give protected α-GalCer **62** in 85% yield (Scheme 2.8). The acid chloride was freshly prepared from hexacosanoic acid with oxalyl chloride in the absence of solvent, and could be used without purification.

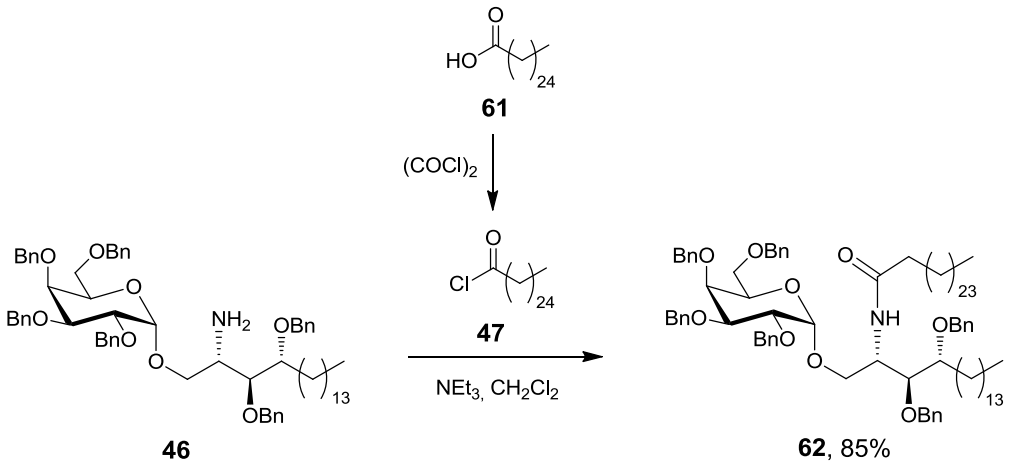

Scheme 2.8. Synthesis of amide **62**.

Finally, hydrogenolysis of the benzyl groups in the presence of palladium over charcoal afforded the desired product **8** in 68% yield (Scheme 2.9). We modified the literature conditions of this debenzylation reaction,[104] with THF being used as the solvent instead of the reported CH_2Cl_2/EtOH. Reaction in THF led to a much faster reaction, which was usually complete within 24 hours. In contrast, reaction in CH_2Cl_2/EtOH was very slow, with benzylated material still present even after 72 hours. Moreover, with this solvent system, the reaction mixture required repeated filtration followed by addition of "fresh" catalyst to achieve complete removal of the benzyl protecting groups.

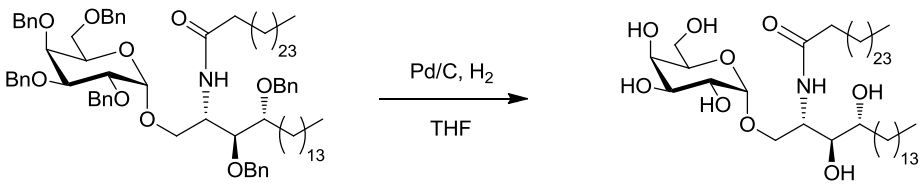

62 **8**, 68%

Scheme 2.9. Hydrogenolysis of **62** led to target compound **8**.

Having prepared the advanced intermediate, amine **46**, and successfully used it to synthesise our first target compound – α-GalCer **8**, we were ready to move on to our target α-GalCer analogues. Although we had not encountered any major problems in the synthesis of α-GalCer, we felt further improvements might still be made, particularly to the final deprotection step in the synthesis.

2.6. Thioamide analogue

With α-GalCer **8** in hand, three steps were required to access the desired thioamide **35** (Scheme 2.12). The key step in this synthesis would involve thionation of the amide and we chose to investigate Lawesson's reagent **63** as a thionating agent in the first instance. Lawesson's reagent[109] is widely used for converting carbonyl compounds such as amides, ketones, lactams and lactones into their thiocarbonyl analogues.[110,111] The reaction proceeds under mild conditions and is now generally preferred over the use of phosphorus pentasulfide (P_2S_5), which requires boiling toluene, pyridine or xylene as solvent, a large excess of the thionating agent and long reaction times.[109,112]

The mechanism of the thionation reaction using Lawesson's reagent **63** is depicted in Scheme 2.10. Lawesson's reagent is in equilibrium with a highly reactive dithiophosphine ylide, which reacts with a carbonyl-containing compound to form a thiaoxaphosphetane.[110] The driving force for the reaction involves the formation of a stable P=O bond in the final cycloreversion step, which is similar to the Wittig reaction.

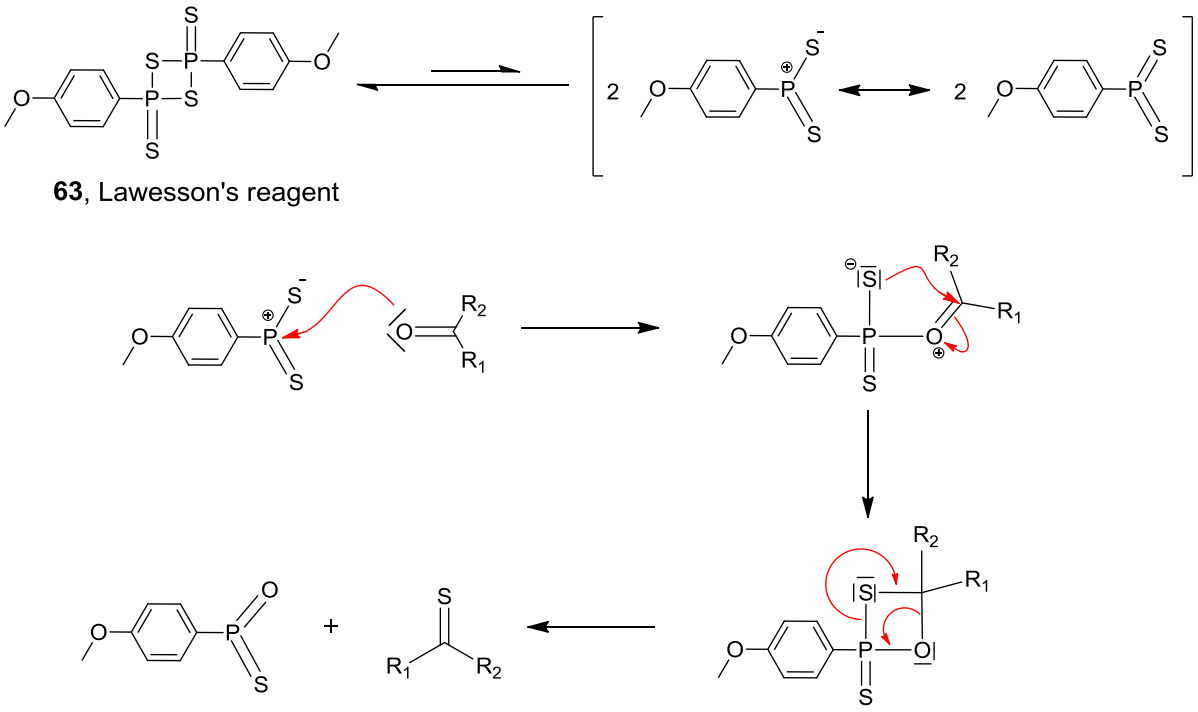

Scheme 2.10. Mechanism of the thionation reaction using Lawesson's reagent.

There are very few examples of direct thionation of amides in the presence of free hydroxyl groups. Nishio *et al.* investigated the thionation of β-, δ-, and κ-hydroxy amides **64**, **67** and **70**, respectively, with Lawesson's reagent.[113-115] Various products were formed in all three cases, including α-β-unsaturated thioamide **65**, mercaptoamide **66**, thiopheneimine **68** and thiones **69** and **71** (Scheme 2.11).

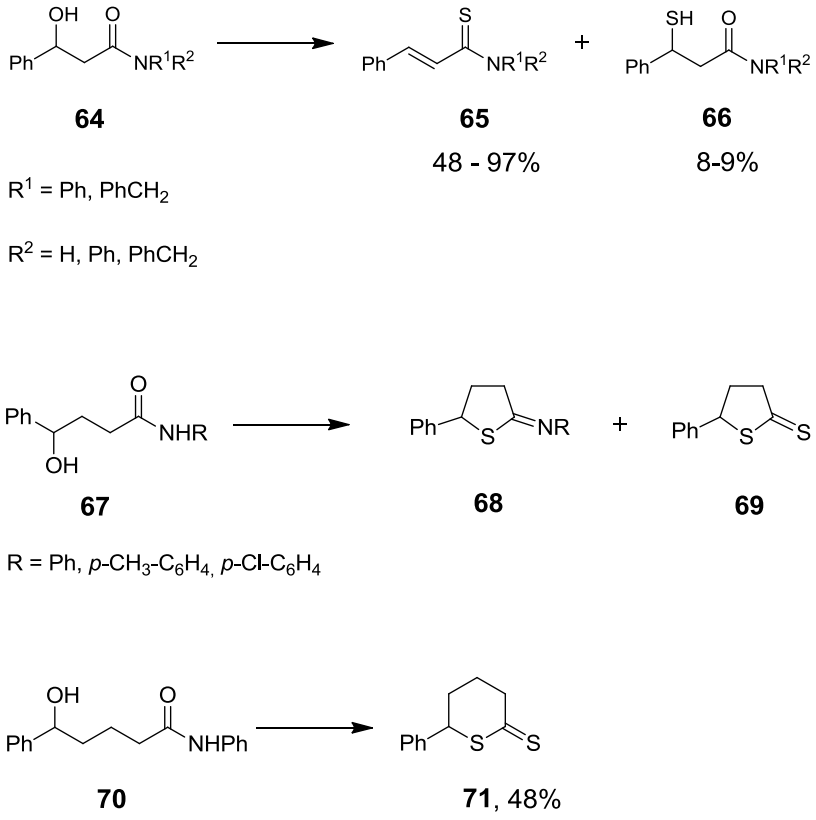

Scheme 2.11. Reaction of β-, γ- and κ-hydroxy amides with Lawesson's reagent.

In light of these results, we were not surprised to observe that performing the thionation of α-GalCer **8** without protecting the hydroxyl groups, resulted in the formation of a range of products. A large amount of unreacted starting material was also present in the reaction mixture, probably owing to the low solubility of the starting material in toluene. Moreover, separating the small amounts of the desired thioamide **35** from the excess of unreacted **8** proved to be difficult owing to their similar behaviour on silica.

A more effective synthesis of thioamide **35** is outlined in Scheme 2.12. We first decided to protect the hydroxyl groups in **8** as acetates, expecting only the amide

group would react with the Lawesson's reagent at 80 ºC in toluene. Thionation of esters is possible using Lawesson's reagent, but the reaction is usually performed in xylene at 140 ºC.[116] Peracetylation of α-GalCer afforded **72** in 94% yield. We were pleased to observe that reaction of **72** with one equivalent of Lawesson's reagent in toluene at 80 ºC for four hours afforded thioamide **73** in 85% yield. Deprotection of the acetyl groups under Zemplén conditions afforded thioamide **35** in 90% yield.

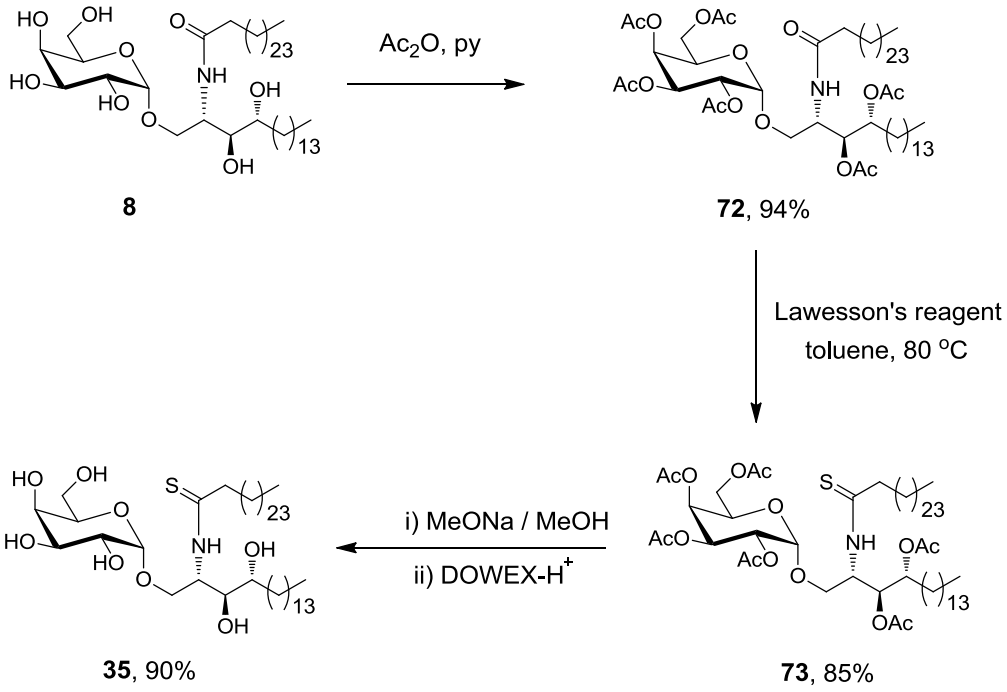

8 **72**, 94% **73**, 85% **35**, 90%

Scheme 2.12. Synthesis of thioamide analogue **35**.

2.7. Synthesis of urea analogue of α-GalCer

Formation of the urea analogue **36** from amine **46** required the synthesis of an appropriate isocyanate. We envisaged this would be accessed by a Curtius rearrangement on the corresponding acid azide.[117,118] Use of hexacosanoic acid **61** as the starting point would lead to a urea product containing 27 atoms (26 carbons and one nitrogen) in the acyl chain. Since CD1d does not readily accommodate acyl chain lengths longer than the C26 chain found in α-GalCer,[119] we chose to start with tetracosanoic acid **74** as this would be processed through to a urea product containing 25 atoms in the acyl chain (24 carbons and one nitrogen). Since the α-GalCer analogue containing a C_{24} acyl chain displays similar biological activity to α-GalCer **8**,[68] we expected any differences in biological activity between a urea analogue containing 25 atoms in the acyl chain (*i.e.* **36**), and α-GalCer **8**, would be attributable to an amide-urea switch and not a result of the slightly truncated acyl chain.

The preparation of isocyanate **48** and urea analogue **36** is summarised in Scheme 2.13. Conversion of the starting tetracosanoic acid **74** to the corresponding acid chloride **75** using the $(COCl)_2$ procedure,[120] followed by treatment with NaN_3 led to the acid azide **76**,[121] which underwent Curtius rearrangement[121] on heating in toluene at reflux for four hours to provide the desired isocyanate **48**. These three steps were performed as a sequence on the same day, without purification of any intermediates to minimise their possible decomposition. Crude isocyanate **48** was

reacted with amine **46** to provide urea **77** in 68% yield (Scheme 2.13). The product was characterised by HRMS and the quaternary resonance corresponding to the carbonyl C=O of the urea was observed at δ 158.8 ppm in the ^{13}C NMR spectrum. The IR spectrum also showed a C=O stretch at 1670 cm^{-1}, providing further evidence of successful functionalisation of amine **77**. Hydrogenolysis of the benzyl groups in urea **77** under our standard conditions, effected global deprotection and afforded our next target, urea **36**.

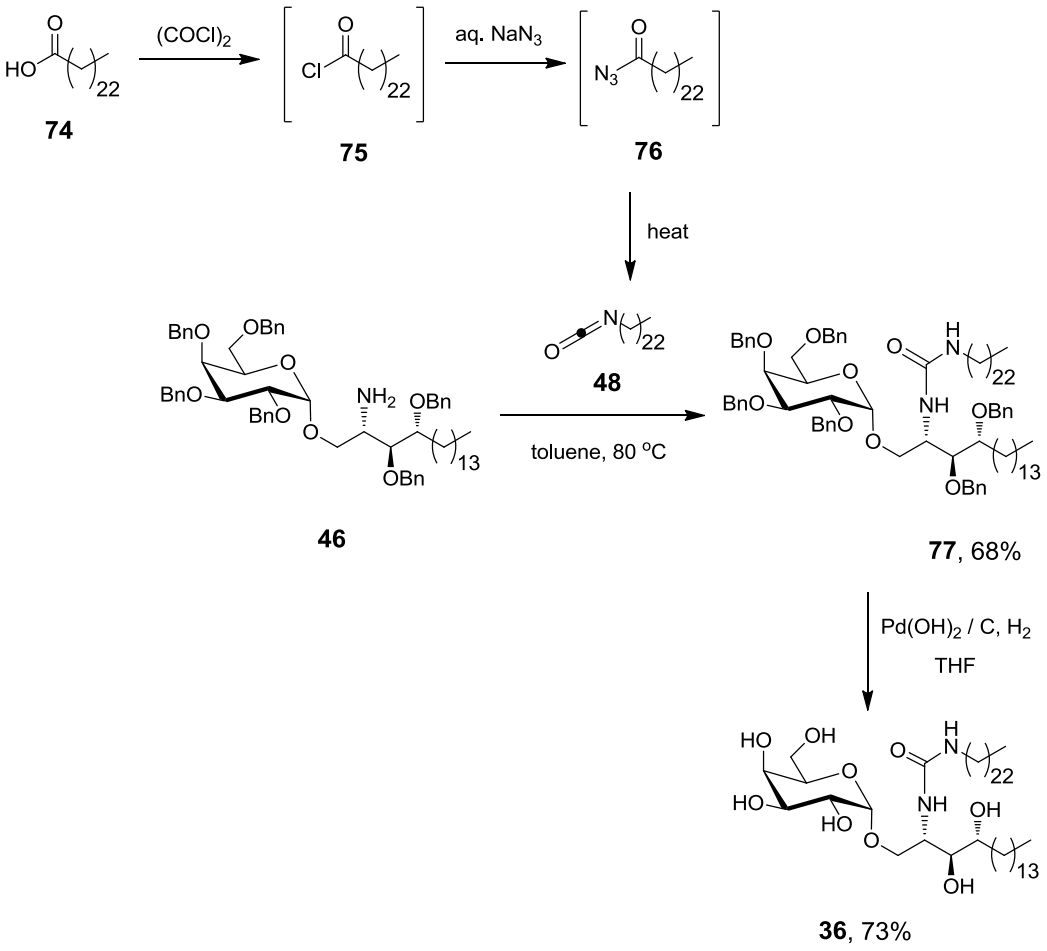

Scheme 2.13. Synthesis of urea analogue **36**.

2.8. Second-Generation Synthesis of α-GalCer

Whilst benzyl ethers are very commonly employed as protecting groups, particularly in carbohydrate chemistry, conformational effects can mean that some groups are particularly stubborn to remove under hydrogenolysis conditions. Indeed, this proved to be the case with one of the benzyl ethers in the phytosphingosine unit of amide **62** and urea **77**. Debenzylation was often slow, and frequently required filtration of the reaction mixture and addition of fresh catalyst to effect complete removal of all benzyl protecting groups.

We envisaged that we could facilitate the hydrogenolysis step in our synthesis by finding alternative protecting groups for the two secondary alcohols in the phytosphingosine acceptor. To this end, we chose to investigate a modified phytosphingosine acceptor **78** in our glycosylation. Whilst the use of an acetal to protect the internal 1,2-diol in our phytosphingosine acceptor would likely necessitate a two-step deprotection *post* glycosylation, we expected the debenzylation step would be easier, and no problems with a late-stage acetal hydrolysis. Moreover, this additional deprotection step would be mitigated by a more straightforward two-step synthesis of acceptor **78** from phytosphingosine **58** (Scheme 2.14),[55,90] compared with the three-step synthesis required to access dibenzyl ether **52**.[96]

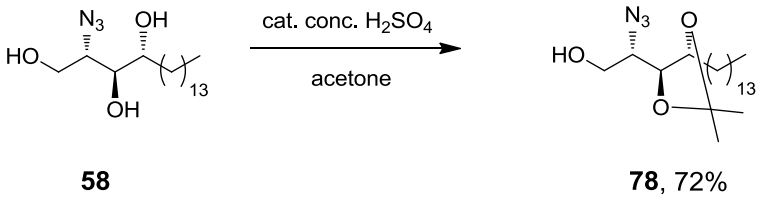

58 **78**, 72%

Scheme. 2.14. Synthesis of modified acceptor **78**.

Although the choice of donor/acceptor pairs can impact on the stereoselectivity of glycosylation reactions, we were pleased to observe that galactoside **79** could be accessed in similarly good yield and once again with complete α-stereoselectivity under our optimised conditions (Scheme 2.15). As an unexpected bonus, purification of **79** proved to be less laborious than for **50**, and probably goes some way to accounting for the slightly higher (71%) isolated yield of the product. The product was confirmed by HRMS and the characteristic α-anomeric proton in the ^{1}H NMR spectrum at 4.93 ppm, which appeared as a doublet with a small coupling constant (1H, d, $J_{1,2}$ 3.6 Hz, H-1'). The characteristic α-anomeric carbon resonance at 98.8 ppm in the ^{13}C NMR spectrum provided further diagnostic data.

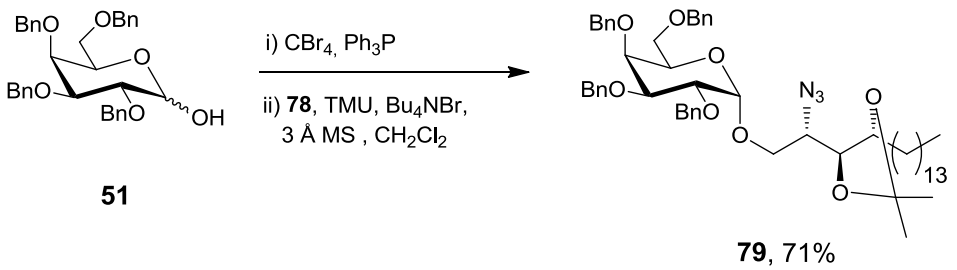

51 **79**, 71%

Scheme 2.15. Synthesis of galactoside **79** with modified acceptor **78**.

Staudinger reduction provided amine **80**, which was acylated, as before, to provide amide **81** (Scheme 2.16). In the next step, the acetal protecting group was hydrolysed with TFA and after evaporation of the volatiles from the reaction mixture, the crude diol product was debenzylated to provide α-GalCer **8**. As expected, hydrogenolysis of four instead of six benzyl ether groups proved to be much faster, taking eight hours instead of the 22 hours required to debenzylate **62**.

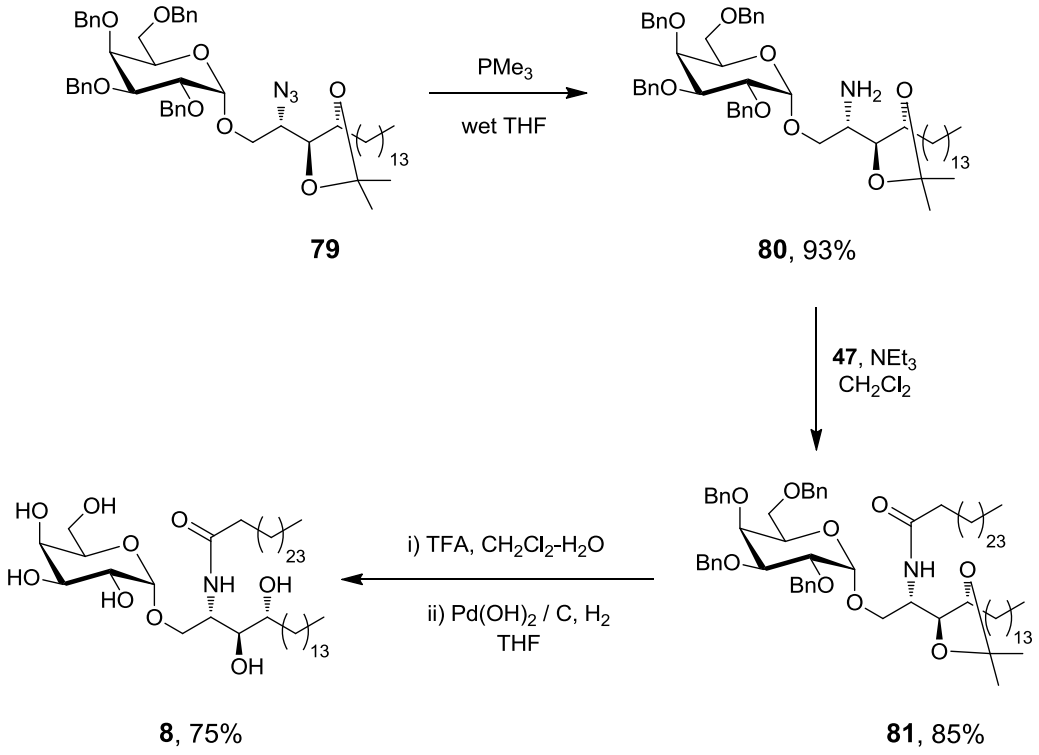

79 **80**, 93%

8, 75% **81**, 85%

Scheme 2.16. Second-generation synthesis of α-GalCer **8**.

2.9. Synthesis of carbamate analogue of α-GalCer

Carbamates are traditionally prepared either by functionalisation of an alcohol with an isocyanate, or by reacting an amine with a chloroformate or synthetic equivalent. Chloroformates are moisture-sensitive, and their preparation requires reaction of an alcohol with difficult-to-handle and highly toxic phosgene or slightly less dangerous triphosgene. We therefore chose to investigate an alternative approach reported by Ghosh *et al.*[122] In this report, Ghosh showed that alcohols react with commercially available *N*,*N*'-disuccinimidyl carbonate in the presence of triethylamine to afford stable and easy-to-handle mixed carbonates, which can then be reacted with an amine to provide the corresponding carbamate.

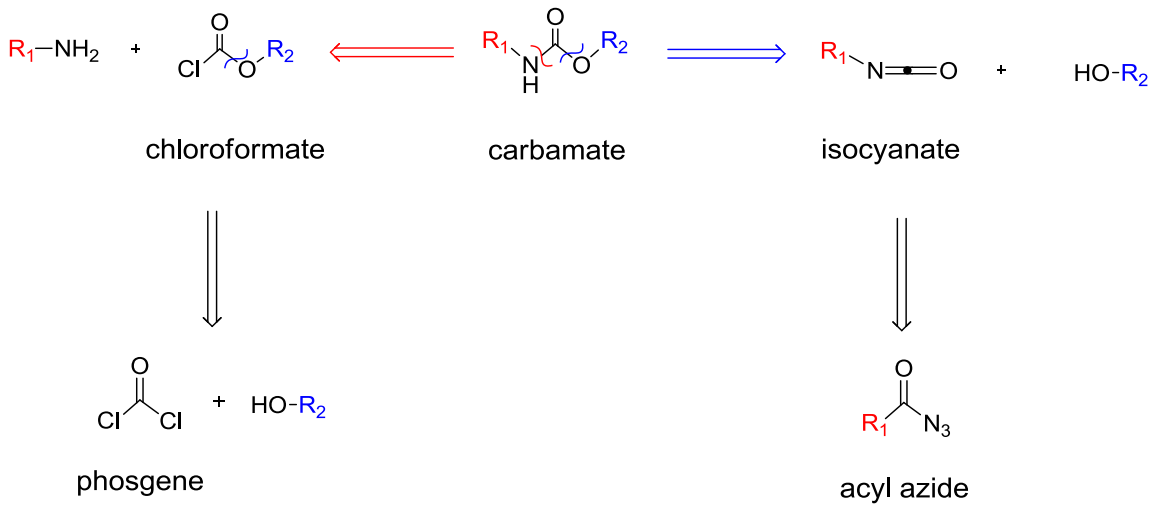

Scheme 2.17. Retrosynthetic analysis for carbamate.

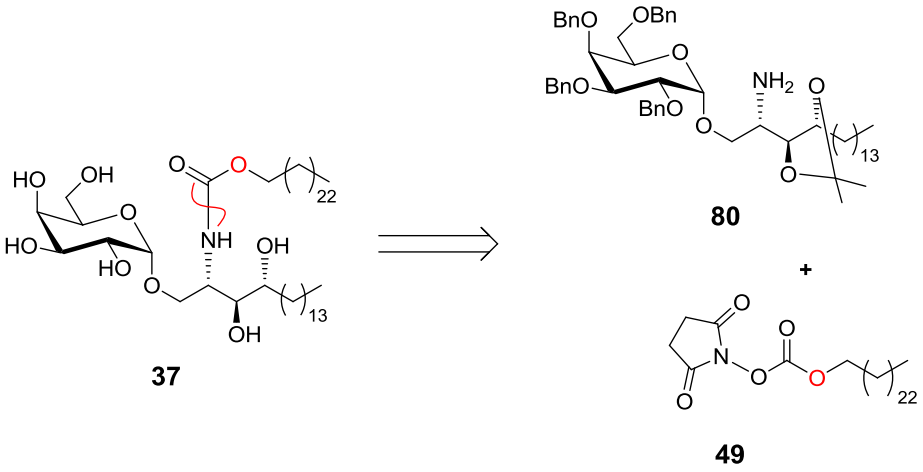

Scheme 2.18. Retrosynthetic analysis of **37**, the carbamate analogue of α-GalCer.

Our next target was the carbamate analogue of α-GalCer **37** (Scheme 2.18). To maintain the optimum length of 26 atoms in the lipid tail, our carbamate analogue required a 24-carbon alkyl chain. We therefore started from tetracosanoic acid **74**, which was reduced to alcohol **82** with $LiAlH_4$ in THF at reflux (Scheme 2.19). Reaction of 1-tetracosanol with 1.5 equivalents of *N*,*N*'-disuccinimidyl carbonate **83** in the presence of 2.5 equivalents of triethylamine afforded mixed carbonate **49** in almost quantitative yield. The product was characterised by HRMS. Further evidence came from the ^{13}C NMR spectrum, which showed a quaternary carbon resonance characteristic for the carbonate carbonyl group at δ 151.6 ppm in addition to a resonance at δ 168.7 ppm corresponding to the imide carbonyls. Mixed carbonate **49** was then reacted with amine **80**, to provide carbamate **84** in very good yield (Scheme 2.19). Formation of the product was confirmed by HRMS and by the chemical shift of the quaternary carbon in the ^{13}C NMR spectrum, which appeared at δ 159.9 ppm. The IR spectrum also showed a C=O stretch at

1689 cm^{-1} as further evidence of carbamate formation. Finally, the protecting groups in carbamate **84** were removed uneventfully in a two-step acetal hydrolysis / debenzylation sequence to provide our final target **37** (Scheme 2.19).

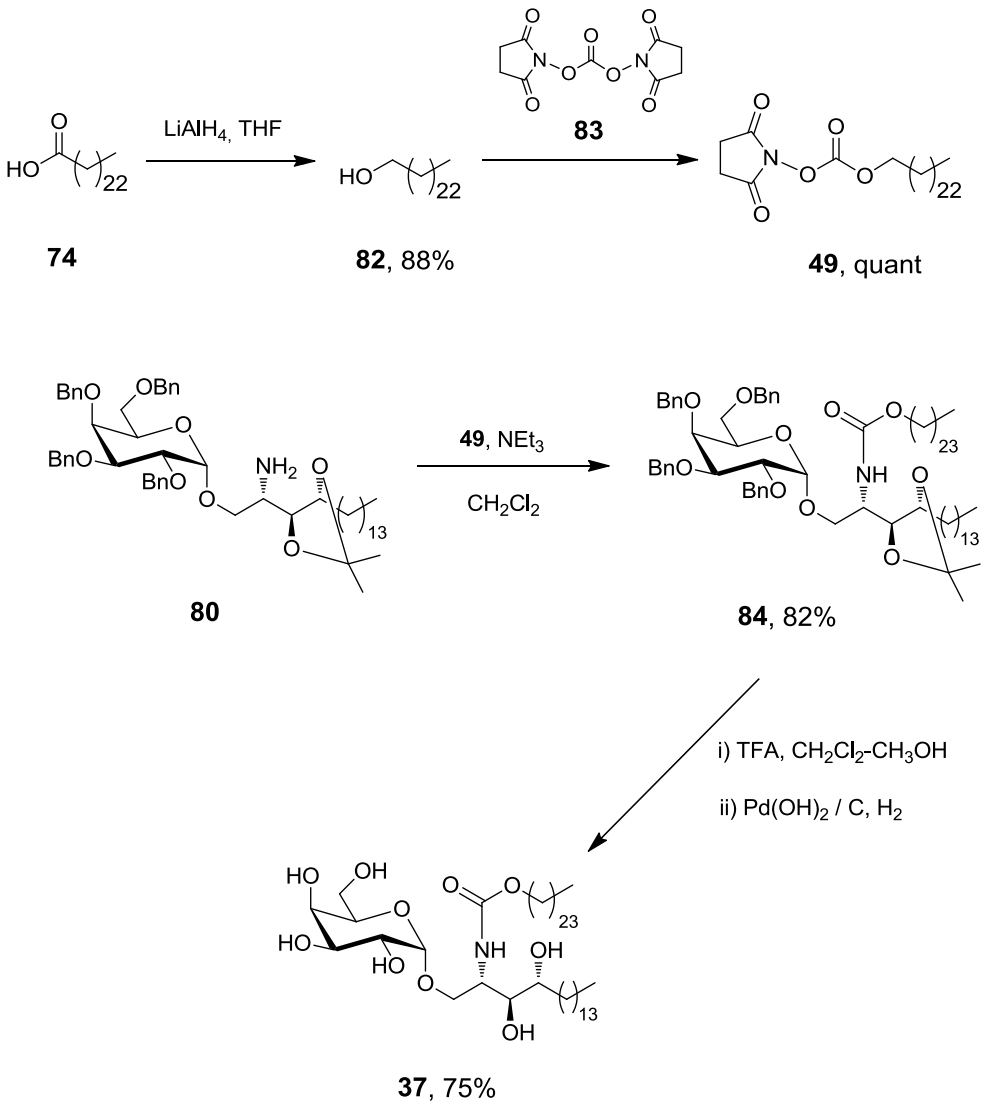

Scheme 2.19. Synthesis of carbamate **37**.

2.10. Synthesis of Threitol Ceramide

Threitol ceramide (ThrCer) **24** is a non-glycosidic analogue of α-GalCer (described previously in Chapter 1.7.2.3). Like α-GalCer, it does not display a biased Th1/Th2 cytokine response and compared with α-GalCer, it is a less potent agonist of CD1d; however it successfully activates iNKT cells without causing their overstimulation, thereby overcoming the problematic iNKT cell activation-induced anergy associated with α-GalCer.[123]

The synthesis of ThrCer **24** has been recently reported by Reddy *et al.*[70] and by our research group.[124] The protecting group strategy employed in both these approaches is slightly different to the synthetic route we chose to follow. We envisaged ThrCer and its three analogues would again be accessed from a common precursor amine **85**, which could then be functionalised in the same fashion as for the α-GalCer series (Scheme 2.20). Amine **85** would be accessed from the corresponding azide **86**, which can be further disconnected to the previously prepared primary alcohol **78** (the acceptor in our improved second-generation glycosylation reaction) and commercially available (+)-2,3-*O*-isopropylidene-L-threitol **88**.

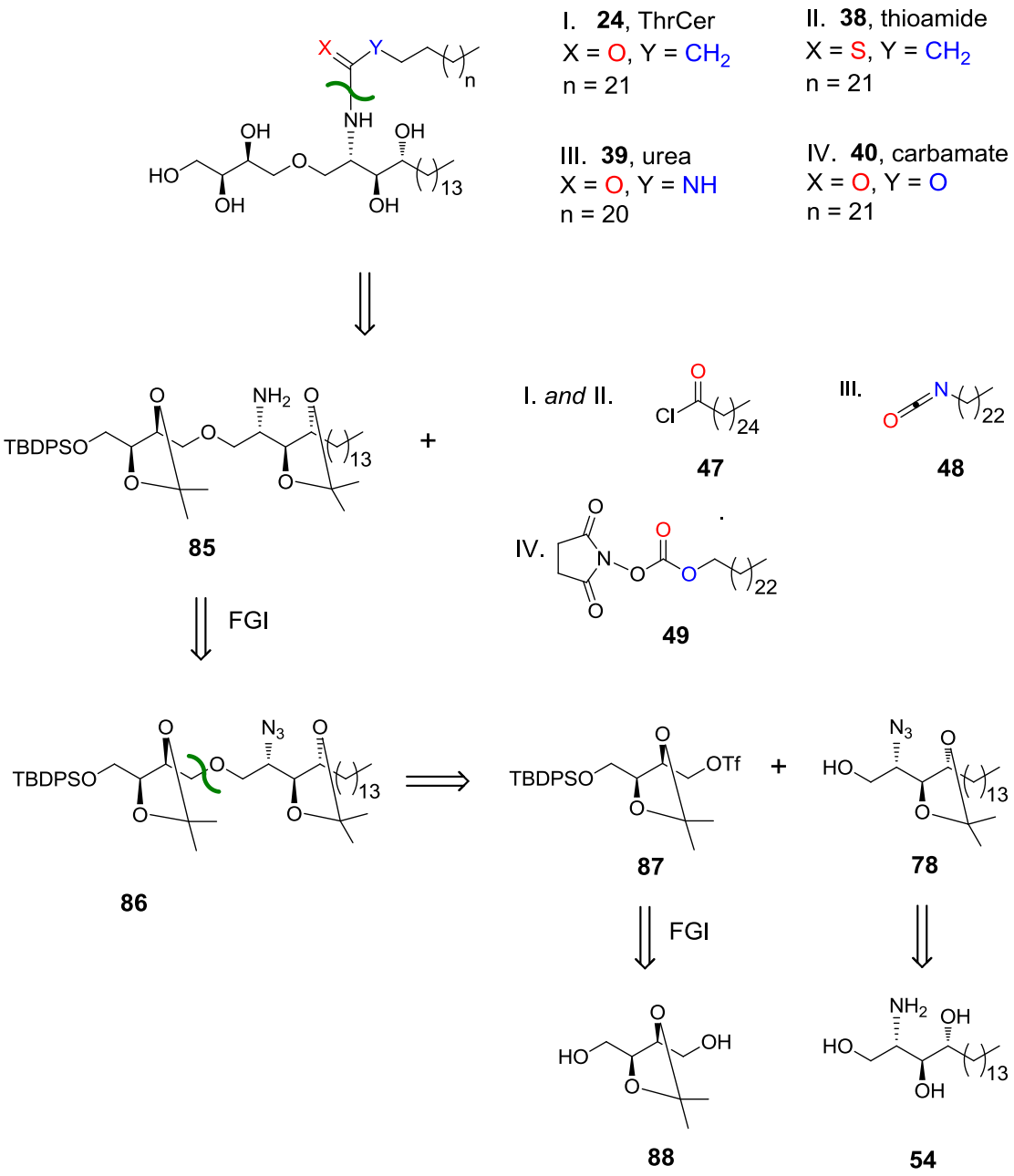

Scheme 2.20. Retrosynthetic analysis of ThrCer **24** and its analogues, thioamide **38**, urea **39** and carbamate **40**.

The protecting groups in the azide **86** were carefully selected to provide an intermediate suitable for the synthesis of ThrCer and its three analogues. Reddy *et al*.[70] used a similar azide **89** in their synthesis of ThrCer, only the primary alcohol on the threitol moiety was protected as a benzyl ether, whilst in our previous report, the same primary alcohol was protected with a bulky TBDPS silyl ether, and the internal 1,2-diol of the threitol unit as a benzylidene acetal **90**.

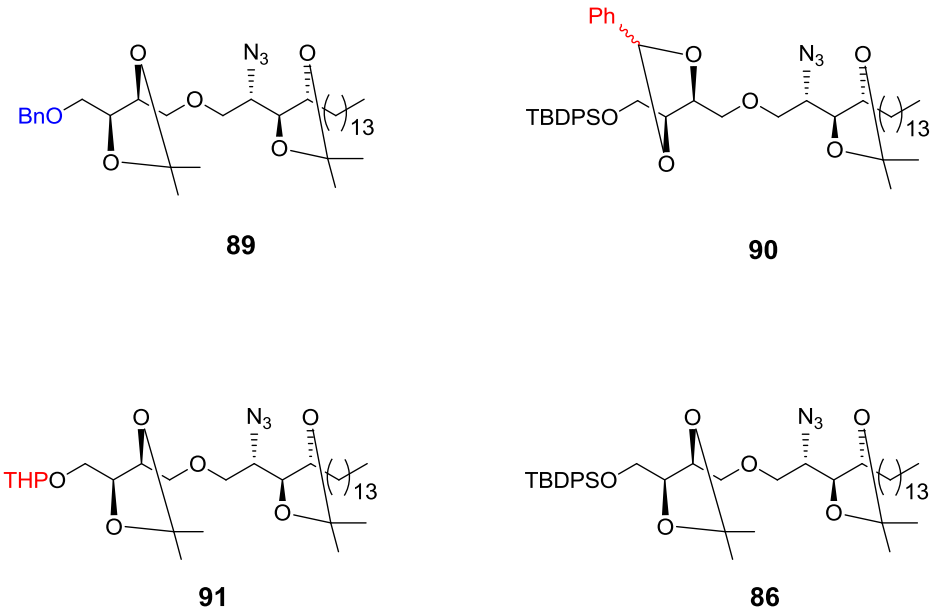

Scheme 2.21. Comparison of protecting group strategy employed in the synthesis of ThrCer.

In our approach, deprotection of all five hydroxyl groups was envisaged as the last step of the synthesis. We wanted to avoid benzyl ethers as these usually require a hydrogenolysis deprotection step, which would prevent us from incorporating

unsaturated acyl chains. We also wanted to protect the two 1,2-diols as isopropylidene acetals and avoid a benzylidene acetal, as this introduces an additional stereocentre, which would render characterisation of the resulting products more difficult. We first considered protecting the primary alcohol of threitol as its tetrahydropyranyl ether **91**, as this would allow us to perform a deprotection of all five hydroxyl groups in a single step; however, like for the benzylidene acetal, the THP-protected derivatives would likely result in diastereoisomeric mixtures. We therefore opted for a bulky TBDPS silyl ether in azide **86**. Whilst this protecting group would entail a two-step deprotection sequence, it might be advantageous to employ an orthogonal protecting group, should we wish to selectively functionalise the primary alcohol of the threitol moiety at a later date.

The synthesis of our precursor amine **85** is summarised in Scheme 2.22. Starting from commercially available (+)-2,3-*O*-isopropylidene-L-threitol **88**, reaction with equimolar quantities of *t*BuPh$_2$SiCl afforded the corresponding mono-silyl ether **92**, which was further reacted with triflic anhydride in pyridine to provide triflate **87**. This intermediate served as our electrophilic coupling partner for an etherification with nucleophilic coupling partner **78**, which was the acceptor we had employed previously in our second-generation glycosylation reaction (see Section 2.9 of this Chapter).

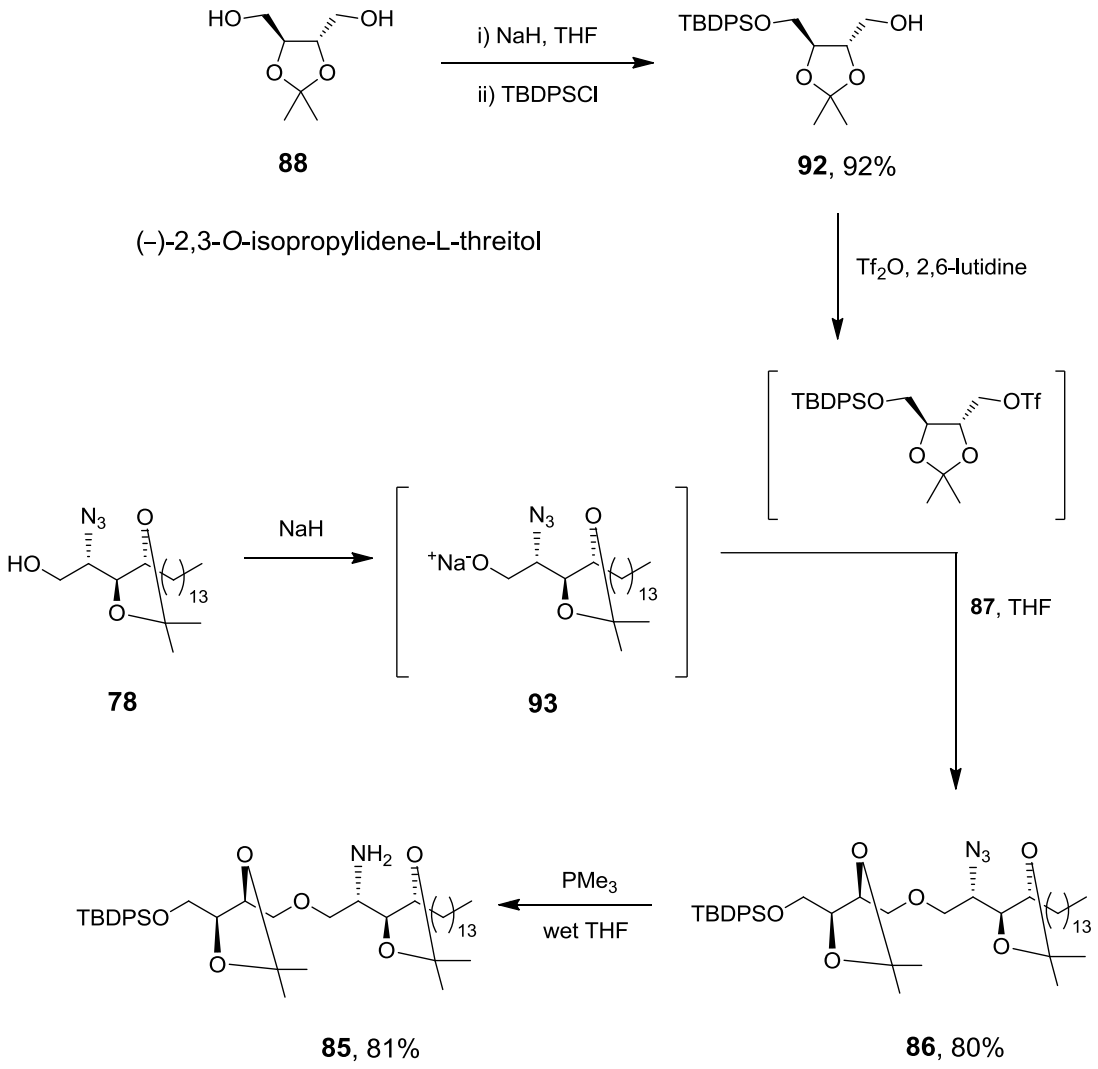

Scheme 2.22. Synthesis of the advanced intermediate amine **85**.

Treatment of alcohol **78** with NaH afforded the corresponding sodium alkoxide **93**, which underwent smooth reaction with triflate **87** to provide the desired ether **86** in 80% yield.[124] Staudinger reduction of the resulting azide using PMe_3[94] provided amine **85** (Scheme 2.22), and thence straightforward access to ThrCer and its three analogues, using the same approaches that were developed for the thioamide **35**, urea **36** and carbamate **37** analogues of α-GalCer.

The synthesis of ThrCer **24** is summarised in Scheme 2.23. Amine **85** was first *N*-acylated with hexacosanoyl chloride **47** to provide amide **94**. The product **94** was confirmed by HRMS. Key spectroscopic signals included the amide carbonyl stretch in the IR spectrum at 1646 cm^{-1}. The amide functionality was further evidenced in the ^{13}C NMR spectrum, which showed the characteristic quaternary carbon environment of a carbonyl at δ 172.4 ppm. In the next steps, silyl ether deprotection with TBAF, followed by acid-catalysed hydrolysis of the acetals provided our target molecule ThrCer **24** as confirmed by HRMS. Analysis of the ^{1}H- and ^{13}C NMR spectra also confirmed the successful removal of the TBDPS silyl ether and two acetals. The IR spectrum showed the OH stretch as further evidence of hydroxyl groups.

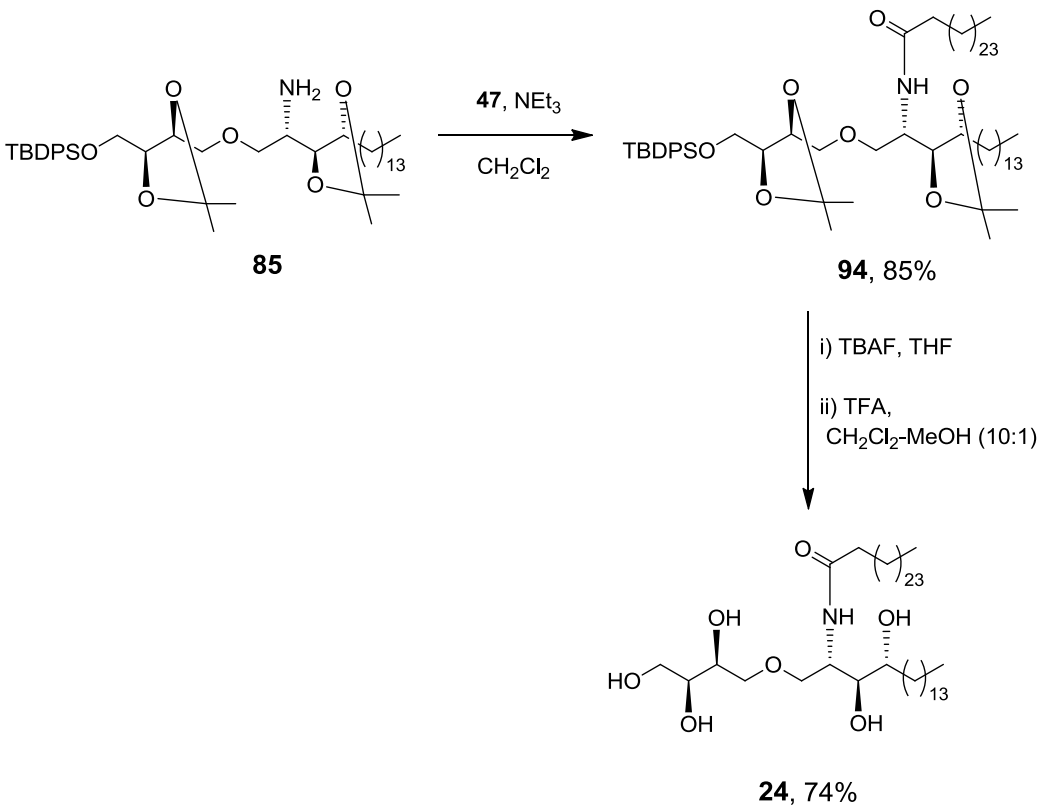

Scheme 2.23. Synthesis of ThrCer **24**.

2.11. Synthesis of thioamide analogue of ThrCer

Scheme 2.24 presents the synthesis of the thioamide **38** analogue of ThrCer, which was prepared in the same fashion as the thioamide analogue of α-GalCer **35** (Chapter 2.6). ThrCer **24** was first peracetylated to give **95**, which underwent thionation, using Lawesson's reagent, to provide thioamide **96** in good yield. Acetate deprotection with sodium methoxide in methanol provided our target compound **38**.

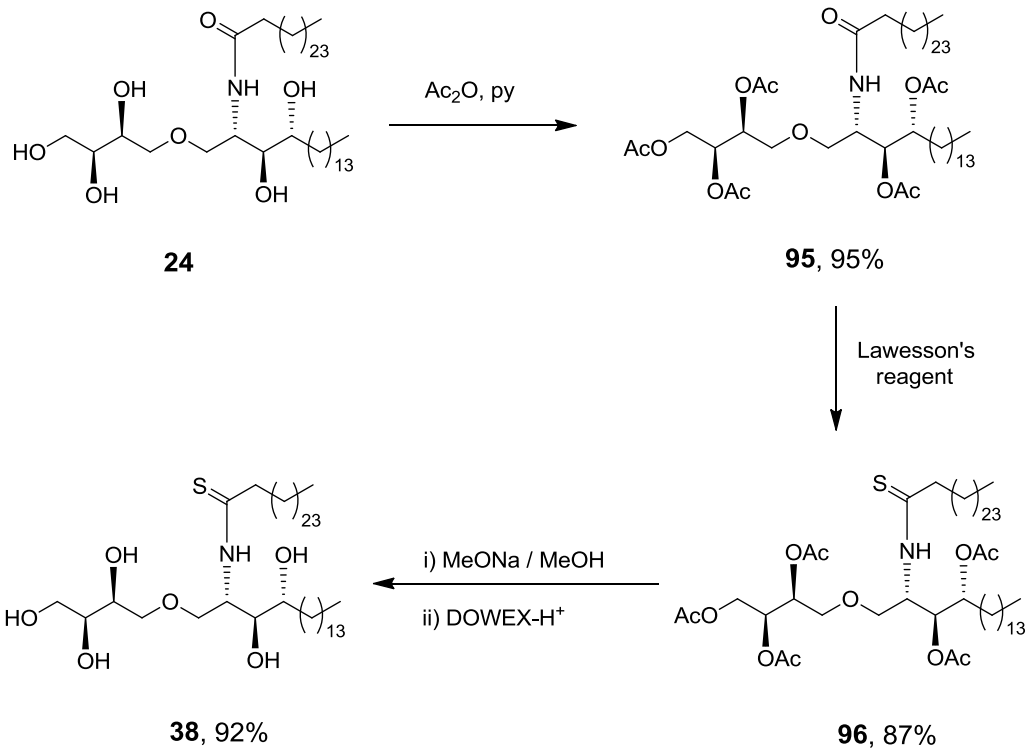

Scheme 2.24. Synthesis of the thioamide analogue of ThrCer **38**.

We also wanted to investigate an alternative approach to thioamide **38**, and perform thionation on the early-stage intermediate amide **94** to minimise handling of the fully deprotected ThrCer **24**. Our alternative approach is summarised in Scheme 2.25. We were pleased to observe that thionation of amide **94** proceeded uneventfully. The product **97** was confirmed by HRMS and spectroscopic data, which provided evidence for the thiocarbonyl C=S group in the ^{13}C NMR spectrum at δ 205.5 ppm. Silyl ether deprotection, followed by hydrolysis of the two isopropylidene acetals, provided the final product **38**.

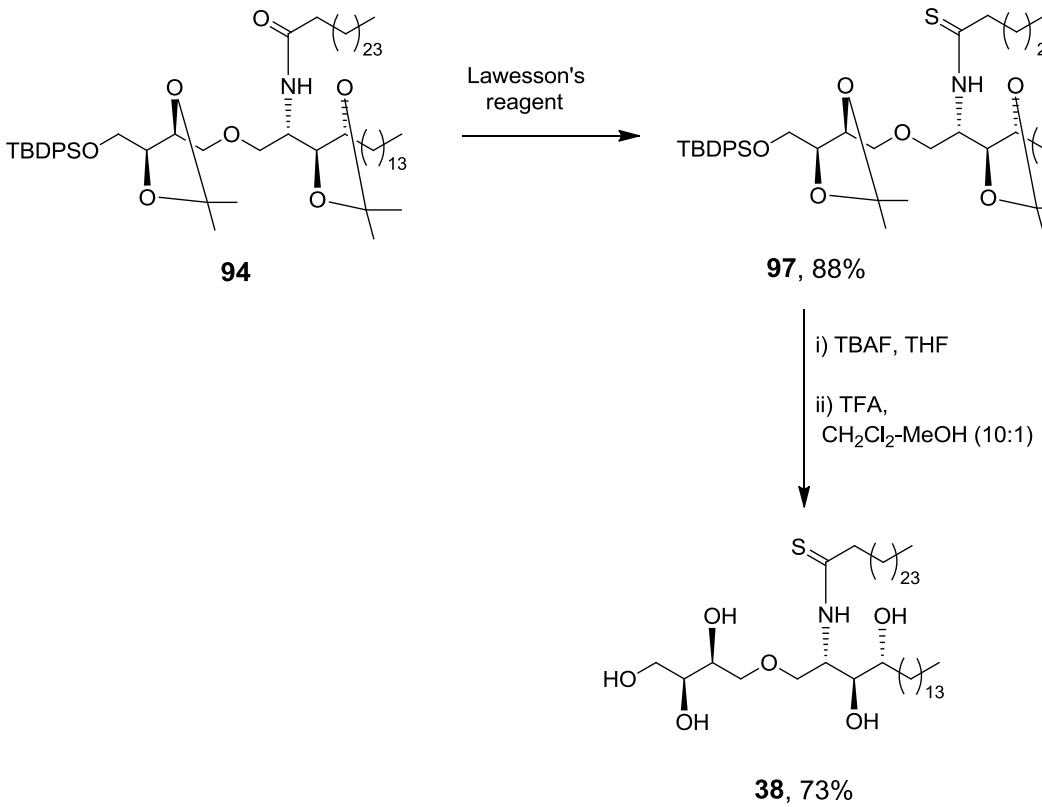

94

97, 88%

38, 73%

Scheme 2.25. Alternative synthesis of thioamide analogue of ThrCer **38** starting from amide **94**.

2.12. Synthesis of urea analogue of ThrCer

Reaction of amine **85** with tricosanyl isocyanate **48** (prepared as previously discussed in Chapter 2.7) in toluene at 80 ºC furnished urea **98**, which underwent our standard two-step deprotection sequence to afford urea analogue **39** in a satisfactory yield. This final compound was insoluble at r.t. in the chloroform / methanol mixture normally used to solubilise these glycolipids for NMR spectroscopic analysis. Fortunately, running the spectra at 40 ºC prevented product precipitation and allowed us to obtain good quality data

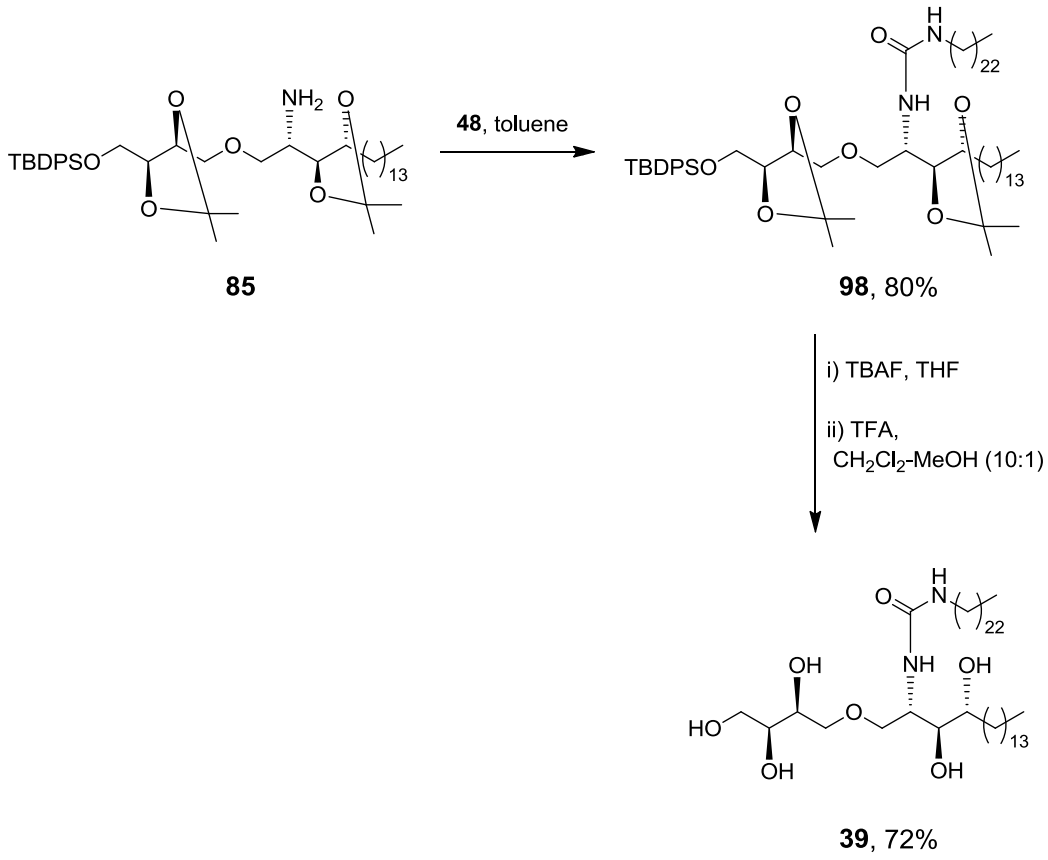

85 **98**, 80%

39, 72%

Scheme 2.26. Synthesis of **39**, the urea analogue of ThrCer.

2.13. Synthesis of carbamate analogue of ThrCer

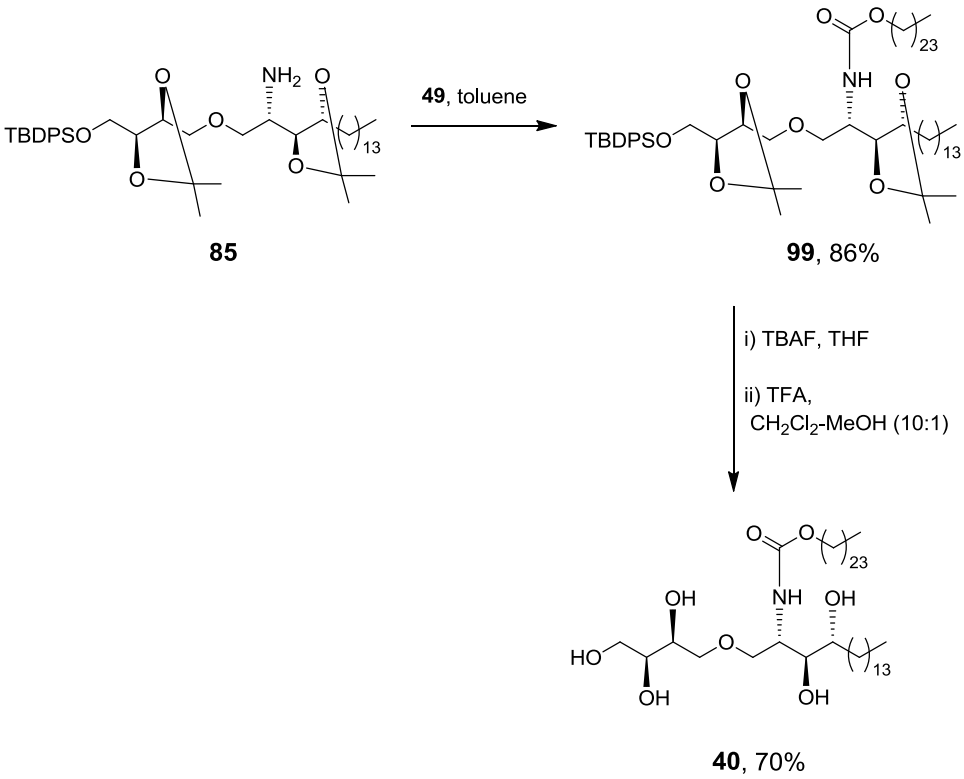

Scheme 2.27. Synthesis of carbamate analogue of ThrCer, **40**.

Treatment of amine **85** with the mixed carbonate **49** derived from the reaction of tetracosanoyl alcohol with *N*,*N*′-disuccinimidyl carbonate (discussed in Chapter 2.9), provided carbamate **99**. After aqueous work-up and silica column chromatography, the product was confirmed by HRMS. Formation of the carbamate function was further evidenced in the ^{13}C NMR spectrum, which revealed a quaternary carbon resonance at 156.0 ppm and a C=O stretch at 1687 cm^{-1} in the IR spectrum. Our standard two-step deprotection sequence provided

carbamate analogue **40**. Carbamate **40** was also found to precipitate from a 2:1 chloroform / methanol mixture at r.t. and ^{1}H- and ^{13}C NMR experiments were performed at 40 ºC in order to obtain good quality data.

Having prepared our target compounds **8**, **24**, **35**-**40**, these were next submitted for biological testing which was carried out in the group of Prof. Vincenzo Cerundolo by Dr John-Paul Jukes and Dr Hemza Ghadbane at the Weatherall Institute of Molecular Medicine in Oxford, UK.

2.14. Biological evaluation of glycolipid antigens: thioamide, urea and carbamate analogues of α-GalCer and ThrCer

In a preliminary screen, our newly synthesised α-GalCer and ThrCer thioamide, urea and carbamate analogues were tested for their ability to stimulate the iNKT cell hybridoma DN32[§], following pulsing of C1R-mCD1d[**] cells with various concentrations of ligands. The concentration of interleukin-2 (IL-2) in the supernatant, released after iNKT cell activation, was measured using an enzyme-linked immunosorbent assay (ELISA) (Figure 2.13 A, B).

Encouragingly, the results of these experiments demonstrated that ThrCer thioamide **38** and ThrCer carbamate **40** induced increased activation compared with ThrCer **24**; however the ThrCer urea analogue **39** led to weak stimulation (Figure 2.13 A). A similar hierarchy was observed for the α-GalCer analogues (Figures 2.13 B), although the differences, particularly at high concentration, were less pronounced (Figure 2.13 B).

[§] DN32 - the Vα14$^+$ NKT cell hybridoma cell lines.

[**] C1R-mCD1d - mouse CD1d-expressing C1R cells.

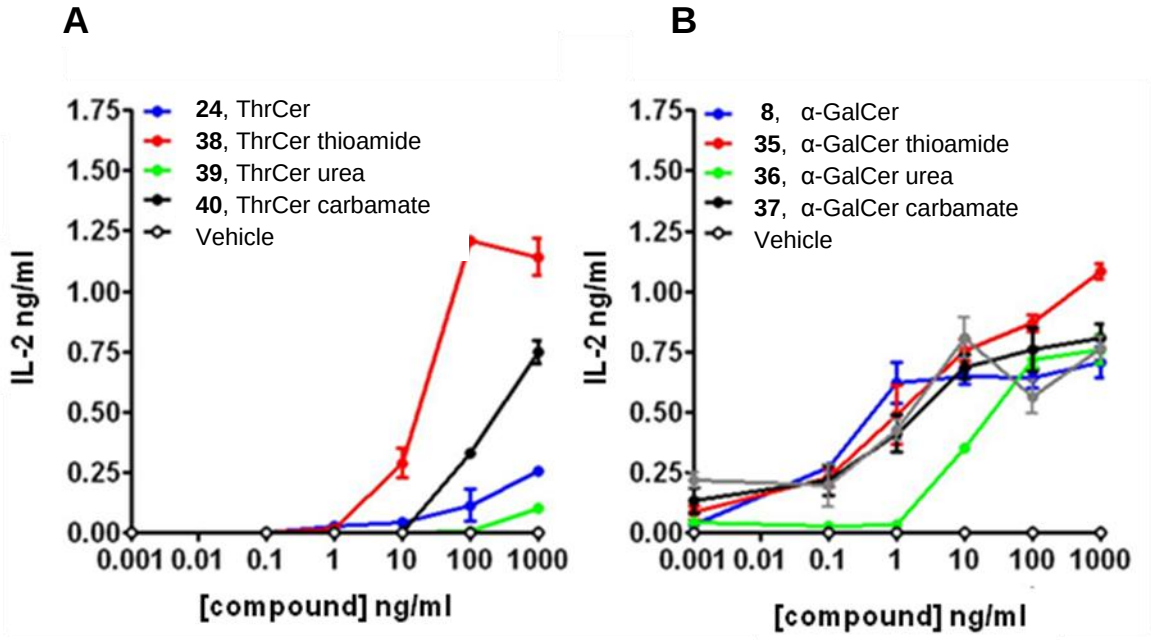

Figure 2.13. **Activation of murine iNKT cells using thioamide, urea and carbamate analogues of ThrCer and α-GalCer.** C1R-mCD1d cells were pulsed with various concentrations of ThrCer analogues (**A**) and α-GalCer analogues (**B**) as indicated and used to stimulate the DN32 hybridoma *in vitro*. The supernatants were tested for the presence of IL-2.

To confirm these findings, human iNKT cells were co-cultured for 40 hours with C1R-hCD1d cells that had been pulsed with 100 ng/ml, 10 ng/ml or 1 ng/ml vehicle, ThrCer **24**, ThrCer thioamide **38**, ThrCer urea **39**, ThrCer carbamate **40** (Figure 2.14 A) and α-GalCer **8**, α-GalCer thioamide **35**, α-GalCer urea **36**, α-GalCer carbamate **37** (Figure 2. 14 B). Cytokine production was again determined by ELISA. The ThrCer analogues stimulated human iNKT cells and in agreement with murine iNKT cell data, the weakest ligand at 100 ng/ml was ThrCer urea **39**, although in this experiment, both the ThrCer thioamide **38** and ThrCer carbamate

40 analogues were comparable to ThrCer **24** (Figure 2.14 A). All the α-GalCer analogues stimulated human iNKT cells showing almost the same activity at 100 ng/ml when compared with α-GalCer, while at 10 ng/ml they stimulated iNKT cells stronger than α-GalCer. Interestingly at that concentration α-GalCer thioamide analogue **35** was found to be 2-fold more potent than α-GalCer **8**. Unlike the ThrCer analogues, all three α-GalCer analogues **35**, **36** and **37** were active even at low concentrations (Figures 2.14 A, B).

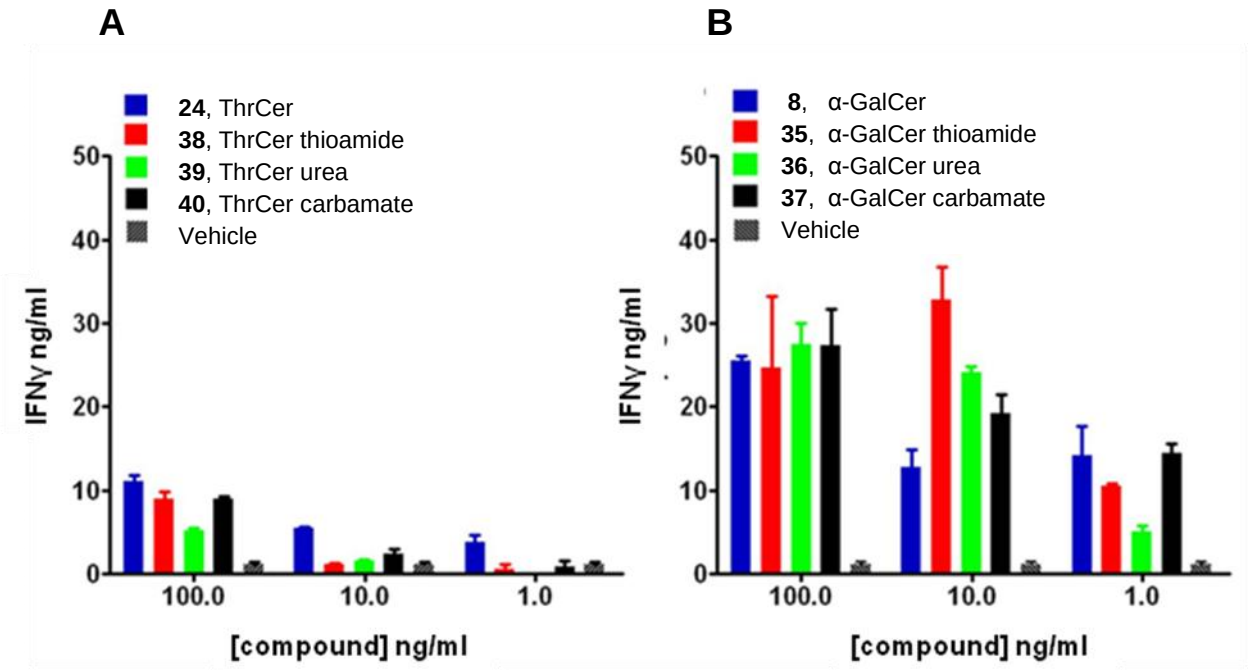

Figure 2.14. **Activation of human iNKT cells using thioamide, urea and carbamate analogues of ThrCer and α-GalCer.** C1R-hCD1d cells were pulsed with various concentrations of ThrCer analogues (**A**) and α-GalCer analogues (**B**) as indicated and used to stimulate human iNKT cells *in vitro*. The supernatants were tested for IFNγ.

Since the two urea derivatives **36** and **39** displayed the weakest activity in our *in vitro* experiments, further studies focused solely on the thioamide and carbamate derivatives of ThrCer and α-GalCer. These analogues were further investigated *in vivo*, alongside the parent compounds and Th2-biasing molecule OCH **13**,[62,125] specifically to assess their ability to effect DC maturation as well as their Th1/Th2 cytokine response profile. To this end, 1 μg lipid was injected intravenously into mice. After 2 h, the mice were tail-bled and IL-4 levels in the serum measured by ELISA (Figure 2.15). At 18 h, the mice were sacrificed and blood serum levels of IFNγ were measured by ELISA (Figure 2.15).

The *in vivo* experiments for the α-GalCer analogues show that the thioamide and carbamate derivatives, **35** and **37**, respectively, both display a slightly more Th1-biasing cytokine response than α-GalCer **8**, resulting from a reduction in IL-4 production relative to the parent α-GalCer **8**, rather than an increase in IFNγ production, which was similar to that generated by α-GalCer **8**. Results for the ThrCer derivatives were more interesting in that these displayed a similar but more pronounced trend. Compared with α-GalCer **8**, ThrCer **24** is a weaker activator of iNKT cells, although it displays a similar Th1-Th2 cytokine profile.[70,123] Very interestingly ThrCer thioamide **38** and ThrCer carbamate **40** displayed no IL-4 production, when assayed at 2 h; however they showed levels of IFNγ production at 18 h that were higher than those shown for ThrCer **24** and only four times lower than that displayed by α-GalCer **8**. Thus ThrCer analogues **38** and **40** appear to be promising Th1-biasing glycolipids.

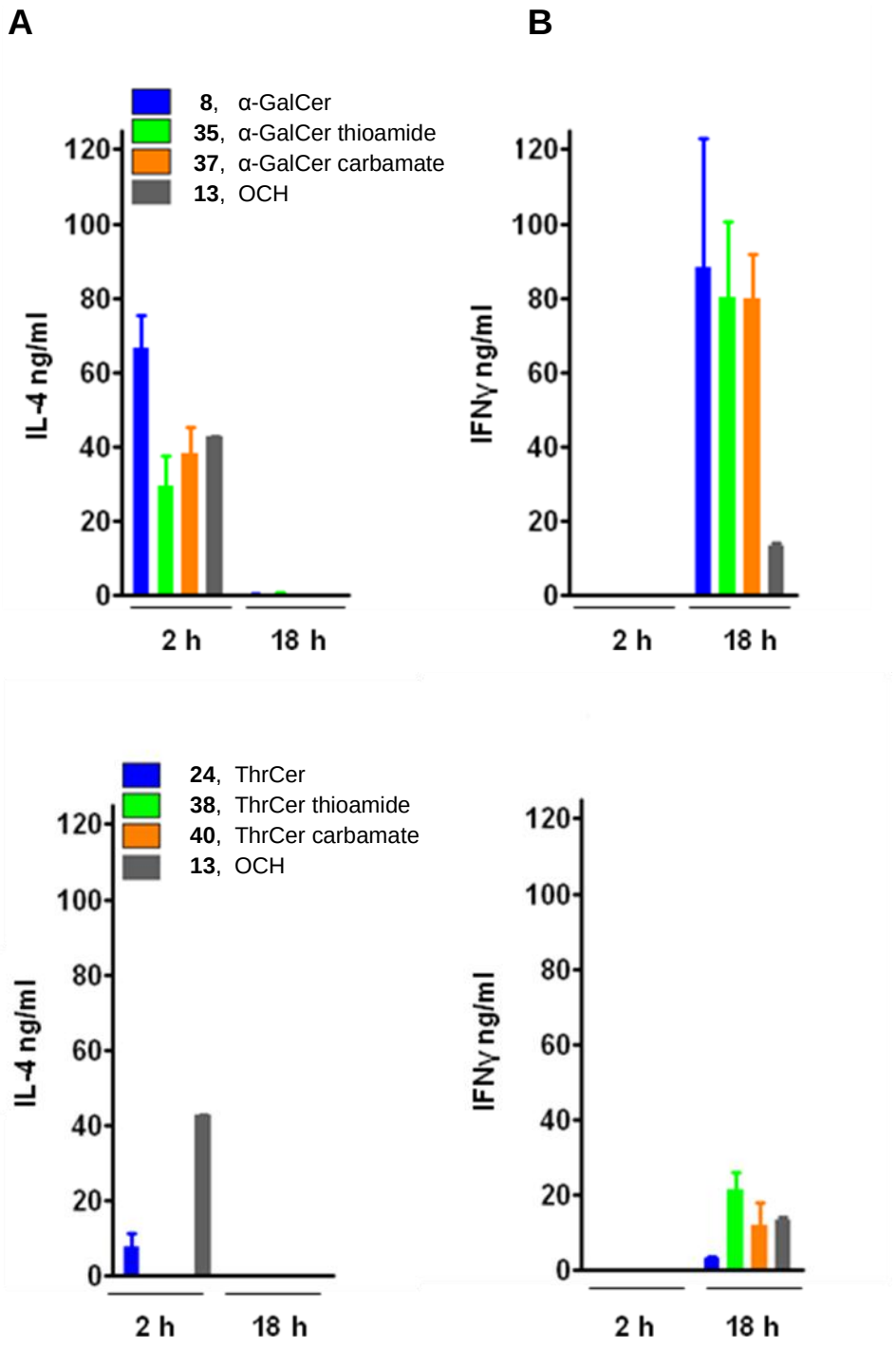

Figure 2.15. IL-4 and IFNγ levels in blood serum taken at the indicated times after injection of mice with glycolipid.

Finally, bacterially-expressed hCD1d and beta-2-microglobulin (β_2m) molecules were refolded with the thioamide, and carbamate analogues of both α-GalCer and ThrCer by oxidative refolding chromatography, and then biotinylated as described previously for use in surface plasmon resonance (SPR) experiments (BIAcore 3000 instrument).[36,126] The urea analogues of α-GalCer and ThrCer could not be refolded, so no SPR data are available for these analogues.

Soluble human iNKT TCR was prepared as described by McCarthy *et al*.[36] SPR experiments were used to measure the affinity and kinetics of human iNKT cell TCRs for hCD1d loaded with α-GalCer, ThrCer, and their thioamide and carbamate analogues (Figure 2.16). To this end, increasing concentrations of TCR were injected for 5 seconds over the indicated complex immobilised on the BIAcore chip until the specific binding reached its plateau. K_d and B_{max} were calculated by fitting the data using a non-linear regression binding kinetics model (GraphPad Prism) (Figure 2.16). Kinetic measurements for the k_{off} were calculated using BIAevaluation software kit; k_{on} values were calculated from the experimental k_{off} and K_d (Figure 2.16 C).

In terms of binding affinity of the TCR for glycolipid-loaded hCD1d, K_d values for the TCR–carbamate–hCD1d complexes in both series were comparable to those measured for the parent compounds. The iNKT TCR exhibited slightly lower binding affinity for hCD1d loaded with α-GalCer-thioamide **35** compared with hCD1d/ α-GalCer, whilst binding affinity for hCD1d loaded with ThrCer-thioamide **38** was interestingly an order of magnitude lower than that for hCD1d/ThrCer **24**. The binding kinetics experiment showed that these lower binding affinities are a

consequence of a faster off rate and a slower on rate of the TCR–thioamide–hCD1d complex compared to CD1d complexes with the parent molecules (Figure 2.16 C). This observation is comparable to the kinetics displayed by the Th2-biasing α-GalCer analogue, OCH **13**.[127] These iNKT cell TCR binding affinity data for the CD1d/glycolipid complexes do not show a clear correlation with the observed cytokine response.

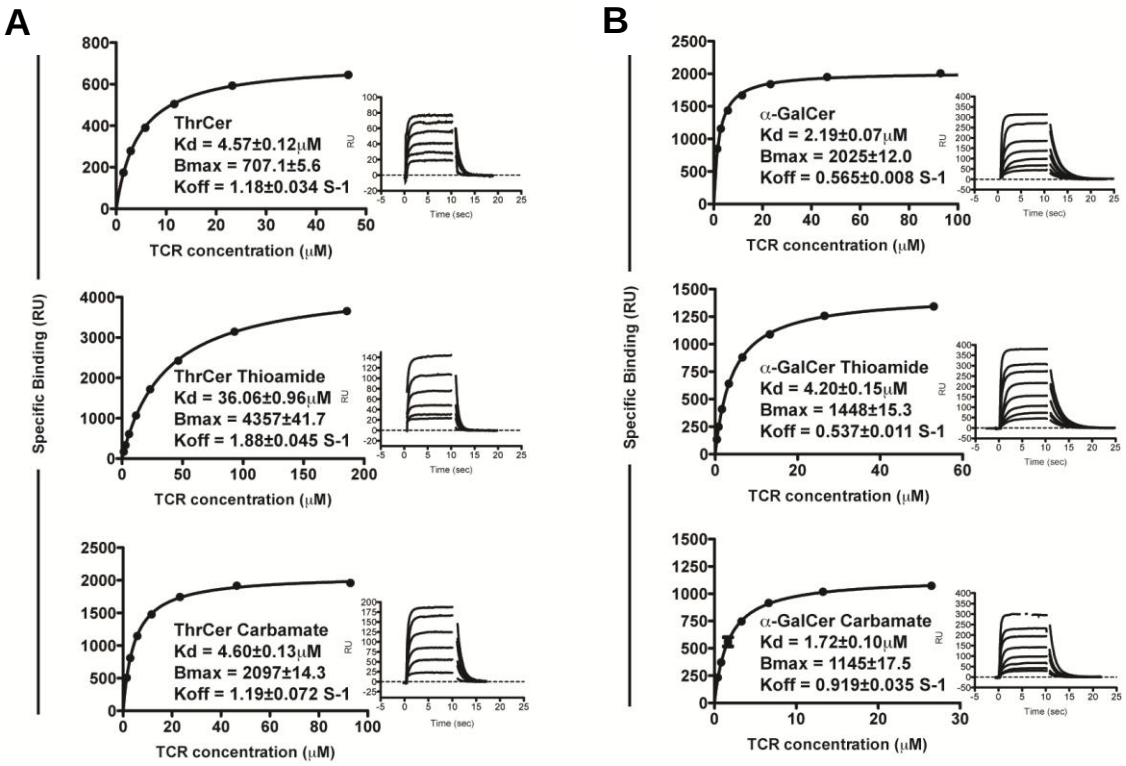

C

Lipid on CD1d	Experimental K_d (μM)	Experimental k_{off} (s^{-1})	Calculated k_{on} (M^{-1} s^{-1})

ThrCer, **24**	4.57 ± 0.12	1.18 ± 0.034	$2.58 \times 10^5 \pm 0.010 \times 10^5$
ThrCer thioamide, **38**	36.06 ± 0.96	1.88 ± 0.045	$5.2 \times 10^5 \pm 0.26 \times 10^4$
ThrCer carbamate, **40**	4.60 ± 0.13	1.19 ± 0.072	$2.59 \times 10^5 \pm 0.017 \times 10^5$
α-GalCer, **8**	2.19 ± 0.07	0.565 ± 0.008	$2.58 \times 10^5 \pm 0.009 \times 10^5$
α-GalCer thioamide, **35**	4.20 ± 0.15	0.537 ± 0.011	$1.28 \times 10^5 \pm 0.05 \times 10^5$
α-GalCer carbamate, **37**	1.72 ± 0.10	0.919 ± 0.035	$5.34 \times 10^5 \pm 0.37 \times 10^5$

Figure 2.16. Binding affinities (left) and kinetics (right) of the iNKT TCR for hCD1d molecules loaded with α-GalCer and ThrCer analogues measured using surface plasmon resonance (SPR). ThrCer analogues (**A**) and α-GalCer analogues (**B**).

A recent study by Sullivan *et al.* made a direct comparison between the Th2-biasing OCH glycolipid **13** and the Th1-biasing *C*-glycosyl analogue of α-GalCer **25**.[127] The group showed that both OCH and the *C*-glycosyl analogue of α-GalCer displayed weaker interactions than α-GalCer with iNKT cell TCRs. The authors attributed differences in cytokine response profiles to other factors including their differing pharmacokinetics properties, and their ability to transactivate other cytokine-releasing T-lymphocytes such as NK cells. When such transactivation requires prolonged lifetime after initial injection, metabolically more stable

glycolipid analogues should function better. A similar observation was made by Taniguchi and co-workers with the neoglycolipid α-carba-GalCer, which also induces a Th1-biased cytokine response profile upon iNKT cell activation.[128] Having replaced the amide residue with metabolically more stable functionality, we expected all three structural analogues, and in particular the non-glycosidic threitol derivatives **38**, **39** and **40**, which are not susceptible to glycosidase-mediated hydrolysis, would exhibit prolonged lifetimes *in vivo*, and for this reason, tentatively postulated that this might lead to Th1-biasing antigens. This hypothesis appears to have been borne out, at least in part, in the ThrCer series with the thioamide and carbamate analogues displaying a cytokine profile that is biased towards Th1. In both α-Gal and Thr series, the urea analogues displayed poor activity and we were unable to obtain binding and kinetics data for these two substrates, which may suggest that the additional NH incorporated into the acyl chain disrupts glycolipid binding and subsequent presentation.

2.15. Conclusion and Future Work

We have designed and synthesised two advanced intermediate amines **46** and **78**, which provided us with easy access to α-GalCer **8** and ThrCer **24** and their thioamide, urea and carbamate analogues.

All of the analogues were found to stimulate iNKT cells by CD1d-mediated presentation to varying degrees; however, the thioamide and carbamate analogues of ThrCer were of particular interest in that they elicted a strongly polarised *in vivo* Th1 response in mice.

ThrCer thioamide **38** may be useful for future investigation since it has the ability to activate both murine and human iNKT cells and elicted a strongly polarised *in vivo* Th1 response in mice. Its low binding affinity for CD1d is analogous to the truncated form of α-GalCer, OCH which has been shown to be rapidly presented on CD1d molecules, compared to α-GalCer.[127] The analysis of the crystal structure of the iNKT TCR-hCD1d–α-GalCer ternary complex suggests that whilst NH in ThrCer thioamide **38** should be able to partake in a strong hydrogen bond with the side-chain hydroxyl of Thr156 in mCD1d (and Thr154 in hCD1d), we expected any hydrogen bonding with a bridging water molecule would be weaker. It is also possible that one of the water molecules might be displaced due to the increased size of the sulfur atom. Attempts are currently on-going to crystallise CD1d with ThrCer **26** and ThrCer thioamide **38** with to understand the mechanism by which the addition of thioamide influences CD1d-TCR interactions.

It would be interesting to investigate further why the urea analogues of α-GalCer and ThrCer showed very weak iNKT cell stimulation. One possibility is that the additional N-H present in the urea can form a hydrogen bond with one of the amino acid residues of CD1d and change the conformation of the glycolipid-CD1d complex which is no longer recognised by iNKT TCR. To test this hypothesis the *N*-methyl urea analogue of α-GalCer and ThrCer should be prepared (Figure 2.17).

Our findings might suggest that increased metabolic stability of the glycolipid is important for favouring a Th1-biased cytokine response. For that reason we also considered moving away from the carboxylic acid derivatives and introducing aromatic and heterocyclic rings into the glycolipid structure that could mimic amide functionality. These amide derivatives would be less conformationally flexible and also more stable *in vivo*. We also envisage the preparation of the thioamide analogue of the *C*-glycosyl α-GalCer derivative, which stimulates a Th1-biased cytokine response (see Chapter 1.7.2.4), would be worthwhile. Direct comparison of the altered biological activity of this analogue with our ThrCer thioamide **38** could provide us with more information on the relation between glycolipid structure and Th1/Th2 bias.

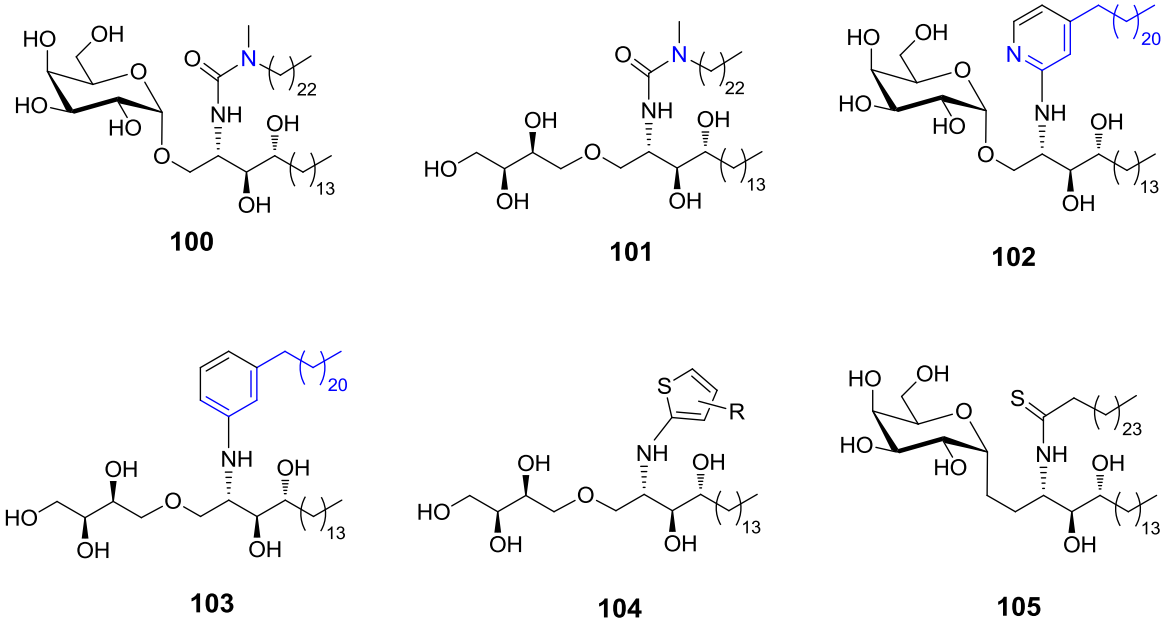

Figure 2.17. Possible future targets.

Chapter 3

Synthesis and Functional Activity of Labelled α-GalCer, ThrCer and Their Unsaturated Analogues

3. Synthesis and functional activity of labelled α-GalCer, ThrCer and their unsaturated analogues

3.1. Target compounds

The mechanisms leading to stimulation of biased Th1/Th2 responses by α-GalCer analogues remain poorly understood. As discussed earlier (see Chapter 1.7.2.1), one hypothesis states that for Th2 type agonists, like OCH **13**, low levels of IFNγ are observed due to the low affinity of the CD1d-OCH complex for the iNKT cell TCR.[36,66] However, another Th2-biasing agonist, α-GalCer(C20:2) **19**, when complexed with mCD1d or hCD1d, has been shown to have high binding affinity for the iNKT cell TCR, similar to that displayed by the most potent CD1d agonist α-GalCer **8**, a molecule which does not show significant skewing in its cytokine profile.[129]

Another hypothesis points at differences in uptake and presentation of various glycolipids. Studies carried out by van den Elzen and co-workers revealed that α-GalCer loading into CD1d occurs mainly in endosomes and requires uptake by endocytosis through a process that is facilitated by extracellular lipid carrying proteins such as apolipoprotein E (ApoE).[130] Further studies[50,131,132] showed that α-GalCer loading and presentation is also facilitated by lipid transfer proteins (LTPs) such as saposins and GM2 activator protein and requires acidic pH. Yu and co-workers[67] demonstrated that Th2-biasing α-GalCer(C20:2) **19** loads directly into cell-surface CD1d and does not require intracellular loading, which leads to much faster presentation. Figure 3.1 outlines the proposed mechanism

leading to stimulation of biased cytokine responses by α-GalCer and its analogues.

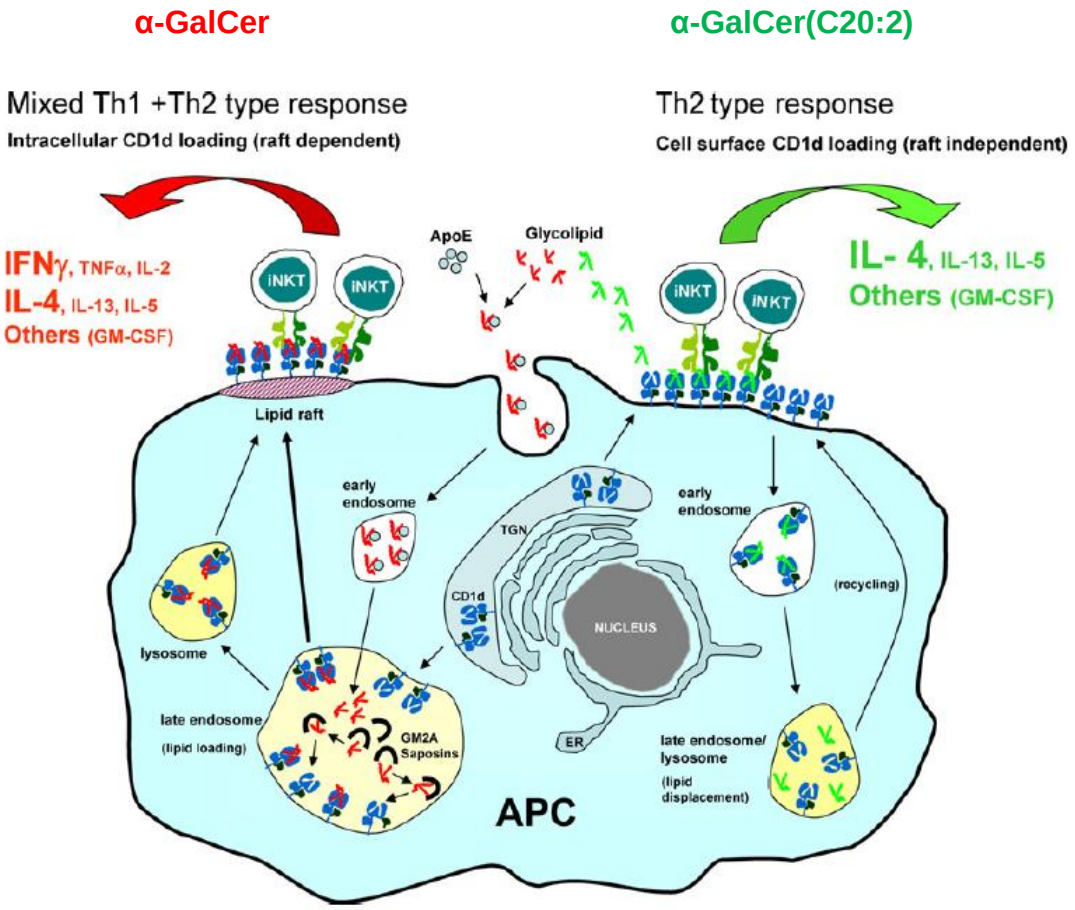

Figure 3.1. **Proposed mechanism leading to stimulation of Th2-biased cytokine responses by α-GalCer and its analogues.** α-GalCer requires intracellular processing and loading into CD1d protein in late endosomes. α-GalCer(C20:2), on the contrary, binds to CD1d at the cell surface without endosomal processing and activates iNKT cells resulting in Th2 type response.

Figure adapted from ref [3]. Permission to reproduce figure was obtained from *Elsevier* through RightsLink® - licence number 2812141231176.

To further study intracellular trafficking of exogenous glycolipids and to better understand the relationship between the cytokine profile of iNKT agonists and their differences in loading and presentation, we desired a series of labelled derivatives of α-GalCer, ThrCer and their unsaturated C20:2 analogues (Figure 3.2). Our first target was biotinylated ThrCer **106**. The synthesis and biological evaluation of this molecule would first confirm that the location of the label and linker did not impact on functional activity, as it is important that labelled analogues mimic the unlabelled glycolipids closely to provide useful information.

Having confirmed the biotin label did not significantly modify functional activity of ThrCer, we would then prepare α-GalCer derivative **108** and α-GalCer(C20:2) derivative **109**, each bearing differently coloured fluorescent labels. The same modifications would be applied in the ThrCer series. A green label would be attached to α-GalCer and ThrCer, and a red label to their unsaturated analogues α-GalCer(C20:2) and ThrCer(C20:2). Incubating cell lines with a pair of differently fluorescent α-GalCer derivatives, and separately with similar ThrCer analogues, would allow us to use multicolour fluorescence detection. The resulting cellular images should reveal the location and distribution of the different CD1d bound glycolipids and allow their direct comparison. For example, we would expect to see red colouration at the cell surface where the presentation of α-GalCer(C20:2) occurs and green areas in the intracellular compartments and at the cell surface, since α-GalCer(C26) needs to be first internalised before presentation to iNKT TCR can take place.

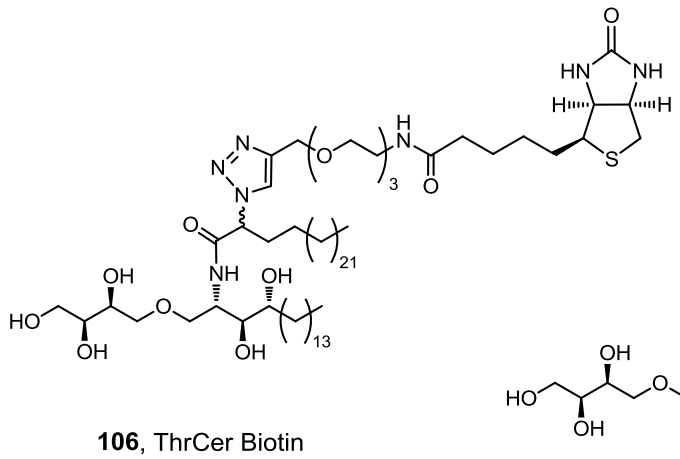

106, ThrCer Biotin

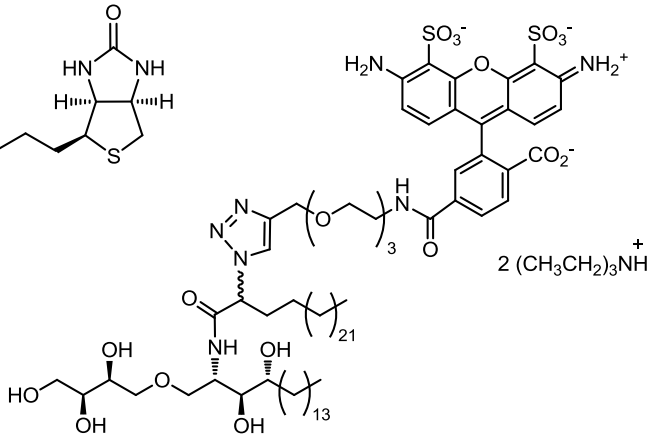

107, ThrCer Alexa 488 "green"

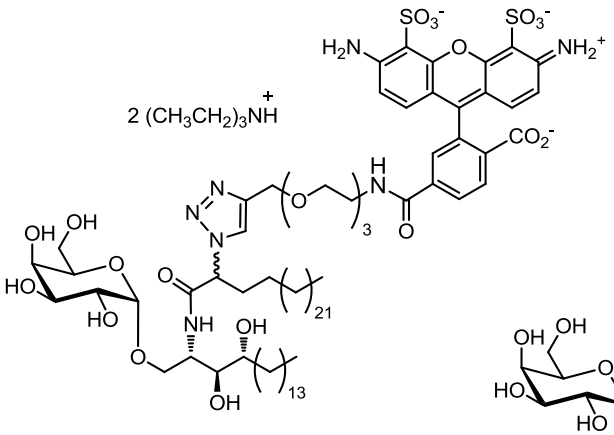

108, α-GalCer Alexa 488 "green"

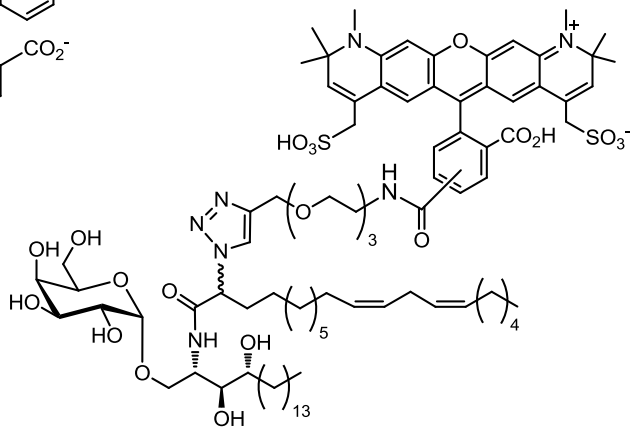

109, α-GalCer Alexa 594 "red"

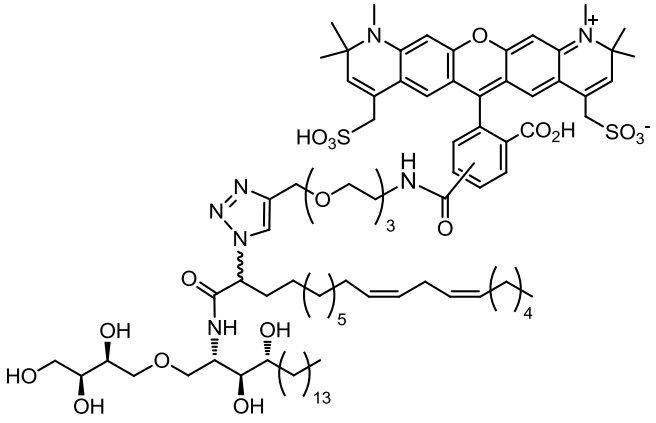

110, ThrCer Alexa 594 "red"

Figure 3.2. Target molecules: biotinylated ThrCer **106**, ThrCer Alexa 488 **107**, α-GalCer Alexa 488 **108**, α-GalCer Alexa 594 **109**, ThrCer 594 **110**.

Alexa Fluor® dyes, although very expensive, are now frequently used for conjugates with histological applications, providing the high fluorescence quantum yield and high photostability required to detect biological structures with excellent selectivity and sensitivity.[133] Figure 3.3 outlines alternative dyes commonly used in fluorescence microscopy, flow cytometry, and nucleic acid-based detection: cyanine dye Cy3 **111**, Oregon Green® **112** from the rhodamine class and a boron-dipyrromethane example, namely BODIPY TR **113**. However Alexa Fluor® dyes and their bioconjugates have more desirable properties including resistance to photobleaching, aqueous solubility, relative insensitivity to pH changes, high molar extinction coefficients and favourable quantum yields.[134]

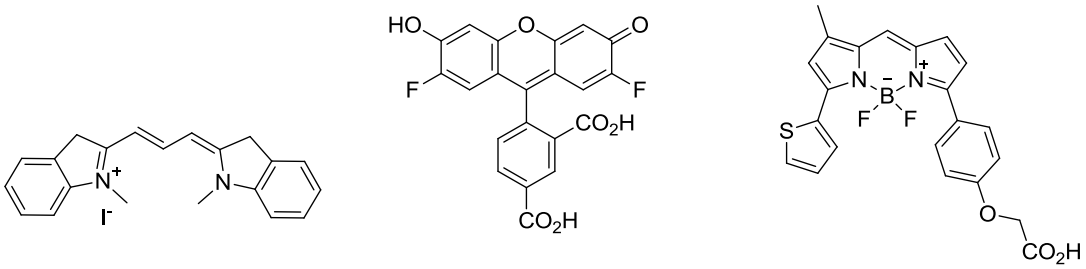

111, Cy3 **112**, Oregon Green **113**, BODIPY TR

Figure 3.3. Examples of commonly used fluorescent dyes: cyanine Cy3 **111**, rhodamine Oregon Green **112** and BODIPY TR **113**.

We first had to identify a label attachment point which would be common for all our target molecules. Chemical labelling studies of α-GalCer **8** have previously introduced the label at either the terminus of the *N*-acyl chain[135-137] or at the C(6)OH of the galactose residue,[138,139] both of which were deemed unsuitable for our purposes. We argued that a ThrCer analogue possessing a biotin label (and

any other for that matter) at the terminus of the *N*-acyl chain would result in the label being buried deep inside the A' pocket of the protein molecule (assuming such an analogue still binds in a similar conformation to ThrCer) and therefore unavailable for streptavidin or anti-biotin Ab recognition. Appending a label to the sugar residue in ThrCer was also rejected since all three alcohol groups in this truncated sugar unit are important for TCR recognition. We therefore considered alternative sites in the glycolipid, which would preserve binding and at the same time allow the biotin label to be recognised by some type of reporter group. Although an X-ray structure of the ThrCer-CD1d complex has so far eluded us, our working hypothesis assumes that ThrCer **24** adopts a similar bound conformation as does α-GalCer **8** in the CD1d molecule;[45,46,74] thus the *N*-acyl chain of ThrCer occupies the hydrophobic A' pocket of the protein and the ceramide base the less voluminous F' pocket, leaving the polar sugar residue surface-exposed for TCR recognition. An examination of the available X-ray structures of α-GalCer[45] and various other glycolipids bound to CD1d[44,127,140,141] and the related iNKT cell TCR ternary complexes,[46,74,142] encouraged us to consider the α-methylene unit in the *N*-acyl chain as a potential derivatisation site. Moreover, of the first set of glycolipid CD1d agonists, which were isolated from the marine sponge *Agelas mauritianus*,[34] AGL-548 is a potent synthetic analogue.[143] This glycolipid is structurally identical to α-GalCer apart from it possessing a hydroxyl group in the α-position (*S* configuration) of the *N*-acyl chain. Early studies had shown that deleting this hydroxyl functionality (which generates α-GalCer **8**) has no significant impact on activity.[143] Analysis of the X-ray structures of the α-GalCer-CD1d complex[45] and the α-GalCer-CD1d-TCR complex[46,74] revealed this site in the

glycolipid lies close to the surface of the CD1d molecule in the glycolipid-protein-TCR complex. Based on this analysis, we decided to introduce our labels into the α-position of the *N*-acyl chain of all our glycolipids.

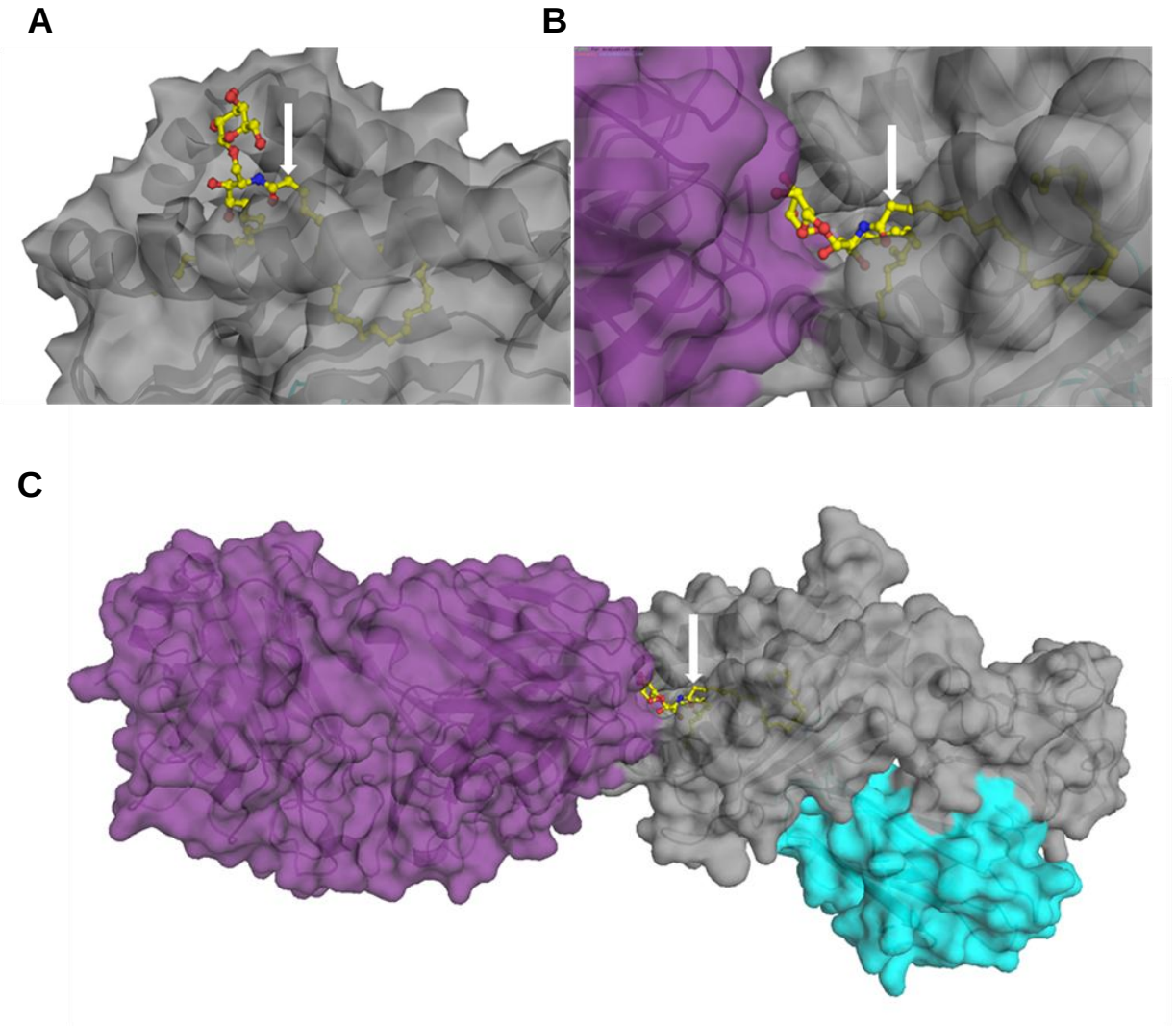

Figure 3.4. Chosen label attachment point (pointed with white arrow) at the α-position of the acyl chain of α-GalCer, showing that this part of the molecule is not buried inside the CD1d protein in the α-GalCer-CD1d complex (**A**) and is also exposed in the iNKT TCR– α-GalCer– CD1d ternary complex (**B**, **C**). Surfaces: grey – CD1d, purple – iNKT TCR, cyan – β_2m. (**A** - generated from 1ZT4,[45] **B**, **C** – generated from 2PO6[46] with Pymol).

We chose not to couple our labels directly to the glycolipid (junction of three components of the α-GalCer-CD1d-TCR complex), and instead attach these through a linker to minimise their impact on binding to CD1d protein, and recognition by the iNKT TCR. Owing to its widespread use elsewhere for similar purposes an oligo(ethylene glycol) spacer group was chosen to separate the biotin label from the 'active' ThrCer portion of the molecule.[144-146] Such a linker would also impart favourable solubility properties on the late-stage products in a range of organic solvents.[147,148] A triethylene glycol spacer unit was deemed to be of sufficient length to ensure the label in our targets would extend away from the TCR recognition site so as not to interrupt antigen presentation, and allow its own uninhibited recognition by streptavidin (in the case of biotin).

3.2. Retrosynthetic analysis

The general retrosynthetic analysis of labelled glycolipids **106**, **107**, **108**, **109** and **110** is outlined in Scheme 3.1. Considering the very high unit cost of the fluorescent labels and to minimise difficult-to-handle, water-soluble labelled products, we decided to install the label of choice in the final step of the synthesis.

We identified α-azido fatty acid chlorides and the previously prepared precursor amine **85** and modified (PMB protecting groups instead of Bn in galactose ring) amine **80** (see Chapter 2) as the starting materials for all of our syntheses. The resulting α-azido amide would then be reacted with the alkyne-terminated oligoethylene glycol linker **114** in a “click” reaction to provide the desired 1,2,3-triazole, which after global deprotection, would provide the primary amine ready to be coupled with a commercially available, amine-reactive biotin or fluorophore derivative leading to our target compounds.

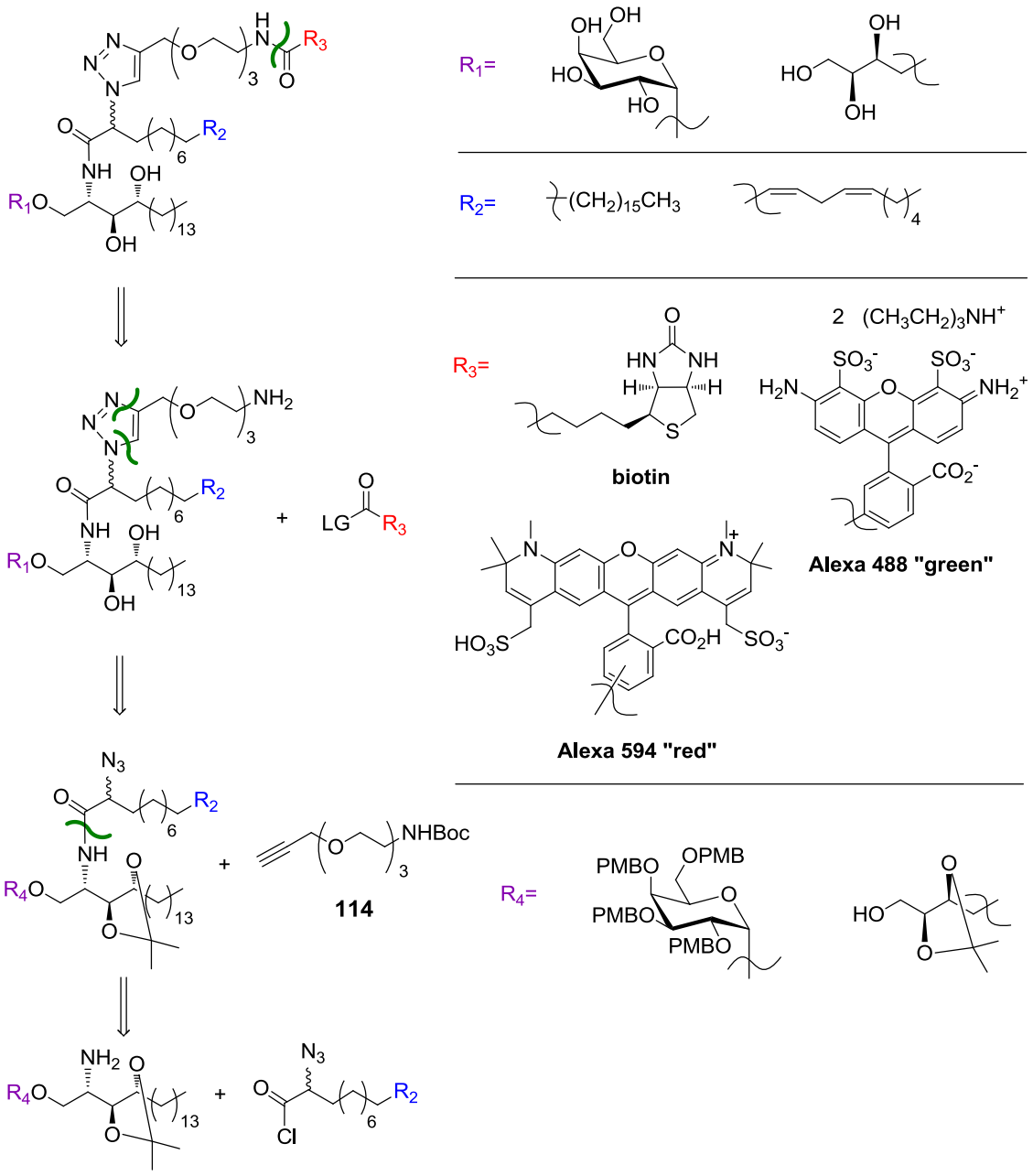

Scheme 3.1. Retrosynthetic analysis of biotinylated ThrCer **106**, ThrCer and α-GalCer derivatives **107** and **108** labelled with green Alexa 488 fluorescent label; and α-GalCer(C20:2) and ThrCer(C20:2) derivatives **109**, **110** labelled with red Alexa 594.

3.3. Synthesis of biotinylated ThrCer

Biotinylation of ThrCer had been performed before in our research group;[149] however, we wanted to refine the previous synthesis of **106** to provide a late-stage intermediate amine **122**, which could be coupled with any amine-reactive label such as the *N*-succinimidyl ester of biotin **123** or an activated ester of a fluorescent label such as Alexa Fluor®.

We first had to prepare α-azido hexacosanoic acid **116**, which would also be used in the synthesis of our target labelled molecules **107** and **108**.

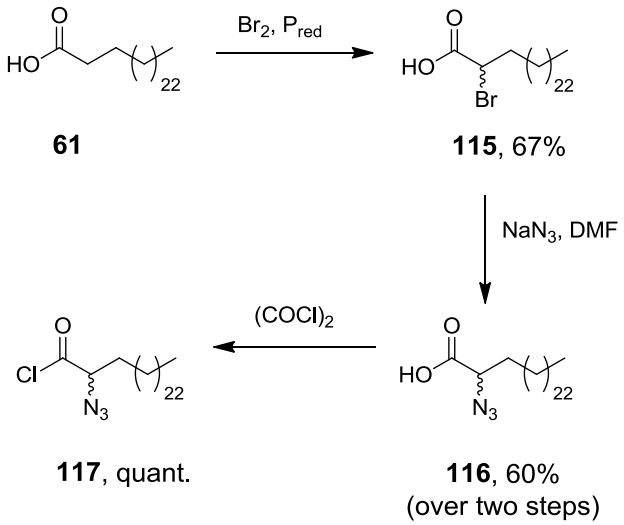

Scheme 3.2. Synthesis of α-azido hexacosanoyl chloride **117**.

α-Azido hexacosanoic acid **116** was prepared in two steps from hexacosanoic acid **61** (Scheme 3.2). Thus treatment of acid **61** with bromine in the presence of red phosphorus provided the corresponding α-bromo acid bromide, and then α-bromo acid **115** after aqueous work up,[150] which was converted into α-azido acid **116** by reaction with NaN_3 in DMF.[151] Treatment of acid **116** with oxalyl chloride generated the corresponding acid chloride **117**, which was reacted directly with amine **118** to provide the desired amide **119** as an inseparable 1:1 mixture of epimers (Scheme 3.3).

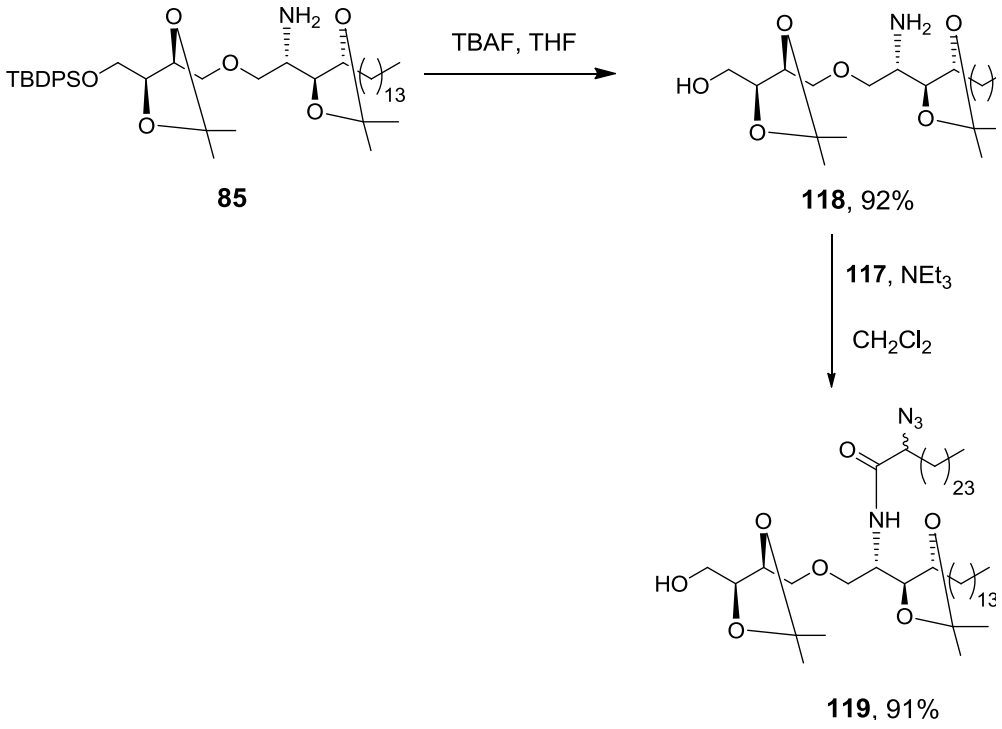

Scheme 3.3. Synthesis of amide **119**.

Linker **114** was prepared in four steps starting from commercially available 2-[2-(2-chloroethoxy)ethoxy]ethanol **120**, which was first reacted with NaN_3 to provide the corresponding azide, in which the hydroxyl group was then treated with NaH and

reacted directly with propargyl bromide to give alkyne **121** in 70% overall yield (Scheme 3.3). The product was characterised by HRMS and the quaternary resonance corresponding to the alkynyl *C*≡CH was observed at δ 158.8 ppm in the ^{13}C NMR spectrum. The IR spectrum showed a strong N_3 stretch at 2099 cm^{-1} providing further evidence of successful formation of the product **121**. Staudinger reduction of the azido group under our standard conditions provided the corresponding amine, which was next *N*-Boc-protected to give linker **114** in 82% yield after two steps. The product **114** was confirmed by HRMS. Key spectroscopic signals included the carbamate carbonyl stretch in the IR spectrum at 1706 cm^{-1}. The carbamate functionality was further evidenced in the ^{13}C NMR spectrum, which showed the characteristic quaternary carbon environment of a carbonyl at δ 154.2 ppm.

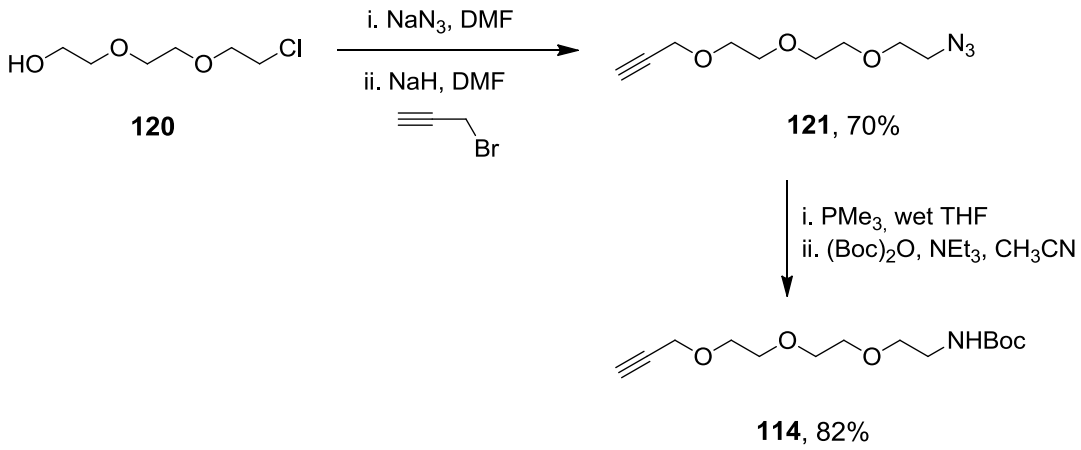

Scheme 3.6. Synthesis of linker **114**.

Click reaction[152,153] of azide **119** with alkyne **114** proceeded uneventfully and with complete regioselectivity to afford the desired 1,4-disubstituted 1,2,3-triazole **121**, which was isolated as a 1:1 mixture of epimers. At this stage we were able to observe two epimers by TLC analysis; however, their chromatographic separation was not possible. Formation of the product was confirmed by HRMS. Further evidence came from the ^{13}C NMR spectrum, which showed a quaternary carbon resonance at δ 145.4 ppm and a *C*H resonance at δ 122.3 ppm characteristic for the 1,4-disubstituted 1,2,3-triazole. From this, the proton of the triazole ring H-1’’’’ was then identified by 2-D chemical shift-correlated spectroscopy (HSQC) and appeared as two broad singlets in the ^{1}H NMR spectrum in the region of 7.71-7.75 ppm for one epimer and in the region of 7.76-7.82 ppm for second epimer. Final global deprotection with trifluoroacetic acid provided the corresponding amine **122**, which underwent smooth coupling with the *N*-hydroxysuccinimide activated ester of biotin **123** to provide our target,[154] biotinylated ThrCer **106** as a 1:1 epimeric mixture (Scheme 3.7). Both epimers were now separable by careful column chromatography on silica, which provided us with 5 mg of the less polar epimer (epimer A) and 4 mg of the more polar epimer (epimer B).

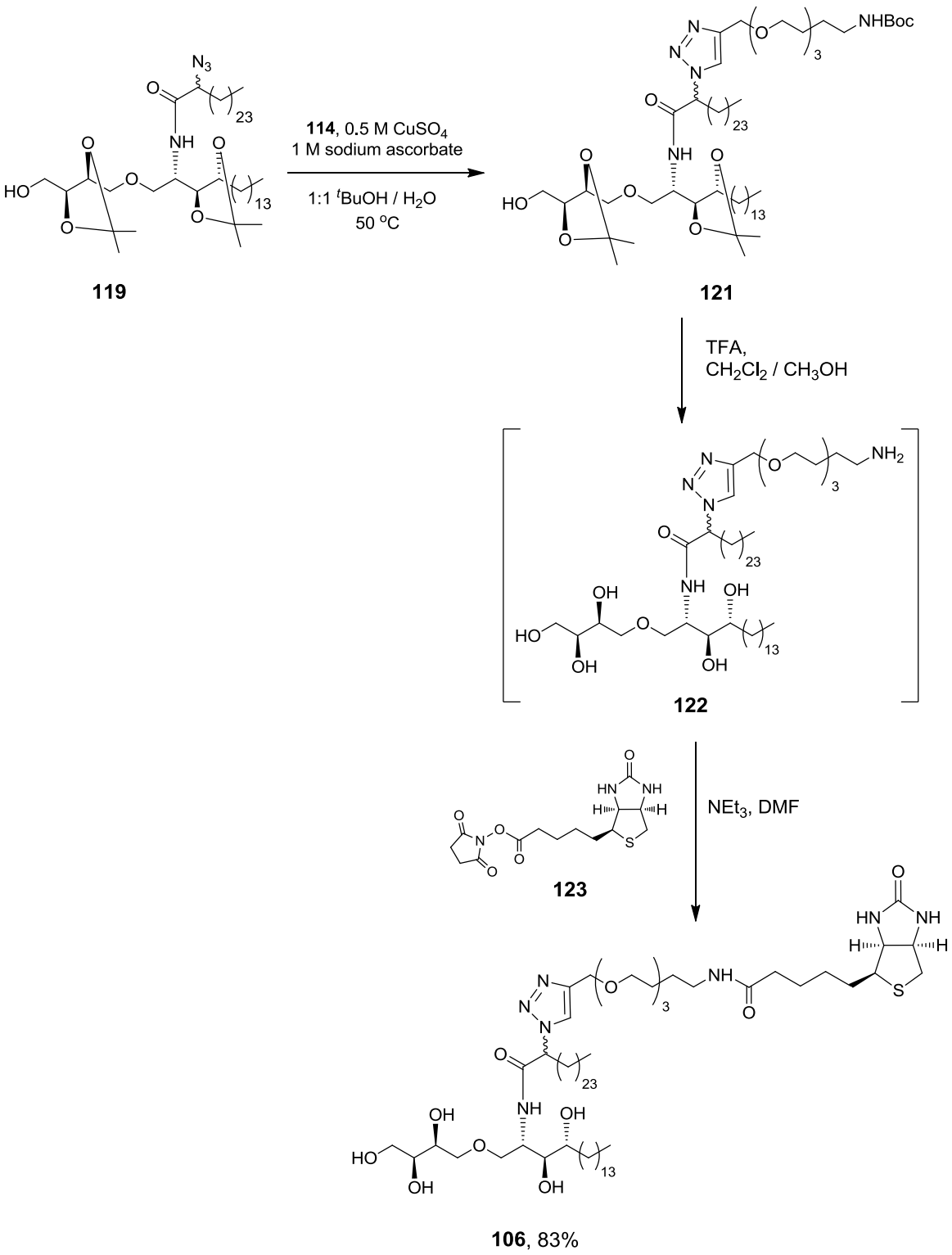

Scheme 3.7. Synthesis of biotinylated ThrCer **106**.

The epimeric mixture **106** and the single epimers A and B were submitted for biological testing, which was carried out in the group of Prof. Vincenzo Cerundolo by Dr John-Paul Jukes and Dr Hemza Ghadbane at the Weatherall Institute of Molecular Medicine in Oxford, UK.

3.4. Biological evaluation of biotinylated ThrCer

The epimeric mixture and single epimers of biotinylated ThrCer **106** were next tested separately for their ability to be loaded on to hCD1d or mCD1d molecules as detected by the binding of tetrameric iNKT cell TCR (Figure 3.3 A) or the stimulation of murine iNKT cells (Figure 3.3 B). Whilst the mixture of epimers behaved similarly to ThrCer **24**, when tested separately, it was apparent that the two epimers displayed different activity: iNKT cell TCR recognition of the CD1d–single epimer complex was noticeably weaker when the less polar (on silica) epimer (epimer A) was employed (Figure 3.3 A). These results were confirmed using mCD1d C1R cells and murine iNKT cell hybridomas (DN32) where the differences between epimer A and B became even more apparent (Figure 3.3 B). As a consequence of the difference in functional activity between the two epimers, the biological results using the 1:1 mixture were similar to those using purified epimer B, and for this reason, all subsequent experiments described below were performed with the more readily accessed epimeric mixture of **106**.

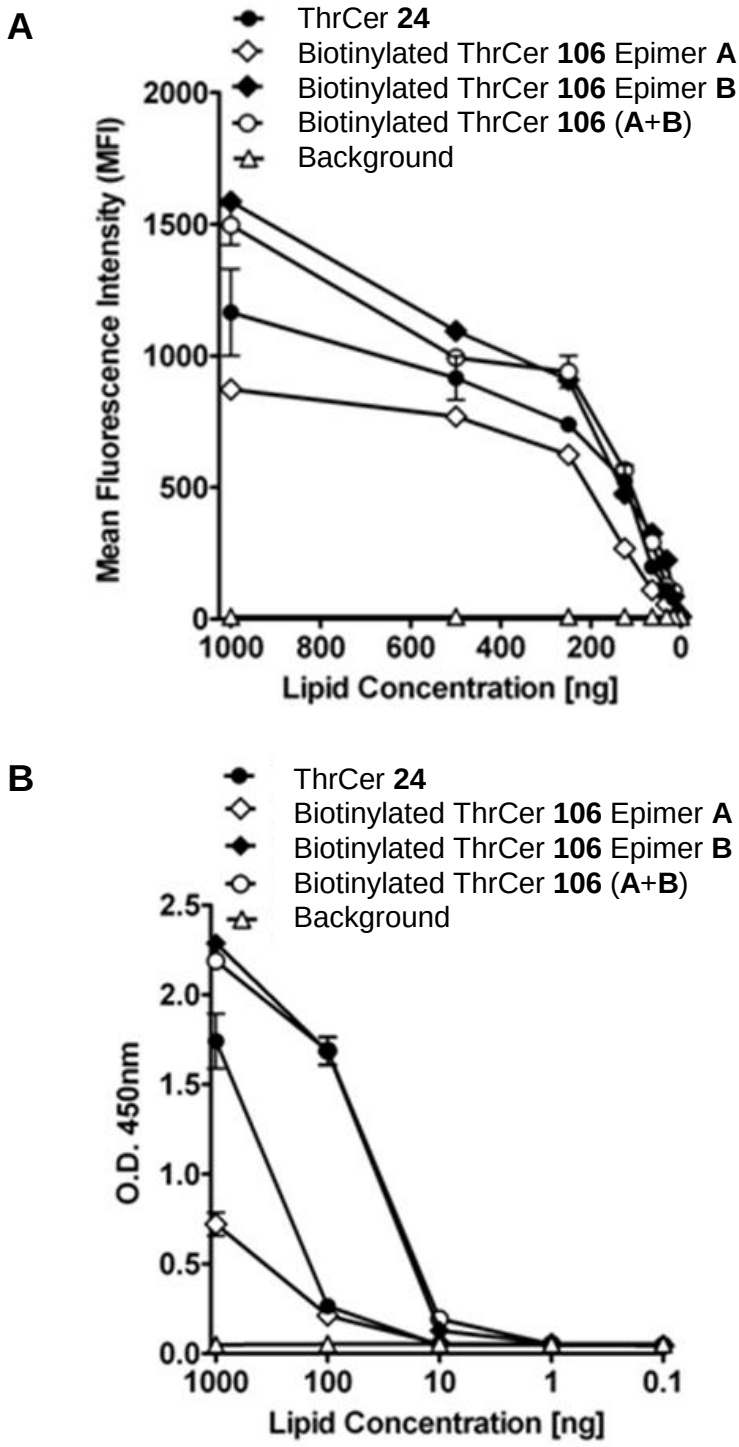

Figure 3.3. iNKT cell recognition of ThrCer **24** and biotinylated ThrCer **106**, epimer A, epimer B and 1:1 mixture of epimers A+B. (**A**) The recognition of **24** and **106** by human iNKT TCR tetramer was assessed by FACS following co-incubation of fluorescent human iNKT cell TCR and hCD1d C1R cells loaded with indicated lipids. (**B**) The activation of iNKT cells (DN32) was examined following overnight culture with mCD1d C1R cells pulsed with **24** and **106**. IL-2 production in supernatant was measured by ELISA after 24 h.

Functional experiments were next performed with both ThrCer **24** and biotinylated ThrCer **106** to assess whether or not the presence of the biotin moiety linked to ThrCer alters optimal loading on to CD1d molecules and presentation to human iNKT cells. To this end, we first analysed the ability of $CD1d^+$ target cells pulsed with both compounds to be recognised by human iNKT cells.[70] The results of these experiments are summarised in Figure 3.4 and demonstrate that both ThrCer **24** and the active epimer of biotinylated ThrCer **106** are capable of sensitising iNKT cells to a similar level, as defined by IFNγ secretion (analysed after 36 h by ELISA[70] (Figure 3.3)). We extended these results by employing a second protocol based on the use of a soluble human iNKT cell TCR tetramer,[36] which was used as a staining reagent for $CD1d^+$ target cells pulsed with a range of concentrations of biotinylated ThrCer **106** (Figure 3.3). These results again indicate that the biotin label and linker in the active epimer of **106** do not alter optimal loading on to CD1d molecules, since the biotin moiety remains available for binding to streptavidin and anti-biotin (Figure 3.3 A/B), and still allows iNKT TCR tetramer binding (Figure 3.4). Significantly, it is possible to co-localise the iNKT TCR tetramer and biotin moiety using streptavidin (Figure 3.5).

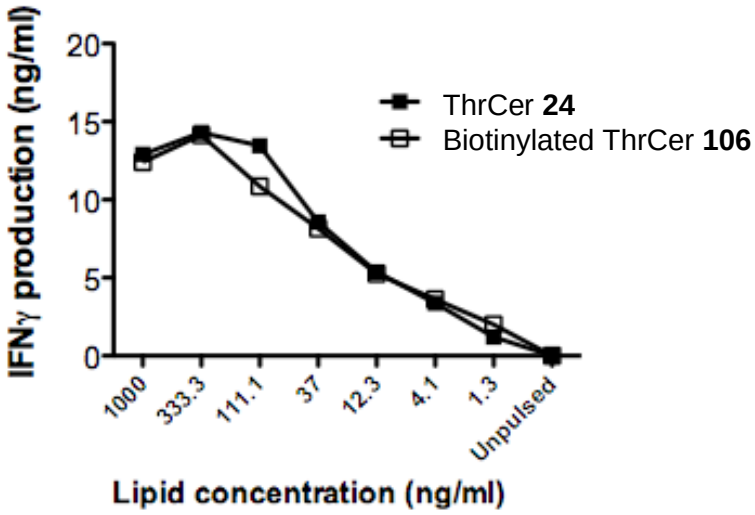

Figure 3.4. Biotinylated ThrCer **106** activates human iNKT cells *in vitro*. A human iNKT cell line was incubated with C1R hCD1d cells pulsed with ThrCer **24** (black squares) or biotinylated ThrCer **106** (1:1 epimeric mixture) (open squares) at various concentrations. IFNγ secretion was analysed after 36 h by ELISA.

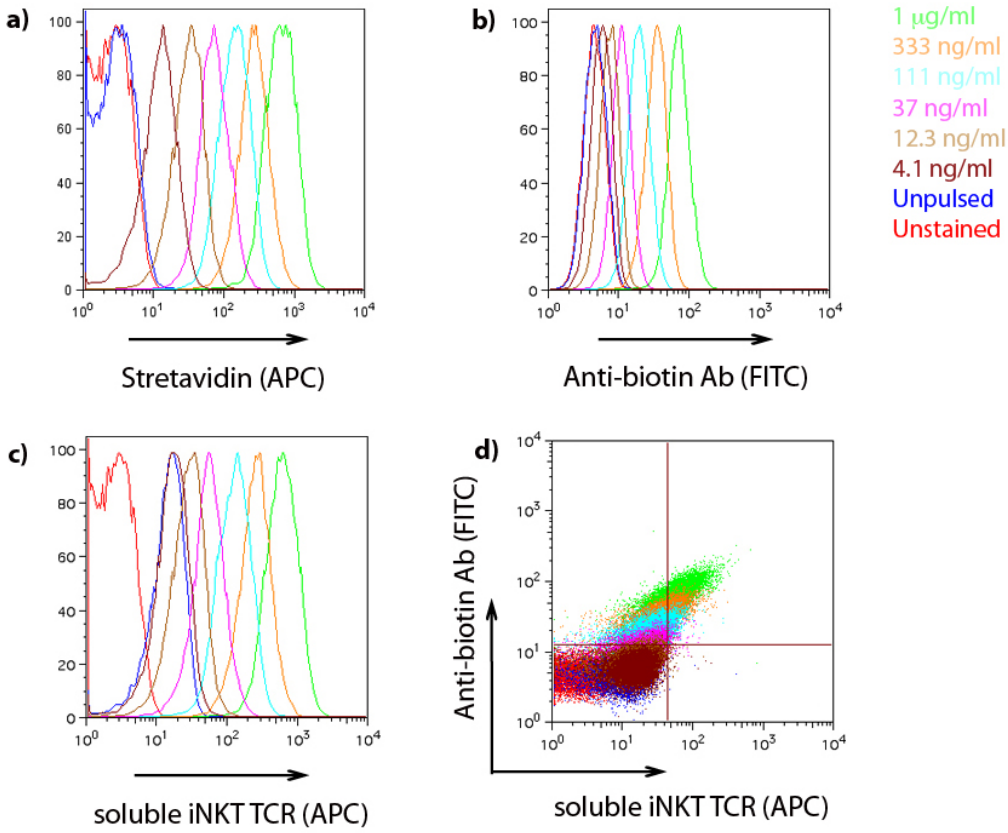

Figure 3.5. Detection of biotinylated ThrCer **106** (1:1 epimeric mixture) on the surface of APCs. C1R hCD1d cells were pulsed with the indicated concentrations of biotinylated ThrCer for 16 h and then stained with **a)** fluorescent streptavidin (APC), **b)** anti-biotin Ab (FITC), **c)** soluble iNKT TCR tetramer (APC). Panels **a**, **b** and **c** depict histogram overlays of the indicated fluorescence intensities. The dot plot shown in panel **d** depicts a double staining with the soluble iNKT TCR (APC) and anti-biotin Ab (FITC).

At this stage of the study, we did not know the absolute stereochemistry at the triazole tethering site of the more active epimer although our previous analysis of the crystal structure of the α-GalCer-CD1d-TCR ternary complex[46,74] suggested that substituting the *pro-S* hydrogen in the α-methylene unit would exert fewer

conformational changes on the iNKT cell TCR-CD1d-glycolipid complex and also allow the biotin label to protrude away from this complex to allow its recognition.

A

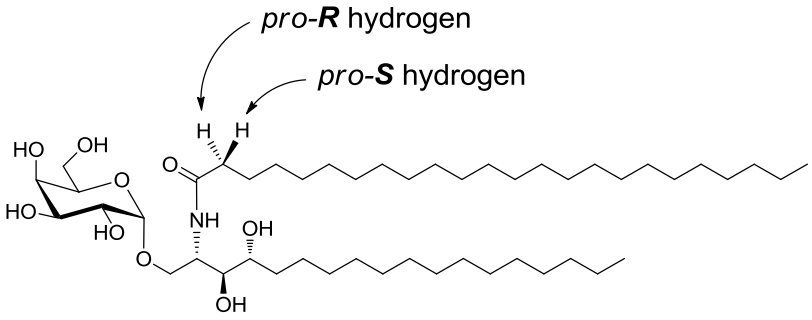

B

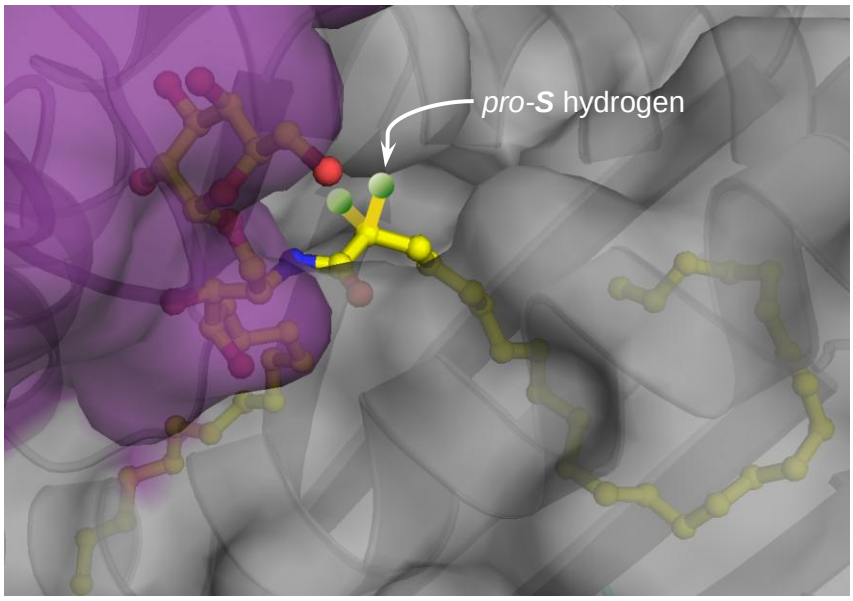

Figure 3.6. (**A**) Representation of the *pro-S* hydrogen and *pro-R* hydrogens in the α-GalCer structure. (**B**) *Pro-S* hydrogen in the α-position of the *N*-acyl chain of α-GalCer pointing away from the interior of the CD1d protein in the crystal structure of the iNKT TCR – α-GalCer – hCD1d ternary complex. Cartoon representation was obtained with PyMol from 2PO6.[46]

In summary, we have shown that attaching a biotin label through a tri(ethylene glycol) spacer to the α-position of the *N*-acyl chain in ThrCer **24** generates a functionally active labelled analogue **106**. Whilst introducing a label at this site necessarily introduces a new stereogenic centre into the molecule, and therefore a mixture of diastereoisomers when racemic azido acid **116** is employed, these two epimers can be separated by chromatography. Although the two epimers display different functional behaviour, the relatively large difference between the two means that the more active epimer **106 B** dominates the behaviour of the epimeric mixture, and obviates the need to use the diastereoisomerically pure active epimer for biological studies.

More generally, this study has shown that the α-site of the *N*-acyl chain should be a viable location for introducing labels into other ceramide-based CD1d agonists (and potentially other bioactive glycolipids). Furthermore, whilst this study involved the introduction of a biotin label, our synthetic strategy has been designed to allow the late-stage incorporation of other labels (*e.g.* fluorophores, lumophores) and we were now ready to prepare Alexa-labelled derivatives of ThrCer and α-GalCer.

3.5. Synthesis of ThrCer(C26:0) labelled with Alexa 488

With advanced intermediate amine **122** in hand we were also ready to perform a coupling reaction with an amine-reactive fluorescent label. To prepare Alexa 488 labelled ThrCer **107** we chose to use the commercially available Alexa Fluor® 488 carboxylic acid, 2,3,5,6-tetrafluorophenyl ester **124**, which unfortunately comes with a high cost of £230 per 1 mg. Our biggest challenge would be to perform the coupling reaction efficiently on small scale; however we knew that providing 0.5-1 mg of labelled compound would be sufficient for our collaborators to carry out many biological assays.

Amine **122** was reacted with Alexa 488 active ester **124** in the presence of NEt_3 in DMF to provide the final product **107** in 73% yield (1.2 mg of isolated product). Owing to the small amount of isolated material, its high molecular mass (Figure 3.2), the charged nature of the material and the fact that it was an epimeric mixture, analysis of the ^1H NMR spectra proved to be very difficult. TLC analysis however showed two bright fluorescent products that were not contaminated with any of the starting materials and gave a positive test for glycolipids with Molisch's reagent (α-naphtol solution 10 wt. % in ethanol) and lipid stain (phosphomolybdic acid solution 5 wt. % in ethanol).

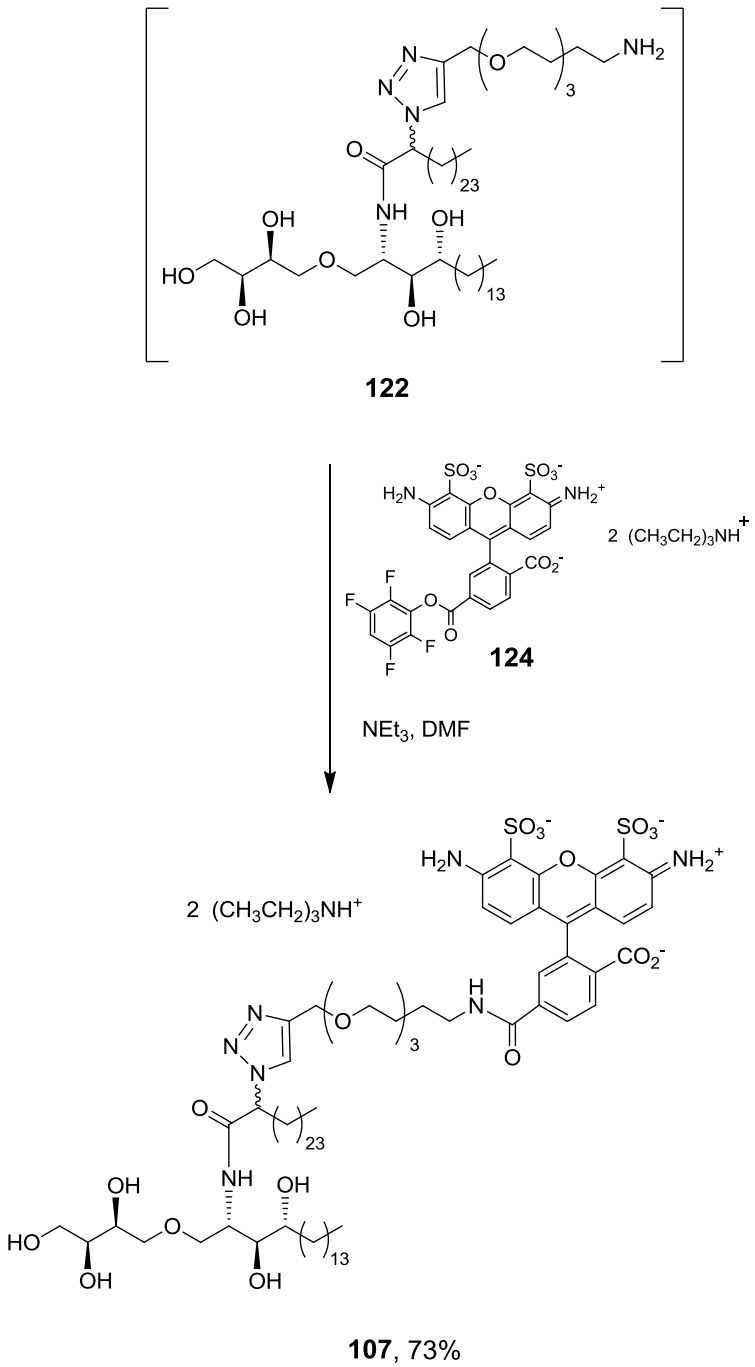

Scheme 3.8. Synthesis of Alexa 488-labelled ThrCer **107**.

3.6. Synthesis of α-GalCer(C26:0) labelled with Alexa 488

To access the corresponding α-GalCer derivative labelled with Alexa 488 **108**, we first considered using our previously prepared amine **80** (See Chapter 2.8), which could be coupled with α-azido hexacosanoyl chloride and then processed as before after removal of the protecting groups. However, the intermediate amine **80** bears four benzyl ether groups whose removal would likely cause a problem in our next target **109**, which incorporates a skipped diene in the acyl chain. We therefore decided to further optimise our glycosylation reaction, and investigate the use of a new galactosyl donor containing PMB protecting groups, which we envisaged could be removed selectively under acidic conditions.

p-Methoxybenzyl (PMB) ethers have been used widely in carbohydrate chemistry.[155] These electron-rich ethers can be selectively removed by oxidation with, for example, 2,3-dichloro-5,6-dicyano-1,4-benzoquinone (DDQ), without affecting alkenes, acetals, epoxides and silyl ethers.[156] They can also be cleaved with trifluoroacetic acid (TFA) without affecting azido groups, acetates and *O*-glycosidic linkages in oligosaccharides.[157] For our purposes, the employment of PMB groups in the glycosyl donor would result in a potentially more efficient approach to amine **131**. In analogy with amine **122**, a final deprotection step with TFA would remove four PMB groups, the isopropylidene acetal and the Boc group.

Our new donor precursor, 2,3,4,6-tetra-*O*-*p*-methoxybenzyl-galactose **126**, was prepared in two steps (Scheme 3.9). Previously prepared tetraol **56** (see Chapter 2.2) was first treated with NaH and the resulting alkoxide was reacted with *p*-

methoxybenzyl chloride to afford thioglycoside **125** in 90% yield. This step required the reaction temperature to be raised to 60 ºC for the reaction to go to completion, whereas with benzyl bromide, r.t. had been sufficient to generate the tetra benzyl ether in almost quantitative yield. The thioglycoside **125** was then hydrolysed with *N*-bromosuccinimide in an acetone/water mixture (10:1) to yield the hemiacetal **126** as a 1:1 mixture of diastereoisomers.[158]

We were pleased to find that the glycosylation reaction of donor precursor **126** with acceptor **78** under our standard conditions resulted in glycoside **127** with complete α-selectivity and in 70% yield (Scheme 3.9). The product was confirmed by HRMS and the characteristic α-anomeric proton in the ^{1}H NMR spectrum at δ 4.93 ppm, which appeared as a doublet with a small coupling constant (1H, d, $J_{1,2}$ 3.6 Hz, H-1'). The ^{13}C NMR spectrum also showed the diagnostic α-anomeric carbon resonance at δ 98.8 ppm.

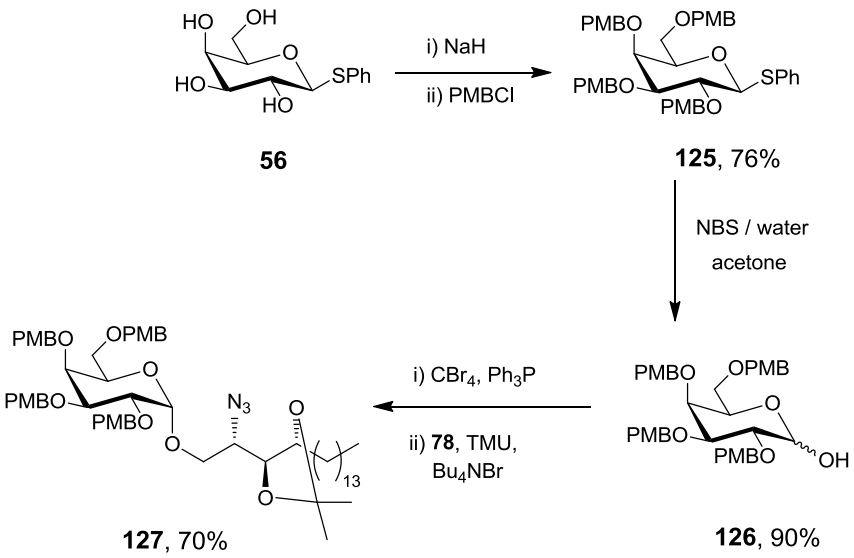

Scheme 3.9. Synthesis of galactoside **127** using new donor **126**.

The next steps involved a Staudinger reaction to afford amine **128**, which was acylated with acid chloride **117** to provide amide **129** as a 1:1 mixture of epimers (Scheme 3.10). Formation of the product **129** was evidenced by HRMS and in the ^{13}C NMR spectrum, two characteristic amide C=O quaternary resonances were observed for both epimers at δ 168.6 and δ 168.9 ppm. From this, the H-2'' protons were identified by 2-D chemical shift-correlated spectroscopy (HMBC) and the resonances for the corresponding C(2'') carbons for both epimers at δ 64.2 and δ 64.5 ppm (by HSQC). The IR spectrum showed a characteristic azido stretch at 2100 cm^{-1}, and a carbonyl amide C=O stretch at 1720 cm^{-1} provided further evidence of successful functionalisation of amine **128** with α-azido-hexacosanoyl chloride **117**. Click reaction performed on azide **129** with linker **114** resulted in the desired 1,2,3-triazole **130** as a 1:1 mixture of epimers.

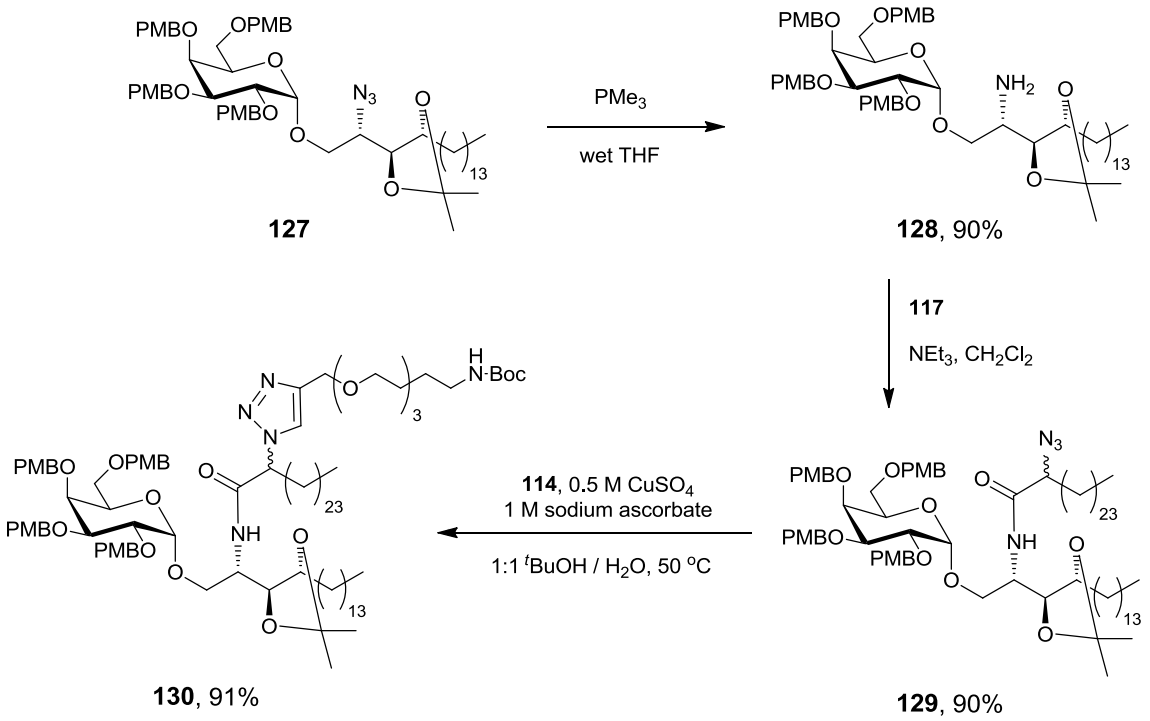

Scheme 3.10. Synthesis of 1,4-disubstituted 1,2,3-triazole **130**.

Scheme 3.11 outlines the synthesis of target molecule **108**. Treatment of **130** with TFA afforded amine **131**, which was purified by chromatography and confirmed by HRMS. Amine **131** was next reacted with the 2,3,5,6-tetrafluorophenyl ester of Alexa Fluor® 488 **124** in the presence of NEt_3 in DMF. This reaction was performed, as previously, on 1 mg (Alexa Fluor® 488) scale. The product **108** was purified from the starting materials by flash column chromatography using a cartridge pre-packed with 100 mg of silica. Working on such small scale and with a mixture of epimers prevented us from obtaining full characterisation data of the product; however, we were able to confirm the formation of the product by HRMS.

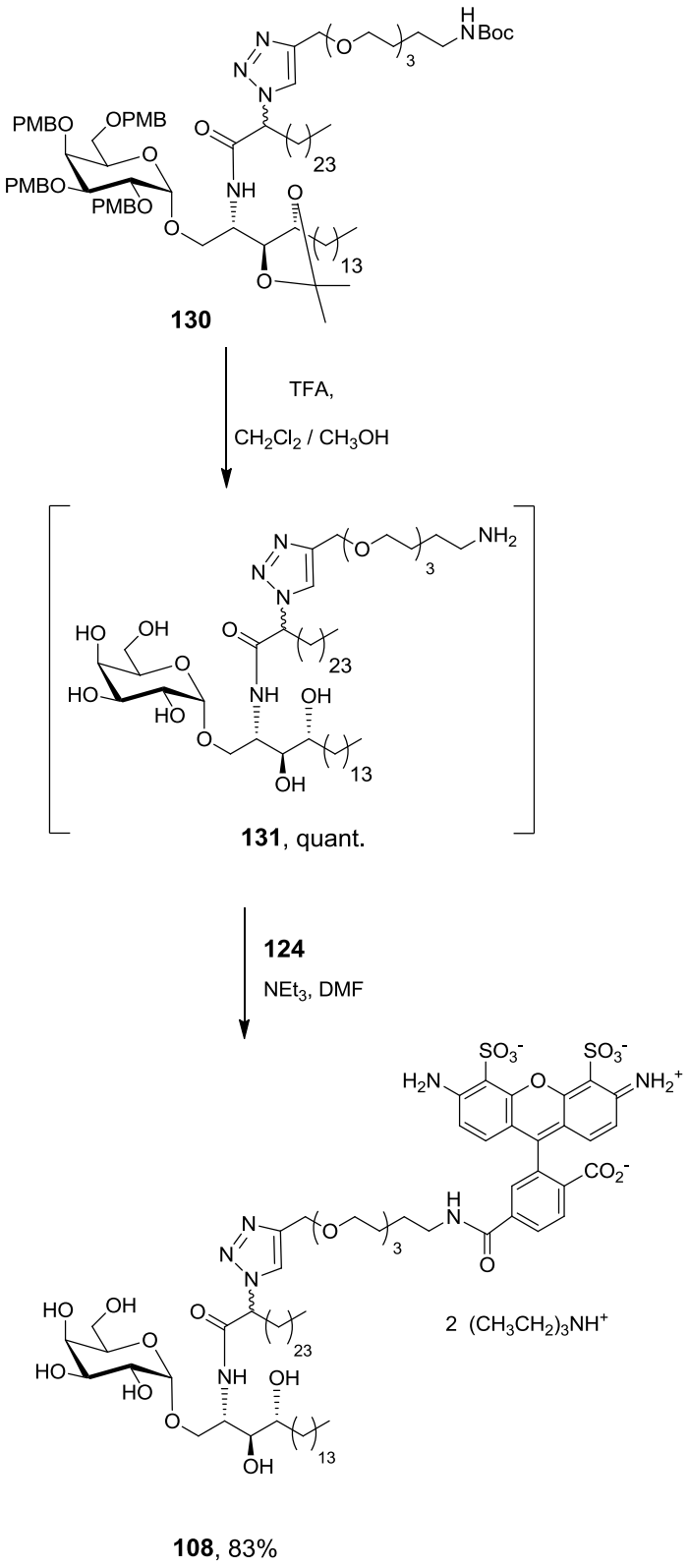

Scheme 3.11. Synthesis of target molecule α-GalCer derivative labelled with Alexa 488 **108**.

To summarise, we further optimised our glycosylation reaction by introducing 2,3,4,6-tetra-*O*-*p*-methoxybenzyl-galactose **126** as a new donor precursor. Since all the protecting groups in the glycoside product can be removed (in a single step) under acidic conditions, this modification opened up the possibility of coupling unsaturated carboxylic acids, which forms the subject of the next Section.

3.7. Synthesis of α-GalCer(C20:2) labelled with Alexa 594

With amine **128** in hand we could now focus on the preparation of α-azido-eicosadienoic carboxylic acid. The high cost of *cis*-11,14-eicosadienoic acid (*circa* £100 / 100 mg, SIGMA-ALDRICH) encouraged us to develop a synthesis of α-azido-eicosadienoic acid from the much cheaper linoleic acid (£43 / 5 g, SIGMA-ALDRICH). For convenience, the α-azido acid would be synthesised in racemic form in the first instance, which would necessarily generate a final product as a mixture of a diastereoisomers. If necessary, an enantioselective route would be investigated at a later stage.

The retrosynthetic analysis of (*Z*,*Z*)-2-azido-eicosa-11,14-dienoic acid **132** is outlined in Scheme 3.12. Starting from inexpensive *cis*-9,12-linoleic acid **138** requires the addition of two carbons to the 18-carbon alkyl chain. These would be introduced sequentially, proceeding *via* aldehyde **135** (19-carbons in length), which would undergo a Strecker reaction to provide the corresponding α-amino-nitrile **134** (20 carbons in total) and after subsequent hydrolysis, α-amino-eicosadienoic acid **133**. The final step in our approach would require an amine-azide conversion in a diazo transfer reaction.[90] Goddard-Borger *et al*. optimised this reaction for the preparation of α-azido acids from natural α-amino acids and therefore, we presumed it would also work as a final step in our synthesis of **132**.

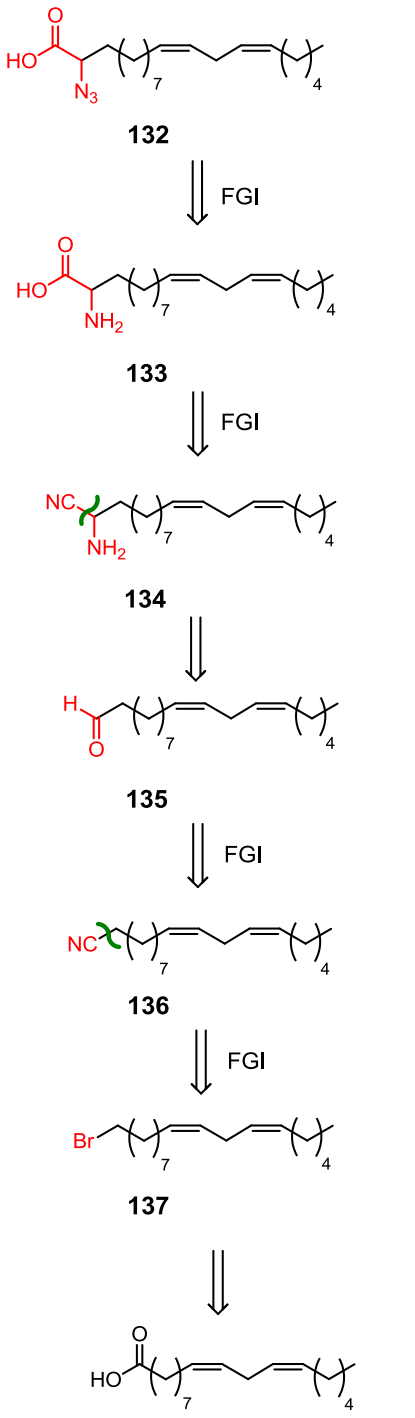

Scheme 3.12. Retrosynthetic analysis of (*Z*,*Z*)-2-azido-eicosa-11,14-dienoic acid **132**.

The Strecker reaction[159,160] is a well-known method for preparing α-amino nitriles, from which the corresponding α-amino acids can be obtained by hydrolysis of the nitrile. Furthermore enantioselective variants of the reaction, employing chiral auxiliaries[161,162] or asymmetric catalysts;[163,164] opens up the possibility of rendering our route to **132** enantioselective at a later stage.

Our synthesis of α-azido acid **132**, began with the conversion of linoleic acid **138** into its methyl ester, which was then reduced with $LiAlH_4$ to the corresponding alcohol **139**.[165] In the next step, **139** was reacted with the Appel reagents (CBr_4, PPh_3) to provide bromide **137**,[165] which, upon treatment with NaCN in DMSO,[166] afforded nitrile **136**. DIBAL-H reduction, and subsequent hydrolysis of the intermediate imine, afforded aldehyde **135**.[167] The product was confirmed by HRMS and further evidenced by the ^{13}C NMR spectrum, which showed the characteristic C=O resonance of an aldehyde at δ 202.8 ppm, and by the ^{1}H NMR spectrum, in which the aldehyde proton appeared as a triplet [δ 9.77 ppm (1H, t, *J* 1.9, C*H*O)]. IR analysis revealed an aldehyde C=O stretch at 1742 cm^{-1}.

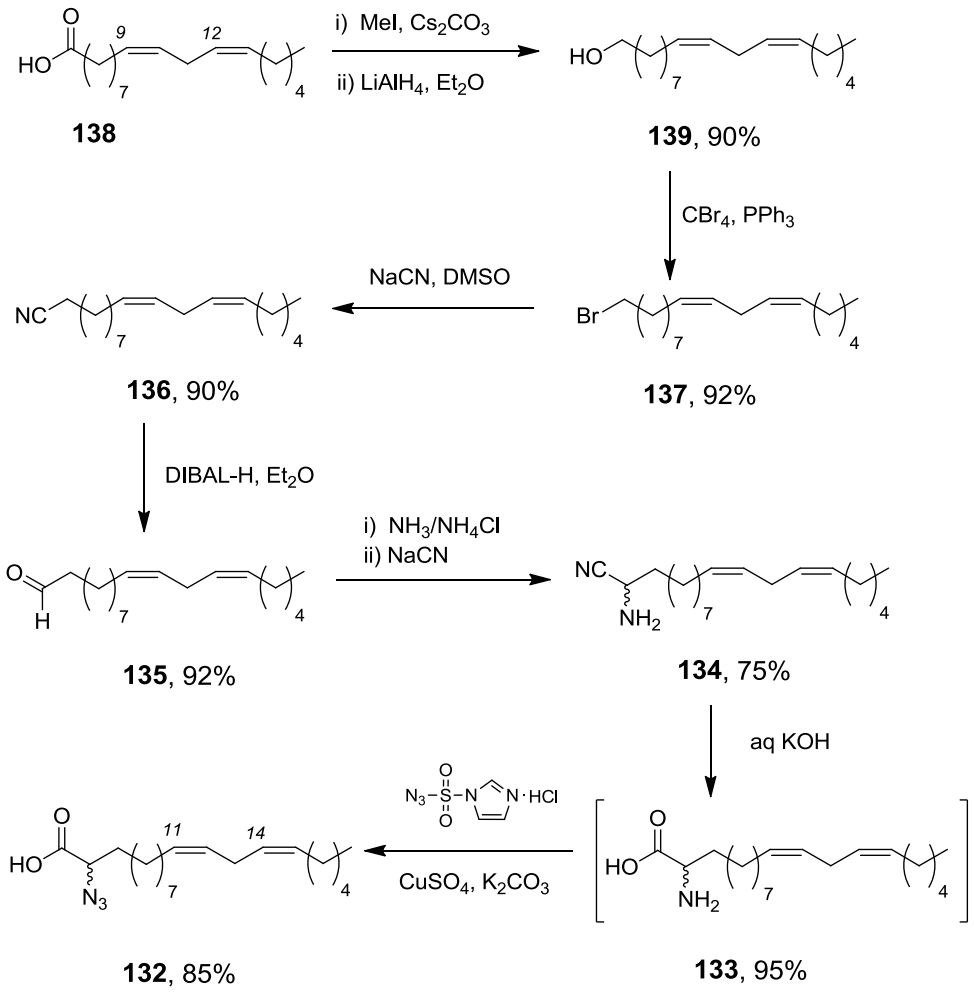

Scheme 3.13. Synthesis of (*Z*,*Z*)-2-azido-eicosa-11,14-dienoic acid **132**.

In the next step, aldehyde **135** was converted to α-aminonitrile **134** using the Strecker reaction. The general mechanism of this transformation is summarised in Scheme 3.14. The first steps involve *in situ* generation of HCN from the cyanide salt and ammonium chloride and acid-catalysed imine formation. Cyanide anions react more rapidly with the iminium species than with the starting aldehyde, to generate an α-aminonitrile, which can then be hydrolysed to the corresponding α-amino acid.

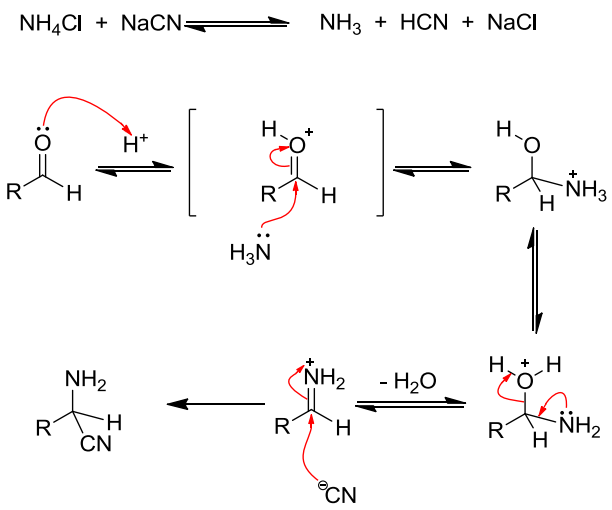

Scheme 3.14. The general mechanism of the Strecker reaction.

Aldehyde **135** underwent a one-pot Strecker reaction[168] to afford racemic α-aminonitrile **134** in a satisfactory 75% yield. The product was confirmed by HRMS. The ^{13}C NMR spectrum of **134** showed a quaternary carbon resonance for the nitrile group at δ 122.2 ppm and only one CH resonance in the alkyl region at δ 43.4 ppm. The product was further evidenced in the IR spectrum with a characteristic C≡N stretch at 2246 cm^{-1} and a broad amine stretch at 3343 cm^{-1}. Nitrile **134** was then hydrolysed under basic conditions[169] by heating with 40% aqueous potassium hydroxide solution for 8 hours, followed by work-up with 10% aqueous HCl solution, to provide crude α-amino acid **133**, which was used in the next step without further purification. The final step involved conversion of **133** into the corresponding α-azido acid **132**,[90] which was evidenced by HRMS and confirmed by ^{13}C NMR spectroscopic analysis, where the quaternary carbon resonance for the carboxylic acid group appeared at δ 176.1 ppm and the CH resonance for the α-carbon at δ 61.7 ppm. The IR spectrum showed a C=O stretch

at 1719 cm^{-1}, a characteristic azide stretch at 2108 cm^{-1} and a very broad stretch for the O-H group in the range of 3400-2500 cm^{-1}, providing further evidence of successful formation of target molecule **132**. The two *cis* double bonds remained unchanged throughout the synthesis, and always appeared in the ^{13}C NMR spectra as four CH resonances in the region of δ 128-130 ppm.

We next converted carboxylic acid **132** into the corresponding acid chloride **140** under mild reaction conditions (Scheme 3.15). Here we wanted to avoid heating the acid in neat oxalyl chloride[††], conditions which might affect the skipped diene present in the acyl chain. Acid **132** was therefore reacted with two equivalents of oxalyl chloride in the presence of catalytic amount of DMF in dichloromethane at 0 ^{o}C.[170]

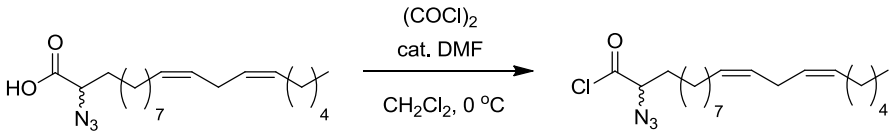

132 **140**, quant.

Scheme 3.15. Synthesis of acid chloride **140**.

[††] We had employed these conditions for the conversion of hexacosanoic acid **61** and α-azido-hexacosanoic acid **132** into the corresponding acid chlorides.

Previously prepared intermediate amine **128** was successfully acylated with the resulting acyl chloride **140**, affording amide **141** in 85% yield as a 1:1 mixture of epimers. Formation of the product **141** was evidenced by HRMS and in the ^{13}C NMR spectrum by two characteristic amide C=O quaternary resonances for both epimers at δ 168.8 and δ 168.9 ppm. From this, the H-2'' protons were identified by 2-D chemical shift-correlated spectroscopy (HMBC) and the resonances for the corresponding C(2'') carbons for both epimers at δ 64.3 and δ 64.6 ppm (by HSQC). Four CH resonances for the two double bonds were identified in the ^{13}C NMR spectrum at δ 127.9, 128.8, 130.0, 130.2 ppm. The IR spectrum showed a characteristic azido stretch at 2103 cm^{-1} and a carbonyl amide C=O stretch at 1683 cm^{-1}, providing further evidence of successful functionalisation of amine **128** with α-azido acid chloride **140**. Azide **141** underwent click reaction with linker **114**, to afford the desired 1,2,3-triazole **142** as a 1:1 mixture of epimers.

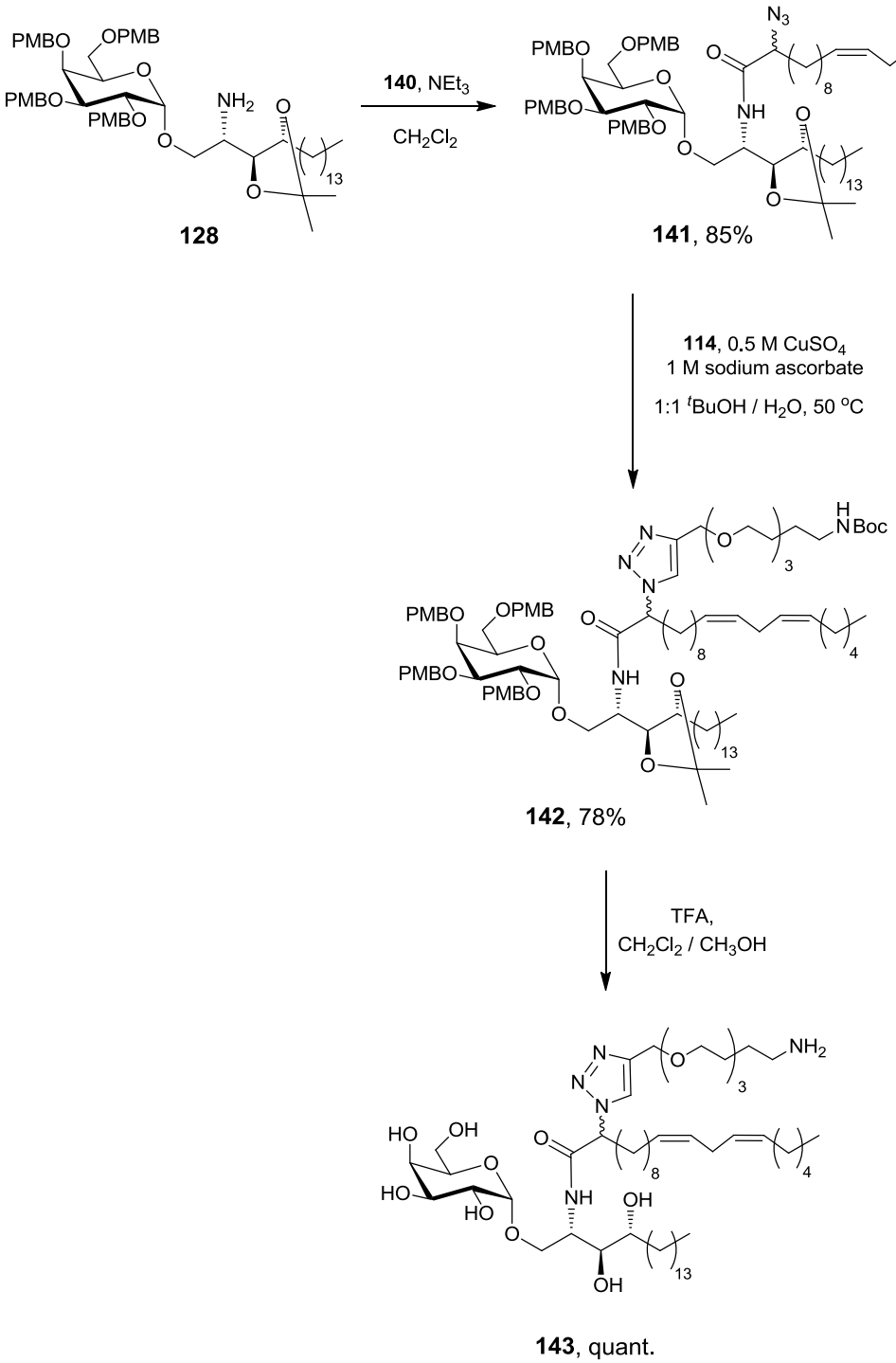

Scheme 3.15. Synthesis of advanced intermediate amine **143**.

Treatment of **142** with TFA and purification by chromatography resulted in amine **143**, as confirmed by HRMS, which was reacted with the succinimidyl ester of Alexa Fluor® 594 carboxylic acid **144** in the presence of NEt_3 in DMF. This reaction was performed as previously on 1 mg (1.2 μmol of Alexa Fluor® 594) scale. The amide product **109** was purified from the starting materials by flash column chromatography using a cartridge prepacked with 100 mg of silica. As was the case for **107** *and* **108**, the small scale of this reaction, working with a mixture of epimers and now regioisomers‡‡ prevented us from obtaining full characterisation data of the product **109**; however in the preliminary biological experiment this labelled glycolipid was found to activate iNKT cells in a similar way as its unlabelled derivative.

‡‡ Alexa Fluor® 594 succinimidyl ester is only available as a mixture of 5- and 6-regioisomers, which after reaction with our amine **143** results in formation of four possible products adding even more complexity to the spectroscopic data.

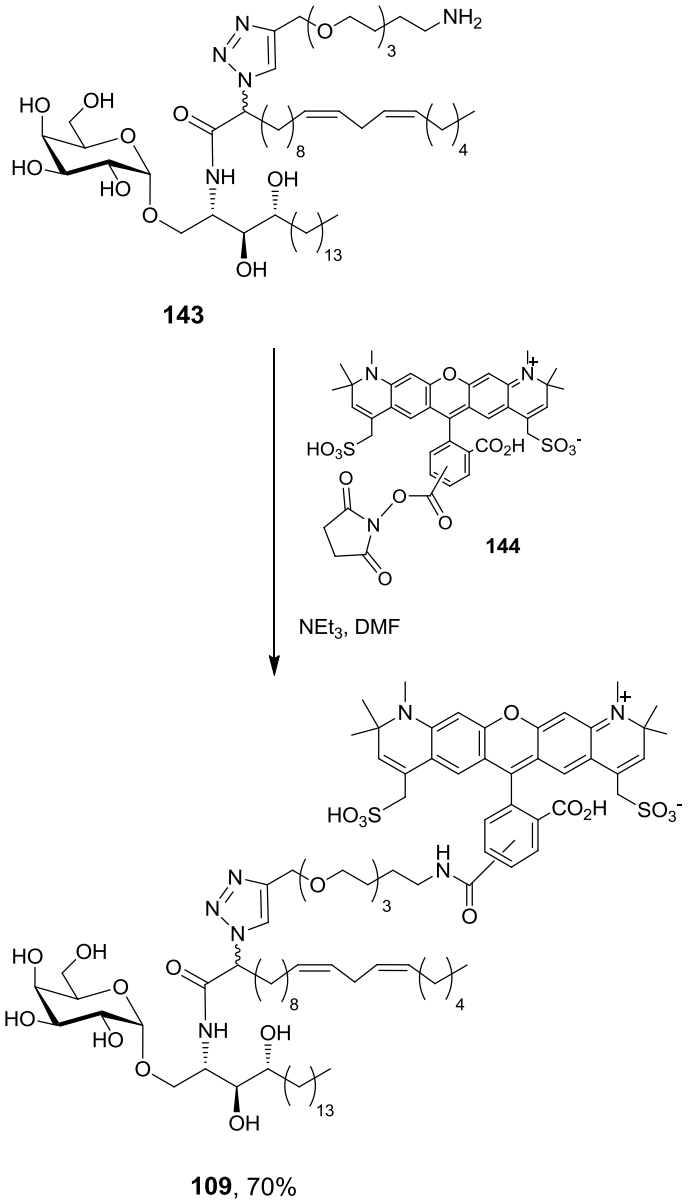

Scheme 3.16. Synthesis of α-GalCer(C20:2) derivative **109** labelled with Alexa 594.

3.8. Synthesis of ThrCer(C20:2) labelled with Alexa 594

Our last target molecule ThrCer(C20:2) labelled with Alexa 594 **110** was prepared in four steps as for α-GalCer derivative **109**. The synthesis of **110** is outlined in Schemes 3.17 and 3.18. Amine **118** was first *N*-acylated with acid chloride **140** to provide amide **145** as a 1:1 mixture of epimers. The product **145** was confirmed by HRMS. Key spectroscopic signals included the amide carbonyl stretch in the IR spectrum at 1660 cm^{-1} and a characteristic azido stretch at 2100 cm^{-1}. The amide functionality was further evidenced in the ^{13}C NMR spectrum, which showed two characteristic quaternary carbon environments of a carbonyl for both epimers at δ 168.9 ppm and at 168.9 ppm. Click reaction of azide **145** and previously prepared alkyne **114** proceeded uneventfully and with complete regioselectivity to afford the desired 1,4-disubstituted triazole **146** as a 1:1 mixture of epimers. Treatment of **146** with TFA afforded amine **147**, which was purified by chromatography and confirmed by HRMS.

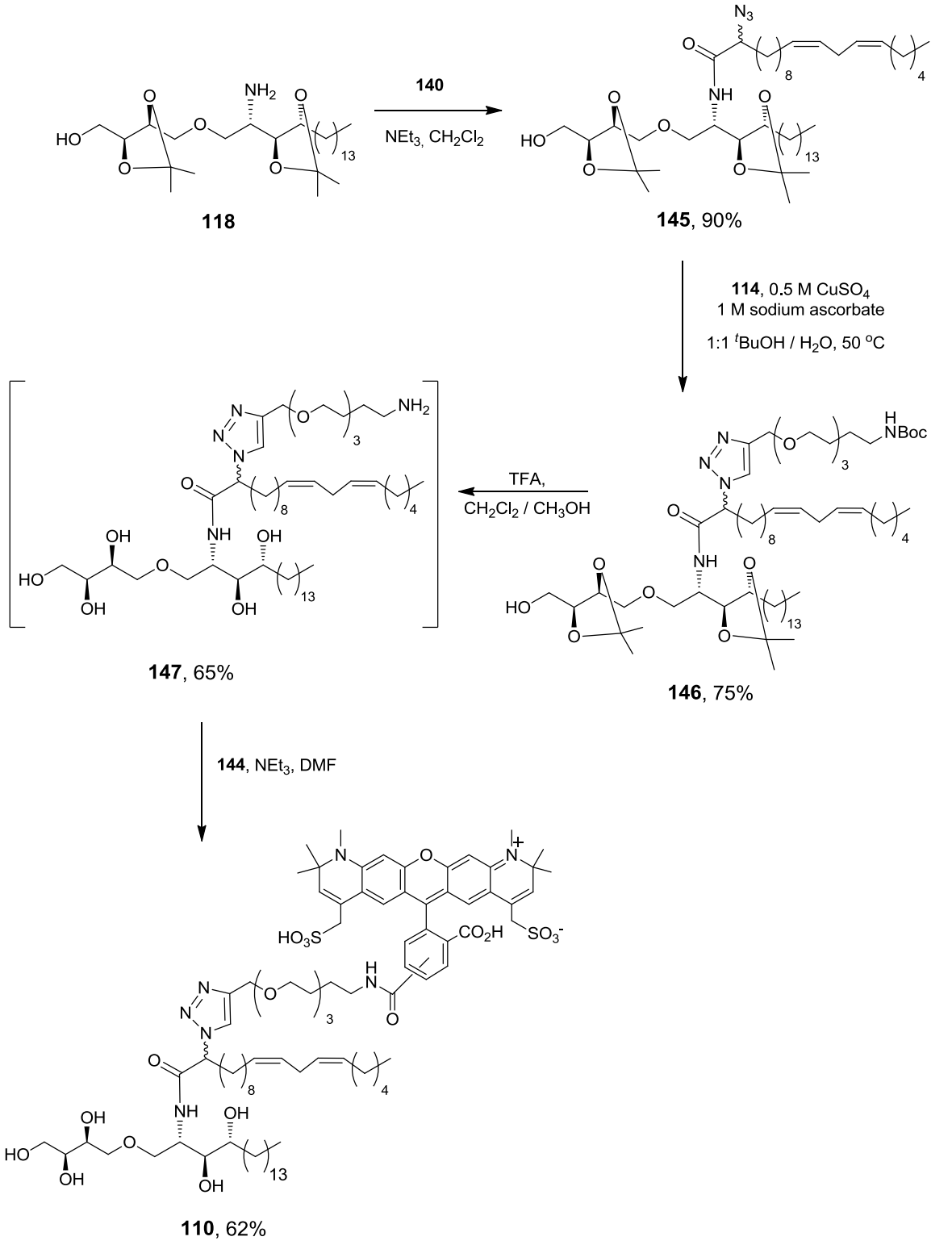

Scheme 3.17. Synthesis of ThrCer(C20:2) derivative **110** labelled with Alexa 594.

Amine **147** was then reacted with the succinimidyl ester of Alexa Fluor® 594 carboxylic acid **144** in the presence of NEt_3 in DMF. This reaction was again performed on 1 mg (Alexa Fluor® 594) scale. The amide product **110** was purified from the starting materials by flash column chromatography using a cartridge pre-packed with 100 mg of silica. As was the case for **107**, the small scale of this reaction, working with a mixture of epimers and regioisomers prevented us from obtaining full characterisation data of the product **110**; however in the preliminary biological experiment this labelled glycolipid was also found to activate iNKT cells in a similar way as its unlabelled derivative ThrCer(C20:2).

Alexa labelled glycolipids **107**, **108**, **109** and **110** were submitted for biological testing, which was carried out in the group of Prof. Vincenzo Cerundolo by Dr John-Paul Jukes and Dr Hemza Ghadbane at the Weatherall Institute of Molecular Medicine in Oxford, UK.

3.9. Biological evaluation of Alexa-labelled glycolipids

The Alexa-conjugated α-GalCer and ThrCer (C26 and C20:2) compounds **107**-**110** were tested for their ability to stimulate iNKT cells. Splenocytes from C57 BL/6 mice were pulsed with various concentrations of ligands. The concentration of IFNγ in the supernatant released after iNKT cell activation was measured using ELISA. The results of these experiments demonstrated that Alexa-conjugated α-GalCer activated iNKT cells, although this was considerably weaker then the parent compound (Figure 3.7 A). Moreover, the Alexa-conjugated ThrCer were found to be inactive when cultured with C57 BL/6 splenocytes (Figure 3.7 A).

In parallel, the Alexa-conjugated α-GalCer and ThrCer (C26 and C20:2) compounds **107**-**110** were further tested for their ability to bind to biotinylated tetramerised human iNKT TCR, as previously described by McCarthy *et al*.[36] Thus, C1R-hCD1d cells were pulsed with lipids to determine the binding affinity of iNKT TCR tetramer (as determined by MFI) by FACS.

The Alexa 594-labelled α-GalCer(C20:2) **109** was shown to bind as well as the parent compound **19** although the Alexa 488-conjugated α-GalCer(C26) **108** bound considerably weaker than its parent compound α-GalCer **8** (Figure 3.7 B). Although the Alexa-conjugated ThrCer derivatives were found to be inactive when cultured with C57 BL/6 splenocytes (Figure 3.7 A), the binding assay showed only moderate binding with the Alexa 594-labelled ThrCer(C20:2) **110**, and this was

considerably weaker for the Alexa 488-conjugated ThrCer(C26) **107**, when compared to the parent compound (Figure 3.6 B).

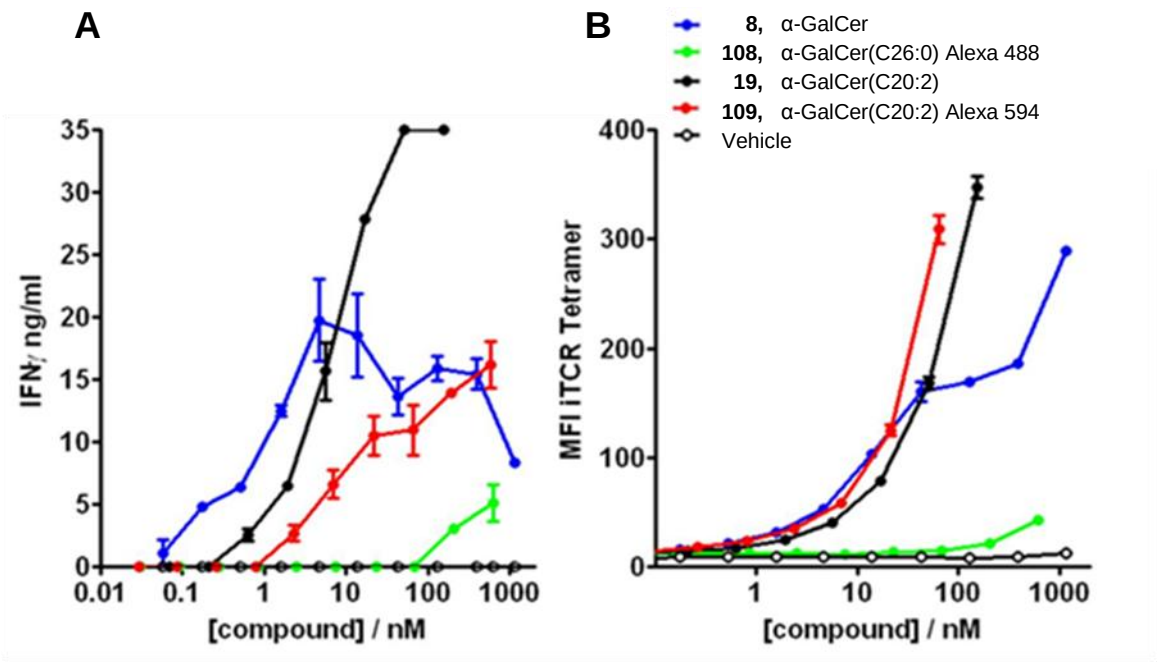

Figure 3.7. **Testing the activation of murine iNKT cells using Alexa-labelled α-GalCer.** Splenocytes from C57BL/6 mice were cultured for 48 hours in the presence of vehicle, α-GalCer(C26) **8**, α-GalCer(C26) Alexa 488 **108**, α-GalCer(C20:2) **19** and α-GalCer(C20:2) Alexa 594 **109** *in vitro* (**A**). The supernatants were analysed for the presence of IFNγ by ELISA. C1R-hCD1d cells were pulsed with vehicle, α-GalCer(C26) **8**, α-GalCer(C26) Alexa 488 **108**, α-GalCer(C20:2) **19** and α-GalCer(C20:2) Alexa 594 **109** to determine the binding affinity using biotinylated tetramerised iNKT TCR. Mean fluorescent intensity (MFI) as determined by fluorescence-activated cell sorting (FACS).

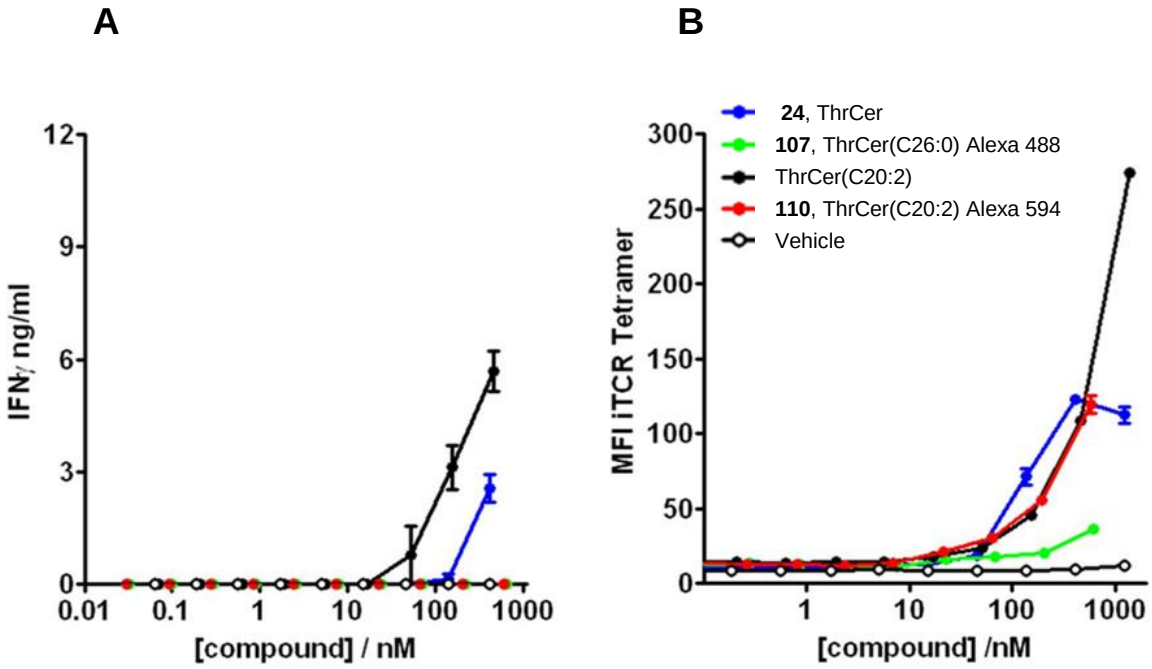

Figure 3.8. **Testing the activation of murine iNKT cells using Alexa-labelled ThrCer.** Splenocytes from C57BL/6 mice were cultured for 48 hours in the presence of vehicle, ThrCer (C26), ThrCer-Alexa 488 (C26), ThrCer (C20:2) and ThrCer-Alexa 594 (C20:2) *in vitro* (**A**). The supernatants were analysed for the presence of IFN-γ by ELISA. C1R-hCD1d cells were pulsed with vehicle, ThrCer (C26), ThrCer-Alexa 488 (C26), ThrCer (C20:2) and ThrCer-Alexa 594 (C20:2) to determine the binding affinity using biotinylated tetramerised iNKT TCR. Mean fluorescent intensity (MFI) as determined by FACS (**B**).

Alexa-594-conjugated α-GalCer(C20:2) **109** showed comparable binding to hCD1d as the parent compound (C20:2) and was able to stimulate murine iNKT cells. However, the Alexa-594-conjugated ThrCer, despite binding in a cell-free system to hCD1d was inactive when tested with murine iNKT cells. Both Alexa-488-conjugated α-GalCer and ThrCer were either significantly weaker (α-GalCer) or

inactive (ThrCer) in comparison to their corresponding parent compound in both assays.

At this stage it is not clear why saturated derivatives **107** and **108** failed to activate iNKT cells whilst their unsaturated analogues showed activity and binding similar (or better) than the parent unlabelled compounds. It is unclear whether the Alexa-488-conjugated analogues compromised binding and hence activation of iNKT cells or whether these compounds require C20:2 ceramides for binding and activity. Future work will assess the choice of the label and its effect on the solubility of the resulting conjugates. It was previously reported by Moqbel and co-workers[171] that in some cases the negative charge of fluorophores may cause a non-specific electrostatic interaction with positively charged cell structures. In these few cases, conventional neutral dyes, such as BODIPY FL, rhodamine, or Texas Red, may be better alternatives.[133] Alexa 488 is doubly negative charged with diethylammonium counter ions, while Alexa 596 comes as a zwitterion. Based on the information provided in the introduction of this Chapter, it may be that the Alexa 594-labelled glycolipids are more easily presented to iNKT TCR at the surface of the cell, while Alexa 488-labelled glycolipids, like α-GalCer **8**, require additional intracellular processing, which proves to be difficult for labelled compounds.

3.10. Conclusions and future work

We successfully synthesised biotinylated ThrCer **106** and showed that attaching a biotin label through a tri(ethylene glycol) spacer to the α-position of the *N*-acyl chain in ThrCer **24** generates a functionally active labelled analogue **106**. Whilst introducing a label at this site necessarily introduces a new stereogenic centre into the molecule, and therefore a mixture of diastereoisomers when racemic azido acid **116** is employed, these two epimers can be separated by careful chromatography.

Continuation of this work in our group has since led to an enantioselective synthesis of (*S*)-2-azido-hexacosanoic acid, which provided biotinylated ThrCer **106** as a single epimer of known configuration, allowing us to confirm the identity of the more active epimer B. Gratifyingly, this more active diastereoisomer corresponded to the more polar epimer prepared using racemic α-azido acid **116**, which is in complete agreement with our predictions that this epimer should better orient the label away from the TCR and therefore have minimal impact on iNKT cell activity.

The synthesis of ThrCer and α-GalCer analogues containing Alexa fluorescent labels proved to be challenging in respect to the small scale of the final step. However, we were able to provide two labelled derivatives that showed activity towards iNKT cells and which might be useful for *in vivo* imaging. The labelled derivatives of α-GalCer and ThrCer need to be further optimised and alternative labels will probably need to be examined. Ongoing work in the group involves

labelling α-GalCer and ThrCer with red Alexa 594, which should allow us to test whether or not the green Alexa 488 was the problem with α-GalCer **108** and ThrCer **107**.

Chapter 4

Synthesis and biological activity of Gal*p*-α-(1→2)-ThrCer

4. Synthesis and biological activity of Gal*p*-α-(1→2)-ThrCer

4.1. Introduction to Gal*p*-α-(1→2)-ThrCer

Among the numerous analogues of α-GalCer, Gal*p*-α-(1→2)-Gal*p*-α-1-Cer **148** (Figure 4.1) has proven to be a valuable tool for studying iNKT cell-mediated immunity. Gal*p*-α-(1→2)-Gal*p*-α-1-Cer **148** is a derivative of α-GalCer **8**, in which the 2'*O*-position of the galactose moiety is α-glycosylated with a second D-galactose unit. Determination of the crystal structure of the iNKT TCR–hCD1d–α-GalCer complex[46] revealed an important role for the free hydroxyl group in the C-2'-position of α-GalCer (see Chapter 1.6), as this forms a hydrogen bond to the side-chain carboxylate of Asp151, which is crucial for the antigenicity of α-GalCer.

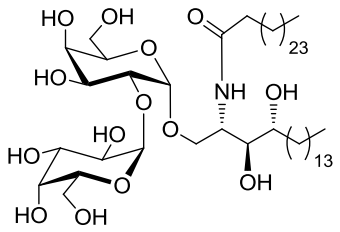

148

Figure 4.1. Structure of Gal*p*-α-(1→2)-Gal*p*-α-1-Cer **148**.

Although some disaccharide glycosphingolipid antigens can be recognised by iNKT TCR without prior processing, the responses to Gal*p*-α-(1→2)-Gal*p*-α-1-Cer **148** require removal of the terminal galactose to permit interaction with the TCR.[172] In this case, a lysosomal enzyme, α-galactosidase A, is responsible for hydrolysing the terminal glycoside and generating the antigenic α-GalCer **8**.

As it requires intracellular processing, Gal*p*-α-(1→2)-Gal*p*-α-1-Cer **148** has proven to be a very useful tool to assess the lipid antigen presentating capacity of professional antigen presenting cells, like dendritic cells.[130] Indeed, it has been shown that cells bearing mutations in enzymes involved in glycosphingolipid processing have altered processing capacity of Gal*p*-α-(1→2)-Gal*p*-α-1-Cer **148** because of engulfment and lysosomal storage.[173] We have observed that presentation of Gal*p*-α-(1→2)-Gal*p*-α-1-Cer requires lipid transfer proteins belonging to the family of saposins.[174] THP1 cells in which prosaposin has been inactivated by lentiviral transduction of shRNA sequences, are impaired in presentation of Gal*p*-α-(1→2)-Gal*p*-α-1-Cer **148** and partly of α-GalCer **8** but not of α-GalCer(C20:2) **19**, which is efficiently loaded from the extracellular milieux.[67] To further investigate the role of saposins in CD1d-mediated lipid antigen presentation, THP1 prosaposin deficient cells were pulsed with the non-glycosidic α-GalCer analogue ThrCer **24**.[123] In addition to being sensitive to cellular fixation, these experiments showed that this lipid is also dependent on saposin activity. We wished to extend these results using a galactosylated derivative of ThrCer.

The synthesis of Gal*p*-α-(1→2)-Gal*p*-α-1-Cer **148** has been recently reported.[175] We decided to prepare the analogous Gal*p*-α-(1→2)-ThrCer **149** (Figure 4.2), which we hoped would provide a similarly useful molecular tool for studying the biological pathways of this important non-glycosidic analogue of α-GalCer. In particular, this glycosylated ThrCer analogue would be useful for studying the kinetics and cellular site of glycolipid loading, which is known to play a critical role in dictating the outcome of iNKT cell activation.[129]

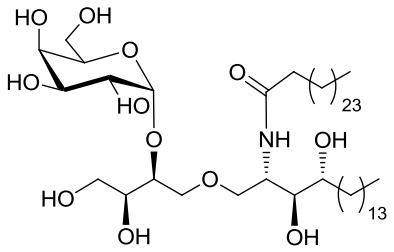

149

Figure 4.2. Structure of target molecule Gal*p*-α-(1→2)-ThrCer **149**.

4.2. Retrosynthetic analysis

The retrosynthesis of Gal*p*-α-(1→2)-ThrCer **149** is summarised in Scheme 4.1. We envisaged that the first step in the synthesis of our target molecule would involve formation of the disaccharide **153**, which would be obtained from commercially available methyl 3,4-*O*-isopropylidene-L-threonate **154** and 2,3,4,6-tetra-*O*-*p*-methoxybenzyl-D-galactose **126**. The key challenge in this step would involve the stereoselective synthesis of the α-glycosidic linkage using a relatively hindered secondary alcohol as the glycosyl acceptor. Reduction of the ester to the primary alcohol in the resulting disaccharide, and formation of the corresponding triflate **152** would then allow a Williamson etherification with a suitably protected phytosphingosine base **78**. Unmasking the amine **150** and acylation with hexacosanoyl chloride **47** would complete the assembly of the four fragments, leaving a one-step global deprotection of the four PMB ether protecting groups and two acetals to deliver our target molecule **149**.

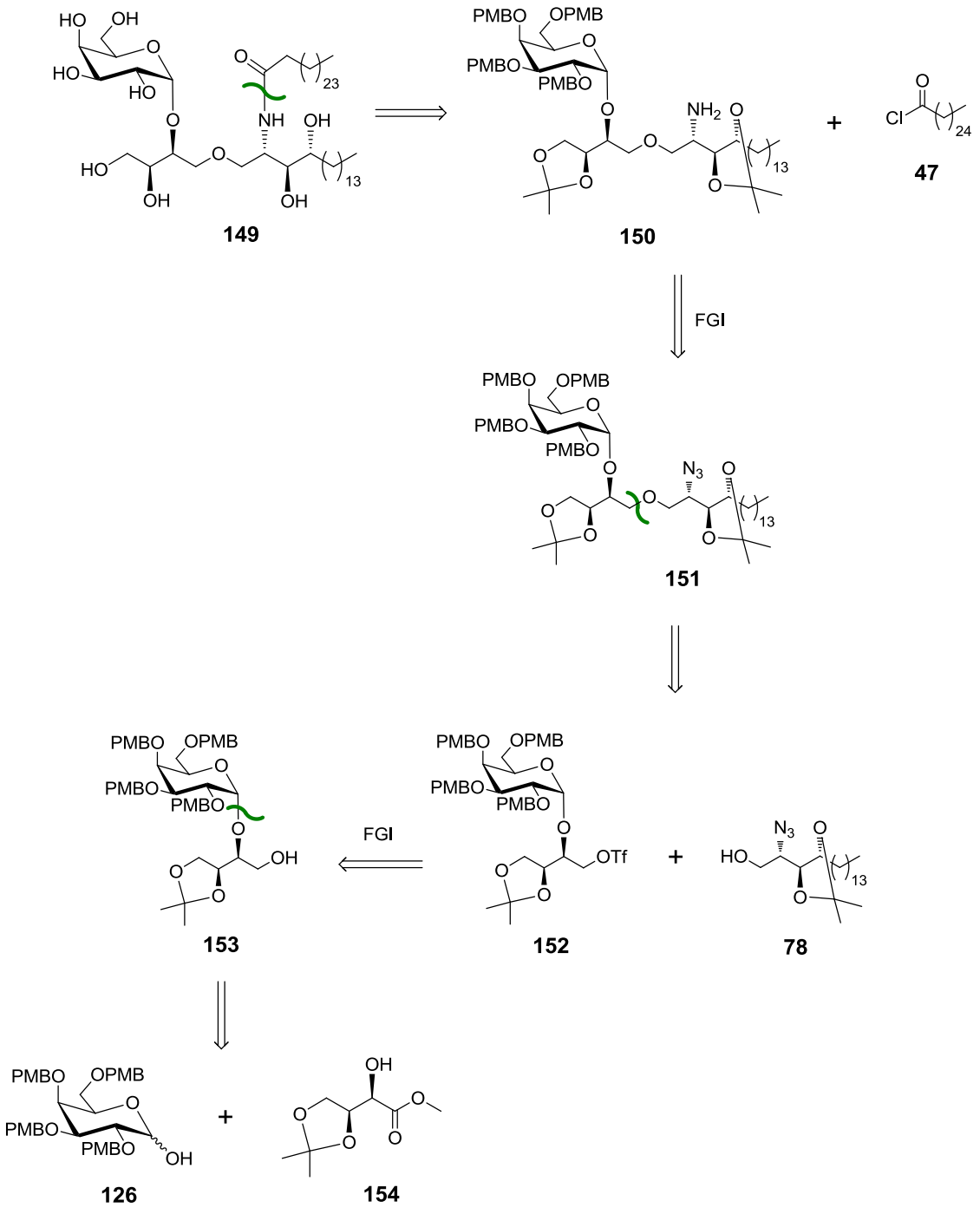

Scheme 4.1. Retrosynthetic analysis of Gal*p*-α-(1→2)-ThrCer **149**.

4.3. Synthesis of Gal*p*-α-(1→2)-ThrCer

In Chapter 3.2 we demonstrated that PMB-protected galactose **126** worked well as the donor in a highly α-stereoselective glycosylation. Reaction of PMB-protected galactose **126** with methyl 3,4-*O*-isopropylidene-L-threonate **154** under our standard glycosylation conditions also provided the desired α-glycoside product **155**. Unfortunately a second α-linked[§§] disaccharide, with the same molecular weight, was also observed in the crude reaction mixture. Although we were unable to separate the two compounds by flash column chromatography, very careful analysis of the NMR spectra of the mixture revealed this second disaccharide product to be α-galactoside **156**. Whilst this compound was the minor product when the reaction was performed on small scale (*e.g.* 0.5 mmol, ratio **155**:**156**, 3:2), it predominated when the glycosylation was scaled up (*e.g.* 1.85 mmol scale, ratio **155**:**156**, 1:3).

[§§] The small vicinal coupling constant between H-1' and H-2' in this disaccharide by-product allowed assignment of the α-configuration [δ_H 5.09 ppm (1H, d, $J_{1,2}$ 3.7 Hz, H-1')].

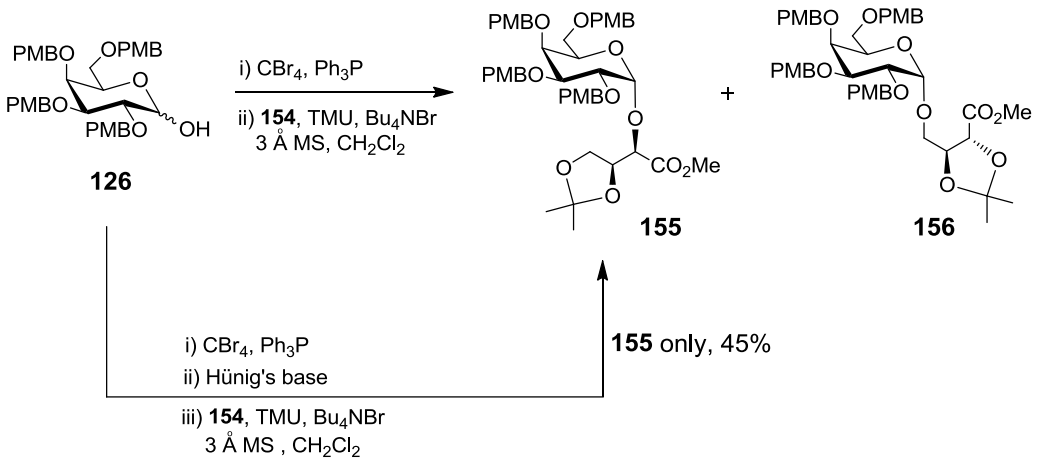

Scheme 4.2. Synthesis of disaccharide **155**.

The easiest resonance to assign in the ^{13}C NMR spectrum of glycosides is the anomeric carbon (C-1'), which usually appears in the region 90-110 ppm. We found two resonances in that region when we analysed a 1:3 mixture of disaccharides **155** and **156**: one resonance for the minor product appeared at δ 96.0 ppm, and a second at δ 98.2 ppm for the major component of the mixture. From this, the corresponding anomeric protons [δ 5.09 ppm (1H, d, *J* 3.7, H-1') and δ 4.91 ppm (1H, d, $J_{1,2}$ 3.5 Hz, H-1'), respectively] were then identified by 2-D chemical shift-correlated spectroscopy (HSQC). Both doublet resonances have small $J_{1,2}$ coupling constants confirming an α-glycosidic linkage in both products. An HMBC experiment revealed strong cross-peaks of $^{3}J_{C\text{-}H}$ coupling for both anomeric carbons, which correlated to two different proton environments in the threitol portion of the molecule (Figure 4.3). The anomeric carbon at δ 98.2 correlated to a proton resonance in the ^{1}H NMR spectrum [δ 3.65 ppm (1H, dd, *J*

11.6, 5.0)], which was assigned by HSQC and COSY experiments as C(4)H_aH_b of the undesired **156** disaccharide. In the same way, the resonance at δ 96.1 ppm correlated to the H2 resonance [δ 4.27 ppm (1H, d, *J* 7.0)]. Thus the major product in this mixture was the undesired disaccharide **156**.

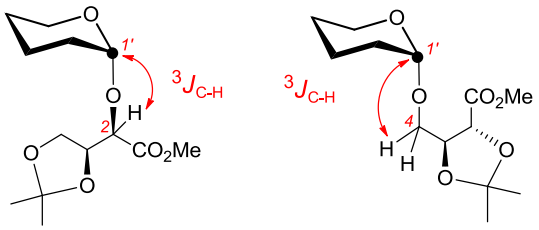

155 minor **156** major

Figure 4.3. HMBC was crucial for assigning the minor **155** and major **156** disaccharides in the mixture.

Aside from generating the reactive glycosyl bromide *in situ,* the Appel agents (PPh_3 and CBr_4) in the glycosylation reaction serve two other useful roles: they function as a scavenger for adventitious water, and when used in excess, are capable of re-generating the active donor from any product that is trapped initially by water rather than the acceptor. However, one of the by-products from this dehydrative glycosylation pathway is HBr, which in our case, presumably catalyses the translational isomerisation of the isopropylidene acetal in **154** from the terminal to the internal 1,2-diol, allowing the remaining primary alcohol to function as a (more reactive) second glycosyl acceptor (Scheme 4.3). Fortunately, we were able to suppress completely this undesirable side-reaction by including Hünig's base as an acid scavenger in the glycosylation reaction mixture.[99] Under

these modified conditions, the desired disaccharide **155** was isolated in a satisfactory 45% yield as a single α-stereoisomer.

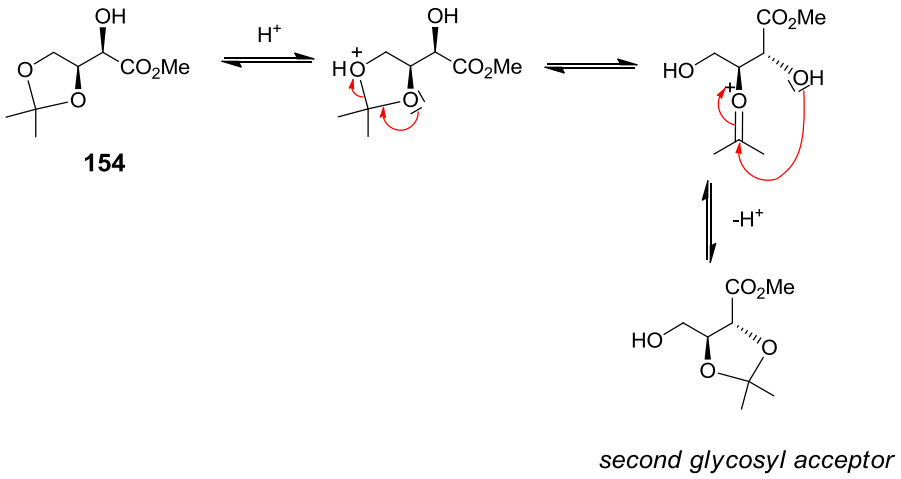

Scheme 4.3. Proposed mechanism of the acid-catalysed isopropylidene acetal migration in **154**.

With disaccharide **155** in hand, reduction of the ester with $LiAlH_4$ afforded primary alcohol **153** in 92% yield. We next decided to combine disaccharide **153** with a phytosphingosine coupling partner using a Williamson etherification. Applying the same method as had been used successfully in the synthesis of ThrCer **24** (see Chapter 2.7), we envisaged converting the primary alcohol of the disaccharide **153** into the corresponding triflate and reacting this with the alkoxide of phytosphingosine **78** would deliver our desired product.

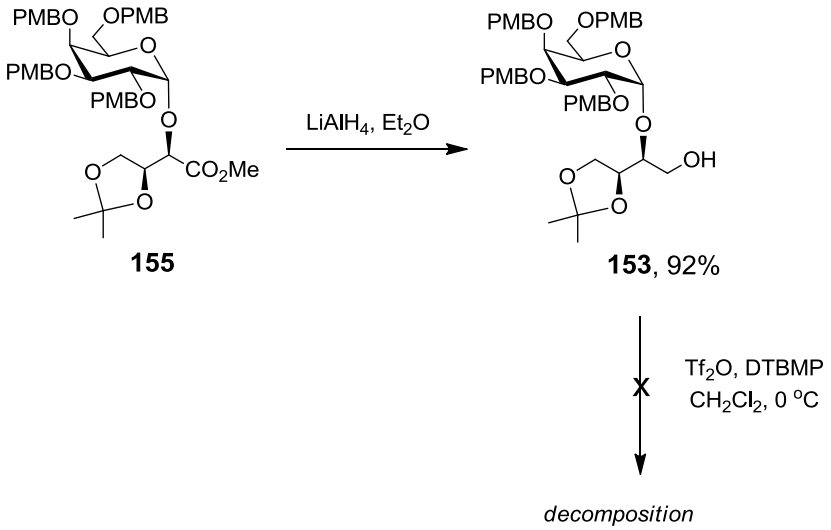

155 **153**, 92%

Scheme 4.4. Unsuccessful attempt at triflate formation using alcohol **153**.

Unfortunately the corresponding triflate **152** proved to be unstable (Scheme 4.4) and we were unable to effect Williamson ether formation. The colour of the reaction mixture turned from colourless to black immediately after adding an equimolar amount of triflic anhydride to the solution of **153** and 2 equivalents of acid scavenger, 2,6-di-*tert*-butyl-4-methylpyridine (DTBMP), at 0 ºC in dichloromethane. TLC analysis of the resulting reaction mixture revealed the formation of more than four by-products, which were difficult to separate. The ^{1}H NMR spectrum of the crude reaction mixture was also too complicated to assign any of the by-products; however, a significant reduction of resonances in the aromatic proton region, when compared with the ^{1}H NMR spectrum of the starting material **153**, suggested partial deprotection of the PMB groups.

We next wanted to check whether or not the etherification step would work if the triflate were formed on the phytosphingosine instead. Applying the same reaction conditions as before, but this time using alcohol **78**, TLC analysis of the reaction mixture showed the formation of a less polar product, suggesting that triflate formation had been successful. However, its reaction with the sodium alkoxide of the alcohol in disaccharide **153** provided none of the desired etherification product.

78

Scheme 4.5. Reversing the electrophile and nucleophile coupling partners failed to provide the desired ether product.

At this juncture, whilst a range of other coupling partners could have been investigated, we had concurrently been investigating the glycosylation reaction using 2,3,4,6-tetra-*O*-benzyl-D-galactose **51** as the latent glycosyl donor. Under our optimised reaction conditions, where Hünig's base was employed as an acid scavenger to prevent acetal migration in the threonate acceptor, the desired disaccharide **157** was obtained in a moderate 45% yield, again as a single α-anomer (Scheme 4.6). We were not surprised that the isolated yield was lower than for the α-selective glycosylation reaction employed in the synthesis of α-GalCer (64%, see Chapter 2.3) as the sterically hindered secondary alcohol of acceptor **154** is less reactive than the primary alcohol of phytosphingosine **78**.

Moreover, separating the product **157** from the unreacted starting materials proved to be difficult, and prevented us from using an excess of the acceptor, which could also account for the observed lower yield.

$LiAlH_4$ effected reduction of the ester in **157** to provide alcohol **158** in 95% yield, which was converted into triflate **159** by treatment with Tf_2O in the presence of the acid scavenger, 2,6-di-*tert*-butyl-4-methylpyridine (DTBMP). As expected, triflate **159** proved to be more stable than its analogue containing PMB protecting groups; however it was still used directly and without purification in the etherification step with the sodium alkoxide of alcohol **78** (Scheme 4.7).[124]

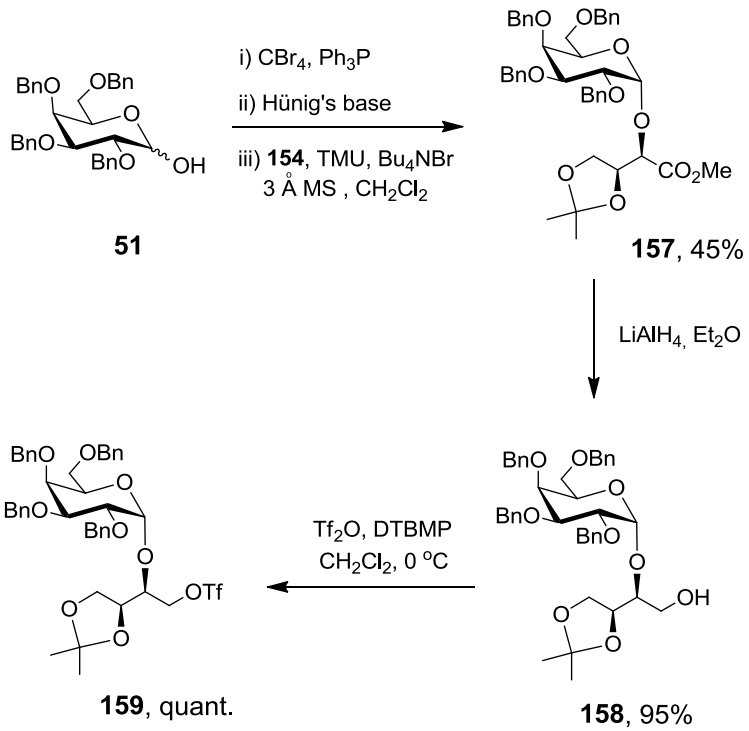

Scheme 4.6. Synthesis of triflate **159**.

Using this pairing, the desired ether **160** was isolated in 72% over the two steps from alcohol **78**. Further processing to the target was straightforward: Staudinger reduction[105,124] of the azide in **160** provided the corresponding amine **161** in 86% yield, which was acylated with hexacosanoyl chloride **47**, prepared as before, from the reaction of hexacosanoic acid with oxalyl chloride,[120] to provide amide **162** in 85% yield. A two-step deprotection involving acetal hydrolysis with aqueous trifluoroacetic acid, followed by hydrogenolysis of the remaining benzyl ethers, delivered our target Gal*p*-α-(1→2)-ThrCer **149** in 75% yield over the two steps (Scheme 4.7).

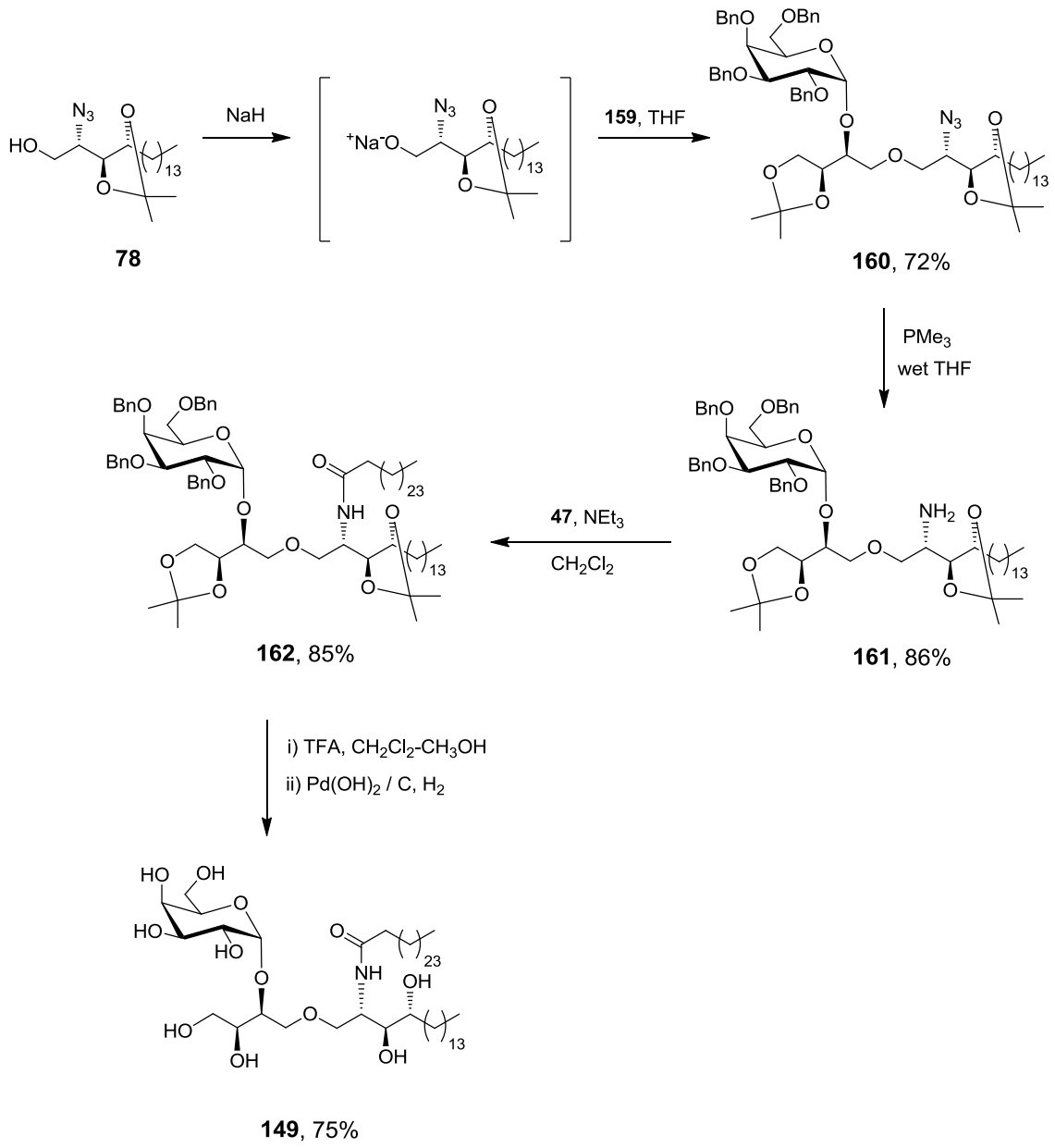

Scheme 4.7. Synthesis of Gal*p*-α-(1→2)-ThrCer **149**.

Our target compound Gal*p*-α-(1→2)-ThrCer **149**, was submitted for biological testing. This work was carried out in the group of Prof. Vincenzo Cerundolo by Dr Mariolina Salio at the Weatherall Institute of Molecular Medicine in Oxford, UK.

4.4. Biological evaluation of Gal*p*-α-(1→2)-ThrCer

Human monocyte-derived dendritic cells (DC) (50000/well) were pulsed with the indicated concentrations of lipids and then a human iNKT cell line was added (30000 cell/well). Supernatants were harvested after 36 hours and assayed for human IFNγ by ELISA.

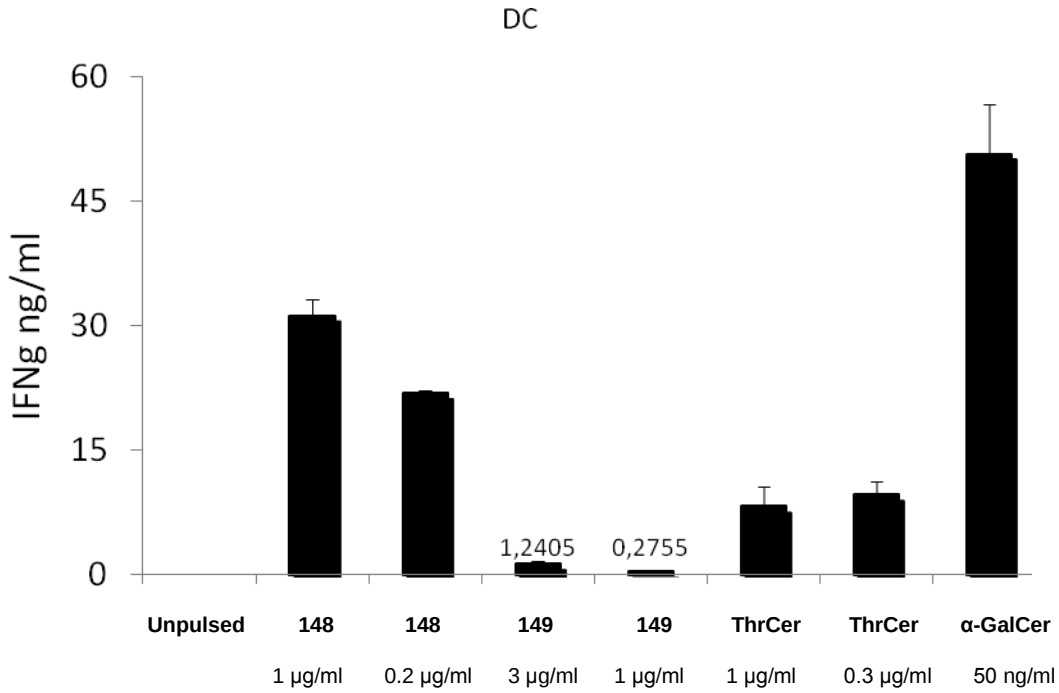

Figure 4.4. **Activation of human iNKT cells using Gal*p*-α-(1→2)-Gal*p*-α-1-Cer, Gal*p*-α-(1→2)-ThrCer, ThrCer, α-GalCer.** C1R-hCD1d cells were pulsed with various concentrations of Gal*p*-α-(1→2)-Gal*p*-α-1-Cer **148**, Gal*p*-α-(1→2)-ThrCer **149**, ThrCer **24**, α-GalCer **8** as indicated and used to stimulate human iNKT cells *in vitro*. The supernatants were tested for IFNγ .

These results demonstrate that Gal*p*-α-(1→2)-ThrCer is presented by DC, albeit weakly, and recognised by iNKT cells.

In another experiment, DC were differentiated from bone marrow precursors of wild type and CD1d/NKT deficient mice for 4 days in 1 ng/ml GM-CSF. DC (33000/well) were pulsed for 16 hours with 20 ng/ml α-GalCer, 200 ng/ml Gal*p*-α-(1→2)-Gal*p*-α-1-Cer, 200 ng/ml ThrCer, 1 µg/ml Gal*p*-α-(1→2)-ThrCer in the presence or absence of 1mM 1-deoxygalactonojirimycin (DGJ) to inhibit α-galactosidase A activity. The cells were extensively washed and incubated with the iNKT hybridoma DN32 (30000 cell/well). Supernatants were harvested after 36 hours and IL-2 secretion measured by ELISA.

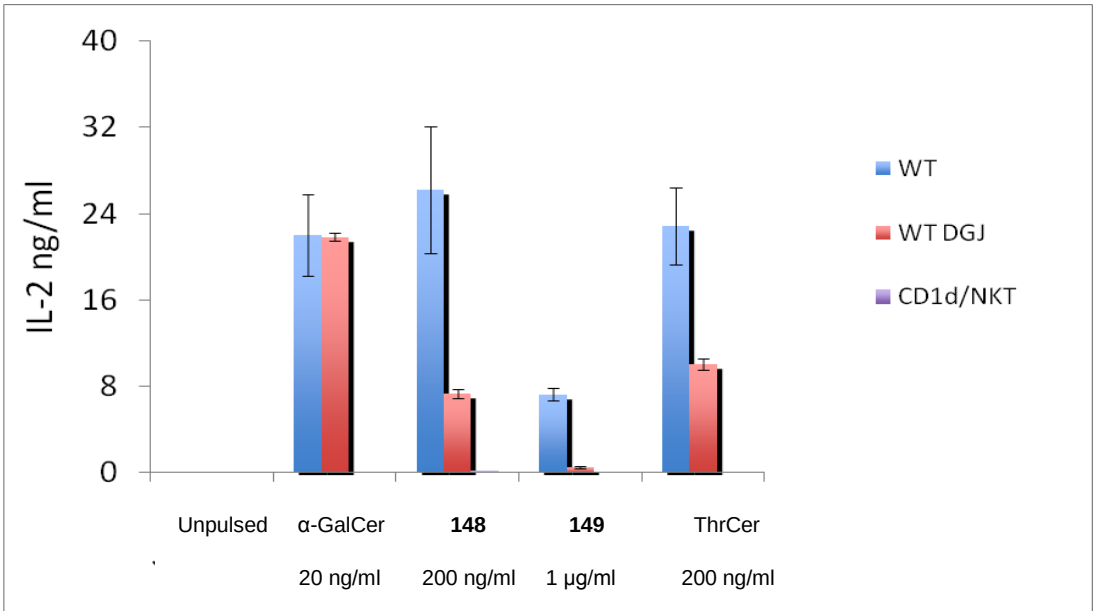

Figure 4.5. **Activation of murine iNKT cells using Gal*p*-α-(1→2)-Gal*p*-α-1-Cer, Gal*p*-α-(1→2)-ThrCer, ThrCer, α-GalCer.** C1R-mCD1d cells were pulsed with various concentrations of Gal*p*-α-(1→2)-Gal*p*-α-1-Cer **148**, Gal*p*-α-(1→2)-ThrCer **149**, ThrCer **24**, α-GalCer **8** as indicated and used to stimulate the DN32 hybridoma *in vitro*. The supernatants were tested for the presence of IL-2.

These results demonstrate that Gal*p*-α-(1→2)-ThrCer is processed in a α-galactosidase A-dependent manner, as presentation is abrogated by treatment with DGJ mice (which are deficient in α-galactosidase A).

4.5. Conclusions and future work

We have successfully completed a stereoselective synthesis of the target molecule Gal*p*-α-(1→2)-ThrCer **149**. In the key step in our synthesis, namely the α-glycosylation, we found that incorporation of an acid scavenger was important to prevent acetal migration in the acceptor **154**.

Preliminary immunological assays have shown that this compound is active and requires intracellular processing by an α-galactosidase enzyme, which requires as cofactor lipid transfer proteins belonging to the saposin family.

Chapter 5

Experimental Section

5. Experimental Section

5.1 General Experimental

Optical rotations were measured using an Optical Activity PolAAr2001 automatic polarimeter. Melting points were determined using open capillaries on a Gallenkamp MPD350 melting point apparatus and are uncorrected. Infrared spectra were recorded either neat as thin films between NaCl discs, on a Perkin Elmer 1600 FTIR spectrometer, or neat on a Perkin Elmer Spectrum 100 fitted with a universal ATR accessory. The intensity of each band is described as s (strong), m (medium) or w (weak), and with the prefix v (very) and suffix br (broad) where appropriate. ^{1}H-NMR spectra were recorded at 500 MHz, 400 MHz, or 300 MHz, using Bruker DRX 500, Bruker AMX 400, Bruker AV 400, Bruker AV 300 and Bruker AC 300 spectrometers. ^{13}C-NMR spectra were recorded at 125 MHz, 100 MHz, or 75 MHz, respectively, using Bruker DRX 500, Bruker AMX 400, Bruker AV 400, Bruker AV 300 and Bruker AC 300 spectrometers. Chemical shifts are reported as values (ppm) referenced to the following solvent signals: $CHCl_3$, δ_H 7.26; $CDCl_3$, δ_C 77.0; CH_3OH, δ_H 3.34; CD_3OD, δ_C 49.9. The term "stack" is used to describe a region where resonances arising from non-equivalent nuclei are coincident, and multiplet, m, to describe a region where resonances arising from a single nucleus (or equivalent nuclei) are coincident but coupling constants cannot be readily assigned. Mass spectra were recorded on a Micromass LCT spectrometer utilising electrospray ionisation (and a MeOH mobile phase), and are reported as (*m/z* (%)). HRMS were recorded on a Micromass LCT spectrometer using a lock mass incorporated into the mobile phase.

All reagents were obtained from commercial sources and used without further purification unless stated otherwise. Anhydrous solvents were purchased from Sigma-Aldrich UK, stored over 4 Å molecular sieves and under an Ar atmosphere. All solutions are aqueous and saturated unless stated otherwise.

Reactions were monitored by TLC using pre-coated aluminium-backed ICN silica plates (60A F_{254}) and visualised by UV detection (at 254 nm) and staining with 5% phosphomolybdic acid in EtOH (MPA spray). Column chromatography was performed on Merck silica gel (particle size 40-63 m mesh) or Fluka 60 (40-60 m mesh) silica gel.

(*2S*,*3S*,*4R*)-*2*-Azido-octadecane-1,3,4-triol (58)

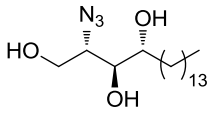

58

Amine **54** (5.00 g, 15.6 mmol), $CuSO_4 \cdot 5H_2O$ (40 mg, 0.16 mmol), and K_2CO_3 (3.23 g, 23.4 mmol) were dissolved in H_2O (50 mL) and the mixture stirred for 10 min at r.t. A solution of imidazole-1-sulfonyl azide hydrochloride[90] (6.00 g, 28.1 mmol, CAUTION: potential explosion risk during purification of this reagent) in CH_2Cl_2 (50 mL) was then added with vigorous stirring. CH_3OH (150 mL) was then added over 30 min through a dropping funnel. After 20 min, the resulting slurry became a transparent pale blue solution, which was stirred vigorously at r.t. for a further 18 h. The mixture was then diluted with $CHCl_3$ (400 mL). The phases were separated and the organic phase was extracted with H_2O (2 × 350 mL). The combined organic phases were dried with Na_2SO_4 and the volatiles were removed under reduced pressure. The crude azide product was re-dissolved in a $CHCl_3$ / CH_2Cl_2 mixture (5:1, 16 mL) and filtered through a silica plug, washing with EtOAc / acetone (9:1) until complete elution of the product. Removal of the solvent under reduced pressure afforded azide **58** as a white solid (4.95 g, 91%): R_f = 0.7 (eluent: EtOAc); mp 92 – 94 °C, (lit. mp 90 °C);[176] $[\alpha]_D^{22}$ + 9.6 (*c* = 1.0, $CHCl_3$) (lit. $[\alpha]_D^{25}$ + 10 (*c* = 1, $CHCl_3$);[177] ν_{max}(film) / cm^{-1} 3261 br (OH), 2916s, 2847s, 2096s (N_3), 1590w, 1461m, 1248m, 1099w, 1058s, 1008m, 923w, 857m, 723s; δ_H(300 MHz, $CDCl_3/CD_3OD$, 2:1) 0.66 (t, *J* 6.5, 3H, C*H*$_3$CH$_2$), 0.95-1.22 (stack, 24H, C*H*$_2$), 1.37-1.42 (stack, 2H, CH(OH)C*H*$_2$CH$_2$), 3.34-3.39 (stack, 3H), 3.58 (dd, *J* 6.1, 5.7,

1H), 3.72 (dd, *J* 3.9, 3.7, 1H); δ_C(75 MHz, $CDCl_3/CD_3OD$, 2:1) 14.4 (CH_3, CH_2CH_3), 23.7 (CH_2), 26.7 (CH_2), 30.5 (CH_2), 30.7 (CH_2), 30.8 (CH_2), 33.1 (CH_2), 33.9 (CH_2), 62.5 (CH_2, CH_2OH), 66.6 (CH, CHN_3), 72.9 (CH, $CHOH$), 76.0 (CH, $CHOH$), some overlap in the methylene resonances; MS (TOF ES+) *m/z* 366.2 ([M + Na]$^+$, 100%); HRMS (TOF ES+) calcd for $C_{18}H_{37}N_3O_3Na$ [M + Na]$^+$ 366.2733, found 366.2728.

Data were in agreement with those reported in the literature.[124,176]

(2*S*,3*S*,4*R*)-2-Azido-1-*O*-trityl-octadecane-1,3,4-triol (59)

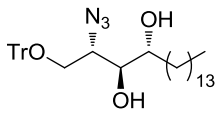

59

TrCl (4.43 g, 15.9 mmol) was added to a solution of alcohol **58** (5.20 g, 15.5 mmol) in pyridine (30 mL) at r.t. The reaction mixture was stirred for 21 h at r.t. and then the solvent was removed under reduced pressure to provide the crude product. Purification by flash column chromatography (15% EtOAc in hexane) afforded trityl ether **59** as a pale yellow oil (5.45 g, 60%): R_f = 0.3 (15% EtOAc in hexane); $[\alpha]_D^{18}$

= +10.5 (*c* = 1.0, $CHCl_3$) (lit. $[\alpha]_D^{20}$ = +8.9 (*c* = 1, $CHCl_3$);[96] ν_{max}(film)/cm^{-1} 3291 (br OH), 2915s, 2848s, 2096m (N_3), 1463m, 1447m, 1249m, 1216w, 1152w, 1099w, 1071m, 1059w, 1010w, 929w, 909w, 757s, 723m, 700s, 667w; δ_H(300 MHz, $CDCl_3$) 0.88 (t, *J* 7.0, 3H, C*H*$_3$CH$_2$), 1.18-1.34 (stack, 23H), 1.36-1.57 (stack, 3H), 1.81 (d, *J* 5.7, 1H, O*H*), 2.35 (d, *J* 5.0, 1H, O*H*), 3.38-3.45 (m, 1H), 3.49-3.59 (stack, 2H), 3.60-3.69 (stack, 2H), 7.20-7.37 (stack, 9H, Ph), 7.40-7.51 (stack, 6H, Ph); δ_C(75 MHz, $CDCl_3$) 14.1 (CH_3, *C*H$_3$CH$_2$), 22.7 (CH_2), 25.6 (CH_2), [29.4, 29.6, 29.7 (CH_2, resonance overlap)], 31.7 (CH_2), 31.9 (CH_2), 62.3 (CH, *C*HN$_3$), 63.5 (CH_2, *C*H$_2$OTr), 72.2 (CH, *C*HOH), 74.2 (CH, *C*HOH), 87.8 (C, *C*Ph$_3$), [127.3, 128.0, 128.5, (CH, Ph)], 137.4 (C, *ipso* Ph); MS (TOF ES+) *m/z* 608.5 ($[M + Na]^+$, 100%); HRMS (TOF ES+) calcd for $C_{37}H_{51}N_3O_3Na$ $[M + Na]^+$ 608.3828, found 608.3836.

Data were in agreement with those reported in the literature.[96]

(2*S*,3*S*,4*R*)-2-Azido-3,4-di-*O*-benzyl-1-*O*-trityl-octadecane-1,3,4-triol (60)

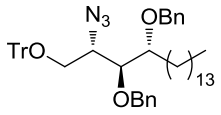

60

NaH (1.095 g of a 60 wt % suspension in mineral oil, 18.24 mmol) was added to a solution of alcohol **59** (4.45 g, 7.60 mmol) in DMF (38 mL) at r.t. The reaction mixture was stirred for 30 min and then cooled to 0 °C. BnBr (1.99 mL, 16.7 mmol) was added dropwise over 3 min and the reaction mixture was stirred for 15 h at r.t. H_2O (40 mL) was then added and the mixture was extracted with Et_2O (2 × 20 mL) and then dried over Na_2SO_4. The drying agent was removed by filtration and the filtrate concentrated under reduced pressure. Purification of the residue by flash column chromatography (5% EtOAc in hexane) afforded dibenzyl ether **60** as a yellow oil (4.66 g, 80%): R_f = 0.3 (5% EtOAc in hexane); $[\alpha]_D^{18}$ = +4.9 (*c* = 1, $CHCl_3$) (lit. $[\alpha]_D^{20}$ = +6.4 (*c* = 1, $CHCl_3$));[96] ν_{max}(film)/cm^{-1} 2923s, 2853s, 2095s (N_3), 1491m, 1449m, 1315w, 1265w, 1209w, 1065s, 899w, 744m, 696s, 632m; δ_H(300 MHz, $CDCl_3$) 0.88 (t, *J* 6.9, 3H, C*H*$_3$CH$_2$), 1.14-1.34 (stack, 23H), 1.35-1.62 (stack, 3H), 3.32-3.41 (stack, 2H), 3.43-3.57 (stack, 3H), 4.37-4.60 (stack, 4H, C*H*$_2$Ph), 7.04-7.11 (stack, 3H, Ph), 7.14-7.32 (stack, 15H, Ph), 7.35-7.47 (stack, 7H, Ph); δ_C(75 MHz, $CDCl_3$) 14.1 (CH_3, *C*H$_3$CH$_2$), 22.7 (CH_2), 25.3 (CH_2), [29.4, 29.7 (CH_2, resonance overlap)], 31.9 (CH_2), 63.2 (CH, *C*HN$_3$), 64.3 (CH_2,

CH_2OTr), 72.0 (CH_2, *C*H_2Ph), 73.5 (CH_2, *C*H_2Ph), 79.2 (CH, *C*HOBn), 79.4 (CH, *C*HOBn), 87.2 (C, *C*Ph_3), [127.0, 127.5, 127.6, 127.8, 128.2, 128.3, 128.7 (CH, Ph, resonance overlap)], 137.9 (C, *ipso* Ph), 138.3 (C, *ipso* Ph,), 143.7 (C, *ipso* Ph); MS (TOF ES+) *m/z* 788.5 ([M + Na]$^+$, 100%); HRMS (TOF ES+) calcd for $C_{51}H_{63}N_3O_3Na$ [M + Na]$^+$ 788.4767, found 788.4774.

Data were in agreement with those reported in the literature.[96]

(2*S*,3*S*,4*R*)-2-Azido-3,4-di-*O*-benzyl-octadecane-1,3,4-triol (52)

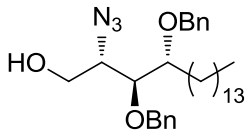

52

A solution of trityl ether **60** (4.61 g, 6.02 mmol) and *p*-TsOH (170 mg, 0.90 mmol) in CH_2Cl_2 / MeOH (60 mL, 3:1) was stirred for 16 h at r.t. The reaction mixture was then washed with $NaHCO_3$ solution (20 mL). The phases were separated and the aqueous phase was extracted with EtOAc (2 × 20 mL) and dried over Na_2SO_4. The drying agent was removed by filtration and the filtrate concentrated under reduced pressure. Purification of the residue by flash column chromatography

(10% EtOAc in hexane) afforded alcohol **52** as a colourless oil (84%, 2.65 g): R_f = 0.2 (10% EtOAc in hexane); $[\alpha]_D^{17}$ = + 5.5 (*c* 1, $CHCl_3$) (lit. $[\alpha]_D^{20}$ = + 5.7 (*c* = 1, $CHCl_3$));[96] ν_{max}(film)/cm^{-1} 3428m (br, OH), 3088w, 3063m, 3030m, 2603, 2532w, 2496w, 2366w, 2335w, 2099s (N_3), 1944w, 1887w, 1810w, 1741w, 1682w, 1644w, 1606w, 1496m, 1454s, 1326m, 1264m, 1208m, 1071s, 1028s, 912w, 844w, 735s, 697s, 608m; δ_H(300 MHz, $CDCl_3$) 0.89 (t, *J* 6.4, 3H, C*H*$_3$), 1.18-1.48 (stack, 24H, alkyl chain), 1.50-1.62 (m, 1H), 1.63-1.75 (m, 1H), 2.55 (app t, *J* 6.6, 1H, O*H*), 3.61-3.74 (stack, 3H), 3.75-3.84 (m, 1H), 3.86-3.95 (m, 1H), 4.55-4.65 (stack, 2H, OC*H*$_2$Ph), 4.66-4.74 (stack, 2H, OC*H*$_2$Ph), 7.31-7.37 (stack, 10H, Ph); δ_C(75 MHz, $CDCl_3$) 14.1 (CH_3, CH_2CH_3), [22.6, 25.4, 29.3, 29.6, 30.1, 31.9 (CH_2, alkyl chain, resonance overlap)], 62.1 (CH_2, CH_2OH), 63.1 (CH, CHN_3), 72.3 (CH_2, CH_2Ph), 73.5 (CH_2, CH_2Ph), 78.9 (CH, *C*HOBn), 80.1 (CH, *C*HOBn), [127.7, 127.9, 128.0, 128.3, 128.4 (CH, Ph, resonance overlap)], 137.4 (C, *ipso* Ph), 137.9 (C, *ipso* Ph); MS (TOF ES+) *m/z* 546.3 ($[M + Na]^+$, 100%); HRMS (TOF ES+) calcd for $C_{32}H_{49}N_3O_3Na$ $[M + Na]^+$ 546.3672, found 546.3657.

Data were in agreement with those reported in the literature.[96]

(2*S*,3*S*,4*R*)-2-Azido-3,4-*O*-isopropylidene-octadecane-1,3,4-triol (78)

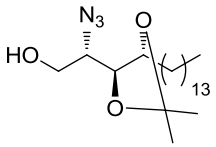

78

98% H_2SO_4 (200 µL) was added dropwise over 2 min to a solution of triol **58** (509 mg, 1.49 mmol) in dry acetone (10 mL) at 0 °C. After 30 min, the reaction mixture was carefully poured into saturated NaOH solution (1 mL), and then evaporated to dryness under reduced pressure. The residue was extracted with EtOAc (15 mL). The organic phase was washed with brine (3 mL), and then dried over Na_2SO_4. Concentration of the filtrate under reduced pressure and purification of the residue by flash column chromatography afforded acetal **78** as a white, low-melting point, amorphous solid (412 mg, 72%): R_f = 0.3 (25% EtOAc in hexane); $[\alpha]_D^{21}$ = +27.5 (*c* = 1.0, $CHCl_3$) (lit. $[\alpha]_D^{22}$ +23 (*c* = 1.0, $CHCl_3$);[124] ν_{max}(film) / cm^{-1} 3414 br (OH), 2919s, 2850s, 2095s (N_3), 1471m, 1382m, 1370m, 1261m, 1208m, 1102m, 1019s, 883m, 826w, 718m; δ_H(300 MHz, $CDCl_3$) 0.88 (t, *J* 6.0, 3H, CH_2CH_3), 1.26-1.30 (stack, 23H), 1.34 (s, 3H, 1 × $C(CH_3)_2$), 1.43 (s, 3H, 1 × $C(CH_3)_2$), 1.50-1.63 (stack, 3H), 2.08 (app. t, *J* 6.0, 1H, CH_2OH), 3.44-3.50 (m, 1H), 3.83-3.91 (m, 1H), 3.94-4.03 (stack, 2H), 4.15-4.21 (m, 1H); δ_C(75 MHz, $CDCl_3$) 14.1 (CH_3, CH_2CH_3), 25.5 (CH_3, 1 × $C(CH_3)_2$), 26.5 (CH_2), 28.0 (CH_3, 1 × $C(CH_3)_2$), 29.35 (CH_2), 29.41 (CH_2), 29.53 (CH_2), 29.58 (CH_2), 29.59 (CH_2), 29.65 (CH_2), 29.68 (CH_2), 29.69 (CH_2), 31.9 (CH_2), 61.2 (CH, CHN_3), 63.9 (CH_2, CH_2OH), 76.6 (CH, *C*HO), 77.7 (CH, *C*HO), 108 (C, $C(CH_3)_2$), some overlap in the methylene resonances; MS (TOF

ES+) *m/z* 406.2 ([M + Na]$^+$, 100%); HRMS (TOF ES+) calcd for $C_{21}H_{41}N_3O_3Na$ [M + Na]$^+$ 406.3046, found 406.3033.

Data were in agreement with those reported in the literature.[124]

(2*S*,3*R*,4*R*)-2-Azido-3,4-di-*O*-benzyl-1-*O*-(2',3',4',6'-tetra-*O*-benzyl-α-D-galactopyranosyl)octadecane-1,3,4-triol (50)

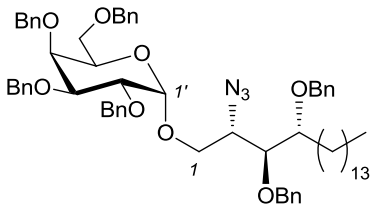

50

Ph_3P (1.46 g, 5.55 mmol) and CBr_4 (1.84 g, 5.55 mmol) were added sequentially to a solution of 2,3,4,6-tetra-*O*-benzyl-D-galactose **51** (1.00 g, 1.85 mmol) in CH_2Cl_2 (10 mL) at r.t. The reaction mixture was stirred for 3 h. In separate flasks, a solution of tetramethyl urea (TMU) (1.2 mL) and Bu_4NBr (1.79 g, 5.55 mmol) in CH_2Cl_2 (5 mL), and a solution of azide **52** (1.46 g, 2.78 mmol) in CH_2Cl_2 (5 mL), were stirred over activated 3 Å MS for 30 min, after which time, these solutions were added dropwise (15 min) *via* syringe sequentially (TMU/Bu_4NBr solution first) to the solution containing the glycosyl donor. The reaction mixture was stirred at r.t. for 3 d until the donor was no longer being consumed (as judged by TLC). The

reaction mixture was then filtered through a silica plug, washed with CH_2Cl_2 (1.2 L) and concentrated under reduced pressure to provide the crude product. Purification of the residue by flash column chromatography (8% EtOAc in hexane) afforded glycoside **50** as a colourless oil (1.21 g, 62%, α-anomer only): R_f = 0.3 (8% EtOAc in hexane); $[\alpha]_D^{18}$ + 22 (*c* 1.4, CH_2Cl_2) (lit $[\alpha]_D^{20}$ = + 26 (*c* 1.4, CH_2Cl_2));[178] ν_{max}(film)/cm^{-1} 2988s, 2972s, 2923s, 2854m, 2097m (N_3), 1721m, 1704m, 1602w, 1585w, 1496w, 1454m, 1405m, 1394m, 1380m, 1314m, 1262s, 1155m, 1066s, 1056s, 1027s, 904m, 805m, 734s, 711s; δ_H(500 MHz, $CDCl_3$) 0.90 (3H, t, *J* 6.9, CH_2CH_3), 1.20-1.35 (23H, stack, alkyl chain methylenes), 1.35-1.45 (m, 1H, alkyl chain CH_aH_b), 1.50-1.58 (m, 1H, C(5)H_aH_b), 1.63-1.71 (m, 1H, C(5)H_aH_b), 3.47-3.54 (stack, 2H, C(6')H_aH_b), 3.60-3.63 (m, 1H, H-4), 3.71-3.76 (stack, 3H, C(1)H_aH_b, H-2, H-3), 3.94-3.98 (stack, 2H, H-4', H-5'), 3.98-4.04 (stack, 2H, H-3', C(1)H_aH_b), 4.08 (dd, *J* 10.0, 3.5, 1H, H-2'), 4.37 (A of AB, *J* 11.8, 1H, C(6')OCH_aH_bPh), 4.45 (B of AB, *J* 11.8, 1H, C(6')OCH_aH_bPh), 4.48 (A of AB, *J* 11.6, 1H, C(4)OCH_aH_bPh), 4.57-4.59 (stack, 2H, C(4)OCH_aH_bPh, C(4')OCH_aH_bPh), 4.63 (A of AB, *J* 11.3, 1H, C(3)OCH_aH_bPh), 4.67 (B of AB, *J* 11.3, 1H, C(3)OCH_aH_bPh), 4.69 (A of AB, *J* 12.0, 1H, C(2')OCH_aH_bPh), 4.74 (A of AB, *J* 11.5, 1H, C(3')OCH_aH_bPh), 4.81 (B of AB, *J* 12.0, 1H, C(2')OCH_aH_bPh), 4.84 (B of AB, *J* 11.5, 1H, C(3')OCH_aH_bPh), 4.91 (d, *J* 3.5, 1H, H-1'), 4.95 (d, *J* 11.5, 1H, C(4')OCH_aH_bPh), 7.22-7.40 (stack, 30H, 6 $\times$ Ph); δ_C(125 MHz, $CDCl_3$) 14.1 (CH_3, CH_2CH_3), [22.6, 25.3, 29.3, 29.6, 29.9, 31.9 (CH_2, alkyl chain, resonance overlap)], 61.9 (CH, C-2), 68.4 (CH_2, C-1), 68.9 (CH_2, C-6'), 69.6 (CH, C-5'), 71.9 (CH_2, C(4)OCH_2Ph), 73.0 (CH_2, C(3')OCH_2Ph), 73.1 (CH_2, C(2')OCH_2Ph), 73.3 (CH_2, C(6')OCH_2Ph), 73.6 (CH_2, C(3)OCH_2Ph), 74.7 (CH_2, C(4')OCH_2Ph), 75.0

(CH, C(4')), 76.3 (CH, C(2')), 78.7 (CH, C(3')), 78.8 (CH, C(3)), 79.2 (CH, C(4)), 98.6 (CH, C(1')), [127.3, 127.4, 127.56, 127.60, 127.7, 127.8, 128.1, 128.2 (CH, Ph, resonance overlap)], 137.9 (C, *ipso* Ph), 138.0 (C, *ipso* Ph), 138.3 (C, *ipso* Ph), 138.58 (C, *ipso* Ph), 138.63 (C, *ipso* Ph), 138.7 (C, *ipso* Ph); MS (TOF ES+) *m/z* 1068.8 ([M + Na]$^+$, 100%); HRMS (TOF ES+) 1068.6063 [M + Na]$^+$, $C_{66}H_{83}N_3O_8Na$ requires 1068.6078; and then unreacted azide **52** was also recovered (445 mg, 45%).

Data were in agreement with those reported in the literature for **50** prepared by a different route.[178]

(2*S*,3*S*,4*R*)-2-Amino-3,4-di-*O*-benzyl-1-*O*-(2',3',4',6'-tetra-*O*-benzyl-α-D-galactopyranosyl)octadecane-1,3,4-triol (46)

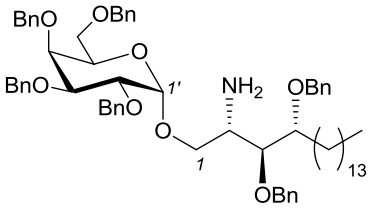

46

PMe_3 (455 μL of a 1.0 M soln in THF, 0.46 mmol) was added dropwise over 5 min to a solution of azide **50** (433 mg, 0.414 mmol) in THF (3.5 mL). The reaction mixture was stirred at r.t. for 4 h after which time, H_2O (3 mL) was added. The

reaction mixture was stirred for 1 h and then concentrated under reduced pressure. The residual H_2O was removed by co-evaporation with toluene (3 × 3 mL) to provide the crude product. Purification of the residue by flash column chromatography (35% EtOAc in hexane) afforded amine **46** as a white solid (300 mg, 72%), which was used directly without further purification. Selected data: R_f = 0.3 (35% EtOAc in hexane); MS (TOF ES+) *m/z* 1020.5 ($[M + H]^+$, 100%); HRMS (TOF ES+) calcd for $C_{66}H_{86}NO_8$ $[M + H]^+$ 1020.6353, found 1020.6357.

(2*S*,3*S*,4*R*)-3,4-Di-*O*-benzyl-1-*O*-(2',3',4',6'-tetra-*O*-benzyl-α-D-galacto-pyranosyl)-2-(hexacosanoylamino)octadecane-1,3,4-triol (62)

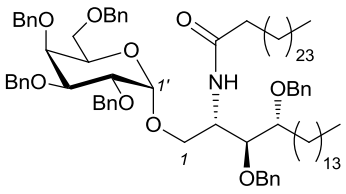

62

A screw-capped glass tube containing a solution of hexacosanoic acid **61** (240 mg, 0.580 mmol) in $(COCl)_2$ (2.0 mL, 23 mmol) was closed tightly and heated at 70 °C for 2 h. After 2 h, the volatiles were removed under a stream of N_2 and the residual solvent removed on the vacuum line (1 h) to provide hexacosanoyl chloride **47** as a pale yellow oil, which was used directly in the next step without further purification (265 mg, quant.): a solution of freshly prepared hexacosanoyl

chloride (265 mg, 0.58 mmol) in CH_2Cl_2 (1.5 mL) was added dropwise over 2 min to an ice-cooled solution of amine **46** (500 mg, 0.49 mmol) and NEt_3 (136 μL, 0.98 mmol) in CH_2Cl_2 (3.5 mL) at 0 ºC. The reaction mixture was stirred at r.t. for 8 h and then diluted with CH_2Cl_2 (20 mL), washed sequentially with $NaHCO_3$ solution (20 mL), brine (4 mL) and then dried over Na_2SO_4. The drying agent was removed by filtration and the filtrate concentrated under reduced pressure. Purification of the residue by flash column chromatography (12% EtOAc in hexane) afforded amide **62** as a white solid (582 mg, 85%): R_f = 0.3 (15% EtOAc in hexane); $[\alpha]_D^{20}$ = + 31.2 (*c* 1, $CHCl_3$) (lit. $[\alpha]_D^{24}$ = + 18.8 (*c* 0.9, $CHCl_3$);[179] mp 75 – 76 ºC (lit. mp 74 – 75 ºC);[179] ν_{max}(film)/cm^{-1} 2918s, 2850s, 1647m (C=O), 1531w, 1496w 1469m, 1454m, 1349w, 1206w, 1115s, 1058s, 952m, 776w, 735s, 695s; δ_H(300 MHz, $CDCl_3$) 0.88 (6H, t, *J* 6.9, 2 × CH_2CH_3), 1.16-1.34 (69H, stack, alkyl chain methylenes), 1.37-1.57 (2H, stack), 1.58-1.72 (1H, m), 1.85-2.00 (2H, stack), 3.36-3.43 (1H, m), 3.44-3.53 (2H, stack), 3.69-3.76 (1H, m), 3.83-3.96 (4H, stack), 3.99-4.08 (2H, stack), 4.09-4.20 (1H, m), 4.32-4.47 (2H, stack), 4.48-4.67 (4H, stack), 4.70-4.86 (6H, stack), 4.92 (1H, d, *J* 11.7), 6.12 (1H, d, *J* 8.7, N*H*), 7.20-7.37 (30H, stack); δ_C(75 MHz, $CDCl_3$) 14.1 (CH_3), 14.7 (CH_3), [22.7, 25.7, 26.1, 29.3, 29.4, 29.7, 31.9, 36.7 (CH_2, alkyl chain, resonance overlap)], 50.3 (CH), 69.6 (CH_2), 69.96 (CH_2), 70.05 (CH), 71.7 (CH_2), 71.8 (CH_2), 72.9 (CH_2), 73.4 (CH_2), 73.6 (CH_2), 73.7 (CH), 74.8 (CH_2), 74.9 (CH), 78.6 (CH), 78.9 (CH), 80.1 (CH), 99.6 (CH, C-1'), [127.4, 127.6, 127.8, 128.2, 128.3 (CH, Ph, resonance overlap)], [137.5, 138.4, 138.5, 138.6 (C, *ipso* Ph, resonance overlap)], 172.8 (C, *C*=O); MS (TOF ES+) *m/z* 1421.6 ($[M + Na]^+$, 100%).

Data were in agreement with those reported in the literature for **62** prepared by a different route.[179]

General procedure for catalytic hydrogenolysis: $Pd(OH)_2/C$ or Pd/C (0.05 eq per benzyl group) was added to a solution of the benzylated compound in THF (0.01 M). H_2 gas was bubbled through the stirred suspension. The progress of the reaction was monitored by TLC. On completion, the reaction mixture was filtered through a plug of Celite, washed with THF and then $CHCl_3$/MeOH (90/10, v/v), and concentrated under reduced pressure to provide the crude product, which was purified by flash column chromatography.

(2*S*,3*S*,4*R*)-1-*O*-(α-D-Galactopyranosyl)-2-(hexacosanoylamino)octadecane-1,3,4-triol (α-GalCer, 8)

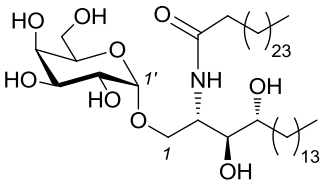

8

Experimental details for the conversion of 62 to 8

Amide **8** (α–GalCer) was prepared from perbenzylated amide **62** (180 mg, 0.129 mmol) and Pd/C (85 mg, 10% wet) in THF (10 mL) according to the general procedure. After 22 h, work-up and purification by flash column chromatography (8% MeOH in $CHCl_3$) afforded amide **8** as an amorphous white solid (75 mg, 68%).

Experimental details for the conversion of 81 to 8

TFA (150 μL) was added dropwise over 1 min to a solution of acetal **81** (120 mg, 0.095 mmol) in CH_2Cl_2 / H_2O (10:1, 0.9 mL). After stirring for 2 h at r.t., the reaction mixture was concentrated under reduced pressure and the residual TFA was removed by co-evaporation with Et_2O (3 × 3 mL) to provide the crude acetal hydrolysis product as a white solid (116 mg, quant.), which was then treated with $Pd(OH)_2/C$ (30 mg, 10% wet) in THF (10 mL) according to the general hydrogenolysis procedure. After 8 h, work-up and purification by flash column

chromatography (8% MeOH in $CHCl_3$) afforded amide **8** as a white solid (61 mg, 75%): R_f = 0.3 (10% MeOH in $CHCl_3$); $[\alpha]_D^{20}$ = + 15.2 (*c* 1, 2:1 $CHCl_3/CH_3OH$) (lit. $[\alpha]_D^{23}$ = + 43.6 (*c* 1, pyridine);[143] mp 188 – 189 °C (lit. mp 189 – 190 °C);[180] ν_{max}(film) / cm^{-1} 3313br (OH), 2918s, 2850s, 1642m (C=O), 1548w, 1468m, 1261m, 1027s, 800s, 721m, 600w; δ_H(400 MHz, 2:1 $CDCl_3/CD_3OD$) 0.83 (6H, t, *J* 6.7, 2 × CH_2CH_3), 1.16-1.40 (68H, stack, alkyl chain methylenes), 1.45-1.63 (4H, stack), 2.16 (2H, app. t, *J* 7.8), 3.46-3.57 (2H, stack), 3.60-3.79 (6H, stack), 3.80-3.87 (1H, m), 3.90 (1H, d, *J* 2.5), 4.11-4.18 (1H, m), 4.86 (1H, d, *J* 3.7), O*H* and N*H* resonances not observed; δ_C(100 MHz, 2:1 $CDCl_3/CD_3OD$) 14.3 (CH_3, 2 × CH_2CH_3), 23.1 (CH_2), 26.29 (CH_2), 26.32 (CH_2), [29.8, 29.9, 30.0, 30.09, 30.13, 30.2 (CH_2, alkyl chain, resonance overlap)], 32.4 (CH_2), 32.9 (CH_2), 36.9 (CH_2), 50.9 (CH), 62.3 (CH_2), 67.8 (CH_2), 69.4 (CH), 70.3 (CH), 70.8 (CH), 71.2 (CH), 72.5 (CH), 75.1 (CH), 100.2 (CH), 175.1 (C, *C*=O); MS (TOF ES+) *m/z* 880.7 ([M + Na]$^+$, 100%); HRMS (TOF ES+) calcd for $C_{50}H_{99}NO_9Na$ [M + Na]$^+$ 880.7218, found 880.7198.

Data were in agreement with those reported in the literature.[180]

(2*S*,3*S*,4*R*)-3,4-Di-*O*-acetyl-1-*O*-(2',3',4',6'-tetra-*O*-acetyl-α-D-galactopyranosyl)-2- (hexacosanoylamino)octadecane-1,3,4-triol (72)

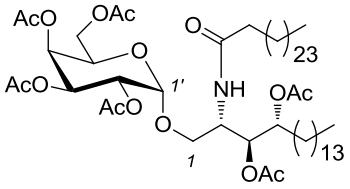

72

Ac_2O (300 μL, 3.2 mmol) was added dropwise over 1 min to a solution of α-GalCer **8** (90 mg, 0.11 mmol) in pyridine (2 mL) and the reaction mixture was stirred at r.t. for 10 h, after which time, the volatiles were removed under reduced pressure. The residue was diluted with CH_2Cl_2 (10 mL), washed sequentially with H_2O (5 mL), $NaHCO_3$ solution (10 mL), brine (3 mL) and then dried over Na_2SO_4. The drying agent was removed by filtration and the filtrate was concentrated under reduced pressure. The crude product was purified by flash column chromatography (25% EtOAc in hexane) to afford hexa-acetate **72** as a white solid (110 mg, 94%): R_f = 0.3 (20% EtOAc in hexane); $[\alpha]^{20}_D$ = +8.4 (*c* 0.5, $CHCl_3$); mp 43 – 44 °C; ν_{max}(film) / cm^{-1} 1745s (C=O), 1683w (C=O); δ_H(75 MHz, $CDCl_3$) 0.87 (t, *J* 6.7, 6H, 2 × CH_2CH_3), 1.12-1.40 (stack, 68H, alkyl chain methylenes), 1.56-1.72 (stack, 4H), 1.98 (s, 3H, C(O)CH_3), 1.99 (s, 3H, C(O)CH_3), 2.04 (s, 3H, C(O)CH_3), 2.06 (s, 3H, C(O)CH_3), 2.09 (s, 3H, C(O)CH_3), 2.13 (s, 3H, C(O)CH_3), 2.27 (t, *J* 7.4, 2H), 3.39 (dd, *J* 10.6, 2.2, 1H), 3.64 (dd, *J* 10.7, 2.6, 1H), 3.97-4.14 (stack, 4H), 4.31-4.41 (m, 1H), 4.90 (d, *J* 3.7, 1H), 5.13 (dd, *J* 10.8, 3.7, 1H), 5.25-5.36 (stack, 2H), 5.44 (d, *J* 3.1, 1H), 6.39 (d, *J* 9.7, 1H); δ_C(100 MHz, $CDCl_3$) 14.1 (CH_3, 2 × CH_2CH_3),

[20.60, 20.66, 20.72, (CH_3, C(O)*C*H_3), resonance overlap], 20.1 (CH_3, C(O)*C*H_3), 22.7 (CH_2), 25.6 (CH_2), 25.7 (CH_2), [29.29, 29.35, 29.40, 29.7 (CH_2, alkyl chain methylenes, resonance overlap)], 31.9 (CH_2), 36.7 (CH_2), 47.8 (CH), 61.8 (CH_2), 66.7 (CH), 67.2 (CH_2), 67.5 (CH), 67.9 (CH), 70.5 (CH), 73.4 (CH), 97.1 (CH), 169.7 (C), 170.1 (C), 170.4 (C), 170.7 (C), 171.1 (C), 172.9 (C), some resonance overlap in *C*=O region; MS (TOF ES+) *m/z* 1132.8 ($[M + Na]^+$, 100%); HRMS (TOF ES+) calcd for $C_{62}H_{111}NO_{15}Na$ $[M + Na]^+$ 1132.7851, found 1132.7860.

(2*S*,3*S*,4*R*)-3,4-Di-*O*-acetyl-1-*O*-(2',3',4',6'-tetra-*O*-acetyl-α-D-galactopyranosyl)-2-(hexacosanethioylamino)octadecane-1,3,4-triol (73)

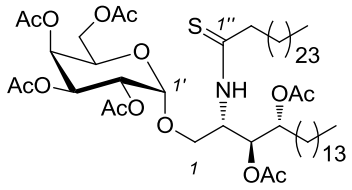

73

Lawesson's reagent (60 mg, 0.15 mmol) was added to a solution of amide **72** (110 mg, 0.10 mmol) in toluene (2 mL) at r.t. The reaction mixture was stirred at 80 ºC for 4 h and then the solvent was removed under reduced pressure. The residue was diluted with CH_2Cl_2 (10 mL), washed sequentially with H_2O (5 mL), $NaHCO_3$ solution (10 mL), brine (2 mL) and then dried over Na_2SO_4. The drying agent was

removed by filtration and the filtrate was concentrated under reduced pressure. Purification of the residue by flash column chromatography (20% EtOAc in hexane) provided thioamide **73** as a pale yellow solid (96 mg, 85%): R_f = 0.3 (15% EtOAc in hexane); $[\alpha]^{20}_{D}$ = +46.0 (*c* 1, $CHCl_3$); mp 47 – 48 °C; ν_{max}(film) / cm^{-1} 1747s (C=O); δ_H(500 MHz, $CDCl_3$) 0.87 (t, *J* 6.8, 6H, 2 × CH_2CH_3), 1.21-1.37 (stack, 68H, alkyl chain methylenes), 1.58-1.69 (stack, 2H, H-5), 1.71-1.82 (stack, 2H, H-3”), 1.99 (s, 3H, C(O)CH_3), 2.00 (s, 3H, C(O)CH_3), 2.03 (s, 3H, C(O)CH_3), 2.07 (s, 3H, C(O)CH_3), 2.08 (s, 3H, C(O)CH_3), 2.12 (s, 3H, C(O)CH_3), 2.66-2.78 (stack, 2H, H-2”), 3.40 (dd, *J* 10.7, 1.9, 1H, C(1)$H_a$$H_b$), 3.65 (dd, *J* 10.7, 2.7, 1H, C(1)$H_a$$H_b$), 3.97-4.07 (stack, 2H, C(6’)$H_a$$H_b$, H-5’), 4.08-4.14 (m, 1H, C(6’)$H_a$$H_b$), 4.75-4.81 (m, 1H, H-4), 4.93 (d, *J* 3.6, 1H, H-1’), 5.08-5.16 (stack, 2H, (including 5.10 (dd, *J* 10.8, 3.7, 1H, H-2’)), H-2’, H-2), 5.37 (dd, *J* 10.8, 3.4, 1H, H-3’), 5.40-5.42 (m, 1H, H-4’), 5.49 (dd, *J* 10.0, 2.4, 1H, H-3), 8.66 (d, *J* 9.2, 1H, N-*H*); δ_C(125 MHz, $CDCl_3$) 14.11 (CH_3, 2 × CH_2CH_3), [20.50, 20.54, 20.62, 20.66, 20.95 (CH_3, C(O)CH_3), resonance overlap], [22.6, 25.5, 27.5, 28.9, 29.2, 29.3, 29.4, 29.5, 29.7, 31.9 (CH_2, alkyl chain methylenes, resonance overlap)], 47.0 (CH_2, C-2”), 53.7 (CH, C-2), 61.7 (CH_2, C-6’), 65.3 (CH_2, C-1), 67.0 (CH, C-5’), 67.3 (CH, C-3’), 67.8 (CH, C-2’), 68.0 (CH, C-4’), 69.8 (CH, C-3), 73.6 (CH, C-4), 96.8 (CH, C-1’), 169.7 (C, C(3)*C*=O), 170.0 (C, C(4’)*C*=O), 170.3 (C, C(3’)*C*=O), 170.4 (C, C(6’)*C*=O), 170.5 (C, C(2’)*C*=O), 171.5 (C, C(4)*C*=O), 207.0 (C, *C*=S); MS (TOF ES+) *m/z* 1148.9 ($[M + Na]^+$, 100%); HRMS (TOF ES+) calcd for $C_{62}H_{111}NO_{14}SNa$ $[M + Na]^+$ 1148.7623, found 1148.7631.

(2*S*,3*S*,4*R*)-1-*O*-(α-D-Galactopyranosyl)-2-(hexacosanethioylamino)-octadecane-1,3,4-triol (35)

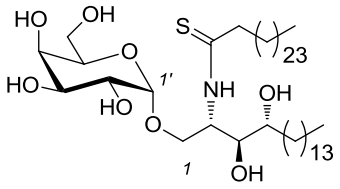

35

NaOMe (10 μL of a 0.5 M soln in MeOH, 0.005 mmol) was added to a solution of hexa-acetate **73** (25 mg, 0.022 mmol) in MeOH (2.5 mL). After stirring at r.t. for 2 h, the reaction mixture was neutralised by the addition of acidic ion-exchange resin (Dowex H CR-S, pre-washed with MeOH (100 mL) and $CHCl_3$ (50 mL)). The solution was filtered and the resin washed with MeOH (25 mL) and $CHCl_3$/MeOH (25 mL, 9:1). The filtrate was concentrated under reduced pressure. Purification of the residue by flash column chromatography (8% MeOH in $CHCl_3$) provided thioamide **35** as a pale yellow solid (17 mg, 90%): R_f = 0.2 (8% MeOH in $CHCl_3$); $[\alpha]^{20}_D$ = +43.2 (*c* 1, $CHCl_3$:CH_3OH, 2:1); mp 136 – 137 °C; ν_{max}(film) / cm^{-1} 3368m br (O–H); δ_H(400 MHz, $CDCl_3$:CD_3OD, 2:1) 0.84 (t, *J* 6.9, 6H, 2 × CH_2CH_3), 1.14-1.44 (stack, 69H, alkyl chain methylenes), 1.45-1.78 (stack, 3H), 2.56-2.66 (stack, 2H), 3.50-3.58 (m, 1H), 3.65-3.83 (stack, 8H), 3.90 (d, *J* 2.9, 1H), 3.96 (dd, *J* 10.9, 4.3, 1H), 4.85 (app. q, *J* 4.3, 1H) 4.94 (d, *J* 3.7, 1H), O*H* resonances not observed; δ_C(100 MHz, $CDCl_3$:CD_3OD, 2:1) 14.3 (CH_3, 2 × CH_2CH_3), 23.1 (CH_2), 26.4 (CH_2), 29.6 (CH_2), [29.9, 30.0, 30.1, 30.17, 30.21 (CH_2, alkyl chain, resonance overlap)], 32.4 (CH_2), 32.7 (CH_2), 47.1 (CH_2), 56.8 (CH), 62.3 (CH_2), 66.8 (CH_2), 69.5 (CH),

70.4 (CH), 70.8 (CH), 71.4 (CH), 72.6 (CH), 73.9 (CH), 100.2 (CH), 206.1 (C, *C*=S); MS (TOF ES+) *m/z* 896.8 ([M + Na]$^+$, 100%); HRMS (TOF ES+) calcd for $C_{50}H_{99}NO_8SNa$ [M + Na]$^+$ 896.6989, found 896.6998.

(2*S*,3*S*,4*R*)-2-Azido-3,4-*O*-isopropylidene-1-*O*-(2',3',4',6'-tetra-*O*-benzyl-α-D-galactopyranosyl)octadecane-1,3,4-triol (79)

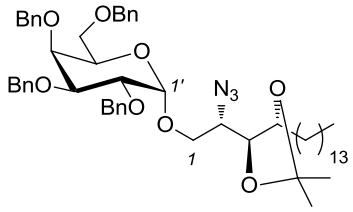

79

Ph_3P (1.46 g, 5.55 mmol) and CBr_4 (1.84 g, 5.55 mmol) were added sequentially to a solution of 2,3,4,6-tetra-*O*-benzyl-D-galactose **51** (1.00 g, 1.85 mmol) in CH_2Cl_2 (10 mL) at r.t. The reaction mixture was stirred for 3 h. In separate flasks, a solution of tetramethylurea (TMU) (1.2 mL) and Bu_4NBr (1.79 g, 5.55 mmol) in CH_2Cl_2 (5 mL), and a solution of azide **78** (1.07 g, 2.78 mmol) in CH_2Cl_2 (5 mL) were stirred over activated 3 Å MS for 30 min, after which time, these solutions were added dropwise (15 min) and sequentially (TMU/Bu_4NBr solution first) to the solution containing the glycosyl donor. The reaction mixture was stirred at r.t. for 3 d until there was no evidence by TLC that the donor was still being consumed. The reaction mixture was then filtered through a silica plug, washing with CH_2Cl_2 (1.2

L) and then concentrated under reduced pressure. Purification of the residue by flash column chromatography (10% EtOAc in hexane) afforded glycoside **79** as a colourless oil (1.56 g, 71%, α-anomer only): R_f = 0.2 (10% EtOAc in hexane); $[\alpha]_D^{22}$ = + 24.8 (*c* 1, $CHCl_3$); lit. $[\alpha]_D^{rt}$ = +32.1 (*c* 2.0, $CHCl_3$);[180] ν_{max}(film) / cm^{-1} 2924s, 2854s, 2099s (N_3), 1497w, 1455m, 1370m, 1249m, 1220m, 1110s, 1059s, 735s, 697s; δ_H(500 MHz, $CDCl_3$) 0.87 (t, *J* 6.8, 3H, CH_2CH_3), 1.20-1.42 (stack, 29H, alkyl chain methylenes, $C(CH_3)_2$), 1.47-1.64 (stack, 3H), 3.44-3.54 (stack, 3H, C(6')H_2, H-2), 3.71 (dd, *J* 10.8, 6.7, 1H, C(1)H_aH_b), 3.91-3.94 (m, 1H, H-4'), 3.95-4.12 (stack, 6H, H-2', H-3', H-5', C(1)H_aH_b, H-3, H-4), 4.39 (A of AB, *J* 11.9, 1H, OC$H_a$$H_b$Ph), 4.47 (B of AB, *J* 11.9, 1H, OC$H_a$$H_b$Ph), 4.56 (A of AB, *J* 11.5, 1H, OC$H_a$$H_b$Ph), 4.70 (A of AB, *J* 12.0, 1H, OC$H_a$$H_b$Ph), 4.71 (A of AB, *J* 11.8, 1H, OC$H_a$$H_b$Ph), 4.79 (B of AB, *J* 12.0, 1H, OC$H_a$$H_b$Ph), 4.84 (B of AB, *J* 11.8, 1H, OC$H_a$$H_b$Ph), 4.93 (d, *J* 3.6, 1H, H-1'), 4.94 (B of AB, *J* 11.5, 1H, OC$H_a$$H_b$Ph), 7.22-7.33 (stack, 16H, Ph), 7.36-7.38 (stack, 4H, Ph); δ_C(125 MHz, $CDCl_3$) 14.1 (CH_3, CH_2CH_3), 22.7 (CH_2), 25.7 (CH_3, 1 × $C(CH_3)_2$), 26.6 (CH_2), 28.1 (CH_3, 1 × $C(CH_3)_2$), [29.3, 29.60, 29.65, 29.69 (CH_2, alkyl chain, resonance overlap)], 31.9 (CH_2), 59.8 (CH, C-2), 69.1 (CH_2, C-6'), 69.6 (CH_2, C-1), 69.9 (CH), 72.9 (CH_2, CH_2Ph), 73.3 (CH_2, CH_2Ph), 73.4 (CH_2, CH_2Ph), 74.7 (CH_2, CH_2Ph), 75.3 (CH, C-4'), 75.4 (CH), 76.6 (CH), 77.8 (CH, C-4), 78.7 (CH), 98.8 (CH, C-1'), 108.2 (C, $C(CH_3)_2$), [127.4, 127.5, 127.60, 127.64, 127.7 (CH, Ph, resonance overlap)], [128.20, 128.25, 128.29, 128.35 (CH, Ph, resonance overlap)], 138 (C, *ipso* Ph), 138.7 (C, *ipso* Ph), 138.9 (C, 2 × *ipso* Ph, resonance overlap); MS (TOF ES+) *m/z* 928.7 ($[M+Na]^+$, 100%); HRMS (TOF ES+) 928.5470 $[M+Na]^+$. $C_{55}H_{75}N_3O_8Na$ requires 928.5452. The unreacted azide was also recovered (394 mg, 37%).

Data were in agreement with those reported in the literature for **79** prepared by a different route.[180]

(2*S*,3*S*,4*R*)-2-Amino-3,4-*O*-isopropylidene-1-*O*-(2',3',4',6'-tetra-*O*-benzyl-α-D-galactopyranosyl)octadecane-1,3,4-triol (80)

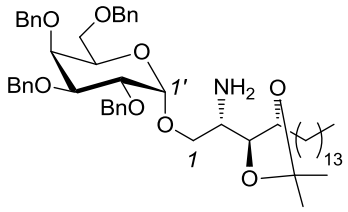

80

PMe_3 (930 μL of a 1.0 M soln in THF, 0.93 mmol) was added dropwise over 5 min to a solution of azide **79** (700 mg, 0.77 mmol) in THF (7 mL). The reaction mixture was stirred at r.t. for 3 h, after which time, H_2O (0.5 mL) was added. The reaction mixture was stirred for 1 h and then concentrated under reduced pressure. The residual H_2O was removed by co-evaporation with toluene (3 × 3 mL) to provide the crude product. Purification by flash column chromatography (25% EtOAc in hexane) afforded amine **80** as a colourless oil (632 mg, 93%): R_f = 0.2 (25% EtOAc in hexane); $[\alpha]^{20}_D$ = +35.6 (*c* 1, $CHCl_3$); ν_{max}(film) / cm^{-1} 3372 br (N–H); δ_H(300 MHz, $CDCl_3$) 0.87 (t, *J* 7.0, 3H, CH_2CH_3), 1.20–1.43 (stack, 24H, alkyl chain methylenes, 1 × $C(CH_3)_2$), 1.37 (s, 3H, 1 × $C(CH_3)_2$), 1.42–1.57 (stack, 5H), 2.99–3.08 (m, 1H), 3.37 (dd, *J* 10.1, 7.6, 1H), 3.48–3.57 (stack, 2H), 3.81–3.98

(stack, 5H), 4.02–4.12 (stack, 2H), 4.38 (A of AB, J_{A-B} 11.8, 1H), 4.46 (B of AB, J_{B-A} 11.8, 1H), 4.57 (d, *J* 11.5, 1H), 4.68 (d, *J* 11.8, 1H), 4.71–4.83 (stack, 3H), 4.91–4.93 (stack, 2H), 7.22–7.39 (stack, 20H, Ph), NH_2 not observed; δ_C(100 MHz, $CDCl_3$) 14.1 (CH_3, CH_2CH_3), 22.7 (CH_2), 25.9 (CH_3, 1 × C(CH_3)$_2$), 26.2 (CH_2), 28.3 (CH_3, 1 × C(CH_3)$_2$), [29.3, 29.7, 29.8 (CH_2, alkyl chain, resonance overlap)], 31.9 (CH_2), 50.7 (CH, $CHNH_2$), 69.0 (CH_2), 69.5 (CH), 72.3 (CH_2), 73.0 (CH_2), 73.3 (CH_2), 73.5 (CH_2), 74.8 (CH_2), 75.0 (CH), 76.8 (CH), 77.9 (CH), 79.0 (CH), 79.1 (CH), 99.0 (CH, C-1'), 107.8 (C, C(CH_3)$_2$), [127.4, 127.5, 127.6, 127.7, 127.8 128.2, 128.3 (CH, Ph, resonance overlap)], 138.0 (C, *ipso* Ph), [138.7, 138.8 (C, 3 × *ipso* Ph, resonance overlap)]; MS (TOF ES+) *m/z* 880.8 ($[M + H]^+$, 100%); HRMS (TOF ES+) calcd for $C_{55}H_{78}NO_8$ $[M + H]^+$ 880.5727, found 880.5721.

(2*S*,3*S*,4*R*)-2-Hexacosanoylamino-3,4-*O*-isopropylidene-1-*O*-(2',3',4',6'-tetra-*O*-benzyl-α-D-galactopyranosyl)octadecane-1,3,4-triol (81)

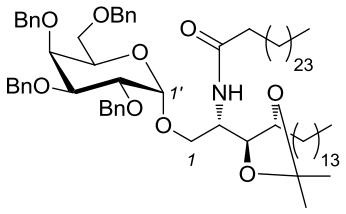

81

A screw-capped glass tube containing a solution of hexacosanoic acid (100 mg, 0.25 mmol) in $(COCl)_2$ (2.0 mL, 23 mmol) was closed tightly and heated at 70 ºC for 2 h, after which time, the volatiles were evaporated under a stream of argon and the tube then placed on a high vacuum line for at least 2 h to remove the residual volatiles. The resulting hexacosanoyl chloride was used directly without further purification: a solution of freshly prepared hexacosanoyl chloride **47** (105 mg, 0.25 mmol) in CH_2Cl_2 (0.5 mL) was added dropwise over 2 min to a solution of amine **80** (132 mg, 0.15 mmol) and NEt_3 (42 μL, 0.30 mmol) in CH_2Cl_2 (1.0 mL) at 0 ºC. The reaction mixture was stirred at r.t. for 12 h and then diluted with CH_2Cl_2 (10 mL), washed sequentially with $NaHCO_3$ solution (10 mL), brine (2 mL) and then dried over Na_2SO_4. The drying agent was removed by filtration and the filtrate concentrated under reduced pressure. Purification of the residue by flash column chromatography provided amide **81** as a white solid (160 mg, 85%): R_f = 0.3 (10% EtOAc in hexane); $[\alpha]_D^{20}$ = + 41.6 (*c* 1, $CHCl_3$); lit. $[\alpha]_D^{rt}$ = + 44.2 (*c* 0.85, $CHCl_3$);[180] mp 87 – 88 °C; ν_{max}(film) / cm^{-1} 2916s, 2849s, 1648m (C=O), 1541m,

1497w, 1469m, 1454m, 1380w, 1370w, 1250w, 1217m, 1158m, 1106s, 1044s, 859m, 881w, 859w, 791w, 733s, 721s; δ_H(500 MHz, $CDCl_3$) 0.87 (t, *J* 6.9, 6H, CH_2CH_3), 1.15-1.34 (stack, 71H, alkyl chain methylenes, 1 × $C(CH_3)_2$), 1.39 (s, 3H, 1 × $C(CH_3)_2$), 1.40-1.47 (stack, 2H, including C(3'')H_aH_b), 1.48-1.56 (stack, 2H), 1.93-2.01 (m, 1H, C(2'')H_aH_b), 2.01-2.09 (m, 1H, C(2'')H_aH_b), 3.37 (dd, *J* 9.4, 5.7, 1H, C(6')H_aH_b), 3.54 (dd, *J* 9.4, 7.0, 1H, C(6')H_aH_b), 3.60 (br d, *J* 9.7, 1H, C(1)H_aH_b), 3.88-3.93 (stack, 3H, H-3', H-4', H-3 or H-4), 3.97 (app t, *J* 6.3, 1H, H-5'), 4.01-4.12 (stack, 4H, H-2', C(1)H_aH_b, H-2, H-3 or H-4), 4.36 (A of AB, J_{A-B} 11.8, 1H, C(6')OCH_aH_bPh), 4.47 (B of AB, J_{B-A} 11.8, 1H, C(6')OCH_aH_bPh), 4.57 (A of AB, J_{A-B} 11.6, 1H, C(4')OCH_aH_bPh), 4.65 (A of AB, J_{A-B} 11.5, 1H, C(2')OCH_aH_bPh), 4.73 (A of AB, J_{A-B} 11.8, 1H, C(3')OCH_aH_bPh), 4.79 (B of AB, J_{B-A} 11.5, 1H, C(2')OCH_aH_bPh), 4.80 (B of AB, J_{B-A} 11.8, 1H, C(3')OCH_aH_bPh), 4.89 (d, *J* 3.7, 1H, H-1'), 4.91 (B of AB, J_{B-A} 11.6, 1H, C(4')OCH_aH_bPh), 6.24 (d, *J* 8.9, 1H, N*H*), 7.21-7.38 (stack, 20H, Ph); δ_C(125 MHz, $CDCl_3$) 14.1 (CH_3, CH_2CH_3), 22.6 (CH_2), 25.6 (CH_2), 25.9 (CH_3, 1 × $C(CH_3)_2$), 26.5 (CH_2), 28.2 (CH_3, 1 × $C(CH_3)_2$), 28.9 (CH_2), [29.31, 29.37, 29.45, 29.55, 29.57, 29.62, 29.66, 29.68 (CH_2, alkyl chain, resonance overlap)], 31.9 (CH_2), 36.7 (CH_2, C-2''), 48.7 (CH, C-2), 69.5 (CH_2, C-6'), 69.9 (CH, C-5'), 70.6 (CH_2, C-1), 73.0 (CH_2, C(3')O*C*H_2Ph), 73.46 (CH_2, C(2')O*C*H_2Ph), 73.54 (CH_2, C(6')O*C*H_2Ph), 74.6 (CH_2, C(4')O*C*H_2Ph), 74.7 (CH, C-4'), 75.4 (CH, C-3 or C-4), 76.8 (CH, C-2'), 77.8 (CH, C-3 or C-4), 78.9 (CH, C-3'), 99.7 (CH, C-1'), 107.8 (C, $(CH_3)_2C$), [127.4, 127.5, 127.7, 127.8, 127.85, 127.91 (CH, Ph, some resonance overlap)], [128.2, 128.31, 128.34, 128.36, 128.40 (CH, Ph, some resonance overlap)], 137.5 (C, *ipso* Ph on C-6'), 138.3 (C, *ipso* Ph), 138.4 (C, *ipso* Ph), 138.6 (C, *ipso* Ph on C-3'), 172.4 (C, *C*=O);

MS (TOF ES+) *m/z* 1281.0 ([M + Na]$^+$, 100%); HRMS (TOF ES+) calcd for $C_{81}H_{127}NO_9Na$ [M + Na]$^+$ 1280.9409, found 1280.9417.

Data were in agreement with those reported in the literature for **81** prepared using different reagents.[180]

(2*S*,3*S*,4*R*)-3,4-Di-*O*-benzyl-1-*O*-(2',3',4',6'-tetra-*O*-benzyl-D-galactopyranosyl)-2-(tricosanylaminocarbonylamino)octadecane-1,3,4-triol (77)

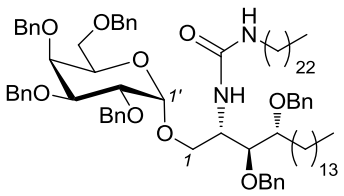

77

A screw-capped glass tube containing a solution of tetracosanoic acid **74** (450 mg, 1.22 mmol) in $(COCl)_2$ (2.0 mL, 23 mmol) was closed tightly and heated at 70 ºC for 2 h. The volatiles were then evaporated under a stream of argon and the tube then placed on a high vacuum line for at least 2 h to remove the residual volatiles. The resulting tetracosanoyl chloride **75** was used directly in the next step without further purification: a solution of freshly prepared tetracosanoyl chloride (450 mg, 1.22 mmol) in THF (5 mL) was added dropwise over 10 min to a solution of NaN_3

(300 mg, 4.62 mmol) in H_2O (0.5 mL) at 0 ºC. The reaction mixture was stirred at r.t. for 5 h. The organic phase was then extracted with cold (~10 ºC) THF (5 mL) and dried over Na_2SO_4. The drying agent was removed by filtration. The solvent was removed under reduced pressure to provide tetracosanoyl azide as a white solid, which was used immediately in the next step: a solution of tetracosanoyl azide (481 mg, 1.22 mmol (assuming quantitative conversion in the previous step)) in toluene (5 mL) was heated under reflux for 4 h, after which time, the reaction mixture was cooled to r.t. The resulting solution of tricosanyl isocyanate product **48** was used directly without further purification in the next step: a solution of amine **46** (150 mg, 0.147 mmol) in toluene (5 mL) was added to a solution of tricosanyl isocyanate (1.22 mmol (assuming quantitative conversion)) in toluene (5 mL) at r.t. The reaction mixture was heated under reflux for 8 h and then concentrated under reduced pressure. Purification of the residue by flash column chromatography (20% EtOAc in hexane) afforded urea **77** as a pale yellow oil (140 mg, 68% based on amine): R_f = 0.3 (20% EtOAc in hexane); $[\alpha]^{20}_D$ = +25.2 (*c* 1, $CHCl_3$); ν_{max}(film) / cm^{-1} 3363m (N-H), 1670m (C=O); δ_H(500 MHz, $CDCl_3$) 0.89 (t, *J* 7.0, 6H, 2 × CH_2CH_3), 1.10-1.39 (stack, 65H, alkyl chain methylenes), 1.39-1.51 (m, 1H, alkyl chain CH_aH_b), 1.56-1.64 (m, 1H, C(5)H_aH_b), 1.64-1.73 (m, 1H, C(5)H_aH_b), 2.90-3.06 (stack, 2H, CH_aH_bNH), 3.33 (dd, *J* 9.5, 5.0, 1H, C(6')H_aH_b), 3.55 (dd, *J* 9.5, 7.0, 1H, C(6')H_aH_b), 3.59-3.64 (m, 1H, H-4), 3.73 (dd, *J* 10.8, 3.1, 1H, C(1)H_aH_b), 3.80-3.88 (stack, 3H, H-2, H-3, H-4'), 3.89 (dd, *J* 10.1, 2.7, 1H, H-3'), 3.98 (app. t, *J* 6.0, 1H, H-5'), 4.05 (dd, *J* 10.1, 3.6, 1H, H-2'), 4.11 (br dd, *J* 10.8, 4.5, 1H, C(1)H_aH_b), 4.38 (A of AB, $J_{A\text{-}B}$ 12.0, 1H, C(6')OCH_aH_bPh), 4.45-4.48 (stack, 2H, C(6')OCH_aH_bPh, C(4)OCH_aH_bPh), 4.54 (A of AB, $J_{A\text{-}B}$ 11.3, 1H, C(3)OCH_aH_bPh),

4.57 (A of AB, $J_{A\text{-}B}$ 11.8, 1H, C(4')OCH_aH$_b$Ph), 4.61 (B of AB, $J_{B\text{-}A}$ 12.6, 1H, C(4)OCH$_a$$H_b$Ph), 4.66 (A of AB, $J_{A\text{-}B}$ 11.7, 1H, C(2')OCH_aH$_b$Ph), 4.75 (A of AB, $J_{A\text{-}B}$ 11.8, 1H, C(3')OCH_aH$_b$Ph), 4.78 (B of AB, $J_{B\text{-}A}$ 11.3, 1H, C(3)OCH$_a$$H_b$Ph), 4.79 (B of AB, $J_{B\text{-}A}$ 11.7, 1H, C(2')OCH$_a$$H_b$Ph), 4.81 (B of AB, $J_{B\text{-}A}$ 11.8, 1H, C(3')OCH$_a$$H_b$Ph), 4.87 (d, *J* 3.6, 1H, H-1'), 4.93 (B of AB, $J_{B\text{-}A}$ 11.8, 1H, C(4')OCH$_a$$H_b$Ph), 5.00 (d, *J* 7.8, 1H, C(2)N*H*), 7.23-7.38 (stack, 30H, 6 × Ph), CH$_2$N*H* not observed; δ_C(125 MHz, $CDCl_3$) 14.1 (CH_3, 2 × CH_2*C*H$_3$), [22.7, 26.0, 26.9, 29.4, 29.7, 29.9, 30.3, 31.9 (CH_2, alkyl chain methylenes, resonance overlap)], 40.3 (CH_2, *C*H$_2$NH), 51.7 (CH, C-2), 69.9 (CH_2, C-6'), 70.1 (CH, C-5'), 71.0 (CH_2, C-1), 71.9 (CH_2, C(4)O*C*H$_2$Ph), 73.1 (CH_2, C(3')O*C*H$_2$Ph), 73.4 (CH_2, C(2')O*C*H$_2$Ph), 73.6 (CH_2, C(6')O*C*H$_2$Ph), 73.8 (CH_2, C(3)O*C*H$_2$Ph), 74.6 (CH_2, C(4')O*C*H$_2$Ph), 75.0 (CH, C-3), 76.8 (CH, C-2'), 78.8 (CH, C-3'), 79.9 (CH, C-4'), 80.3 (CH, C-4), 99.8 (CH, C-1'), [127.5, 127.6, 127.67, 127.70, 127.84, 127.88, 127.9, 128.25, 128.28, 128.34, 128.37, 128.5 (CH, Ph, resonance overlap)], 137.39 (C, *ipso* Ph), 138.42 (C, *ipso* Ph), 138.48 (C, *ipso* Ph), 138.67 (C, *ipso* Ph), 138.72 (C, *ipso* Ph), 138.8 (C, *ipso* Ph), 158.8 (C, *C*=O); MS (TOF ES+) *m/z* 1408.0 ([M + Na]$^+$, 100%); HRMS (TOF ES+) calcd for $C_{90}H_{132}N_2O_9Na$ [M + Na]$^+$ 1407.9831, found 1407.9844. The unreacted amine was also recovered (40 mg, 83%).

(2*S*,3*S*,4*R*)-1-*O*-(α-D-Galactopyranosyl)-2-(tricosanylaminocarbonylamino)-octadecane-1,3,4-triol (36)

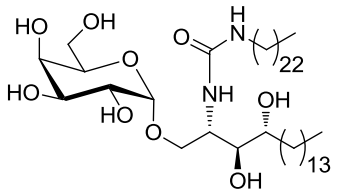

36

Urea **36** was prepared from perbenzylated urea **77** (115 mg, 0.083 mmol) and Pd/C (26.5 mg, 10% wet) in THF (10 mL) according to the general procedure for catalytic hydrogenolysis. After 22 h, work-up and purification by flash column chromatography (6% MeOH in $CHCl_3$) afforded urea **36** as an amorphous, white solid (51 mg, 73%): R_f = 0.23 (6% MeOH in $CHCl_3$); $[\alpha]^{18}_D$ = +28.0 (*c* 0.5, $CHCl_3$); mp 154 – 155 °C; ν_{max}(film) / cm^{-1} 3363m (N-H), 1670m (C=O); δ_H(500 MHz, $CDCl_3$) 0.68 (t, *J* 6.5, 6H, 2 × CH_2CH_3), 1.06-1.10 (stack, 62H, alkyl chain methylenes), 1.22-1.27 (stack, 2H), 1.33-1.36 (m, 1H), 1.48-1.52 (m, 1H), 1.67-1.69 (stack, 2H), 2.83-2.96 (stack, 2H, CH_2NH), 3.28-3.31 (m, 1H, H-3), 3.33-3.36 (m, 1H, H-4), 3.49-3.63 (stack, 6H, H-3', 2 × H-6', H-2', H-5', C(1)H_aH_b), 3.66 (dd, *J* 10.5, 4.5, 1H, C(1)H_aH_b), 3.72 (br d, *J* 2.5, 1H, H-4'), 3.97 (dd, *J* 9.0, 4.5, 1H, H-2), 4.67 (d, *J* 3.5, 1H, H-1'); δ_C(125 MHz, $CDCl_3$) 13.5 (CH_3, 2 × CH_2CH_3), [22.3, 25.1, 25.5, 26.6, 29.0, 29.1, 29.3, 29.4, 29.8, 31.5, 32.7 (CH_2, alkyl chain methylenes, resonance overlap)], 39.8 (CH_2, CH_2NH), 50.6 (CH, C-2), 61.5 (CH_2, C-6'), 67.6 (CH_2, C-1), 68.6 (CH, C-2'), 69.4 (CH, C-4'), 70.0 (CH, C-3'), 70.5 (CH, C-5'), 72.1 (CH, C-4), 75.2 (CH, C-3), 99.4 (CH, C-1'), 158.9 (C, *C*=O); MS (TOF ES+) *m/z*

867.9 ([M + Na]$^+$, 100%); HRMS (TOF ES+) calcd for $C_{48}H_{96}N_2O_9Na$ [M + Na]$^+$ 867.7014, found 867.7026.

Tetracosan-1-ol (82)

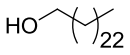

82

A solution of tetracosanoic acid (2.00 g, 5.43 mmol) in THF (10 mL) was added dropwise to a suspension of $LiAlH_4$ (310 mg, 8.14 mmol) in THF (45 mL) over 5 min at r.t. The mixture was heated under reflux for 4 h, cooled to r.t. and then quenched carefully with freshly prepared saturated Na_2SO_4 solution (10 mL), followed by the addition of anhydrous $MgSO_4$ (600 mg). The mixture was stirred vigorously for 10 min, filtered through a pad of Celite and washed with THF (2 $\times$ 40 mL). Removal of the solvent under reduced pressure and purification of the residue by flash column chromatography (10% EtOAc in toluene) provided tetracosan-1-ol as a white solid (1.69 g, 88%): R_f = 0.3 (10% EtOAc in hexane); mp 76 – 77 °C (lit. 76.0 – 76.5 °C);[181] ν_{max}(film) / cm^{-1} 3488 br (OH), 2974m, 2917m, 2849m, 1462w, 1356w, 1181w, 1065s, 907m, 720w, 658w, 581w; δ_H(300 MHz, $CDCl_3$) 0.87 (t, *J* 6.7, 3H, CH_2CH_3), 1.16-1.39 (stack, 40H, alkyl chain methylenes), 1.40-1.45 (stack, 2H), 1.51-1.62 (stack, 2H), 3.64 (t, *J* 6.6, 2H), O*H* resonance not observed; δ_C(75 MHz, $CDCl_3$) 14.1, (CH_3, CH_2CH_3), 22.7 (CH_2),

25.7 (CH_2), 26.5 (CH_2), 28.2 (CH_3), 28.8 (CH_2), 29.1 (CH_2), [29.3, 29.4, 29.7, 29.8 (CH_2, alkyl chain, resonance overlap)], 31.9 (CH_2), 32.8 (CH_2), 63.1 (CH_2); MS (TOF ES+) *m/z* 377.5 ($[M + Na]^+$, 100%); HRMS (TOF ES+) calcd for $C_{24}H_{50}ONa$ $[M + Na]^+$ 377.3759, found 377.3755.

Data were in agreement with those reported in the literature.[182]

Carbonic acid, 2,5-dioxo-1-pyrrolidinyl tetracosanyl ester (49)

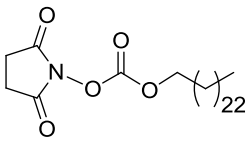

49

N,*N*′-Disuccinimidyl carbonate **83** (190 mg, 0.75 mmol) was added to a solution of tetracosan-1-ol (177 mg, 0.50 mmol) and NEt_3 (210 μL, 1.5 mmol) in dry CH_3CN (2.5 mL) at r.t. The resulting mixture was stirred at r.t. for 4 h and then concentrated under reduced pressure. The residue was diluted with $NaHCO_3$ solution (10 mL) and extracted with EtOAc (2 × 10 mL). The combined extracts were washed with brine (5 mL) and dried over Na_2SO_4. Evaporation of the solvent under reduced pressure provided the corresponding mixed carbonate **49** as a white solid, which was used directly in the next step (248 mg, quant.): R_f = 0.3 (25% EtOAc in hexane); ν_{max}(film) / cm^{-1} 1711m (C=O), 1693m (C=O); δ_H(300

MHz, $CDCl_3$) 0.88 (t, *J* 7.0, 3H, CH_2CH_3), 1.16-1.46 (stack, 42H, alkyl chain methylenes), 1.51-1.80 (stack, 2H), 2.84 (s, 4H), 4.31 (t, *J* 6.6, 2H); δ_C(100 MHz, $CDCl_3$) 14.1 (CH_3, CH_2CH_3), 22.7 (CH_2), 28.4 (CH_2), [29.1, 29.36, 29.42, 29.5, 29.7 (CH_2, alkyl chain, resonance overlap)], 31.9 (CH_2), 71.7 (CH_2), 151.6 (C, O*C*=O), 168.7 (C, N*C*=O); MS (TOF ES+) *m/z* 518.5 ($[M + Na]^+$, 100%); HRMS (TOF ES+) calcd for $C_{29}H_{53}NO_5Na$ $[M + Na]^+$ 518.3821, found 518.3817.

(2*S*,3*S*,4*R*)-3,4-*O*-Isopropylidene-1-*O*-(2',3',4',6'-tetra-*O*-benzyl-α-D-galacto-pyranosyl)-2-(tetracosanyloxycarbonylamino)octadecane-1,3,4-triol (84)

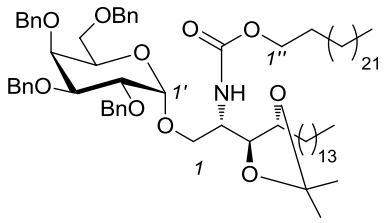

84

A solution of carbonic acid, 2,5-dioxo-1-pyrrolidinyl tetracosanyl ester (50 mg, 0.10 mmol) in CH_2Cl_2 (0.5 mL) was added to a stirred solution of amine **80** (60 mg, 0.068 mmol) and NEt_3 (24 μL, 0.17 mmol) in CH_2Cl_2 (1 mL). The resulting mixture was stirred at r.t. until no mixed carbonate remained as determined by TLC (4 h). The mixture was then diluted with CH_2Cl_2 (8 mL) and washed sequentially with $NaHCO_3$ solution (10 mL) and brine (10 mL). The organic phase was dried over Na_2SO_4 and the solvent was evaporated under reduced pressure. Purification of

the residue by flash column chromatography (5% EtOAc in toluene) provided carbamate **84** as a colourless oil (70 mg, 82%): R_f = 0.3 (10% EtOAc in hexane); $[\alpha]^{20}_D$ = +36.8 (*c* 1, $CHCl_3$); ν_{max}(film) / cm^{-1} 1689m (C=O); δ_H(500 MHz, $CDCl_3$) 0.88 (t, *J* 6.8, 6H, 2 × CH_2CH_3), 1.24-1.34 (stack, 64H, alkyl chain methylenes, $C(CH_3)_2$), 1.39-1.51 (stack, 8H), 1.57-1.59 (stack, 3H), 1.63-1.67 (m, 1H), 3.45 (dd, *J* 9.3, 6.3, 1H, C(6')H_aH_b), 3.52 (dd, *J* 9.3, 6.5, 1H, C(6')H_aH_b), 3.66-3.70 (m, 1H, H-3), 3.77-3.84 (m, 1H, H-2), 3.91-3.98 (stack, 6H, H-3', H-4', H-5', C(1)H_aH_b, H-4', C(1")H_aH_b), 4.03-4.11 (stack, 3H, H-2', C(1)H_aH_b, C(1")H_aH_b), 4.38 (A of AB, $J_{A\text{-}B}$ 11.8, 1H, C(6')OCH_aH_bPh), 4.49 (B of AB, $J_{B\text{-}A}$ 11.8, 1H, C(6')OCH_aH_bPh), 4.56 (A of AB, $J_{A\text{-}B}$ 11.5, 1H, OCH_aH_bPh), 4.67 (A of AB, $J_{A\text{-}B}$ 11.7, 1H, OCH_aH_bPh), 4.74 (A of AB, $J_{A\text{-}B}$ 11.7, 1H, C(2')OCH_aH_bPh) 4.78 (B of AB, $J_{B\text{-}A}$ 11.7, 1H, OCH_aH_bPh), 4.83 (B of AB, $J_{B\text{-}A}$ 11.7, 1H, C(2')OCH_aH_bPh), 4.92 (B of AB, $J_{B\text{-}A}$ 11.5, 1H, OCH_aH_bPh), 4.95 (d, *J* 3.6, 1H, H-1'), 5.32 (br d, *J* 9.5, 1H, N*H*), 7.23-7.35 (stack, 18H, Ph), 7.38-7.39 (stack, 2H, Ph); δ_C(125 MHz, $CDCl_3$) 14.1 (CH_3, 2 × CH_2CH_3), 22.7 (CH_2), 25.9 (CH_2, CH_3, resonance overlap), 26.5 (CH_2), 28.2 (CH_3), 28.8 (CH_2), 29.1 (CH_2), [29.3, 29.4, 29.7, 29.8 (CH_2, alkyl chain, resonance overlap)], 32.0 (CH_2), 50.7 (CH), 65.1 (CH_2), 69.3 (CH_2), 69.7 (CH), 69.9 (CH_2), 73.1 (CH_2), 73.2 (CH_2), 73.6 (CH_2), 74.7 (CH_2), 74.9 (CH), 75.5 (CH), 76.8 (CH), 77.8 (CH), 79.0 (CH), 99.2 (CH, C-1'), 107.7 (C, $C(CH_3)_2$), [127.5, 127.6, 127.8, 127.9 (CH, Ph, resonance overlap)], [128.23, 128.26, 128.34, 128.36, 128.4 (CH, Ph, resonance overlap)], 137.8 (C, *ipso* Ph), 138.6 (C, 2 × *ipso* Ph), 138.8 (C, *ipso* Ph), 155.9 (C, *C*=O); MS (TOF ES+) *m/z* 1283.0 ($[M + Na]^+$, 100%); HRMS (TOF ES+) calcd for $C_{80}H_{125}NO_{10}Na$ $[M + Na]^+$ 1282.9201, found 1282.9244.

(2*S*,3*S*,4*R*)-1-*O*-(α-D-Galactopyranosyl)-2-(tetracosanyloxycarbonylamino)-octadecane-1,3,4-triol (37)

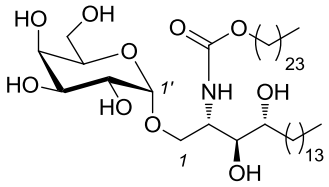

37

TFA (120 μL) was added dropwise over 1 min to a solution of acetal **84** (60 mg, 0.048 mmol) in CH_2Cl_2 / CH_3OH (2:1, 0.6 mL). After stirring for 2 h at r.t., the reaction mixture was concentrated under reduced pressure and the residual TFA was removed by co-evaporation with Et_2O (3 × 3 mL) to provide the acetal hydrolysis product as a white solid (58 mg, quant.), which was treated with $Pd(OH)_2$/C (15 mg, 10% wet) and H_2 in THF (6 mL) according to the general hydrogenolysis procedure. After 6 h, work-up and purification by flash column chromatography (8% MeOH in $CHCl_3$) afforded carbamate **37** as an amorphous white solid (31 mg, 75%): R_f = 0.3 (8% MeOH in $CHCl_3$); $[\alpha]^{18}_D$ = +46.0 (*c* 1, $CHCl_3$); mp 166 – 167 °C; ν_{max}(neat) / cm^{-1} 3388s br (OH), 1683m (C=O); δ_H(500 MHz, $CDCl_3$:CD_3OD, 2:1) 0.63 (t, *J* 6.8, 6H, 2 × CH_2CH_3), 0.91-1.12 (stack, 66H, alkyl chain methylenes), 1.22-1.48 (stack, 4H), 3.27-3.38 (stack, 2H), 3.39-3.58 (stack, 6H), 3.64-3.75 (stack, 4H), 3.77-3.84 (m, 1H), 4.65 (d, *J* 3.4, 1H, H-1'), O*H* and N*H* resonances not observed; δ_C(125 MHz, $CDCl_3$:CD_3OD, 2:1) 13.4, 22.2, 25.3, 25.4, 28.6, 28.7, 28.9, 29.2, 31.4, 32.1, 51.3, 61.4, 64.8, 67.1, 68.5, 69.4, 69.9, 70.4, 71.5, 74.4, 99.3, 156.9 (significant resonance overlap in the alkyl chain

methylene resonances); MS (TOF ES+) *m/z* 882.4 ([M + Na]$^+$, 100%); HRMS (TOF ES+) calcd for $C_{49}H_{97}NO_{10}Na$ [M + Na]$^+$ 882.7010, found 882.7000.

1-*O*-(*tert*-Butyldiphenylsilyl)-2,3-*O*-isopropylidene-L-threitol (92)

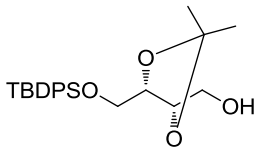

92

A solution of (+)-2,3-*O*-isopropylidene-L-threitol **88** (1.000 g, 6.162 mmol) in THF (15 mL) was added dropwise over 10 min to a suspension of NaH (60% dispersion in mineral oil, 271 mg, 6.782 mmol) in THF (30 mL) at 0 ^oC. After 30 min, a solution of ^{t}BuPh$_2$SiCl (1.864 g, 6.782 mmol) in THF (15 mL) was added dropwise over 20 min. After stirring at r.t. for 12 h, the reaction was quenched by the sequential addition of MeOH (5 mL) and $NaHCO_3$ solution (60 mL). The phases were separated and the aqueous phase was washed with CH_2Cl_2 (3 $\times$ 60 mL). The combined organic phases were washed with brine (60 mL), dried (Na_2SO_4), filtered and the solvent was evaporated under reduced pressure. The residue was purified by silica gel flash column chromatography (eluent: 15% EtOAc in hexanes) to provide silyl ether **92** as a colourless oil (2.265 g, 92%); R_f = 0.25 (15% EtOAc in hexanes); $[\alpha]_D^{21}$ = 3.5 (c 1, $CHCl_3$) (lit. $[\alpha]_D^{22}$ = +8.5 (c 0.2, $CHCl_3$);[183] ν_{max}(film) /

cm^{-1} 3465br (OH), 3071w, 3049w, 2986m, 2931s, 2858s, 1589w, 1473m, 1463m, 1428s, 1380m, 1371m, 1246m, 1216m, 1113s, 1080s, 823m, 704s; δ_H(300 MHz, $CDCl_3$) 1.06 (s, 9H, (C*H*$_3$)$_3$C), 1.39 (s, 3H, (C*H*$_3$)$_2$C), 1.41 (s, 3H, (C*H*$_3$)$_2$C), 2.03-2.11 (m, 1H, CH_2O*H*), 3.61-3.86 (stack, 4H), 3.91-4.01 (m, 1H), 4.03-4.11 (m, 1H), 7.34-7.48 (stack, 6H, Ph), 7.61-7.70 (stack, 4H, Ph); δ_C(100 MHz, $CDCl_3$) 19.1 (C, (CH_3)$_3$*C*)], [26.8, 26.9, 27.0 (CH_3, (*C*H$_3$)$_3$C, (*C*H$_3$)$_2$C)], 62.5 (CH_2, *C*H_2O), 64.1 (CH_2, *C*H_2O), 77.4 (CH, *C*HO), 79.5 (CH, *C*HO), 109.1 (C, (CH_3)$_2$*C*), 127.7 (CH, Ph), 129.8 (CH, Ph), 132.8 (C, *ipso* Ph), 135.5 (CH, Ph); MS (TOF ES+) *m/z* 423.3 ([M + Na]$^+$, 100%); HRMS (TOF ES+) calcd for $C_{23}H_{32}O_4SiNa$ [M + Na]$^+$ 423.1968, found 423.1956.

Data were in agreement with those reported in the literature.[183,184]

(2*S*,3*S*,4*R*)-2-Azido-1-*O*-[4'-*O*-*tert*-butyldiphenylsilyl-2',3'-*O*-isopropylidene-L-threitol]-3,4-*O*-isopropylidene-octadecane-1,3,4-triol (86)

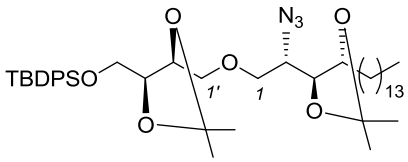

86

Tf_2O (235 µL, 1.40 mmol) was added dropwise over 10 min to a solution of alcohol **92** (561 mg, 1.40 mmol) and 2,6-di-*tert*-butylpyridine (346 µL, 1.54 mmol) in CH_2Cl_2 (14 mL) at 0 °C. After 30 min, the reaction mixture was diluted with CH_2Cl_2 (15 mL) and the resulting solution washed sequentially with cold H_2O (2 × 30 mL) and brine (10 mL), dried (Na_2SO_4) and filtered. Removal of the solvent under reduced pressure provided crude triflate **87** as a colourless oil [R_f = 0.7 (15% EtOAc in hexanes)], which was used immediately in the next etherification step. A solution of alcohol **78** (505 mg, 1.32 mmol) in THF (10 mL) was treated with NaH (60% in mineral oil, 56.0 mg, 1.40 mmol) at 0 ^{o}C. After 1 h, a solution of triflate **87** (assuming 100% conversion, 1.40 mmol) in THF (5 mL) was added dropwise over 5 min. The resulting solution was stirred at this temperature for 1 h and then at r.t. for 12 h. The reaction was then quenched by the addition of MeOH (2 mL) followed by $NaHCO_3$ solution (10 mL). The phases were separated and the aqueous phase was extracted with CH_2Cl_2 (3 × 20 mL). The combined organic fractions were washed with brine (15 mL) and dried (Na_2SO_4), filtered and the solvent was removed under reduced pressure. The residue was purified by flash

column chromatography (eluent: 5% EtOAc in hexanes) R_f = 0.2 (5% EtOAc in hexanes) to provide ether **86** as a colourless oil (815 mg, 80%); R_f = 0.6 (10% EtOAc in hexane); $[\alpha]_D^{21}$ = + 10.0 (*c* 1, $CHCl_3$); ν_{max}(film) / cm^{-1} 2925s, 2855s, 2098s (N_3), 1589w, 1463m, 1428m, 1379m, 1369s, 1218s, 1112s, 1082s, 822s, 701s; δ_H(300 MHz, $CDCl_3$): 0.88 (t, *J* 7.0, 3H, CH_2CH_3), 1.08 (s, 9H, $C(CH_3)_3$), 1.20-1.43 (stack, 35H, alkyl chain methylenes and 4 × acetonide CH_3), 1.49-1.63 (stack, 3H), 3.58-3.75 (stack, 4H), 3.76-3.88 (stack, 3H), 3.91-3.99 (stack, 2H), 4.10-4.24 (stack, 2H), 7.34-7.47 (stack, 6H, Ph), 7.64-7.72 (stack, 4H, Ph); δ_C(100 MHz, $CDCl_3$) 14.1 (CH_3, CH_2CH_3), 19.2 (C, $C(CH_3)_3$), 22.7 (CH_2), 25.7 (CH_3, 1 × CH_3 from 1,2-*anti*-diol acetonide), 26.4 (CH_2), 26.8 (CH_3, 1 × CH_3 from 1,2-*syn*-diol acetonide), 27.0 (CH_3, $C(CH_3)_3$), 27.1 (CH_3, 1 × CH_3 from 1,2-*syn*-diol acetonide], 28.2 (CH_3, 1 × CH_3 from 1,2-*anti*-diol acetonide), [29.3, 29.7 (CH_2, alkyl chain, some resonance overlap)], 31.9 (CH_2), 60.0 (CH), 64.2 (CH_2), 72.4 (CH_2), 80.0 (CH_2), 75.8 (CH), 77.8 (CH), 77.9 (2 × CH), 108.2 (C, $(CH_3)_2C$), 109.4 (C, $(CH_3)_2C$), 127.7 (CH, Ph), 129.7 (CH, Ph), 133.2 (C, *ipso* Ph), 135.6 (CH, Ph); MS (TOF ES+) *m/z* 788.7 ($[M + Na]^+$, 100%); HRMS (TOF ES+) calcd for $C_{44}H_{71}N_3O_6SiNa$ $[M + Na]^+$ 788.5010, found 788.5015.

(2*S*,3*S*,4*R*)-2-Amino-1-*O*-[4'-*O*-*tert*-butyldiphenylsilyl-2',3'-*O*-isopropylidene-L-threitol]-3,4-*O*-isopropylidene-octadecane-1,3,4-triol (85)

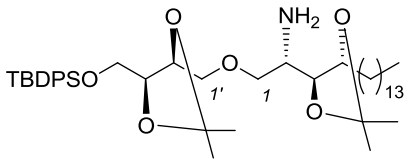

85

PMe_3 (0.7 mL of a 1.0 M soln in THF, 0.7 mmol) was added dropwise over 2 min to a solution of azide **86** (500 mg, 0.65 mmol) in THF / H_2O (7 mL, 15:1). The reaction mixture was stirred at r.t. for 4 h and then concentrated under reduced pressure. The residual H_2O was removed by co-evaporation with toluene (3 × 3 mL) to provide the crude amine product. Purification of the residue by flash column chromatography (30% EtOAc in hexane) afforded amine **85** as a colourless oil (433 mg, 90%): R_f = 0.3 (30% EtOAc in hexane); $[\alpha]^{20}_D$ = +45.6 (*c* 1, $CHCl_3$); ν_{max}(film) / cm^{-1} 3076w, 1113s, 1083s, 702s; δ_H(300 MHz, $CDCl_3$) 0.88 (t, *J* 7.0, 3H, H-18), 1.08 (s, 9H, C(CH_3)$_3$), 1.20-1.43 (stack, 35H, alkyl chain methylenes and acetonide CH_3), 1.49-1.63 (stack, 3H), 3.58-3.75 (stack, 4H), 3.76-3.88 (stack, 3H), 3.91-3.99 (stack, 2H), 4.10-4.24 (stack, 2H), 7.34-7.47 (stack, 6H, Ph), 7.64-7.72 (stack, 4H, Ph); δ_C(100 MHz, $CDCl_3$): 14.1 (CH_3, C-18), 19.2 (CH_2), 22.7 (CH_2), 25.7 (CH_3), 26.4 (CH_2), [26.8, 27.0, 27.1, 28.2 (CH_3, C(CH_3)$_2$, C(CH_3)$_3$, some resonance overlap], [29.3, 29.7 (CH_2, alkyl chain, some resonance overlap)], 31.9 (CH_2), 60.0 (CH), 64.2 (CH_2), 72.4 (CH_2), 80.0 (CH_2), 75.8 (CH), 77.8 (CH), 77.9 (2 × CH), 108.2 (C, (CH_3)$_2$*C*), 109.4 (C, (CH_3)$_2$*C*),

[127.7, 129.7 (CH, Ph, some resonance overlap)], 133.2 (C, *ipso* Ph), 135.6 (CH, Ph, some resonance overlap); MS (TOF ES+) *m/z* 740.6 ([M + H]$^+$, 100%); HRMS (TOF ES+) calcd for $C_{44}H_{74}NO_6Si$ [M + H]$^+$ 740.5285, found 740.5293.

(2*S*,3*S*,4*R*)-1-*O*-[4'-*O*-*tert*-Butyldiphenylsilyl-2',3'-*O*-isopropylidene-L-threitol]-2- Hexacosanoylamino-3,4-*O*-isopropylidene-octadecane-1,3,4-triol (94)

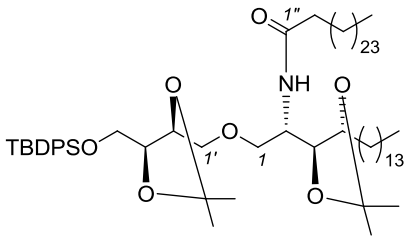

94

A screw-capped glass tube containing a solution of hexacosanoic acid (163 mg, 0.41 mmol) in $(COCl)_2$ (2.0 mL, 23 mmol) was closed tightly and heated at 70 ºC for 2 h. The volatiles were then evaporated under a stream of argon and the tube then placed on a high vacuum line for at least 2 h to remove the residual volatiles. The resulting hexacosanoyl chloride **47** was used directly without further purification: a solution of freshly prepared hexacosanoyl chloride **47** (187 mg, 0.41 mmol) in CH_2Cl_2 (1 mL) was added dropwise over 2 min to a solution of amine **85** (250 mg, 0.34 mmol) and NEt_3 (95 μL, 0.68 mmol) in CH_2Cl_2 (3 mL) at 0 ºC. The reaction mixture was stirred at r.t. for 12 h and then diluted with CH_2Cl_2 (10 mL), washed sequentially with $NaHCO_3$ solution (10 mL), brine (2 mL) and then dried

over Na_2SO_4. The drying agent was removed by filtration and the filtrate concentrated under reduced pressure. Purification of the residue by flash column chromatography provided amide **94** as a colourless oil (323 mg, 85%): R_f = 0.3 (10% EtOAc in hexane); $[\alpha]^{20}_D$ = +11.8 (*c* 1, $CHCl_3$); ν_{max}(film) / cm^{-1} 1646m (C=O); δ_H(300 MHz, $CDCl_3$) 0.88 (t, *J* 7.0, 6H, 2 × CH_2CH_3), 1.06 (s, 9H, $C(CH_3)_3$), 1.16-1.36 (stack, 69H, including (1.32 (s, 3H, $C(CH_3)_2$), alkyl chain methylenes, 1 × $C(CH_3)_2$), 1.40 (s, 3H, $C(CH_3)_2$), 1.41 (s, 3H, $C(CH_3)_2$), 1.42 (s, 3H, $C(CH_3)_2$), 1.45-1.66 (stack, 6H), 2.05-2.18 (stack, 2H), 3.49-3.67 (stack, 3H), 3.74-3.89 (stack, 4H), 4.00-4.23 (stack, 4H), 5.71 (br d, *J* 9.2, 1H), 7.34-7.48 (stack, 6H, Ph), 7.63-7.72 (stack, 4H, Ph); δ_C(100 MHz, $CDCl_3$) 14.1 (CH_3, C-18, C-26"), 22.7 (CH_2), 25.7 (CH_2), 25.8 (CH_3, $C(CH_3)_2$), 26.5 (CH_2), 26.9 (CH_3, $C(CH_3)_3$), 27.1 (CH_3, $C(CH_3)_2$), 27.2 (CH_3, $C(CH_3)_2$), 28.1 (CH_3, $C(CH_3)_2$), 29.1 (CH_2), [29.33, 29.37, 29.38, 29.43, 29.67, 29.68, 29.69, 29.71, 29.73 (CH_2, alkyl chain, some resonance overlap)], 31.9 (CH_2), 37.0 (CH_2), 48.2 (CH), 64.2 (CH_2), 71.3 (CH_2), 72.6 (CH_2), 76.0 (CH), 77.8 (CH), 77.9 (CH), 78.1 (CH), 107.9 (C, $(CH_3)_2C$), 109.5 (C, $(CH_3)_2C$), [127.75, 127.76, 129.79, 129.82, (CH, Ph, some resonance overlap)], 133.1 (C, *ipso* Ph), [135.61, 135.62 (CH, Ph, some resonance overlap)], 172.4 (C, *C*=O); MS (TOF ES+) *m/z* 1140.5 ($[M + Na]^+$, 100%); HRMS (TOF ES+) calcd for $C_{70}H_{123}NO_7Na$ $[M + Na]^+$ 1140.8967, found 1140.8977.

(2*S*,3*S*,4*R*)-1-*O*-[4'-*O*-*tert*-Butyldiphenylsilyl-2',3'-*O*-isopropylidene-L-threitol]-2-hexacosanethioylamino-3,4-*O*-isopropylidene-octadecane-1,3,4-triol (97)

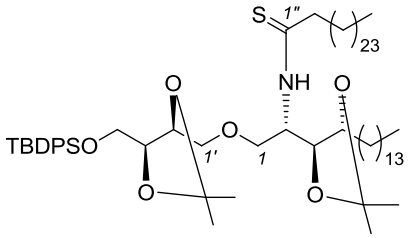

97

Lawesson's reagent (81 mg, 0.2 mmol) was added to a solution of amide **94** (145 mg, 0.13 mmol) in toluene (2 mL) at r.t. The reaction mixture was stirred at 80 ºC for 5 h and then the solvent was removed under reduced pressure. The residue was diluted with CH_2Cl_2 (10 mL), washed sequentially with H_2O (5 mL), $NaHCO_3$ solution (10 mL), brine (2 mL) and then dried over Na_2SO_4. The drying agent was removed by filtration and the filtrate was concentrated under reduced pressure. Purification of the residue by flash column chromatography (15% EtOAc in hexane) provided thioamide **97** as a pale yellow oil (130 mg, 88%): R_f = 0.3 (15% EtOAc in hexane); $[\alpha]^{20}_D$ = +36.8 (*c* 0.5, $CHCl_3$); ν_{max}(film) / cm^{-1} 1258s, 1083s, 736s, 702s; δ_H(300 MHz, $CDCl_3$) 0.88 (t, *J* 7.0, 6H, 2 × CH_2CH_3), 1.06 (s, 9H, $C(CH_3)_3$), 1.17-1.35 (72H, stack, including (1.31 (s, 3H, $C(CH_3)_2$), alkyl chain methylenes, 1 × $C(CH_3)_2$), 1.39 (s, 3H, $C(CH_3)_2$), 1.41 (s, 3H, $C(CH_3)_2$), 1.42 (s, 3H, $C(CH_3)_2$), 1.44-1.58 (stack, 3H), 2.49-2.67 (stack, 2H), 3.49-3.58 (m, 1H), 3.61-3.72 (stack, 2H), 3.74-3.91 (stack, 5H), 4.05-4.21 (stack, 2H), 4.28-4.35 (dd, *J* 7.7, 5.9, 1H), 4.77-4.88 (m, 1H), 7.30-7.49 (stack, 6H, Ph), 7.60-7.75 (stack, 4H, Ph); δ_C(100 MHz, $CDCl_3$) 14.1 (CH_3, C-18, C-26"), 22.7 (CH_2), 25.6 (CH_3,

C(CH_3)$_2$), 26.7 (CH_2), 26.9 (CH_3, C(CH_3)$_3$), 27.0 (CH_3, C(CH_3)$_2$), 27.2 (CH_3, C(CH_3)$_2$), 27.7 (CH_3, C(CH_3)$_2$), 29.0 (CH_2), [29.37, 29.42, 29.56, 29.59, 29.61, 29.7 (CH_2, alkyl chain, some resonance overlap)], 31.9 (CH_2), 47.6 (CH_2), 54.6 (CH), 64.2 (CH_2), 69.7 (CH_2), 72.6 (CH_2), 75.5 (CH), 77.7 (CH), 77.8 (CH), 77.9 (CH), 108.1 (C, (CH_3)$_2$*C*), 109.5 (C, (CH_3)$_2$*C*), [127.8, 129.8, (CH, Ph, some resonance overlap)], 133.1 (C, *ipso* Ph), 135.6 (CH, Ph, some resonance overlap), 205.5 (C, *C*=S); MS (TOF ES+) *m/z* 1156.8 ([M + Na]$^+$, 100%); HRMS (TOF ES+) calcd for $C_{70}H_{123}NO_6SiSNa$ [M + Na]$^+$ 1156.8738, found 1156.8749.

(2*S*,3*S*,4*R*)-1-*O*-[L-Threitol]-2-(hexacosanylcarbonylamino)octadecane-1,3,4-triol (24)

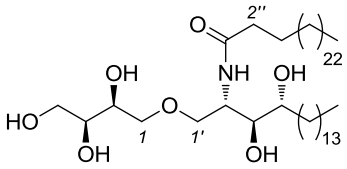

24

TBAF (1.0 M solution in THF, 120 mL, 0.12 mmol) was added to a solution of silyl ether **94** (123 mg, 0.11 mmol) in THF (1 mL) at r.t. After 4 h, NH_4Cl solution (10 mL) was added. The phases were separated and the aqueous phase was extracted with CH_2Cl_2 (3 × 10 mL). The solvent was removed under reduced pressure to provide the corresponding primary alcohol as a white solid (97 mg,

quant.), which was dissolved in CH_2Cl_2 / CH_3OH (10:1, 1.1 mL) and treated with TFA (0.5 mL; dropwise addition over 1 min). After stirring for 2 h at r.t., the reaction mixture was concentrated under reduced pressure and the residual TFA was removed by co-evaporation with Et_2O (3 × 4 mL). Purification of the residue by flash column chromatography (5% CH_3OH in $CHCl_3$) afforded ThrCer **24** as a white-yellow solid (65 mg, 74%): R_f = 0.3 (8% MeOH in $CHCl_3$); $[\alpha]_D$ the insolubility of this amphiphilic compound at r.t. prevented us from obtaining reliable optical rotation data; mp 107–109 °C; ν_{max}(neat) / cm^{-1} 3308br m (O–H, N–H), 2915s, 2849s, 2098w, 1634m (C=O), 1540m, 1471m, 1108m, 1070m, 1026m, 718m; δ_H(500 MHz, d_8-THF, 45 °C) 0.89 (app t, *J* 6.7, 6H, 2 × CH_2CH_3), 1.25-1.63 (stack, 72H, alkyl chain), 2.12 (t, *J* 7.7, 2H, C(O)CH_2), 3.40-3.47 (stack, 2H, H-3', H-4'), 3.47-3.57 (stack, 5H, C(1)H_2, C(4)H_2, H-2 or H-3), 3.59-3.63 (m, 1H, C(1')$H_a$$H_b$), 3.67-3.72 (stack, 2H, C(1')$H_a$$H_b$, H-3 or H-2), 4.14-4.18 (m, 1H, H-2'), 6.93-6.96 (m, 1H, N*H*); δ_C(125 MHz, d_8-THF, 45 °C) 14.3 (CH_3, 2 × CH_2CH_3), [23.5 (CH_2), 26.6 (CH_2), 26.8 (CH_2), 29.3 (CH_2), 30.3 (CH_2), 30.5 (CH_2), 30.59 (CH_2), 30.64 (CH_2), 30.7 (CH_2), 30.8 (CH_2), 32.8 (CH_2), 34.1 (CH_2) alkyl chain methylenes, resonance overlap], 36.9 (CH_2, C(O)CH_2), 51.8 (CH, C-2'), 64.6 (CH_2, C-4), 71.3 (CH, C-2 or C-3), 71.5 (CH_2, C-1'), 73.0 (CH, C-4'), 73.1 (CH, C-3 or C-2), 74.1 (CH_2, C-1), 76.7 (CH, C-3'), 173.0 (C, *C*=O); MS (TOF ES+) *m/z* 822.7 ($[M+Na]^+$, 100%); HRMS (TOF ES+) calcd for $C_{48}H_{97}NO_7Na$ $[M+Na]^+$ 822.7163, found 822.7175.

Data were in agreement with those reported in the literature.[124]

(2'*S*,3'*S*,4'*R*)-2'-Hexacosanethioylamino-1'-*O*-[L-threitol]-octadecane-1',3',4'-triol (38)

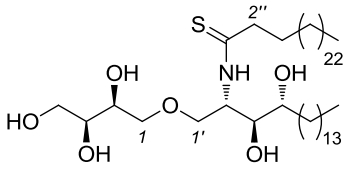

38

TBAF (1.0 M solution in THF, 120 μL, 0.12 mmol) was added to a solution of silyl ether **97** (125 mg, 0.11 mmol) in THF (1 mL) at r.t. After 4 h, NH_4Cl solution (10 mL) was added. The phases were separated and the aqueous phase was extracted with CH_2Cl_2 (3 × 10 mL). The solvent was removed under reduced pressure to provide the resulting primary alcohol as a white solid (98 mg, quant.), which was dissolved in CH_2Cl_2 / CH_3OH (10:1, 1.1 mL) and treated with TFA (0.5 mL; dropwise addition over 1 min). After stirring for 2 h at r.t., the reaction mixture was concentrated under reduced pressure and the residual TFA was removed by co-evaporation with Et_2O (3 × 4 mL). Purification of the residue by flash column chromatography (5% CH_3OH in $CHCl_3$) afforded pentaol **38** as a pale yellow solid (65 mg, 73%): R_f = 0.3 (8% CH_3OH in $CHCl_3$); $[\alpha]_D$ the insolubility of this amphiphilic compound at r.t. prevented us from obtaining reliable optical rotation data; mp 96 – 97 °C; ν_{max}(film) / cm^{-1} 3324s br (O–H); δ_H(500 MHz, $CDCl_3$:CD_3OD, 2:1) 0.83 (t, *J* 7.0, 6H, 2 × CH_2CH_3), 1.11-1.41 (stack, 69H, alkyl chain methylenes), 1.43-1.74 (stack, 3H), 2.60 (t, *J* 8.1, 2H, C(3")H_2), 3.48-3.54 (stack, 3H, C(1')H_2, H-4), 3.55-3.63 (stack, 3H, C(4')H_2, H-3'), 3.64-3.72 (stack, 2H,

C(1)H_aH_b, H-3), 3.74-78 (m, 1H, H-2'), 3.80-3.86 (m, 1H, C(1)H_aH_b), 4.83-4.88 (m, 1H, H-2); δ_C(125 MHz, $CDCl_3$:CD_3OD, 2:1) 14.2 (CH_3, 2 × CH_2CH_3), 22.9 (CH_2), 26.2 (CH_2), 29.3 (CH_2), [29.6, 29.7, 29.8, 30.0 (CH_2, alkyl chain, resonance overlap)], 32.2 (CH_2), 32.7 (CH_2, C-5), 46.9 (CH_2, C-2"), 56.1 (CH, C-2), 63.7 (CH_2, C-4'), 69.6 (CH_2, C-1), 70.6 (CH, C-2'), 72.2 (CH, C-3'), 73.0 (CH_2, C-4), 73.2 (CH_2, C-1'), 74.1 (CH, C-3), 205.9 (C, *C*=S); MS (TOF ES+) *m/z* 838.7 ($[M + Na]^+$, 100%); HRMS (TOF ES+) calcd for $C_{50}H_{99}NO_8SNa$ $[M + Na]^+$ 838.6934, found 838.6946.

(2'*S*,3'*S*,4'*R*)-3',4'-Di-*O*-acetyl-1'-*O*-(2,3,4-tri-*O*-acetyl-L-threitol]-2'-(hexacosanoylamino)octadecane-1',3',4'-triol (95)

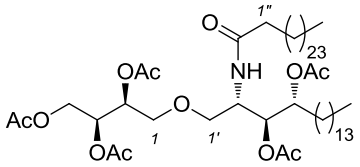

95

Ac_2O (420 μL, 4.5 mmol) was added dropwise over 1 min to a solution of ThrCer **24** (120 mg, 0.15 mmol) in pyridine (2 mL). The reaction mixture was stirred at r.t. for 10 h, after which time, the volatiles were removed under reduced pressure. The residue was diluted with CH_2Cl_2 (10 mL), washed sequentially with H_2O (5 mL), $NaHCO_3$ solution (10 mL), brine (3 mL) and then dried over Na_2SO_4. The drying

agent was removed by filtration and the filtrate was concentrated under reduced pressure. The crude product was purified by flash column chromatography (25% EtOAc in hexane) to afford hexa-acetate **95** as a white solid (144 mg, 95%): R_f = 0.26 (25% EtOAc in hexane); $[\alpha]^{20}_D$ = +18.4 (*c* 1, $CHCl_3$); ν_{max}(film) / cm^{-1} 2917 s, 2850s, 1739s, 1650m, 1540w, 1468m, 1371m, 1220s, 1132m, 1046m, 978w, 720m, 682m; δ_H(500 MHz, $CDCl_3$) 0.88 (t, *J* 7.1, 6H, CH_2CH_3), [1.21-1.33 (stack, 68H, alkyl chain methylenes)], 1.53-1.72 (stack, 4H, C(5')H_aH_b, C(2")H_aH_b,), 2.01 (s, 3H, C(4')COCH_3), 2.05 (s, 3H, C(4)COCH_3), 2.08 (stack, 6H, C(2)COCH_3, C(3)COCH_3), 2.10 (s, 3H, C(4')COCH_3), 2.22 (t, *J* 7.6, 2H, C(1")H_aH_b), 3.41 (A of ABX, dd, *J* 9.7, 3.2, 1H, C(1')H_aH$_b$), 3.43-3.48 (stack, 2H, C(1)H_aH$_b$, C(1')H$_a$$H_b$), 3.53 (B of ABX, dd, *J* 10.9, 5.6, 1H, C(1)H$_a$$H_b$), 4.04 (dd, *J* 11.8, 6.8, 1H, C(4)H_aH$_b$), 4.26-4.32 (stack, 2H, C(4)H$_a$$H_b$, H2'), 4.89-4.93 (m, 1H, H4'), 5.12-5.18 (stack, 2H, H2, H3'), 5.28-5.33 (m, 1H, H3), 6.21 (1H, br d, *J* 9.2, N*H*); δ_c(125 MHz): 14.1 (CH_3, C18', C25''), 20.7 (CH_3, (C4)CO*C*H$_3$), 20.75 (2 x CH_3, (C2)CO*C*H$_3$, (C3)CO*C*H$_3$), 20.8 (CH_3, (C3')CO*C*H$_3$), 21.0 (CH_3, (C4')CO*C*H$_3$), 22.7 (CH_2), (alkyl chain, some resonance overlap)], 25.6 (CH_2), 25.7 (CH_2, C2''), 28.0 (CH_2, C5'), [29.3-29.4 (CH_2, alkyl chain, some resonance overlap)], [29.4, 29.56, 29.58, 29.7 (CH_2, alkyl chain, some resonance overlap)], 31.9 (CH_2), 36.6 (CH_2, C1''), 47.9 (CH, C2'), 62.2 (CH_2, C4), 69.17 (CH_2, C1), 69.24 (CH, C3), 69.66 (CH, C2), 69.72 (CH_2, C1'), 71.8 (CH, C3'), 73.2 (CH, C4'), 169.8 (C, (C3')*C*OCH$_3$), 170.2 (2 x C, (C2)*C*OCH$_3$, (C3)*C*OCH$_3$), 170.5 (C, (C4)*C*OCH$_3$), 170.8 (C, (C4')*C*OCH$_3$), 173.0 (C, C=O); MS (TOF ES+) *m/z* 1032.6 ($[M + Na]^+$, 100%); HRMS (TOF ES+) calcd for $C_{68}H_{120}N_2O_7SiNa$ ($[M+Na]^+$) 1032.7691, found 1032.7698.

(2'*S*,3'*S*,4'*R*)-3,4-Di-*O*-acetyl-1-*O*-(2,3,4-tri-*O*-acetyl-L-threitol]-2'-(hexacosa-thioylamino)octadecane-1',3',4'-triol (96)

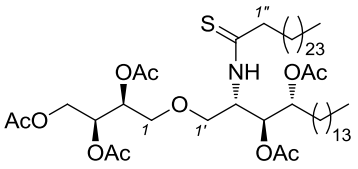

96

Lawesson's reagent (60 mg, 0.12 mmol) was added to a solution of amide **95** (102 mg, 0.10 mmol) in toluene (2 mL) at r.t. The reaction mixture was stirred at 80 ºC for 4 h and then the solvent was removed under reduced pressure. The residue was diluted with CH_2Cl_2 (10 mL), washed sequentially with H_2O (5 mL), $NaHCO_3$ solution (10 mL), brine (2 mL) and then dried over Na_2SO_4. The drying agent was removed by filtration and the filtrate was concentrated under reduced pressure. Purification of the residue by flash column chromatography (20% EtOAc in hexane) provided thioamide **96** as a pale yellow solid (92 mg, 87%): R_f = 0.26 (20% EtOAc in hexane); $[\alpha]_D^{20}$= +54.0 (*c* 1, $CHCl_3$); δ_H(500 MHz, $CDCl_3$): 0.88 (t, *J* 7.1, 6H, CH_2CH_3), [1.19-1.36 (stack, 68H, alkyl chain methylenes)], 1.54-1.64 (m, 1H, C(5')H_aH_b), 1.66-1.83 (stack, 3H, C(5')H_aH_b, C(2")H_aH_b), [2.04, 2.05, 2.08, 2.09, 2.11, (stack, 15H, 5 x COCH_3)], 2.63-2.74 (stack, 2H, C(1")H_aH_b), 3.46 (A of ABX, dd, *J* 10.8, 5.2, 1H, C(1)H_aH_b), 3.53-3.58 (stack, 2H, C(1)H_aH_b, C(1')H_aH_b), 3.61 (B of ABX, dd, *J* 10.0, 3.1, 1H, C(1')H_aH_b), 4.04 (A of ABX, dd, *J* 11.8, 6.9, 1H, C(4)H_aH_b), 4.30 (B of ABX, dd, *J* 10.0, 3.1, 1H, C(4)H_aH_b), 4.86-4.91 (m, 1H, H4'), 5.05-5.12 (m, 1H, H2'), 5.16 (app q, *J* 10.1, 5.2, 1H, H2), 5.28 (dd, *J* 8.0, 3.2,

1H, H3'), 5.31-5.33 (m, 1H, H3), 8.07 (br d, *J* 9.0, 1H, N*H*); δ_C(125 MHz): 14.1 (CH_3, C18', C25''), [20.7, 20.8, 21.0 (CH_3, 5 x CO*C*H_3, some resonance overlap), 22.7 (CH_2), 25.5 (CH_2), 28.8 (CH_2, C5'), 29.0 (CH_2), 29.4 (CH_2 ,C2''), [29.5, 29.6, 29.7, (CH_2, alkyl chain, some resonance overlap)], 31.9 (CH_2), 47.2 (CH_2, C1''), 53.8 (CH, C2'), 62.2 (CH_2, C4), 68.3 (CH_2, C1'), 69.2 (CH, C3), 69.3 (CH_2, C1), 69.6 (CH, C2), 71.5 (CH, C3'), 73.1 (CH, C4'), 169.9 (C, (C3')*C*OCH_3), 170.1 (C, (C2)*C*OCH_3), 170.2 (C, (C3)*C*OCH_3), 170.5 (C, (C4)*C*OCH_3), 170.9 (C, (C4')*C*OCH_3), 206.8 (C, *C*=S); MS (TOF ES+) *m/z* 1048.9 ($[M + Na]^+$, 100%); HRMS (TOF ES+) calcd for $C_{68}H_{120}N_2O_7SiNa$ ($[M+Na]^+$) 1048.7463, found 1048.7466.

(2*S*,3*S*,4*R*)-1-*O*-[4'-*O*-*tert*-Butyldiphenylsilyl-2',3'-*O*-isopropylidene-L-threitol]-3,4-*O*-isopropylidene-2-(tetracosanyloxycarbonylamino)octadecane-1,3,4-triol (98)

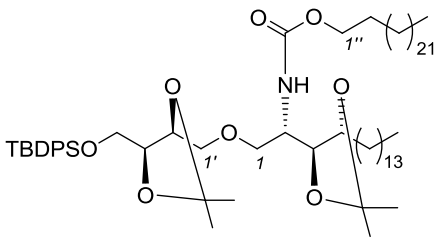

98

A solution of carbonic acid, 2,5-dioxo-1-pyrrolidinyl tetracosanyl ester (110 mg, 0.21 mmol) in CH_2Cl_2 (0.5 mL) was added to a stirred solution of amine **85** (104 mg, 0.14 mmol) and NEt_3 (42 μL, 0.3 mmol) in CH_2Cl_2 (1 mL). The resulting mixture was stirred at r.t. until no mixed carbonate remained as determined by TLC (5 h). The mixture was then diluted with CH_2Cl_2 (10 mL) and washed sequentially with $NaHCO_3$ solution (10 mL) and brine (10 mL). The organic phase was dried over Na_2SO_4 and the solvent was evaporated under reduced pressure. Purification of the residue by flash column chromatography (10% EtOAc in toluene) provided carbamate **99** as a colourless oil (135 mg, 86%): R_f = 0.3 (10% EtOAc in hexane); $[\alpha]^{22}_D$ = +28.8 (*c* 0.5, $CHCl_3$); ν_{max}(film) / cm^{-1} 1687m (C=O); δ_H(500 MHz, $CDCl_3$) 0.88 (t, *J* 7.1, 6H, 2 × CH_2CH_3), 1.06 (s, 9H, $C(CH_3)_3$), 1.26-1.34 (stack, 70H, alkyl chain methylenes), 1.40 (s, 6H, $C(CH_3)_2$), 1.42 (s, 3H, $C(CH_3)_2$), 1.59 (s, 3H, $C(CH_3)_2$), 3.52-3.65 (stack, 3H, C(1)H_aH_b, C(1')H_aH_b), 3.74-3.81 (stack, 3H, C(4')H_aH_b,, C(1)H_aH_b), 3.82-3.90 (stack, 2H, H-3', H-2), 3.98 (m, 1H, C(1")H_aH_b), 4.00-4.11 (stack, 3H, H-3, H-4, C(1")H_aH_b), 4.14-4.20 (m, 1H, H-2'), 4.97 (br d, *J* 9.5, 1H, N*H*), 7.36-7.46 (stack, 6H, Ph), 7.66-7.70 (stack, 4H, Ph);

δ_C(125 MHz, $CDCl_3$) 14.1 (CH_3, C-18, C-24”), 19.2 (C, $(CH_3)_3CSi$), 22.7 (CH_2), 25.8 (CH_3, $C(CH_3)_2$), 25.9 (CH_2), 26.4 (CH_2), 26.8 (CH_3, $C(CH_3)_3$), 27.0 (CH_3, $C(CH_3)_2$), 27.2 (CH_3, $C(CH_3)_2$), 28.1 (CH_3, $C(CH_3)_2$), 28.9 (CH_2), 29.1 (CH_2), 29.4 (CH_2), [29.6, 29.7 (CH_2, alkyl chains, some resonance overlap)], 31.9 (CH_2), 50.3 (CH, C-2), 64.1 (CH_2, C-4’), 65.2 (CH_2, C-1”), 71.6 (CH_2, C-1), 72.6 (CH_2, C-1’), 75.9, (CH, C-3), 77.7 (CH, C-2’), 77.8 (CH, C-4), 78.2 (CH, C-3’), 107.8 (C, $(CH_3)_2C$), 109.4 (C, $(CH_3)_2C$), [127.7, 129.75, 129.79, (CH, Ph, some resonance overlap)], 133.2 (C, *ipso* Ph), 135.6 (CH, Ph, some resonance overlap), 156.0 (C, *C*=O); MS (TOF ES+) *m/z* 1142.7 ($[M + Na]^+$, 100%); HRMS (TOF ES+) calcd for $C_{69}H_{121}NO_8SiNa$ $[M + Na]^+$ 1142.8759, found 1142.8767.

(2*S*,3*S*,4*R*)-2-Tetracosanyloxycarbonylamino-1-*O*-[L-threitol]-octadecane-1,3,4-triol (40)

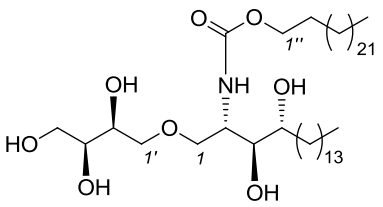

40

TBAF (1.0 M solution in THF, 180 μL, 0.18 mmol) was added to a solution of silyl ether **99** (179 mg, 0.16 mmol) in THF (1.5 mL) at r.t. After 4 h, NH_4Cl solution (10 mL) was added. The phases were separated and the aqueous phase was extracted with CH_2Cl_2 (3 × 10 mL). The solvent was removed under reduced pressure to provide the crude primary alcohol as a white solid (141 mg, quant.), which was dissolved in CH_2Cl_2 / CH_3OH (10:1, 1.2 mL) and treated with TFA (0.6 mL; dropwise addition over 1 min). After stirring for 2 h at r.t., the reaction mixture was concentrated under reduced pressure and the residual TFA was removed by co-evaporation with Et_2O (3 × 4 mL) to provide the crude product, which was purified by flash column chromatography (10% CH_3OH in $CHCl_3$) to afford pentaol **40** as a pale yellow solid (90 mg, 70%): R_f = 0.3 (10% CH_3OH in $CHCl_3$); $[\alpha]_D$ the insolubility of this amphiphilic compound at r.t. prevented us from obtaining reliable optical rotation data; mp 55 – 56 °C; ν_{max}(film) / cm^{-1} 3340m br (O–H), 1683s (C=O); δ_H(500 MHz, $CDCl_3$:CD_3OD, 2:1) 0.83 (t, *J* 7.2, 6H, 2 × CH_2CH_3), 1.16-1.45 (stack, 65H, alkyl chain methylenes), 1.46-1.68 (stack, 5H), 3.12-3.20 (m, 1H), 3.49-3.64 (stack, 8H), 3.67-3.79 (stack, 2H), 3.85-4.07 (stack, 3H), O*H*

resonances not observed; δ_C(125 MHz, $CDCl_3$:CD_3OD, 2:1) 14.2 (CH_3, 2 × CH_2CH_3), 20.1 (CH_2), 23.0 (CH_2), 24.1 (CH_2), 26.2 (CH_2), [29.5, 29.7, 30.0, 30.4, (CH_2, alkyl chains, some resonance overlap)], 32.3 (CH_2), 32.9 (CH_2), 52.1 (CH), 63.9 (CH_2), 65.8 (CH_2), 70.8 (CH), 71.2 (CH_2), 72.5 (CH), 72.8 (CH), 73.4 (CH_2), 75.5 (CH), 157.7 (C, *C*=O); MS (TOF ES+) *m/z* 824.8 ([M + Na]$^+$, 100%); HRMS (TOF ES+) calcd for $C_{50}H_{99}NO_8SNa$ [M + Na]$^+$ 809.6955, found 824.6940.

(2*S*,3*S*,4*R*)-1-*O*-[4'-*O*-*tert*-Butyldiphenylsilyl-2',3'-*O*-isopropylidene-L-threitol]-3,4-*O*-isopropylidene-2-(tricosanylaminocarbonylamino)-octadecane-1,3,4-triol (98)

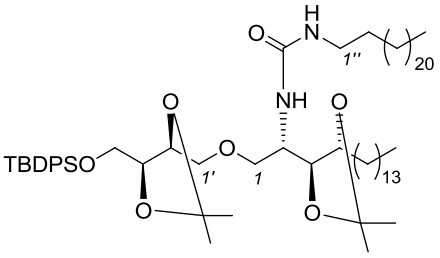

98

A solution of amine **85** (155 mg, 0.21 mmol) in toluene (1.5 mL) was added to a solution of tricosanyl isocyanate **48** (121 mg, 0.33 mmol; prepared as reported previously (see page 198) in the synthesis of urea **77**) in toluene (1 mL) at r.t. The reaction mixture was heated under reflux for 8 h and then concentrated under reduced pressure to provide the crude product. Purification of the residue by flash column chromatography (15% EtOAc in hexane) afforded urea **98** as a pale yellow

oil (186 mg, 80% based on amine): R_f = 0.3 (10% EtOAc in hexane); $[\alpha]^{22}_{D}$ = +48.8 (*c* 1, $CHCl_3$); ν_{max}(film) / cm^{-1} 1632m (C=O); δ_H(500 MHz, $CDCl_3$) 0.88 (t, *J* 7.1, 6H, 2 × CH_2CH_3), 1.06 (s, 9H, $C(CH_3)_3$), 1.21-1.32 (stack, 68H, alkyl chain methylenes), 1.39 (s, 3H, 1 × $C(CH_3)_2$), 1.40 (s, 3H, 1 × $C(CH_3)_2$), 1.41 (s, 3H, 1 × $C(CH_3)_2$), 1.61 (s, 3H, 1 × $C(CH_3)_2$), 3.03-3.17 (stack, 2H, C(1")H_aH_b), 3.53-3.60 (stack, 2H, C(1')H_aH_b, C(1)H_aH_b), 3.65 (dd, *J* 10.5, 3.2, 1H, C(1')H_aH_b), 3.72-3.80 (stack, 3H, C(4')H_aH_b, C(1)H_aH_b), 3.82-3.87 (m, 1H, H-3'), 3.92-3.97 (m, 1H, H-2), 4.04-4.11 (stack, 2H, H-3, H-4), 4.13-4.18 (m, 1H, H-2'), 4.31 (br s, 1H, CH_2NH), 4.49 (br d, *J* 9.2, 1H, CHNH), 7.37-7.46 (stack, 6H, Ph), 7.64-7.70 (stack, 4H, Ph); δ_C(125 MHz, $CDCl_3$) 14.1 (CH_3, 2 × CH_2CH_3), 19.2 (C, $C(CH_3)_3$), 22.7 (CH_2), 25.8 (CH_3, 1 × $C(CH_3)_2$), 26.4 (CH_2), 26.8 (CH_3, $C(CH_3)_3$), 26.9 (CH_2), 27.1 (CH_3, 1 × $C(CH_3)_2$), 27.2 (CH_3, 1 × $C(CH_3)_2$), 28.1 (CH_3, 1 × $C(CH_3)_2$), 29.1 (CH_2), [29.4, 29.7 (CH_2, alkyl chain, resonance overlap)], 30.2 (CH_2), 31.9 (CH_2), 40.6 (CH_2, C-1"), 49.7 (CH, C-2), 64.3 (CH_2, C-4'), 72.0 (CH_2, C-1), 72.7 (CH_2, C-1'), 76.3 (CH, C-3), 77.3 (CH, C-2'), 77.9 (CH, C-4), 78.2 (CH, C-3'), 107.8 (C, $C(CH_3)_2$), 109.5 (C, $C(CH_3)_2$), 127.8 (CH, Ph), 129.8 (CH, Ph), 133.1 (C, *ipso* Ph), 135.6 (CH, Ph), 157.4 (C, *C*=O); MS (TOF ES+) *m/z* 1127.7 ($[M + Na]^+$, 100%); HRMS (TOF ES+) calcd for $C_{68}H_{120}N_2O_7SiNa$ $[M + Na]^+$ 1127.8763, found 1127.8737.

(2*S*,3*S*,4*R*)-1-*O*-[L-Threitol]-2-(tricosanylaminocarbonylamino)octadecane-1,3,4-triol (39)

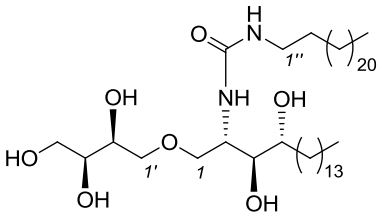

39

TBAF (1.0 M solution in THF, 170 μL, 0.17 mmol) was added to a solution of silyl ether **98** (167 mg, 0.15 mmol) in THF (1.5 mL) at r.t. After 4 h, NH_4Cl solution (10 mL) was added. The phases were separated and the aqueous phase was extracted with CH_2Cl_2 (3 × 10 mL). The solvent was removed under reduced pressure to provide a white solid (primary alcohol product, 130 mg, quant.), which was dissolved in CH_2Cl_2 / CH_3OH (10:1, 1.2 mL). TFA (0.6 mL) was added dropwise over 1 min. After stirring for 2 h at r.t., the reaction mixture was concentrated under reduced pressure and the residual TFA was removed by co-evaporation with Et_2O (3 × 4 mL) to provide the crude product, which was purified by flash column chromatography (10% CH_3OH in $CHCl_3$) to afford the pentaol **39** as a white solid (85 mg, 72%): R_f = 0.3 (10% CH_3OH in $CHCl_3$); $[\alpha]_D$ the insolubility of this amphiphilic compound at r.t. prevented us from obtaining reliable optical rotation data; mp 131 – 132 °C; ν_{max}(film) / cm^{-1} 3344s br (O–H), 1607s (C=O); δ_H(500 MHz, $CDCl_3$:CD_3OD, 2:1) 0.84 (t, *J* 6.9, 6H, 2 × CH_2CH_3), 1.15–1.55 (stack, 67H, alkyl chain methylenes), 1.58–1.69 (m, 1H), 2.99–3.15

(stack, 2H), 3.46–3.66 (stack, 8H), 3.71–3.80 (stack, 2H), 3.93–3.99 (m, 1H), O*H* and N*H* resonances not observed; δ_C(125 MHz, $CDCl_3$:CD_3OD, 2:1) 14.3 (CH_3, 2 × CH_2CH_3), 23.2 (CH_2), 26.4 (CH_2), 27.4 (CH_2), [29.8, 29.9, 30.1, 30.2, 30.3 (CH_2, alkyl chain, resonance overlap)], 30.7 (CH_2), 32.4 (CH_2), 33.5 (CH_2), 40.7 (CH_2), 51.2 (CH), 64.1 (CH_2), 70.7 (CH), 72.1 (CH_2), 72.5 (CH), 73.5 (CH), 73.9 (CH_2), 75.9 (CH), 159.9 (C, *C*=O); MS (TOF ES+) *m/z* 809.8 ($[M + Na]^+$, 100%); HRMS (TOF ES+) calcd for $C_{50}H_{99}NO_8SNa$ $[M + Na]^+$. 809.6959, found 809.6950.

α-Bromo hexacosanoic acid (115)

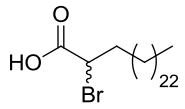

115

A mixture of hexacosanoic acid (600 mg, 1.51 mmol) and red phosphorus (47 mg, 1.5 mmol) was heated to 95 °C and Br_2 (270 µL, 5.29 mmol) was added dropwise over 2 min at this temperature with stirring. The mixture was stirred for 6 h and then cooled to r.t., diluted with Et_2O (30 mL) and washed with H_2O (30 mL). The aqueous phase was extracted with Et_2O (2 × 30 mL), and the combined organic fractions were washed with brine (10 mL), dried with $MgSO_4$, filtered and the solvent was removed under reduced pressure to yield the α-bromo acid as a white solid, which was recrystallised from hexanes and used without further purification in the next reaction (481 mg, 67%). R_f = 0.35 (30% EtOAc in hexane); mp 73 - 74

°C (from hexane); ν_{max}(film) / cm^{-1} 3300-2600w v br (OH), 2915s, 2849s, 1715m (C=O), 1697s (C=O), 1477w, 1462m, 1429w, 1241w (br), 1164w, 1120w, 906w, 725m, 662m; δ_H(300 MHz, $CDCl_3$) 0.88 (t, *J* 6.8, 3H, CH_2CH_3), 1.21-1.33 (stack, 44H, alkyl chain), 1.95-2.21 (m, 2H, CH_2CHBr), 4.24 (app t, *J* 7.6, 1H, CH_2CHBr), O*H* not observed; δ_c(100 MHz, $CDCl_3$) 14.1 (CH_3, CH_2CH_3), 22.7 (CH_2), 27.2 (CH_2), 28.8 (CH_2), [29.3, 29.4, 29.5, 29.7, 29.8 (CH_2, alkyl chain, resonance overlap)], 32.0 (CH_2), 34.7 (CH_2, CH_2CHBr), 45.4 (CH, CH_2CHBr), 176.0 (C, *C*=O); *m/z* (TOF ES–) 475.3 ([M(^{81}Br isotopomer) – H]$^-$, 100%), 473.3 (100, [M(^{79}Br isotopomer) – H]$^-$). HRMS *m/z* (TOF ES–) calcd for $C_{26}H_{50}{}^{79}BrO_2$ [M – H]$^-$ 473.2994, found 473.2989.

α-Azido hexacosanoic acid (116)

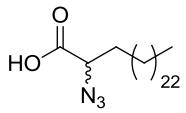

116

NaN_3 (690 mg, 10.6 mmol) was added to a solution of α-bromo acid **115** (481 mg, 1.01 mmol) in DMF (5 mL). The reaction mixture was stirred vigorously at 60 °C. After 48 h, the reaction mixture was allowed to cool to r.t., diluted with Et_2O (20 mL) and washed with 1 M hydrochloric acid (50 mL). The phases were separated

and the aqueous phase was extracted with Et_2O (2 × 25 mL). The combined organic fractions were washed with brine (20 mL) and dried with $MgSO_4$. Removal of the volatiles under reduced pressure and purification of the residue by flash column chromatography (eluent 15% EtOAc in toluene) afforded α-azido acid **116** as a white solid (394 mg, 60% over 2 steps from hexacosanoic acid); R_f = 0.2 (30% EtOAc in hexane); mp 77 - 78 °C; ν_{max}(neat) / cm^{-1} 3300-2600w v br (OH), 2915s, 2849s, 2124m (N_3), 1717m (C=O), 1471m, 1256m, 717m; δ_H(300 MHz, $CDCl_3$) 0.88 (t, *J* 6.9, 3H, CH_2CH_3), 1.19-1.40 (stack, 41H, CH_2 resonances in alkyl chain), 1.41-1.54 (stack, 3H,), 1.72-1.96 (stack, 2H, CH_2CHN_3), 4.24 (dd, *J* 8.3, 5.2, 1H, CH_2CHN_3), OH resonance not observed; δ_c(100 MHz, $CDCl_3$): 14.1 (CH_3, CH_2CH_3), 22.7 (CH_2), 25.7 (CH_2), 29.1 (CH_2), [29.4, 29.5, 29.7 (CH_2, alkyl chain, significant resonance overlap)], 31.3 (CH_2), 32.0 (CH_2, CH_2CHN_3), 61.9 (CH, CH_2CHN_3), 176.6 (C, *C*=O); MS (TOF ES–) *m/z* 436.4 ($[M - 1]^-$, 100%); HRMS (TOF ES–) calcd for $C_{26}H_{50}N_3O_2$ $[M - 1]^-$ 436.3903, found 436.3920.

(2*S*,3*S*,4*R*)-2-Amino-1-*O*-[2',3'-*O*-isopropylidene-L-threitol]-3,4-*O*-isopropylidene-octadecane-1,3,4-triol (118)

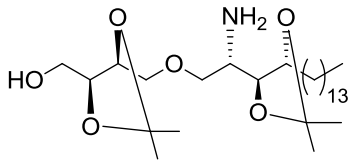

118

TBAF (1.0 M solution in THF, 1.1 mL, 1.1 mmol) was added to a solution of silyl ether **85** (750 mg, 0.98 mmol) in THF (10 mL) at r.t. After 4 h, NH_4Cl solution (10 mL) was added. The phases were separated and the aqueous phase was extracted with CH_2Cl_2 (3 × 10 mL). The solvent was removed under reduced pressure and the residue purified by flash column chromatography (eluent: 25% EtOAc in hexanes) to provide alcohol **118** as a colourless oil (490 mg, 95%). R_f = 0.35 (30% EtOAc in hexane); $[\alpha]_D^{21}$ = 22.0 (*c* 1, $CHCl_3$); ν_{max}(film) / cm^{-1} 3487br (OH), 2923s, 2098s (N_3), 1458w, 1370m, 1250s, 1219s, 1168m, 1058s, 989m, 846s, 707w; δ_H(300 MHz, $CDCl_3$) 0.87 (t, *J* 6.2, 3H, CH_2CH_3), 1.22-1.34 (stack, 25H,), 1.40-1.45, (stack, 9H,), 1.46-1.65 (stack, 4H), 1.99 (dd, *J* 7.8, 4.8, 1H, O*H*), 3.51-4.18 (broad stack, 11H,); δ_C(100 MHz, $CDCl_3$) 14.1 (CH_3), 22.7 (CH_2), 25.6 (CH_3, (CH_3)$_2$C), 26.4 (CH_2), 27.0 (CH_3, (CH_3)$_2$C, some resonance overlap), 28.1 (CH_3, (CH_3)$_2$C), [29.4, 29.6 (CH_2, alkyl chain, some resonance overlap)], 31.9 (CH_2), 59.9 (CH), 62.3 (CH_2), 71.9 (CH_2), 72.9 (CH_2), 75.6 (CH), 76.0 (CH), 77.8 (CH), 79.4 (CH), 108.3 (C, (CH_3)$_2$*C*)), 109.4 (C, (CH_3)$_2$*C*)); MS (TOF ES+) *m/z*

550.5 ([M + Na]$^+$, 100%); HRMS (TOF ES+) calcd for $C_{28}H_{53}N_3O_6Na$ [M + Na]$^+$ 550.3832, found 550.3853.

(2*S*,3*S*,4*R*)-2-[2''-Azido-hexacosanoylamino]-1-*O*-[2',3'-*O*-isopropylidene-L-threitol]octadecane-*O*-isopropylidene-octadecane-1,3,4-triol (119)

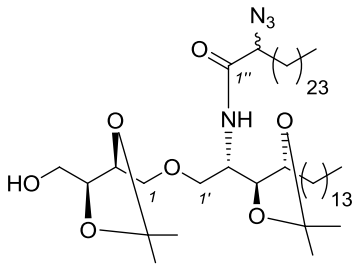

119

A solution of α-azido acid **116** (44 mg, 0.11 mmol) in $(COCl)_2$ (2 mL) was heated at 70 °C. After 2 h, the volatiles were removed under a stream of N_2 and the residual solvent removed on the vacuum line (1 h) to provide the corresponding acid chloride **117** as a pale yellow oil, which was used directly in the next step without further purification (50 mg, quant.): A solution of freshly prepared acid chloride **117** (50 mg, 0.11 mmol) in CH_2Cl_2 (0.6 mL) was added dropwise over 2 min to a solution of amine **118** (69 mg, 0.14 mmol) and NEt_3 (32 µL, 0.23 mmol) in CH_2Cl_2 (0.8 mL) at 0 ºC. The reaction mixture was stirred at rt for 12 h and then diluted with CH_2Cl_2 (10 mL), washed sequentially with $NaHCO_3$ solution (10 mL), brine (2 mL) and then dried over Na_2SO_4. The drying agent was removed by filtration and

the filtrate concentrated under reduced pressure. Purification of the residue by flash column chromatography provided amide **119** as a colourless oil (92 mg, 91%, 1:1 mixture of epimers). Data on epimeric mixture: R_f = 0.3 (20% EtOAc in hexane); ν_{max}(film) / cm^{-1} 3309br (OH), 2918s, 2859s, 2109m (N_3), 1651m, 1534w, 1467m, 1370m, 1245m, 1218m, 1072m, 872w, 756s, 722m; δ_H(500 MHz, $CDCl_3$) 0.87 (t, *J* 6.8, 6H, 2 × CH_2CH_3), 1.20-1.34 (stack, 68H), 1.39-1.43 (stack, 12H), 1.44-1.56 (stack, 2H), 1.74-1.94 (stack, 2H, incl. C(3")H_2), 2.25-2.31 (br OH), 3.52-3.61 (stack, 2H, C(1')H_aH_b for both epimers, C(1)H_aH_b for both epimers), 3.62-3.71 (stack, 2H, C(1)H_aH_b for both epimers, C(4)H_aH_b for both epimers), 3.74-3.83 (stack, 2H, C(4)H_aH_b for both epimers, C(1')H_aH_b for both epimers), 3.88-3.95 (stack, 1.5H, C(2")*H* for epimer 1, C(3)*H* for both epimers), 3.91-4.04 (stack, 1.5H, C(2")*H* for epimer 2, C(2)*H* for both epimers), 4.05-4.20 (stack, 3H, C(2')*H* for both epimers, C(3')*H* for both epimers, C(4')*H* for both epimers), 6.48-6.56 (stack, 1H, N*H* for both epimers); δ_C(125 MHz, $CDCl_3$): 14.0 (CH_3, C18', C26"), 22.6 (CH_2), 25.2 (CH_2), 25.4 (CH_2), [25.62, 25.67 (CH_3, $C(CH_3)_2$ of 1,2-*anti* diol for both epimers], 26.4 (CH_2), 26.5 (CH_2), [26.90, 26.94, 26.97 (CH_3, $C(CH_3)_2$ of 1,2-*syn* diol for both epimers (resonance overlap))], [27.8, 27.9 (CH_3, $C(CH_3)_2$ of 1,2-*anti* diol for both epimers)], [29.0, 29.1, 29.16, 29.21, 29.27, 29.34, 29.42, 29.44, 29.56, 29.59, 29.6, 29.7 (CH_2, alkyl chain, some resonance overlap)], 31.9 (CH_2), 32.1 (CH_2), 32.2 (CH_2), [48.4, 48.6 (CH, C2')], [62.3, 62.4, (CH_2, C4)], [64.2, 64.5 (CH, C2")], 71.3 (CH_2, C1'), [71.71, 71.73 (CH_2, C1)], [75.9, 76.0 (CH, C4')], [76.4, 76.5 (CH, C2)], [77.6, 77.7 (CH, C3')], [79.2, 79.3 (CH, C3)], [108.0, 108.1 (C, $(CH_3)_2C$ of 1,2-*anti* diol)], [109.28, 109.30 (C, $(CH_3)_2C$ of 1,2-*syn* diol)], [168.8,

168.9 (C, *C*=O)]; MS (TOF ES+) *m/z* 943.7 $[M + Na]^+$, 100%; HRMS (TOF ES+) calcd for $C_{54}H_{104}N_4O_7Na$ $[M + Na]^+$ 943.7803, found 943.7800.

3-(2-(2-(2-(2-*t*-butoxycarbonyl)aminoethoxy)ethoxy)ethoxy)prop-1-yne (114)

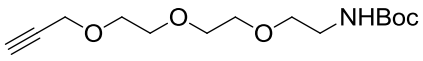

114

Di-*tert*-butyl dicarbonate (120 mg, 0.56 mmol) was added to a solution of 3-(2-(2-(2-aminoethoxy)ethoxy)ethoxy)prop-1-yne[144] (55 mg, 0.28 mmol) and NEt_3 (58 µL, 0.42 mmol) in CH_3CN (3 mL). After stirring for 6 h at r.t., the volatiles were removed under reduced pressure and the residue was purified by flash column chromatography (30% EtOAc in hexane) to afford Boc amide **114** as a dark yellow oil (74 mg, 92%). R_f = 0.2 (30% EtOAc in hexane); ν_{max}(film) / cm^{-1} 3351br , 2869m, 1706s (C=O), 1509m, 1455w, 1368m, 1249m, 1218m, 1117s, 1070s, 865w, 755s, 1391w, 1365m, 1271m, 1248m, 1170s, 1095s, 1033m, 864w, 780w; δ_H(300 MHz, $CDCl_3$) 1.43 (s, 9H, C(C*H*$_3$)$_3$), 2.43 (t, *J* 2.4, 1H, ≡C*H*), 3.26-3.35 (stack, 2H), 3.50-3.57 (stack, 2H), 3.58-3.76 (stack, 8H), 4.18-4.23 (stack, 2H), 5.04 (br s, 1H, N*H*); δ_C(100 MHz, MeOD) 28.4 (CH_3, C(*C*H$_3$)$_3$), 40.4 (CH_2), 58.4 (CH_2), 69.1 (CH_2), 70.2 (CH_2), 70.2 (CH_2), 70.4 (CH_2), 70.5 (CH_2), 74.6 (CH), 79.2

(C), 79.6 (C), 154.2 (C, *C*=O); MS (TOF ES+) *m/z* 310.1 $[M + Na]^+$, 100%; HRMS (TOF ES+) calcd for $C_{14}H_{25}NO_5Na$ $[M + Na]^+$ 310.1630, found 310.1617.

Triazole 121

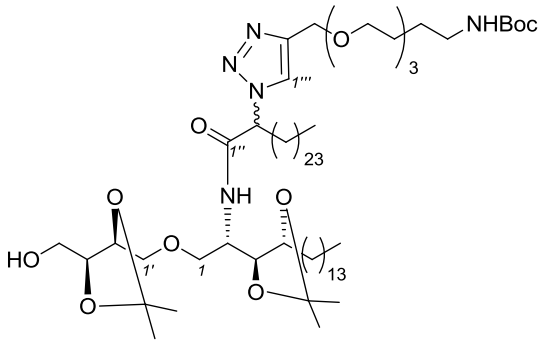

121

$CuSO_4$ solution (7 µL of a 0.5 M solution, 7 µmol) and sodium ascorbate solution (30 µL of a 1 M solution, 30 µmol) were added to a solution of azide **119** (65 mg, 0.074 mmol) and alkyne **114** (34 mg, 0.11 mmol) in ^tBuOH / H_2O (1 mL, 1:1) at r.t. The reaction mixture was heated for 10 h at 50 °C and then diluted with $CHCl_3$ (10 mL), and washed with brine (3 mL). The phases were separated and the aqueous layer was extracted with $CHCl_3$ (2 × 5 mL). The combined organic layers were dried over Na_2SO_4 and the volatiles were removed under reduced pressure. Purification of the residue by flash column chromatography (gradient: $CHCl_3$ to 5% CH_3OH in $CHCl_3$) afforded 1,2,3-triazole **121** as a colourless oil (78 mg, 87%,

isolated as a 2:1 mixture of epimers). Data on epimeric mixture: R_f = 0.2[***] (5% CH_3OH in $CHCl_3$); ν_{max}(film) / cm^{-1} 3319br (OH), 2917s, 2850s, 1700m (C=O), 1659m (C=O), 1545w, 1471m, 1368m, 1249m, 1218m, 1117s, 1070s, 865w, 755s; δ_H(500 MHz, $CDCl_3$) 0.88 (t, *J* 6.8, 6H, 2 × CH_2CH_3), 1.19-1.32 (stack, 73H, incl. 1 × $C(CH_3)_2$ of 1,2-*anti* diol), 1.38-1.40 (stack, 6H, 1 × $C(CH_3)_2$ of 1,2-*anti* diol, 1 × $C(CH_3)_2$ of 1,2-*syn* diol), 1.41 (s, 3H, 1 × $C(CH_3)_2$ of 1,2-*syn* diol), 1.44 (s, 9H, $C(CH_3)_3$), 2.03-2.12 (m, 1H, C(3")H_aH_b), 2.17-2.27 (m, 1H, C(3")H_aH_b), 2.40-2.72 (br s, 1H, O*H*), 3.25-3.36 (stack, 2H, CH_2NHBoc), 3.40-3.46 (m, 1H, C(1')H_aH_b), 3.50-3.58 (stack, 4H, CH_2CH_2NHBoc, C(1)H_2), 3.59-3.65 (stack, 4H), 3.65-3.69 (stack, 2H), 3.69-3.74 (stack, 3H, incl. C(4)H_aH_b), 3.74-3.79 (stack, 2H, C(4)H_aH_b, C(1')H_aH_b), 3.87-3.99 (stack, 2H, incl. C(2)*H*), 4.00-4.07 (stack, 2H), 4.07-4.15 (m, 1H, C(2')*H*), 4.66-4.73 (stack, 2H, C(3'")H_2), [4.95-4.98 (m, 0.34H, C(2'')*H* for minor epimer), 5.00-5.15 (stack, 1.66H, C(2")*H* for major epimer, N*H*Boc)], [6.59-6.69 (m, 0.66H, CON*H* for major epimer), 6.78-6.84 (m, 0.34H, CON*H* for minor epimer)], [7.71-7.75 (s, 0.34H, C(1'")*H* for minor epimer), 7.76-7.82 (s, 0.66H, C(1'")*H* for major epimer)]; δ_C(125 MHz, $CDCl_3$) 14.1 (CH_3, C18', C26"), 22.7 (CH_2), 25.6 (CH_3, $C(CH_3)_2$ of 1,2-*anti* diol), 25.8 (CH_2), 26.48 (CH_2), 26.50 (CH_2), 26.9 (CH_3, $C(CH_3)_2$ of 1,2-*syn* diol), 27.1 (CH_3, $C(CH_3)_2$ of 1,2-*syn* diol), 27.9 (CH_3, $C(CH_3)_2$ of 1,2-*anti* diol), 28.4 (CH_3, $C(CH_3)_3$), [28.9, 29.0, 29.1, 29.3, 29.4, 29.5, 29.7 (CH_2, alkyl chain, some resonance overlap)], 31.5 (CH_2), 31.9 (CH_2), 32.4 (CH_2, C3"), 32.7 (CH_2), 40.4 (CH_2, CH_2NHBoc), [48.8 (CH, C2' for minor epimer), 49.0 (CH, C2' for major epimer)], 61.8 (CH_2), 62.7 (CH_2, C4), [64.6 (CH, C2" for major epimer *and* CH_2, C3'", resonance overlap), 65.6 (CH, C2" for minor epimer)],

[***] The two epimers can be observed by TLC; however they have very similar R_f values.

[69.9, 70.0, 70.2, 70.50, 70.52 (CH_2, 5 × CH_2O in PEG linker)], 70.9 (CH_2, C1'), 71.7 (CH_2, C1), 75.8 (CH), 76.5 (CH), 79.1 (CH), [79.4 (CH *and* C, incl. O*C*$(CH_3)_3$, resonance overlap)], 108.1 (C, $(CH_3)_2C$ of 1,2-*anti* diol), 109.2 (C, $(CH_3)_2C$ of 1,2-*syn* diol), 122.3 (CH, C1'"), 145.4 (C, C2'"), 156.0 (C, *C*=ONHBoc), 167.3 (C, *C*=ONH); MS (TOF ES+) *m/z* 1230.9 $[M + Na]^+$, 100%; HRMS (TOF ES+) *m/z* calcd for $C_{68}H_{129}N_5O_{12}Na$ $[M + Na]^+$ 1230.9535, found 1230.9541.

Biotinylated ThrCer (106)

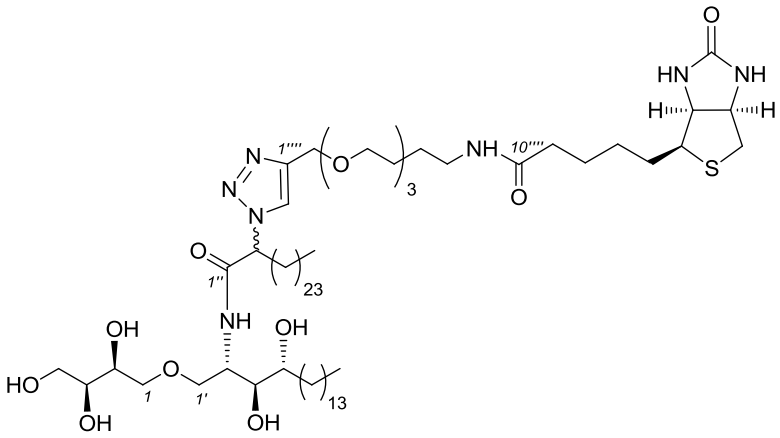

106

TFA (60 µL) was added dropwise over 1 min to a solution of Boc amide **121** (60 mg, 0.050 mmol) in CH_2Cl_2 / CH_3OH (2:1, 0.6 mL). After stirring overnight at r.t., the reaction mixture was concentrated under reduced pressure and the residual TFA was removed by co-evaporation with Et_2O (3 × 3 mL) to provide crude amine

122 as a white solid (51 mg, quant.), which was used in the step without further purification: selected data: MS (TOF ES+) *m/z* 1029.1 ([M + H]$^+$, 100%); HRMS (TOF ES+) *m/z* 1028.8572 [M + H]$^+$. $C_{57}H_{114}N_5O_{10}$ requires 1028.8566.

NEt_3 (33 µL, 0.24 mmol) was added to a solution of crude amine (51 mg, 0.050 mmol) in DMF (0.5 mL). After stirring for 1 h at r.t., (+)-biotin *N*-hydroxysuccinimide ester **123** (10 mg, 0.029 mmol) was added. The reaction mixture was stirred for 12 h at r.t. and then the volatiles were removed under reduced pressure. Purification of the residue by flash column chromatography (eluent: first EtOAc to remove *N*-hydroxysuccinimide by-product, then gradient 1-10% CH_3OH in $CHCl_3$) afforded biotinylated ThrCer **106** as a white solid (52 mg, 83%, 1:1 mixture of epimers); data on mixture unless stated otherwise: R_f = 0.3 for epimer A, R_f = 0.2 for epimer B (10% CH_3OH in $CHCl_3$); ν_{max}(film) / cm^{-1} 3333br (OH), 2921m, 2852m, 1672s (C=O), 1467m, 1352w, 1203s, 1184s, 1133s, 908w, 840m, 800m, 722s; δ_H(500 MHz, $CDCl_3$/CD_3OD, 2:1) 0.66 (t, *J* 6.7, 6H, 2 × CH_2CH_3), 0.91-1.15 (stack, 66H), 1.17-1.28 (stack, 4H), 1.32-1.55 (stack, 6H, incl. C(12'")H_2 (middle of stack), C(14'")H_aH_b (LHS of stack), C(14"')H_aH_b (RHS of stack)), 1.81-1.90 (stack, 1H, C(3")H_aH_b), 1.91-2.03 (stack, 3H, C(3")H_aH_b, C(11'")H_2), 2.51 (d, *J* 12.8, 1H, C(18'")H_aH_b), 2.68-2.74 (stack, 1H, C(18'") H_aH_b), 2.92-3.00 (stack, 1H, C(15'")H), 3.15-3.21 (stack, 2H, C(9'")H_2), 3.23-3.54 (stack, 18.5H, incl. C(1')H_aH_b for both epimers, C(4'")H_2), 3.55-3.66 (stack, 1.5H, incl. C(1')H_aH_b for epimer A (LHS of stack), C(1')H_aH_b for epimer B (RHS of stack)), 3.95-4.02 (stack, 1H, C(2')H (epimer A, LHS of stack; epimer B, RHS of stack)), 4.08-4.14 (stack, 1H, C(16'")H), 4.27-4.32 (stack, 1H, C(17'")H), 4.45-4.49 (stack, 2H, C(3'")H_2), 5.08-

5.14 (app. q, *J* 6.7, 1H, C(2")H), 7.79 (s, 1H, C(1"')H); δ_C(125 MHz, $CDCl_3/CD_3OD$, 2:1) 13.4 (CH_3, C18', C26" (resonance overlap)), 22.2 (CH_2), 25.1 (CH_2, C(12'")), 25.2 (CH_2), 25.3 (CH_2), 25.4 (CH_2), 25.5 (CH_2), 27.7 (CH_2), 28.0 (CH_2), 28.58 (CH_2), 28.63 (CH_2), [29.1, 29.2, 29.3, 29.4 (CH_2, alkyl chain, some resonance overlap)], 31.5 (CH_2), 31.9 (CH_2), 32.3 (CH_2, C(3")), 32.5 (CH_2), 35.2 (CH_2, C(11'")), [38.72, 38.78 (CH_2, C(9'") for both epimers)], [39.81, 39.84 (CH_2, C(18'") for both epimers)], [49.8, 49.9 (CH, C(2') for both epimers)], 55.3 (CH, C(15'")), 59.9 (CH, C(17'")), 61.6 (CH, C(16'")), [63.00, 63.05 (CH_2, C(4) for both epimers)], [63.6, 63.7 (CH, C(2") for both epimers)], [63.79, 63.83 (CH_2, C(3'") for both epimers)], 69.2 (CH_2, C(4'")), 69.4 (CH_2, PEG chain), [69.46, 69.51 (CH, for both epimers)], [69.54, 69.57, 69.84, 69.87, 69.90, 69.92 (3 × CH_2, PEG chain for both epimers)], [70.0, 70.1 (CH_2, C(1') for both epimers)], [71.4, 71.5 (CH, for both epimers)], [72.0, 72.1 (CH, for both epimers)], [72.9, 73.1 (CH_2, C(1) for both epimers)], 73.8 (CH, C(3')), [122.2, 122.3 (CH, C(1'") for both epimers)], [144.1, 144.2 (C, C(2'") for both epimers)], [163.95, 164.04 (C, NH*C*=ONH for both epimers)], [167.98, 168.04 (C, C(1") for both epimers)], [174.21, 174.23 (C, C(10'") for both epimers)]; MS (TOF ES+) *m/z* 1277.1 ($[M + Na]^+$, 100%); HRMS (TOF ES+) calcd for $C_{67}H_{127}N_7O_{12}SNa$ $[M + Na]^+$ 1276.9161, found 1276.9182.

Careful column chromatography (eluent: gradient 3-8% CH_3OH in $CHCl_3$) on a small sample of the purified mixture of epimers allowed their separation. Selected data for epimer A – (less polar), R_f = 0.3 (10% CH_3OH in $CHCl_3$); δ_H(500 MHz, $CDCl_3/CD_3OD$, 2:1) 0.66 (t, *J* 6.7, 6H, 2 × CH_2CH_3), 0.91-1.15 (stack, 66H), 1.17-1.28 (stack, 4H), 1.32-1.55 (stack, 6H, incl. C(12'")H_2 (middle of stack),

C(14’”)H_aH$_b$ (LHS of stack), C(14’”)H$_a$$H_b$ (RHS of stack)), 1.81-1.90 (stack, 1H, C(3”)H_aH$_b$), 1.91-2.03 (stack, 3H, C(3”)H$_a$$H_b$, C(11’”)$H_2$), 2.51 (d, *J* 12.8, 1H, C(18’”)H_aH$_b$), 2.68-2.74 (m, 1H, C(18’”) H$_a$$H_b$), 2.92-3.00 (m, 1H, C(15’”)H), 3.15-3.21 (m, 2H, C(9’”)H_2), 3.24-3.52 (stack, 18H, incl. C(1’)H_aH$_b$, C(4’”)H_2), 3.57-3.62 (stack, 2H, incl. C(1’)H$_a$$H_b$), 3.97-4.00 (m, 1H, C(2’)H), 4.08-4.14 (m, 1H, C(16’”)H), 4.27-4.32 (m, 1H, C(17’”)H), 4.44-4.47 (stack, 2H, C(3’”)H_2), 5.08-5.12 (t, *J* 6.9, 1H, C(2”)H), 7.77 (s, 1H, C(1”’)H). Selected data for epimer B – (more polar), R_f = 0.2 (10% CH_3OH in $CHCl_3$); δ_H(500 MHz, $CDCl_3$/CD_3OD, 2:1) 0.66 (t, *J* 6.7, 6H, 2 × $CH_2C$$H_3$), 0.91-1.15 (stack, 66H), 1.17-1.28 (stack, 4H), 1.32-1.55 (stack, 6H, incl. C(12’”)H_2 (middle of stack), C(14’”)H_aH$_b$ (LHS of stack), C(14’”)H$_a$$H_b$ (RHS of stack)), 1.81-1.90 (stack, 1H, C(3”)H_aH$_b$), 1.91-2.03 (stack, 3H, C(3”)H$_a$$H_b$, C(11’”)$H_2$), 2.51 (d, 1H, *J* 12.8, C(18’”)H_aH$_b$), 2.68-2.74 (m, 1H, C(18’”) H$_a$$H_b$), 2.92-3.00 (m, 1H, C(15’”)H), 3.15-3.21 (stack, 2H, C(9’”)H_2), 3.22-3.53 (stack, 19H, incl. C(1’)H_aH$_b$, C(4’”)H_2), 3.54-3.60 (m, 1H, C(1’)H$_a$$H_b$), 3.93-3.98 (m, 1H, C(2’)H), 4.08-4.14 (m, 1H, C(16’”)H), 4.27-4.32 (m, 1H, C(17’”)H), 4.45-4.49 (stack, 2H, C(3’”)H_2), 5.07-5.12 (t, *J* 6.8, 1H, C(2”)H), 7.78 (s, 1H, C(1”’)H).

Alexa 488-labelled ThrCer (107)

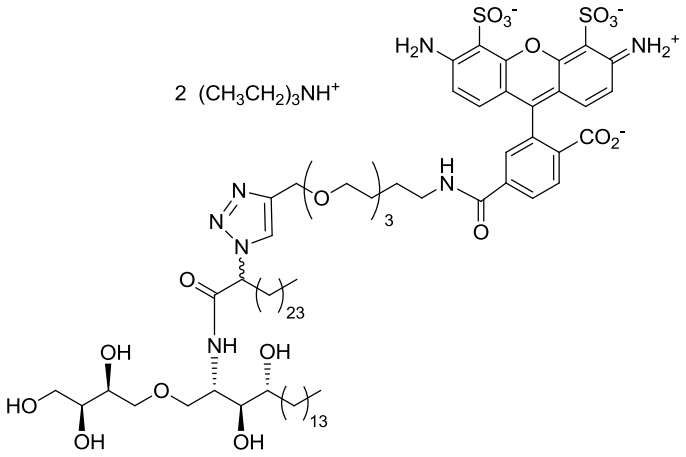

107

TFA (60 µL) was added dropwise over 1 min to a solution of Boc amide **121** (60 mg, 0.050 mmol) in CH_2Cl_2 / CH_3OH (2:1, 0.6 mL). After stirring overnight at r.t., the reaction mixture was concentrated under reduced pressure and the residual TFA was removed by co-evaporation with Et_2O (3 × 3 mL) to provide crude amine **122** as a white solid (51 mg, quant.), which was used in the step without further purification: selected data: MS (TOF ES+) *m/z* 1029.1 ($[M + H]^+$, 100%); HRMS (TOF ES+) calcd for $C_{57}H_{114}N_5O_{10}$ $[M + H]^+$ 1028.8566, found 1028.8572.

NEt_3 (1 µL, 7.2 µmol) was added to a solution of crude amine **122** (2.3 mg, 2.3 µmol) in DMF (10 µL). After stirring for 1 h at r.t., Alexa Fluor® 488 carboxylic acid, 2,3,5,6-tetrafluorophenyl ester **124** (1.0 mg, 1.1 µmol) was added. The reaction mixture was stirred for 12 h at r.t. and then the volatiles were removed under reduced pressure. Purification of the residue by flash column chromatography (eluent: gradient 0-50% CH_3OH in $CHCl_3$) afforded compound **107** as a red solid

(1.2 mg, 73%); selected data: R_f = 0.3 for epimer A, R_f = 0.2 for epimer B in 65:35:4 $CHCl_3$ / MeOH / aq. NH_3.

(2*S*,3*S*,4*R*)-2-Azido-3,4-*O*-isopropylidene-1-*O*-(2',3',4',6'-tetra-*O*-*p*-methoxybenzyl-D-galactopyranosyl)octadecane-1,3,4-triol (127)

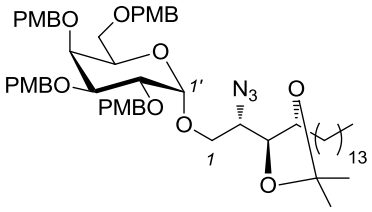

127

Ph_3P (1.46 g, 5.55 mmol) and CBr_4 (1.84 g, 5.55 mmol) were added sequentially to a solution of 2,3,4,6-tetra-*O*-*p*-methoxybenzyl-D-galactose **126** (1.22 g, 1.85 mmol) in CH_2Cl_2 (10 mL) at r.t. The reaction mixture was stirred for 3 h. In separate flasks, a solution of tetramethylurea (TMU) (1.2 mL) and Bu_4NBr (1.79 g, 5.55 mmol) in CH_2Cl_2 (5 mL), and a solution of azide **78** (1.07 g, 2.78 mmol) in CH_2Cl_2 (5 mL) were stirred over activated 3 Å MS for 30 min, after which time, these solutions were added dropwise (15 min) and sequentially (TMU/Bu_4NBr solution first) to the solution containing the glycosyl donor. The reaction mixture was stirred at r.t. for 3 d until there was no evidence by TLC that the donor was still being consumed. The reaction mixture was then filtered through a silica plug, washing

with CH_2Cl_2 (1.2 L) and then concentrated under reduced pressure. Purification of the residue by flash column chromatography (15% EtOAc in hexane) afforded glycoside **127** as a colourless oil (1.33 g, 70%, α-anomer only): R_f = 0.3 (20% EtOAc in hexane); δ_H(300 MHz, $CDCl_3$) 0.88 (t, *J* 6.8, 3H, CH_2CH_3), 1.20-1.42 (stack, 28H, alkyl chain methylenes, $C(CH_3)_2$), 1.47-1.70 (stack, 4H), 3.36-3.54 (stack, 3H), 3.70 (dd, *J* 10.8, 6.7, 1H), 3.75-4.17 (stack, 19H), 4.27-4.54 (stack, 3H), 4.56-4.67 (stack, 2H), 4.68-4.79 (stack, 2H), 4.80-4.91 (stack, 2H), 6.76-6.96 (stack, 8H), 7.13-7.23 (stack, 4H), 7.24-7.37 (stack, 4H); δ_C(100 MHz, $CDCl_3$) 14.1 (CH_3, CH_2CH_3), 22.7 (CH_2), 25.7 (CH_3, 1 × $C(CH_3)_2$), 26.6 (CH_2), 28.1 (CH_3, 1 × $C(CH_3)_2$), 29.31 (CH_2), 29.34 (CH_2), [29.57, 29.59, 29.63, 29.64, 29.65, 29.68 (CH_2, alkyl chain, resonance overlap)], 31.9 (CH_2), [55.22, 55.24 (CH_3, 4 × $ArOCH_3$ resonance overlap)], 59.8 (CH), 68.8 (CH_2), 69.6 (CH_2), 69.8 (CH), 72.5 (CH_2), 72.9 (CH_2), 73.0 (CH_2), 74.2 (CH_2), 74.7 (CH) , 75.4 (CH), 76.2 (CH), 77.8 (CH), 78.4 (CH), 98.9 (CH), 108.2 (C, $C(CH_3)_2$), [113.56, 113.60, 113.68, 113.73 (CH, Ar *ortho* to OMe)], [129.16, 129.23, 129.4, 129.9 (CH, Ar *meta* to OMe)], [130.1, 130.8, 131.05, 131.09 (C, Ar *para* to OMe)], [159.01, 159.02, 159.1, 159.2 (C, Ar *ipso* to OMe)].

(2*S*,3*S*,4*R*)-2-Amino-3,4-*O*-isopropylidene-1-*O*-(2',3',4',6'-tetra-*O*-*p*-methoxybenzyl-D-galactopyranosyl)octadecane-1,3,4-triol (128)

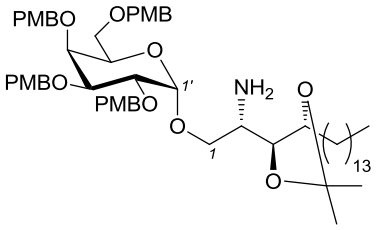

128

PMe_3 (1.53 mL of a 1.0 M soln in THF, 1.53 mmol) was added dropwise over 5 min to a solution of azide **127** (1.30 g, 1.27 mmol) in THF (10 mL). The reaction mixture was stirred at r.t. for 3 h, after which time, H_2O (0.5 mL) was added. The reaction mixture was stirred for 1 h and then concentrated under reduced pressure. The residual H_2O was removed by co-evaporation with toluene (3 × 3 mL) to provide the crude product. Purification by flash column chromatography (40% EtOAc in hexane) afforded amine **128** as a colourless oil (1.14 g, 90%): R_f = 0.3 (40% EtOAc in hexane); ν_{max}(film) / cm^{-1} 3380 br (N–H), 2923s, 2854s, 1497m, 1454s, 1368m, 1244m, 1216m, 1096s, 1057s, 909s, 872w, 732s, 697s; δ_H(300 MHz, $CDCl_3$) 0.88 (t, *J* 7.0, 3H, CH_2CH_3), 1.14-1.61 (stack, 32H, alkyl chain methylenes, $C(CH_3)_2$), 3.11-3.22 (m, 1H), 3.35-3.52 (stack, 3H), 3.70-4.18 (stack, 20H), 4.28-4.53 (stack, 3H), 4.54-4.78 (stack, 5H), 4.79-4.88 (stack, 2H), 6.75-6.93 (stack, 8H), 7.09-7.36 (stack, 8H); δ_C(100 MHz, $CDCl_3$) 14.1 (CH_3, CH_2CH_3), 22.7 (CH_2), 25.9 (CH_3, 1 × $C(CH_3)_2$), 26.3 (CH_2), 28.1 (CH_3, 1 × $C(CH_3)_2$), [29.3, 29.7 (CH_2, alkyl chain, resonance overlap)], 31.9 (CH_2), 50.9 (CH), [55.2 (CH_3, 4 ×

ArO*C*H_3 resonance overlap)], 68.8 (CH_2), 69.6 (CH_2), 69.8 (CH), 72.5 (CH_2), 72.9 (CH_2), 73.0 (CH_2), 74.2 (CH_2), 74.7 (CH), 75.4 (CH), 76.2 (CH), 77.8 (CH), 78.4 (CH), 98.9 (CH), 108.2 (C, *C*(CH_3)$_2$), [113.56, 113.60, 113.68, 113.73 (CH, Ar *ortho* to OMe)], [129.16, 129.23, 129.4, 129.9 (CH, Ar *meta* to OMe)], [130.1, 130.8, 131.05, 131.09 (C, Ar *para* to OMe)], [159.01, 159.02, 159.1, 159.2 (C, Ar *ipso* to OMe)].

(2'*S*,3'*S*,4'*R*)-2'-[2''-Azido-hexacosanoylamino]-1'-*O*-[2,3,4,6-tetra-*O*-benzyl-D-galactopyranosyl]octadecane-*O*-isopropylidene-octadecane-1',3',4'-triol (129)

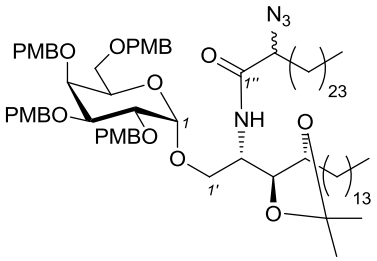

129

A solution of α-azido acid **116** (88 mg, 0.22 mmol) in $(COCl)_2$ (2 mL) was heated at 70 °C. After 2 h, the volatiles were removed under a stream of N_2 and the residual solvent removed on the vacuum line (1 h) to provide the corresponding acid chloride **117** as a pale yellow oil, which was used directly in the next step without further purification (100 mg, quant.): A solution of freshly prepared acid chloride **117** (100 mg, 0.22 mmol) in CH_2Cl_2 (1.0 mL) was added dropwise over 2 min to a solution of amine **128** (280 mg, 0.28 mmol) and NEt_3 (32 µL, 0.23 mmol) in CH_2Cl_2 (2.0 mL) at 0 ºC. The reaction mixture was stirred at rt for 12 h and then diluted with CH_2Cl_2 (20 mL), washed sequentially with $NaHCO_3$ solution (20 mL), brine (5 mL) and then dried over Na_2SO_4. The drying agent was removed by filtration and the filtrate concentrated under reduced pressure. Purification of the residue by flash column chromatography provided amide **129** as a colourless oil (281 mg, 90%, 1:1 mixture of epimers). Data on epimeric mixture: R_f = 0.3 (20% EtOAc in hexane); ν_{max}(film) / cm^{-1} 2922s, 2852s, 2105m (N_3), 1685m, 1613m, 1513s, 1465m, 1368m, 1247s, 1037s, 821s, 729s; δ_H(500 MHz, $CDCl_3$) 0.84-0.89 (stack,

6H, 2 × CH_2CH_3), 1.16-1.50 (stack, 56H), 1.61-1.86 (stack, 2H, C(3")H_2), 3.34-3.40 (stack, 1H, C(6')H_aH_b for both epimers), 3.41-3.46 (stack, 1H, C(6')H_aH_b for both epimers), 3.58-3.62 (stack, 1H, C(1)H_aH_b for both epimers), 3.67-3.70 (m, 0.5H, C(2")*H* for epimer 1), 3.74-3.81 (stack, 12H, 4 × $ArOCH_3$ for both epimers, *and* 1H, C(2")*H* for epimer 2), 3.82-3.89 (stack, 3H, C(3')*H* for both epimers, C(4')*H* for both epimers, C(5')*H* for both epimers), 3.89-4.00 (stack, 3H, C(1)H_aH_b for both epimers, C(4)*H* for both epimers, C(2')*H* for both epimers), 4.03-4.09 (stack, 1H, C(2)*H* for both epimers), 4.09-4.18 (stack, 1H, C(3)*H* for both epimers), 4.27 (A of AB, J_{A-B} 11.6, 1H, C(6')OCH_aH_bAr for epimer 1), 4.28 (A of AB, J_{A-B} 11.6, 1H, C(6')OCH_aH_bAr for epimer 2), 4.40 (B of AB, J_{B-A} 11.6, 1H, C(6')OCH_aH_bAr for epimer 1), 4.42 (B of AB, J_{B-A} 11.6, 1H, C(6')OCH_aH_bAr for epimer 1), 4.46 (A of AB, J_{A-B} 11.2, 1H, C(4')OCH_aH_bAr for epimer 1), 4.47 (A of AB, J_{A-B} 11.2, 1H, C(4')OCH_aH_bAr for epimer 2), 4.56 (A of AB, J_{A-B} 11.2, 1H, C(2')OCH_aH_bAr for epimer 1), 4.57 (A of AB, J_{A-B} 11.2, 1H, C(2')OCH_aH_bAr for epimer 2), 4.63 (A of AB, J_{A-B} 11.2, 1H, C(3')OCH_aH_bAr for epimer 1), 4.64 (A of AB, J_{A-B} 11.2, 1H, C(3')OCH_aH_bAr for epimer 2), 4.70 (B of AB, J_{B-A} 11.2, 1H, C(3')OCH_aH_bAr for both epimers), 4.72 (B of AB, J_{B-A} 11.2, 1H, C(2')OCH_aH_bAr for epimer 1), 4.73 (B of AB, J_{B-A} 11.2, 1H, C(2')OCH_aH_bAr for epimer 2), 4.80 (B of AB, J_{B-A}, 1H, C(4')OCH_aH_bAr for both epimers), 4.84-4.87 (stack, 1H, C(1')H, for both epimers), 6.74-6.89 (8H, stack, 8H, Ar), 7.13-7.18 (stack, 4H, Ar), 7.23-7.31 (stack, 4H, Ar); δ_C(125 MHz, $CDCl_3$) [14.1 (CH_3, C18', C26")], [22.7 (CH_2)], [25.6, 25.7 (CH_2, alkyl chain (resonance overlap)], [25.9, 26.0 (CH_3, $C(CH_3)_2$ for both epimers)], 26.6 (CH_2), 26.7 (CH_2), [28.1, 28.2 (CH_3, $C(CH_3)_2$ for both epimers)], [28.96, 29.03, 29.3, 29.4, 29.5, 29.7, (CH_2, alkyl chain, some resonance overlap)], 31.9 (CH_2),

32.0 (CH_2), 32.1 (CH_2), [48.8, 49.1 (CH, C2)], [55.22, 55.24 (CH_3, 4 × Ar*O*CH_3, resonance overlap)], [64.2, 64.5 (CH, C2")], 68.6 (CH_2, C1 for epimer 1), [68.88, 68.91 (CH_2, C6')], 69.0 (CH_2, C1 for epimer 2), 69.8 (CH, C5' for both epimers (resonance overlap)), [72.6, 72.7 (CH_2, C(3')O*C*H_2Ar), [73.08, 73.12, 73.15 (CH_2, C(2')O*C*H_2Ar *and* C(6')O*C*H_2Ar (resonance overlap))], 74.2 (CH_2, O*C*H_2Ar for both epimers (resonance overlap)), [74.4, 74.5 (CH, C4')], [75.1, 75.2 (CH, C3)], 76.5 (CH, C2' for both epimers (resonance overlap)), [77.69, 77.73 (CH, C4)], [78.8, 78.9 (CH, C3')], [99.0, 99.3 (CH, C1')], [107.88, 107.94 (C, $(CH_3)_2C$)], [113.6, 113.73, 113.75 113.77 (CH, Ar *ortho* to OMe)], 127.9 (CH, *C*H=CH), 128.0 (CH, CH=*C*H), [129.0, 129.4, 129.5, 129.8, 129.9, (CH, Ar *meta* to OMe)], 130.0 (CH, *C*H=CH), 130.2 (CH, *C*H=CH), [130.66, 130.75, 130.78, 130.9 (C, Ar *para* to OMe, some resonance overlap)], [159.1, 159.2, 159.3 (C, Ar *ipso* to OMe)], [168.6, 168.9 (C, *C*=O)]; MS (TOF ES+) *m/z* 1442.4 ($[M + Na]^+$, 100%).

Triazole 130

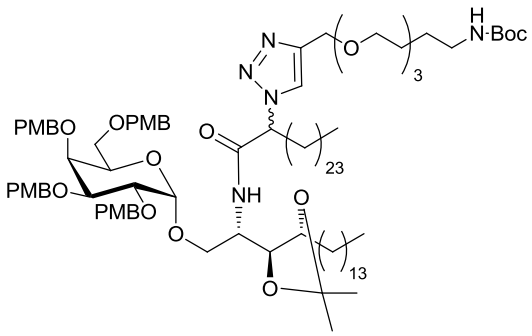

130

$CuSO_4$ solution (14 µL of a 0.5 M solution, 7 µmol) and sodium ascorbate solution (60 µL of a 1 M solution, 60 µmol) were added to a solution of azide **129** (65 mg, 0.15 mmol) and alkyne **114** (66 mg, 0.23 mmol) in $^{t}BuOH$ / H_2O (1 mL, 1:1) at r.t. The reaction mixture was heated for 10 h at 50 °C and then diluted with $CHCl_3$ (20 mL), and washed with brine (10 mL). The phases were separated and the aqueous layer was extracted with $CHCl_3$ (2 × 10 mL). The combined organic layers were dried over Na_2SO_4 and the volatiles were removed under reduced pressure. Purification of the residue by flash column chromatography (gradient: $CHCl_3$ to 5% CH_3OH in $CHCl_3$) afforded 1,2,3-triazole **130** as a colourless oil (231 mg, 91%, isolated as a 1:1 mixture of epimers). Data on epimeric mixture: R_f = 0.2[†††] (40% EtOAc in hexane); ν_{max}(film) / cm^{-1} 3343br (NH), 2923s, 2853s, 1687m (C=O), 1613m (C=O), 1586w, 1513s, 1465m, 1471m, 1367m, 1302m, 1248s, 1173s, 1093s, 1038s, 822m; δ_H(500 MHz, $CDCl_3$) 0.83-0.88 (stack, 6H, 2 × CH_2CH_3), 1.11-1.36 (stack, 69H, alkyl chain methylenes, $C(CH_3)_a(CH_3)_b$), 1.37-1.45 [stack,

[†††] The two epimers can be observed by TLC; however they have very similar R_f values.

16H, including $C(CH_3)_a(CH_3)_b$, $C(CH_3)_3$))], 1.92-2.09 (stack, 2H, C(3")H_2), 3.20-3.35 (stack, 3H, C(6')H_aH_b for both epimers, CH_2NHBoc), 3.39-3.46 (stack, 1H, C(6')H_aH_b for both epimers), 3.47-3.54 (stack, 3H, CH_2CH_2NHBoc, C(1)H_aH_b for both epimers), 3.55-3.73 (stack, 12H, including 4 × PEG CH_2O, C(4''')H_2), 3.75-3.83 (stack, 13H, 4 × $ArOCH_3$ for both epimers, C(3')*H* for epimer 1 *and* C(4')*H* for epimer 1), 3.84-4.16 (stack, 8H, including C(2')*H* for both epimers, C(3')*H* for epimer 2, C(4')*H* for epimer 2, C(1)H_aH_b for both epimers, C(2)*H* for both epimers, C(4)*H* for both epimers, C(3)*H* for both epimers, 1 × PEG CH_2O), 4.24-4.31 (stack, 2H, A of AB, C(6')OCH_aH_bAr for both epimers), 4.40-4.59 (stack, 3H), 4.64-4.76 (stack, 2H), 4.76-4.82 (stack, 2H, including C(1')*H*, for both epimers), 4.90-4.95 (stack, 1H, C(2'')*H* for both epimers), 4.99-5.06 (stack, 1H, N*H*Boc for both epimers), 6.72-6.88 (stack, 8H, Ar), 7.10-7.18 (stack, 4H, Ar), 7.22-7.30 (stack, 4H, Ar), 7.65 (br s, 0.5H, C(1'")*H*) for epimer 1), 7.71 (br s, 0.5H, C(1'")*H*) for epimer 2), CON*H* resonance not observed; δ_C(125 MHz, $CDCl_3$) [14.0, 14.1 14.2 (CH_3, resonance overlap, C18, C26")], 22.5 (CH_2), 22.7 (CH_2), [25.86, 25.89 CH_3, $C(CH_3)_a(CH_3)_b$], 26.5 (CH_2), 28.2 (CH_3, $C(CH_3)_a(CH_3)_b$, 28.4 (CH_3, $C(CH_3)_3$), 28.8 (CH_2), 29.0 (CH_2), [29.2, 29.31, 29.33, 29.4 (CH_2, resonance overlap)], [29.58, 29.63, 29.70 (CH_2, resonance overlap)], 31.5 (CH_2), 31.9 (CH_2), 33.1 (CH_2, C3''), 40.3 (CH_2, CH_2NHBoc), [49.4, 49.5 (CH, C2)], [55.21, 55.24 (CH_3, 4 × $ArOCH_3$, resonance overlap)], [64.3, 64.6 (CH, C2")], 64.7 (CH_2, C3'"), 68.2 (CH_2, C1), [69.1, 69.2 (CH_2, C6', resonance overlap), [70.0, 70.2, 70.4, 70.50, 70.52 (CH_2, 4 × CH_2O in PEG linker)], [72.6, 72.9 (CH_2, OCH_2Ar), [73.04, 73.12, 73.15 (CH_2, OCH_2Ar (resonance overlap))], [74.1, 74.2 (CH_2, OCH_2Ar (resonance overlap)), [74.4, 74.5 (CH, C4')], [75.1, 75.2 (CH, C3)], 76.2 (CH, C2' for both epimers

(resonance overlap)), 77.6 (CH, C4, for both epimers (resonance overlap)], [78.8, 78.9 (CH, C3' for both epimers (resonance overlap)], 79.4 (CH, C3 *and* C, *C*$(CH_3)_3$) [98.9, 99.6 (CH, C1')], [107.87, 107.91 (C, $(CH_3)_2C$)], [113.6, 113.73, 113.75 113.77 (CH, Ar *ortho* to OMe)], [121.8, 122.1 (CH, C1'")], [129.0, 129.4, 129.5, 129.8, 129.9, (CH, Ar *meta* to OMe)], [130.6, 130.7, 130.9 (C, Ar *para* to OMe, some resonance overlap)], [145.4, 145.2 (C, C2'")], [159.1, 159.2, 159.3 (C, Ar *ipso* to OMe)], [167.31, 167,33 (C, CH_2C(O)NH)], [171.1 C of Boc]; MS (TOF ES+) *m/z* 1729.1 $[M + Na]^+$, 100%;

Alexa 488-labelled α-GalCer (108)

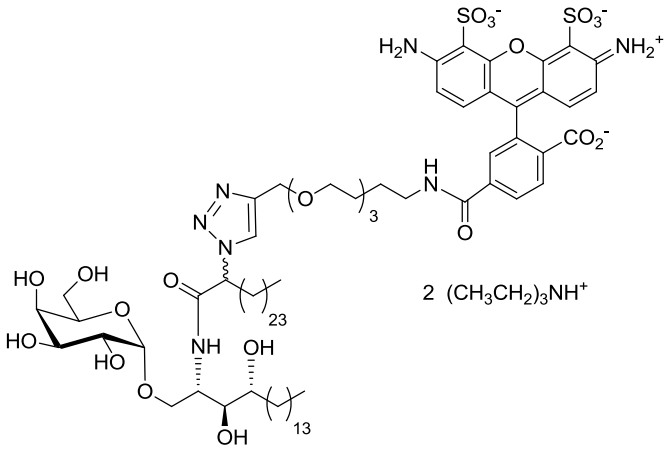

108

TFA (60 µL) was added dropwise over 1 min to a solution of Boc amide **121** (60 mg, 0.050 mmol) in CH_2Cl_2 / CH_3OH (2:1, 0.6 mL). After stirring overnight at r.t., the reaction mixture was concentrated under reduced pressure and the residual TFA was removed by co-evaporation with Et_2O (3 × 3 mL) to provide crude amine **122** as a white solid (51 mg, quant.), which was used in the step without further purification: selected data: MS (TOF ES+) *m/z* 1108.9 ($[M + Na]^+$, 100%); HRMS (TOF ES+) 1108.8462 $[M + Na]^+$. $C_{59}H_{115}N_5O_{12}Na$ requires 1108.8440.

NEt_3 (1 µL, 7.2 µmol) was added to a solution of crude amine **122** (2.5 mg, 2.3 µmol) in DMF (10 µL). After stirring for 1 h at r.t., Alexa Fluor® 488 carboxylic acid, 2,3,5,6-tetrafluorophenyl ester **124** (1.0 mg, 1.1 µmol) was added. The reaction mixture was stirred for 12 h at r.t. and then the volatiles were removed under reduced pressure. Purification of the residue by flash column chromatography (eluent: gradient 0-50% CH_3OH in $CHCl_3$) afforded compound **108** as a red solid

(1.2 mg, 83%); selected data: R_f = 0.3 for epimer A, R_f = 0.2 for epimer B in 65:35:4 $CHCl_3$ / MeOH / aq. NH_3; MS (TOF ES-) *m/z* 1622.9 ($[M + Na - H]^-$, 100%);

(*Z,Z*)-Octadeca-9,12-dien-1-ol (139)

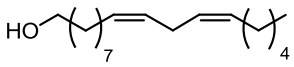

139

Cs_2CO_3 (5.21 g, 16.0 mmol) was added to a solution of linoleic acid **138** (3.00 g, 10.7 mmol) in DMF (10 mL). After stirring for 20 min at r.t., MeI (735 µL, 11.8 mmol) was added to the suspension. After 2 h, the mixture was poured into H_2O (10 mL) and extracted with Et_2O (2 × 20 mL). The organic phases were washed with H_2O (3 × 20 mL), dried over Na_2SO_4, filtered and concentrated under reduced pressure to give the methyl ester as a colourless oil (3.15 g, 100%), which was used in the next step without further purification. A solution of methyl linoleate (3.15 g, 10.7 mmol) in Et_2O (20 mL) was added over 5 min *via* syringe to a stirred suspension of $LiAlH_4$ (0.800 g, 21.0 mmol) in Et_2O (20 mL). After the initial vigorous reaction had subsided, the mixture was heated at reflux for 3 h and then cooled to r.t., poured into NH_4Cl solution (100 mL) and H_2O (20 mL). The layers were separated and the aqueous layer was extracted with Et_2O (3 × 20 mL). The organic layer and the ethereal extracts were combined and the mixture was dried (Na_2SO_4) and concentrated under reduced pressure. The residue was

purified by flash column chromatography (10% EtOAc in hexane) to afford alcohol **139** as a colourless oil (2.57 g, 90%). R_f = 0.3 (15% EtOAc in hexane); ν_{max}(film) / cm^{-1} 3327 br O–H, 3010w, 2925s, 2855m, 1467m, 1378w, 1054m, 986m, 723m; δ_H(300 MHz, $CDCl_3$) 0.86 (t, *J* 6.8, 3H, CH_2CH_3), 1.21-1.42 (stack, 15H, alkyl chain), 1.50-1.63 (stack, 3H), 1.97-2.11 (stack, 4H, 2 × CH_2CH=CH), 2.72-2.82 (m, 2H, CH=CHCH_2CH=CH), 3.64 (t, *J* 6.6, 2H, CH_2OH), 5.27-5.44 (stack, 4H, 2 × C*H*=C*H*), O*H* resonance not observed; δ_c(100 MHz, $CDCl_3$) 14.0 (CH_3, CH_2CH_3), 22.5 (CH_2), 25.6 (CH_2), 25.7 (CH_2), 27.2 (CH_2), [29.2, 29.3, 29.4, 29.5, 29.6 (CH_2, alkyl chain, resonance overlap)], 31.5 (CH_2), 31.7 (CH_2), 62.9 (CH_2, CH_2OH), 127.86 (CH, *C*H=CH), 127.93 (CH, CH=*C*H), 130.0 (CH, *C*H=CH), 130.1 (CH, CH=*C*H); MS (TOF ES+) *m/z* 266.3 ($[M+Na]^+$, 100%); HRMS (TOF ES+) calcd for $C_{18}H_{34}ONa$ ($[M+Na]^+$) 266.2610, found 266.2617

Data were in agreement with those reported in the literature.[165]

(*Z,Z*)-1-Bromo-octadeca-9,12-diene (137)

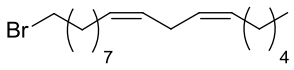

137

CBr_4 (2.43 g, 7.34 mmol) was added in small portions to a cooled (0 °C) solution of alcohol **139** (1.85 g, 6.99 mmol) and PPh_3 (1.93 g, 7.34 mmol) in CH_2Cl_2 (35 mL). The mixture was stirred at r.t. for 16 h and then concentrated under reduced pressure. The residual solid was washed with H_2O (50 mL) and extracted with Et_2O (2 × 50 mL). The ethereal extracts were dried (Na_2SO_4) and concentrated under reduced pressure. The residue was purified by flash column chromatography (hexane) to afford bromide **137** as a colourless oil (2.51 g, 92%). R_f = 0.7 (Hexane); ν_{max}(film) / cm^{-1} 3008m, 2924s, 2854s, 1459m, 723m; δ_H(300 MHz, $CDCl_3$) 0.89 (t, *J* 6.8, 3H, CH_2CH_3), 1.19-1.49 (stack, 16H, alkyl chain), 1.79-1.91 (stack, 2H), 1.98-2.12 (stack, 4H, 2 × CH_2CH=CH), 2.71-2.84 (m, 2H, CH=CHCH_2CH=CH), 3.41 (t, *J* 6.8, 2H, CH_2Br), 5.26-5.45 (stack, 4H, 2 × C*H*=C*H*); δ_c(100 MHz, $CDCl_3$) 14.1 (CH_3, CH_2CH_3), 22.6 (CH_2), 25.6 (CH_2), 27.2 (CH_2), 28.2 (CH_2), 28.7 (CH_2), [29.2, 29.3, 29.6 (CH_2, alkyl chain, resonance overlap)], 31.5 (CH_2), 32.8 (CH_2), 33.9 (CH_2), 127.9 (CH, *C*H=CH), 128.0 (CH, CH=*C*H), 130.0 (CH, *C*H=CH), 130.2 (CH, CH=*C*H); MS (TOF ES+) *m/z* 328.2 ([M(^{79}Br isotopomer)]$^+$, 100%); HRMS (TOF ES+) calcd for $C_{18}H_{33}{}^{79}Br$ ([M(^{79}Br isotopomer)]$^+$) 328.1766, found 328.1762.

Data were in agreement with those reported in the literature.[165]

(*Z,Z*)-1-Cyano-octadeca-9,12-diene (136)

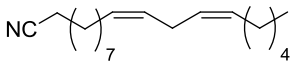

136

A solution of bromide **137** (1.10 g, 3.34 mmol) in DMSO (10 mL) was added over 5 min to a stirred solution of NaCN (180 mg, 3.67 mmol) in DMSO (25 mL) at 40 ºC. Soon after the addition, an exothermic reaction was observed and a salt (NaBr) precipitated. The mixture was stirred and heated at 60 ºC for 40 min, and then poured into ice-water (30 mL) and extracted with Et_2O (2 × 50 mL). The extract was washed sequentially with H_2O (50 mL) and brine (20 mL), dried (Na_2SO_4) and concentrated under reduced pressure. The residue was purified by flash column chromatography (3% EtOAc in hexane) to afford nitrile **136** as a colourless oil (830 mg, 90%). R_f = 0.3 (2% EtOAc in hexane); ν_{max}(film) / cm^{-1} 3009w, 2925s, 2855s, 2246w (C≡N), 1459m, 1398w, 913w, 723s; δ_H(300 MHz, $CDCl_3$) 0.89 (t, *J* 6.9, 3H, CH_2CH_3), 1.23-1.50 (stack, 16H, alkyl chain), 1.59-1.72 (stack, 2H), 1.98-2.12 (stack, 4H, $CH_2CH{=}CHCH_2CH{=}CHCH_2$), 2.34 (t, *J* 7.1, 2H, CH_2CN), 2.73-2.81 (m, 2H, $CH{=}CHCH_2CH{=}CH$), 5.27-5.43 (stack, 4H, 2 × C*H*=C*H*); δ_C(100 MHz, $CDCl_3$) 14.0 (CH_3, CH_2CH_3), 17.0 (CH_2), 22.4 (CH_2), 25.2 (CH_2), 25.5 (CH_2), 27.0 (CH_2), 27.1 (CH_2), [28.5, 28.6, 29.0, 29.1, 29.2, 29.4 (CH_2, alkyl chain, resonance overlap)], 31.4 (CH_2), 119.6 (. C, *C*≡N), 127.7 (CH, *C*H=CH), 127.9 (CH, CH=*C*H), 129.8 (CH, *C*H=CH), 130.0 (CH, CH=*C*H); MS (TOF ES+) *m/z* 298.1 ($[M + Na]^+$, 100%); HRMS (TOF ES+) calcd for $C_{19}H_{33}NNa$ ($[M + Na]^+$) 298.2511, found 298.2500.

(*Z,Z*)-Nonadeca-10,13-dienal (135)

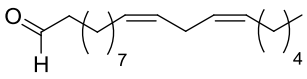

135

DIBALH (10.8 mL of a 1 M soln in CH_2Cl_2, 10.8 mmol,) was added dropwise over 10 min to a stirred solution of nitrile **136** (2.30 g, 8.35 mmol) in CH_2Cl_2 (40 mL) at −78 ºC. The reaction mixture was stirred for 1.5 h and then quenched with ^{i}PrOH (10 mL) and H_2O (5 mL) at −78 ºC before warming to r.t. Silica gel (1.00 g) was added and the resulting mixture was stirred for 1 h, before diluting with EtOAc (50 mL) and filtering through a pad of celite. The filtrate was concentrated under reduced pressure and the residue purified by flash column chromatography (2% EtOAc in hexane) to afford aldehyde **135** as a colourless oil (2.77 g, 92%). R_f = 0.4 (2% EtOAc in hexane); ν_{max}(film) / cm^{-1} 3317 br, 3009m, 2924s, 2854s, 1742m (C=O), 1465m, 1374w, 1240m, 1047w, 723m; δ_H(300 MHz, $CDCl_3$) 0.89 (t, *J* 6.9, 3H, CH_2CH_3), 1.23-1.42 (stack, 16H, alkyl chain), 1.57-1.70 (stack, 2H), 1.98-2.12 (stack, 4H, $CH_2CH{=}CHCH_2CH{=}CHCH_2$), 2.37-2.46 (m, 2H, CH_2CHO), 2.73-2.82 (m, 2H, $CH{=}CHCH_2CH{=}CH$), 5.27-5.44 (stack, 4H, 2 × C*H*=C*H*), 9.77 (t, *J* 1.9, 1H, C*H*O); δ_c(100 MHz, $CDCl_3$): 14.1 (CH_3, CH_2CH_3), 22.1 (CH_2), 22.6 (CH_2), 25.7 (CH_2), 27.2 (CH_2), [29.1, 29.2, 29.3, 29.6 (CH_2, alkyl chain, resonance overlap)], 31.6 (CH_2), 43.9 (CH_2), 127.9 (CH, *C*H=CH), 128.0 (CH, CH=*C*H), 130.1 (CH, *C*H=CH), 130.2 (CH, CH=*C*H), 202.8 (CH, *C*=O); MS (TOF ES+) *m/z* 277.2 ([M –

H]$^+$, 100%); HRMS (TOF ES+) calcd for $C_{19}H_{33}O$ ([M – H]$^+$) 277.2531, found 277.2542.

(*Z,Z*)-2-Amino-1-cyano-nonadeca-10,13-diene (134)

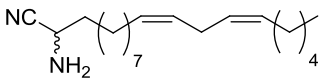

134

A solution of NH_4Cl (350 mg, 6.48 mmol) in aqueous NH_3 (30% solution, 7 mL) was added to a solution of aldehyde **135** (450 mg, 1.62 mmol) in MeOH (8 mL). The reaction mixture was stirred at r.t. for 1 h before NaCN (160 mg, 3.24 mmol) was added. After 24 h, the solvent was removed under reduced pressure. The resulting solid was partitioned between EtOAc (50 mL) and H_2O (50 mL). The separated organic layer was dried over Na_2SO_4 and evaporated under reduced pressure to provide a yellowish residue, which was purified by flash column chromatography (50% EtOAc in hexane) to afford α-amino nitrile **134** as a colourless oil (370 mg, 75%). R_f = 0.3 (40% EtOAc in hexane); ν_{max}(film) / cm^{-1}: 3343 br m (NH_2), 2973m, 2927w, 2883m, 2246w (C≡N), 1453w, 1380w, 1328w, 1274w, 1088m, 1046s, 880s; δ_H(300 MHz, $CDCl_3$): 0.89 (t, *J* 6.9, 3H, CH_2CH_3), 1.19-1.55 (stack, 16H, alkyl chain), 1.60-1.79 (stack, 4H), 1.97-2.11 (stack, 4H, $CH_2CH{=}CHCH_2CH{=}CHCH_2$), 2.77 (app. t *J* 5.9, 2H, CH=CHCH_2CH=CH), 3.67 (t, *J* 7.1, 1H, C*H*NH_2), 5.26-5.44 (stack, 4H, 2 × C*H*=C*H*), resonance for NH_2 not

observed; δ_c(100 MHz, $CDCl_3$): 14.0 (CH_3, CH_2CH_3), 22.5 (CH_2), 25.4 (CH_2), 25.6 (CH_2), 27.1 (CH_2), [28.9, 29.2, 29.3, 29.6 (CH_2, alkyl chain, resonance overlap)], 31.5 (CH_2), 35.3 (CH_2), 43.4 (CH, *C*HNH$_2$), 122.2 (C, *C*≡N), 127.9 (CH, *C*H=CH), 128.0 (CH, CH=*C*H), 130.0 (CH, *C*H=CH), 130.1 (CH, CH=*C*H); MS (TOF ES+) *m/z* 327.3 ([M + Na]$^+$, 100%); HRMS (TOF ES+) calcd for $C_{20}H_{36}N_2Na$ ([M + Na]$^+$) 327.2776, found 327.2767.

(*Z*,*Z*)-2-Amino-eicosa-11,14-dienoic acid (133)

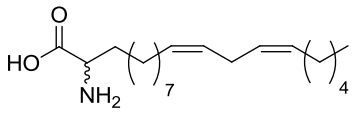

133

40% Aqueous KOH solution (KOH (250 mg, 4.54 mmol) in H_2O (0.5 mL)) was added to a stirred solution of nitrile **134** (138 mg, 0.454 mmol) in EtOH (3 mL). The resulting mixture was heated at 80 °C for 8 h. After cooling the mixture to r.t., H_2O (10 mL) and MeOH (10 mL) were added sequentially. The reaction mixture was cooled to 0 °C, acidified (to pH 3.0) with hydrochloric acid (10 mL of a 10% solution). The mixture was extracted with Et_2O (3 × 20 mL), and then the combined organic extracts were dried with Na_2SO_4 and the volatiles evaporated under reduced pressure to afford the crude α-amino acid **133** as a white solid (140 mg, 95%), which was used in the next step without further purification. R_f = 0.2

(20% MeOH in $CHCl_3$); δ_H(300 MHz, CD_3OD): 0.88 (t, *J* 7.0, 3H, CH_2CH_3), 1.18-1.59 (stack, 16H, alkyl chain), 1.72-1.92 (stack, 4H, alkyl chain), 1.93-2.10 (stack, 4H, $CH_2CH{=}CHCH_2CH{=}CHCH_2$), 2.70 (app. t, *J* 5.7, 2H, $CH{=}CHCH_2CH{=}CH$), 3.89 (t, *J* 6.1, 1H, $CHNH_2$), 5.19-5.36 (stack, 4H, 2 × $CH{=}CH$), 8.83 (d, *J* 5.4, 2H, NH_2), OH resonance not observed; δ_C(100 MHz, $CDCl_3$): 14.5 (CH_3, CH_2CH_3), 23.6 (CH_2), 25.9 (CH_2), 26.6 (CH_2), 28.2 (CH_2), [30.3, 30.4, 30.5, 30.8 (CH_2, alkyl chain, resonance overlap)], 31.5 (CH_2), 32.7 (CH_2), 54.0 (CH, $CHNH_2$), 128.9 (CH, $CH{=}CH$), 129.1 (CH, $CH{=}CH$), 130.9 (CH, $CH{=}CH$), 131.0 (CH, $CH{=}CH$), 171.9 (C, $C{=}O$); MS (TOF ES–) *m/z* 322.2 ($[M - H]^-$, 100%); HRMS (TOF ES–) calcd for $C_{20}H_{36}NO_2$ ($[M - H]^-$, 100%) 322.2746, found 322.2743.

(*Z*,*Z*)-2-Azido-eicosa-11,14-dienoic acid (132)

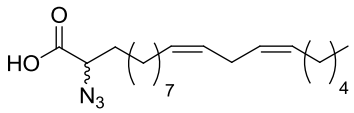

132

Imidazole-1-sulfonyl azide hydrochloride[90] (156 mg, 0.74 mmol, CAUTION: potential explosion risk during purification of this reagent) was added to a suspension of amine **133** (120 mg, 0.37 mmol), $CuSO_4 \cdot 5H_2O$ (2 mg, 2 μmol) and K_2CO_3 (374 mg, 2.71 mmol) in MeOH (5 mL). The mixture was stirred at r.t. for 18 h and then concentrated under reduced pressure. H_2O (15 mL) was added to the residue which was then acidified (to pH 3.0) with hydrochloric acid (5 mL of a 10% solution). The mixture was extracted with EtOAc (3 × 10 mL). The combined organic layers were dried with Na_2SO_4 and the volatiles were removed under reduced pressure. The crude product was purified by flash column chromatography (20% EtOAc in toluene) to afford α-azido acid **132** as a colourless oil (110 mg, 85%). R_f = 0.3 (20% EtOAc in toluene); ν_{max}(film) / cm^{-1} 3400-2500w v br (OH), 2927s, 2856m, 2108s (N_3), 1719s (C=O), 1457m, 1377w, 1186m, 1080m, 907s, 732s; δ_H(300 MHz, $CDCl_3$) 0.89 (t, *J* 6.9, 3H, CH_2CH_3), 1.23-1.52 (stack, 17H, alkyl chain), 1.53-1.70 (m, 1H, alkyl chain), 1.72-1.94 (stack, 2H, alkyl chain), 1.98-2.14 (stack, 4H, $CH_2CH{=}CHCH_2CH{=}CHCH_2$), 2.77 (app. t *J* 5.9, 2H, $CH{=}CHCH_2CH{=}CH$), 3.88 (dd, *J* 8.4, 5.2, 1H, CHN_3), 5.27-5.44 (stack, 4H, 2 × C*H*=C*H*), 10.03 (v br s, 1H, O*H*); δ_c(100 MHz, $CDCl_3$) 14.0 (CH_3, CH_2CH_3), 22.6 (CH_2), 25.6 (CH_2), 25.7 (CH_2), 27.2 (CH_2), [28.9, 29.0, 29.2, 29.3, 29.4, 29.6, 29.7

(CH_2, alkyl chain, resonance overlap)], 31.3 (CH_2), 31.5 (CH_2), 61.7 (CH, *C*HN_3), 127.9 (CH, *C*H=CH), 128.0 (CH, CH=*C*H), 130.0 (CH, *C*H=CH), 130.2 (CH, CH=*C*H), 176.1 (C, *C*=O); MS (TOF ES–) *m/z* 348.3 ($[M - H]^-$, 100%); HRMS (TOF ES–) calcd for $C_{20}H_{34}N_3O_2Na$ ($[M - H]^-$, 100%) 348.2651, found 348.2665.

(2'*S*,3'*S*,4'*R*)-2'-[(*Z*,*Z*)-2''-Azido-eicosa-11,14-dienoylamino]-1'-*O*-[2,3-*O*-isopropylidene-L-threitol]octadecane-*O*-isopropylidene-octadecane-1',3',4'-triol (145)

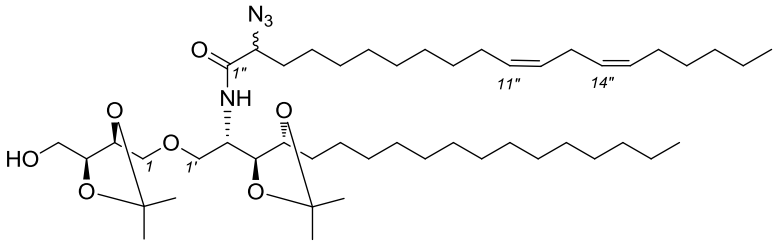

145

DMF (1 µL, 13 µmol) was added to a solution of (*Z,Z*)-2-azido-eicosa-11,14-dienoic acid **132** (45 mg, 0.129 mmol) in CH_2Cl_2 (1 mL) and the mixture was cooled to 0 ºC. A solution of oxalyl chloride (22 µL, 0.258 mmol) in CH_2Cl_2 (0.5 mL) was added dropwise over 2 min. After 2 h, the volatiles were removed under reduced pressure to provide the corresponding acid chloride **140** as a pale yellow oil, which was used directly in the next step without further purification (48 mg, quant.): A solution of freshly prepared acid chloride **140** (48 mg, 0.129 mmol) in CH_2Cl_2 (0.5 mL) was added dropwise over 2 min to a solution of amine **118** (97 mg, 019 mmol) and NEt_3 (36 µL, 0.26 mmol) in CH_2Cl_2 at 0 ºC. The reaction mixture was stirred for 12 h and then diluted with CH_2Cl_2 (10 mL), washed sequentially with $NaHCO_3$ solution (10 mL), brine (2 mL) and then dried over Na_2SO_4. The drying agent was removed by filtration and the filtrate concentrated under reduced pressure. Purification of the residue by flash column chromatography (20% EtOAc in hexane) provided amide **145** as a colourless oil

(97 mg, 90%, 1:1 mixture of epimers); data on epimeric mixture: R_f = 0.3 (25% EtOAc in hexane); ν_{max}(film) / cm^{-1} 3395br (OH), 2925s, 2855s, 2100m (N_3), 1660m (C=O), 1543w, 1465m, 1370m, 1251m, 1219m, 1080m, 1057m, 850w, 721w; δ_H(500 MHz, $CDCl_3$) 0.84-0.88 (stack, 6H, 2 × CH_2CH_3), 1.19-1.41 (stack, 54H), 1.45-1.55 (stack, 2H), 1.71-1.93 (stack, 2H, C(3")H_2), 2.03 (app. q, *J* 7.2, 4H, CH_2CH=$CHCH_2CH$=$CHCH_2$), 2.15-2.20 (br s, 1H, O*H*), 2.75 (app. t, *J* 6.6, 2H, CH=$CHCH_2CH$=CH), 3.51-3.60 (stack, 2H, C(1')H_aH_b for both epimers, C(1)H_aH_b for both epimers), 3.63-3.70 (stack, 2H, C(1)H_aH_b for both epimers, C(4)H_aH_b for both epimers), 3.72-3.80 (stack, 2H, C(4)H_aH_b for both epimers, C(1')H_aH_b for both epimers), 3.87-3.93 (stack, 1.5H, C(2")*H* for epimer 1, C(3)*H* for both epimers), 3.95 (dd, *J* 7.3, 4.6, 0.5H, C(2")*H* for epimer 2), 3.97-4.02 (stack, 1H, C(2)*H* for both epimers), 4.03-4.11 (stack, 2H, C(3')*H* for both epimers, C(4')*H* for both epimers), 4.12-4.18 (stack, 1H, C(2')*H* for both epimers), 5.27-5.39 (stack, 4H, 2 × C*H*=C*H*), 6.46 (d, *J* 9.0, 0.5H, N*H* for epimer 1), 6.49 (d, 0.5H, *J* 9.7, N*H* for epimer 2); δ_C(125 MHz, $CDCl_3$) [14.0, 14.1 (CH_3, C18', C20")], [22.5, 22.7 (CH_2, C3'"'], 25.3 (CH_2), 25.4 (CH_2), 25.6 (CH_2, C13"), 25.7 (CH_3, $C(CH_3)_a(CH_3)_b$ of 1,2-*anti* diol for both epimers (resonance overlap)], 26.5 (CH_2), 26.6 (CH_2), [26.91, 26.94, 26.98 (CH_3, $C(CH_3)_2$ of 1,2-*syn* diol for both epimers (resonance overlap))], [27.18, 27.20 (CH_2, C10", C16")], [27.86, 27.93 (CH_3, $C(CH_3)_a(CH_3)_b$ of 1,2-*anti* diol)], 29.0 (CH_2), [29.16, 29.20, 29.25, 29.33, 29.4, 29.5, 29.6, 29.7 (CH_2, alkyl chain, some resonance overlap)], 31.5 (CH_2), 31.9 (CH_2), [32.1, 32.3 (CH_2, C3")], [48.4, 48.6 (CH, C2')], [62.4, 62.5, (CH_2, C4)], [64.3, 64.6 (CH, C2")], 71.4 (CH_2, C1' for both epimers (resonance overlap)), [71.71, 71.73 (CH_2, C1)], [76.0, 76.1 (CH, C3' or C4')], [76.49, 76.50 (CH, C2)], [77.6, 77.7 (CH, C4' or C3')], [79.2, 79.4

(CH, C3)], [108.1, 108.2 (C, $(CH_3)_2C$ of 1,2-*anti* diol)], [109.29, 109.31 (C, $(CH_3)_2C$ of 1,2-*syn* diol)], 127.9 (CH, *C*H=CH), 128.0 (CH, CH=*C*H), 130.0 (CH, *C*H=CH), 130.2 (CH, CH=*C*H), [168.8, 168.9 (C, *C*=O)]; MS (TOF ES+) *m/z* 855.2 $[M + Na]^+$, 100%; HRMS (TOF ES+) 855.6579 $[M + Na]^+$. $C_{48}H_{88}N_4O_7Na$ requires 855.6551.

Triazole 146

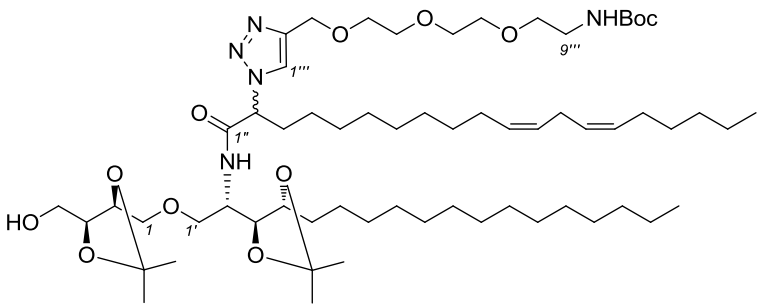

146

$CuSO_4$ solution (10 µL of a 0.5 M aqueous solution, 10 µmol) and sodium ascorbate solution (40 µL of a 1 M aqueous solution, 40 µmol) were added to a solution of azide **145** (80 mg, 0.096 mmol) and alkyne **114** (33 mg, 0.115 mmol) in ^tBuOH / H_2O (1 mL, 1:1) at r.t. The reaction mixture was heated for 10 h at 50 °C and then diluted with $CHCl_3$ (10 mL), and washed with brine (3 mL). The phases were separated and the aqueous layer was extracted with $CHCl_3$ (2 × 5 mL). The combined organic layers were dried over Na_2SO_4 and the volatiles were removed under reduced pressure. Purification of the residue by flash column

chromatography (gradient: 50% → 90% EtOAc in hexane) afforded 1,2,3-triazole **146** as a colourless oil (108 mg, 95%, isolated as 45 mg of a more polar epimer, 40 mg of less polar epimer and 23 mg of 1:1 mixture of two epimers). Data for less polar epimer: R_f = 0.3 (40% EtOAc in hexane); $[\alpha]_D^{20}$ = + 5.6 (*c* 1, $CHCl_3$); ν_{max}(film) / cm^{-1} 3316br (OH), 2924s, 2855s, 1717m (C=O), 1688s (C=O), 1515m, 1458m, 1367s, 1248s, 1220w, 1171w, 1100s, 848w, 723w; δ_H(500 MHz, $CDCl_3$) 0.84-0.89 (stack, 6H, 2 × CH_2CH_3), 1.18-1.34 (stack, 43H, alkyl chain methylenes, $C(CH_3)_a(CH_3)_b$ for 1,2-*anti*-diol), 1.35-1.50 [stack, 22H, including (1.37 (stack, 6H, $C(CH_3)_a(CH_3)_b$ of 1,2-*anti* diol, $C(CH_3)_a(CH_3)_b$ of 1,2-*syn* diol), 1.39 (s, 3H, $C(CH_3)_a(CH_3)_b$ of 1,2-*syn* diol), 1.42 (s, 9H, $C(CH_3)_3$))], 1.98-2.05 (stack, 4H, $CH_2CH{=}CHCH_2CH{=}CHCH_2$), 2.08-2.24 (stack, 2H, C(3")H_2), 2.74 (app. t, *J* 6.8, 2H, $CH{=}CHCH_2CH{=}CH$), 3.25-3.32 (stack, 2H, CH_2NHBoc), 3.40-3.44 (m, 1H, C(1')H_aH_b), 3.48-3.54 (stack, 4H, CH_2CH_2NHBoc, C(1)H_2), 3.58-3.63 (stack, 4H, PEG CH_2O), 3.64-3.72 (stack, 7H, C(4)H_2, C(1')H_aH_b, C(4''')H_2, 2 × PEG CH_2O), 3.85-3.89 (m, 1H, C(2)*H*), 3.90-3.95 (m, 1H, C(3)*H*), 3.93-4.03 (stack, 2H, C(3')*H*, C(4')*H*), 4.06-4.12 (m, 1H, C(2')*H*), 4.66-4.69 (stack, 2H, C(3''')H_2), 4.93-4.99 (m, 1H, C(2'')*H*), 5.02-5.09 (m, 1H, N*H*Boc), 5.26-5.39 (stack, 4H, 2 × C*H*=C*H*), 6.76 (d, *J* 8.3, 1H, N*H*), 7.70 (br s, 1H, C(1''')*H*), O*H* resonance not observed; δ_C(125 MHz, $CDCl_3$) [14.0, 14.1 (CH_3, C18', C26")], 22.5 (CH_2), 22.7 (CH_2), [25.6 (CH_2, $CH{=}CHCH_2CH{=}CH$, *and* CH_3, $C(CH_3)_a(CH_3)_b$ of 1,2-*anti* diol)], 25.9 (CH_2), 26.5 (CH_2), 26.9 (CH_3, $C(CH_3)_a(CH_3)_b$ of 1,2-*syn* diol), 27.1 (CH_3, $C(CH_3)_a(CH_3)_b$ of 1,2-*syn* diol), [27.17, 27.19 (CH_2, $CH_2CH{=}CHCH_2CH{=}CHCH_2$)], 27.9 ($CH_3$, $C(CH_3)_a(CH_3)_b$ of 1,2-*anti* diol), 28.4 (CH_3, $C(CH_3)_3$), 28.9 (CH_2), 29.0 (CH_2), [29.2, 29.32, 29.34, 29.4 (CH_2, resonance overlap)], [29.58, 29.63, 29.70 (CH_2,

resonance overlap)], 31.5 (CH_2), 31.9 (CH_2), 33.1 (CH_2, C3''), 40.4 (CH_2, *C*H_2NHBoc), 48.8 (CH, C2'), 62.7 (CH_2, C4), 64.6 (CH_2, C3'"), 65.6 (CH, C2"), 70.0 (CH_2, C4'''), [70.2, 70.3, 70.50, 70.52 (CH_2, 4 × CH_2O in PEG linker)], 71.0 (CH_2, C1'), 71.6 (CH_2, C1), 75.9 (CH, C3' or C4'), 76.5 (CH, C2), 77.5 (CH, C4' or C3'), 79.4 (CH, C3 *and* C, *C*$(CH_3)_3$), 108.1 (C, $(CH_3)_2$*C* of 1,2-*anti* diol), 109.2 (C, $(CH_3)_2$*C* of 1,2-*syn* diol), 123.2 (CH, C1'"), 127.9 (CH, *C*H=CH), 128.0 (CH, CH=*C*H), 130.0 (CH, *C*H=CH), 130.2 (CH, CH=*C*H), 145.4 (C, C2'"), 167.3 (C, CH_2*C*(O)NH), *C*=O of Boc not observed; MS (TOF ES+) *m/z* 1142.9 $[M + Na]^+$, 100%; HRMS (TOF ES+) calcd for $C_{62}H_{113}N_5O_{12}Na$ $[M + Na]^+$ 1142.8283, found 1142.8251.

Data for more polar epimer: R_f = 0.2 (40% EtOAc in hexane); $[\alpha]_D^{20}$ = + 11.2 (*c* 1, $CHCl_3$); ν_{max}(film) / cm^{-1} 3293br (OH), 2925s, 2854s, 1715m (C=O), 1685m (C=O), 1532m, 1463m, 1368m, 1249m, 1220w, 1108m, 724w; δ_H(500 MHz, $CDCl_3$) 0.84-0.89 (stack, 6H, 2 × CH_2CH_3), 1.19-1.34 (stack, 43H, alkyl chain methylenes, $C(CH_3)_a(CH_3)_b$ for 1,2-*anti*-diol), 1.35-1.50 [stack, 22H, (including 1.37 (6H, stack, $C(CH_3)_a(CH_3)_b$ of 1,2-*anti* diol, $C(CH_3)_a(CH_3)_b$ of 1,2-*syn* diol), 1.39 (s, 3H, $C(CH_3)_a(CH_3)_b$ of 1,2-*syn* diol), 1.42 (s, 9H, $C(CH_3)_3$))], 1.98-2.05 (stack, 5H, $CH_2CH=CHCH_2CH=CHCH_2$, C(3")H_aH_b), 2.16-2.25 (m, 1H, C(3")H_aH_b), 2.74 (app. t, *J* 6.6, 2H, CH=CHCH_2CH=CH), 3.24-3.33 (stack, 2H, CH_2NHBoc), 3.38-3.43 (m, 1H, C(1')H_aH_b), 3.49-3.56 (stack, 4H, CH_2CH_2NHBoc, C(1)H_2), 3.58-3.67 (stack, 6H, PEG CH_2O), 3.64-3.72 (stack, 5H, C(4)H_2, C(1')H_aH_b, 2 × PEG CH_2O), 3.89-3.97 (stack, 2H, C(2)*H*, C(3)*H*), 3.98-4.05 (stack, 2H, C(3')*H*, C(4')*H*), 4.05-4.11 (m, 1H, C(2')*H*), 4.66-4.69 (stack, 2H, C(3'")H_2), 4.99-5.10 (stack, 2H, C(2'')*H*,

N*H*Boc), 5.26-5.39 (stack, 4H, 2 × C*H*=C*H*), 6.57 (d, *J* 8.4, 1H, N*H*), 7.75 (br s, 1H, C(1'")*H*), O*H* resonance not observed; δ_C(125 MHz, $CDCl_3$) [14.0, 14.1 (CH_3, C18', C20")], 22.5 (CH_2), 22.7 (CH_2), [25.6 (CH_2, CH=CH*C*H_2CH=CH, *and* CH_3, C(*C*H_3)$_a$(CH_3)$_b$ of 1,2-*anti* diol)], 25.8 (CH_2), 26.5 (CH_2), 26.9 (CH_3, C(*C*H_3)$_a$(CH_3)$_b$ of 1,2-*syn* diol), 27.1 (CH_3, C(CH_3)$_a$(*C*H_3)$_b$ of 1,2-*syn* diol), [27.17, 27.19 (CH_2, *C*H_2CH=CHCH$_2$CH=CH*C*H_2)], 27.9 (CH_3, C(CH_3)$_a$(*C*H_3)$_b$ of 1,2-*anti* diol), 28.4 (CH_3, C(*C*H_3)$_3$), 29.0 (CH_2), 29.1 (CH_2), [29.22, 29.27, 29.31, 29.33, 29.4 (CH_2, resonance overlap)], [29.6, 29.7 (CH_2, resonance overlap)], 31.5 (CH_2), 31.9 (CH_2), 32.4 (CH_2, C3''), 40.3 (CH_2, *C*H_2NHBoc), 49.0 (CH, C2'), 62.7 (CH_2, C4), 64.6 (CH_2, C3'" *and* CH, C2"), [70.0, 70.2, 70.49, 70.51 (CH_2, 5 × CH_2O in PEG linker, resonance overlap)], 70.9 (CH_2, C1'), 71.7 (CH_2, C1), 75.8 (CH, C3' or C4'), 76.7 (CH, C2 or C3), 77.5 (CH, C4' or C3'), 79.1 (CH, C3 or C2 *and* C, *C*(CH_3)$_3$), 108.1 (C, (CH_3)$_2$*C* of 1,2-*anti* diol), 109.2 (C, (CH_3)$_2$*C* of 1,2-*syn* diol), 122.2 (CH, C1'"), 127.9 (CH, *C*H=CH), 128.0 (CH, CH=*C*H), 130.0 (CH, *C*H=CH), 130.2 (CH, CH=*C*H), 145.5 (C, C2'"), 156.0 (C, O*C*(O)NH), 167.3 (C, amide *C*=O);

Alexa 594-labelled ThrCer (110)

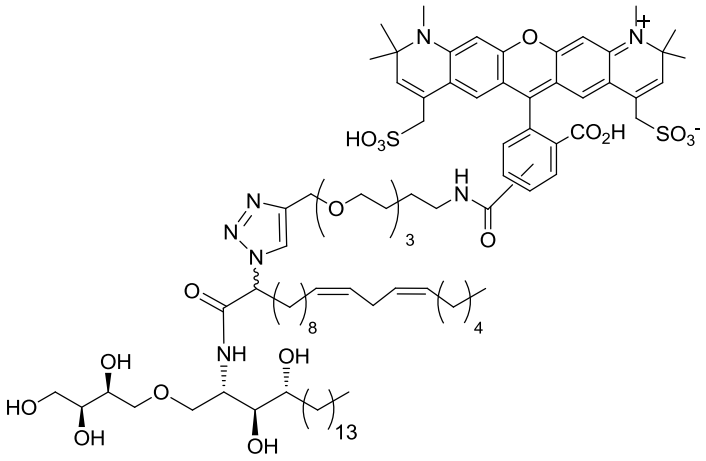

110

TFA (60 µL) was added dropwise over 1 min to a solution of Boc amide **146** (60 mg, 0.050 mmol) in CH_2Cl_2 / CH_3OH (2:1, 0.6 mL). After stirring overnight at r.t., the reaction mixture was concentrated under reduced pressure and the residual TFA was removed by co-evaporation with Et_2O (3 × 3 mL) to provide crude amine **147** as a white solid (51 mg, quant.), which was used in the step without further purification.

NEt_3 (1 µL, 7.2 µmol) was added to a solution of crude amine **147** (2.1 mg, 2.3 µmol) in DMF (10 µL). After stirring for 1 h at r.t., Alexa Fluor® 488 carboxylic acid, succinimidyl ester **144** (1.2 mg, 1.1 µmol) was added. The reaction mixture was stirred for 12 h at r.t. and then the volatiles were removed under reduced pressure. Purification of the residue by flash column chromatography (eluent: gradient 0-50% CH_3OH in $CHCl_3$) afforded compound **110** as a dark blue solid (0.7 mg, 62%); selected data: R_f = 0.3 for epimer A, R_f = 0.2 for epimer B in 65:35:4 $CHCl_3$ / MeOH / aq. NH_3;

(2*S*,3*S*,4*R*)-2-(*Z*,*Z*)-2''-Azido-eicosa-11'',14''-dienoylamino-3,4-*O*-isopropylidene-1-*O*-(2',3',4',6'-tetra-*O*-benzyl-α-D-galactopyranosyl)octadecane-1,3,4-triol (141)

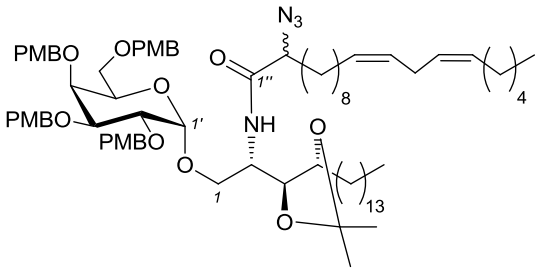

141

DMF (1 µL, 13µmol) was added to a solution of (*Z,Z*)-2-azido-eicosa-11,14-dienoic acid (32 mg, 0.093 mmol) in CH_2Cl_2 (1 mL) and the mixture was cooled to 0 ºC. A solution of oxalyl chloride (16 µL, 0.186 mmol) in CH_2Cl_2 (0.5 mL) was added dropwise over 2 min. After 2 h, the volatiles were removed under reduced pressure to provide the corresponding acid chloride **140** as a pale yellow oil, which was used directly in the next step without further purification (48 mg, quant.): A solution of freshly prepared acid chloride **140** (34 mg, 0.093 mmol) in CH_2Cl_2 (0.5 mL) was added dropwise over 2 min to a solution of amine **128** (57 mg, 0.062 mmol) and NEt_3 (18 µL, 0.013 mmol) in CH_2Cl_2 at 0 ºC. The reaction mixture was stirred for 12 h and then diluted with CH_2Cl_2 (10 mL), washed sequentially with $NaHCO_3$ solution (10 mL), brine (2 mL) and then dried over Na_2SO_4. The drying agent was removed by filtration and the filtrate concentrated under reduced pressure. Purification of the residue by flash column chromatography (20% EtOAc in hexane) provided amide **141** as a colourless oil (70 mg, 85%, 1:1 mixture of epimers); data on epimeric mixture: R_f = 0.3 (20% EtOAc in hexane); ν_{max}(film) /

cm^{-1} 2923s, 2853m, 2103m (N_3), 1683m, (C=O), 1586w, 1513s, 1464m, 1368w, 1302m, 1247s, 1172m, 1092m, 1038s, 822m, 720w; δ_H(500 MHz, $CDCl_3$) 0.84-0.90 (stack, 6H, 2 × CH_2CH_3), 1.16-1.40 (stack, 54H), 1.41-1.52 (stack, 2H), 1.61-1.86 (stack, 2H, C(3")H_2), 1.99-2.07 (stack, 4H, $CH_2CH{=}CHCH_2CH{=}CHCH_2$), 2.73-2.78 (stack, 2H, $CH{=}CHCH_2CH{=}CH$), 3.33-3.41 (stack, 1H, C(6')H_aH_b for both epimers), 3.42-3.47 (stack, 1H, C(6')H_aH_b for both epimers), 3.58-3.65 (stack, 1H, C(1)H_aH_b for both epimers), 3.67-3.71 (m, 0.5H, C(2")*H* for epimer 1), 3.74-3.81 (stack, 12H, 4 × $ArOCH_3$ for both epimers, *and* 1H, C(2")*H* for epimer 2), 3.81-3.89 (stack, 3H, C(3')*H* for both epimers, C(4')*H* for both epimers, C(5')*H* for both epimers), 3.90-4.01 (stack, 3H, C(1)H_aH_b for both epimers, C(4)*H* for both epimers, C(2')*H* for both epimers), 4.02-4.10 (stack, 1H, C(2)*H* for both epimers), 4.11-4.19 (stack, 1H, C(3)*H* for both epimers), 4.27 (A of AB, J_{A-B} 11.6, 1H, C(6')OCH_aH_bAr for epimer 1), 4.28 (A of AB, J_{A-B} 11.6, 1H, C(6')OCH_aH_bAr for epimer 2), 4.40 (B of AB, J_{B-A} 11.6, 1H, C(6')OCH_aH_bAr for epimer 1), 4.42 (B of AB, J_{B-A} 11.6, 1H, C(6')OCH_aH_bAr for epimer 1), 4.46 (A of AB, J_{A-B} 11.2, 1H, C(4')OCH_aH_bAr for epimer 1), 4.47 (A of AB, J_{A-B} 11.2, 1H, C(4')OCH_aH_bAr for epimer 2), 4.56 (A of AB, J_{A-B} 11.2, 1H, C(2')OCH_aH_bAr for epimer 1), 4.57 (A of AB, J_{A-B} 11.2, 1H, C(2')OCH_aH_bAr for epimer 2), 4.63 (A of AB, J_{A-B} 11.2, 1H, C(3')OCH_aH_bAr for epimer 1), 4.64 (A of AB, J_{A-B} 11.2, 1H, C(3')OCH_aH_bAr for epimer 2), 4.70 (B of AB, J_{B-A} 11.2, 1H, C(3')OCH_aH_bAr for both epimers), 4.72 (B of AB, J_{B-A} 11.2, 1H, C(2')OCH_aH_bAr for epimer 1), 4.73 (B of AB, J_{B-A} 11.2, 1H, C(2')OCH_aH_bAr for epimer 2), 4.81 (B of AB, J_{B-A}, 1H, C(4')OCH_aH_bAr for both epimers), 4.89 (stack, 1H, C(1')H, for both epimers), 5.27-5.41 (stack, 4H, 2 × $CH{=}CH$), 6.75-6.89 (stack, 8H, Ar), 7.12-7.19 (stack, 4H, Ar), 7.23-7.32 (stack, 4H,

Ar); δ_C(125 MHz, $CDCl_3$) [14.0, 14.1 (CH_3, C18', C20")], [22.6, 22.7 (CH_2)], [25.6, 25.7 (CH_2, alkyl chain *and* C13" (resonance overlap)], [25.9, 26.0 (CH_3, C(CH_3)$_2$ for both epimers)], 26.6 (CH_2), 26.7 (CH_2), [27.18, 27.23 (CH_2, C10", C16")], [28.1, 28.2 (CH_3, C(CH_3)$_2$ for both epimers)], 28.1 (CH_2), [28.95, 29.02, 29.25, 29.30, 29.32, 29.35, 29.38, 29.45, 29.48, 29.54, 29.57, 29.62, 29.65, 29.69, (CH_2, alkyl chain, some resonance overlap)], 31.5 (CH_2), 31.9 (CH_2, C3"), 32.0 (CH_2), 32.1 (CH_2), [48.8, 49.1 (CH, C2)], [55.21, 55.24 (CH_3, 4 × ArOCH_3, resonance overlap)], [64.3, 64.6 (CH, C2")], 68.6 (CH_2, C1 for epimer 1), [68.88, 68.91 (CH_2, C6')], 69.0 (CH_2, C1 for epimer 2), 69.8 (CH, C5' for both epimers (resonance overlap)), [72.6, 72.7 (CH_2, C(3')OCH_2Ar), [73.07, 73.12, 73.15 (CH_2, C(3')OCH_2Ar *and* C(3')OCH_2Ar (resonance overlap))], 74.2 (CH_2, C(4')OCH_2Ar for both epimers (resonance overlap)), [74.4, 74.5 (CH, C4')], [75.1, 75.2 (CH, C3)], 76.2 (CH, C2' for both epimers (resonance overlap)), [77.68, 77.72 (CH, C4)], [78.8, 78.9 (CH, C3')], [99.0, 99.2 (CH, C1')], [107.87, 107.93 (C, $(CH_3)_2C$)], [113.6, 113.73, 113.75 113.77 (CH, Ar *ortho* to OMe)], 127.9 (CH, *C*H=CH), 128.0 (CH, CH=*C*H), [129.0, 129.4, 129.5, 129.8, 129.9, (CH, Ar *meta* to OMe)], 130.0 (CH, *C*H=CH), 130.2 (CH, *C*H=CH), [130.6, 130.7, 130.9 (C, Ar *para* to OMe, some resonance overlap)], [159.1, 159.2, 159.3 (C, Ar *ipso* to OMe)], [168.8, 168.9 (C, *C*=O)]; MS (TOF ES+) *m/z* 1353.8 $[M + Na]^+$, 100%; HRMS (TOF ES+) calcd for $C_{79}H_{118}N_4O_{13}Na$ $[M + Na]^+$ 1353.8593, found 1353.8610.

Triazole 142

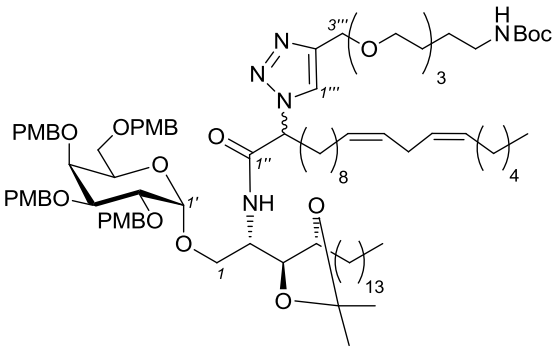

142

$CuSO_4$ solution (10 µL of a 0.5 M aqueous solution, 10 µmol) and sodium ascorbate solution (40 µL of a 1 M aqueous solution, 40 µmol) were added to a solution of azide **145** (100 mg, 0.075 mmol) and alkyne **114** (32 mg, 0.115 mmol) in ^{t}BuOH / H_2O (1 mL, 1:1) at r.t. The reaction mixture was heated for 10 h at 50 °C and then diluted with $CHCl_3$ (10 mL), and washed with brine (3 mL). The phases were separated and the aqueous layer was extracted with $CHCl_3$ (2 × 5 mL). The combined organic layers were dried over Na_2SO_4 and the volatiles were removed under reduced pressure. Purification of the residue by flash column chromatography (gradient: 50% → 90% EtOAc in hexane) afforded 1,2,3-triazole **142** as a colourless oil (95 mg, 78% %, 1:1 mixture of epimers); data on epimeric mixture: R_f = 0.3 (40% EtOAc in hexane); ν_{max}(film) / cm^{-1} 2916s, 2849m, 1789m, 1735, 1473m, 1368w, 1302m, 1206s, 1075m, 1172m, 909s, 730s; δ_H(500 MHz, $CDCl_3$) 0.84-0.89 (stack, 6H, 2 × CH_2CH_3), 1.12-1.36 (stack, 44H, alkyl chain methylenes, $C(CH_3)_a(CH_3)_b$), 1.37-1.44 [stack, 16H, including $C(CH_3)_a(CH_3)_b$, $C(CH_3)_3$))], 1.92-2.08 (stack, 6H, $CH_2CH{=}CHCH_2CH{=}CHCH_2$, C(3")$H_2$), 2.73 (app.

t, *J* 6.7, 2H, CH=CHC*H*$_2$CH=CH), 3.21-3.33 (stack, 3H, C(6')*H*$_a$H$_b$ for both epimers, C*H*$_2$NHBoc), 3.39-3.46 (stack, 1H, C(6')H$_a$*H*$_b$ for both epimers), 3.47-3.54 (stack, 3H, C*H*$_2$CH$_2$NHBoc, C(1)*H*$_a$H$_b$ for both epimers), 3.55-3.74 (stack, 12H, including 4 × PEG C*H*$_2$O, C(4''')*H*$_2$), 3.75-3.82 (stack, 13H, 4 × ArOC*H*$_3$ for both epimers, C(3')*H* for epimer 1 *and* C(4')*H* for epimer 1), 3.84-4.16 (stack, 8H, including C(2')*H* for both epimers, C(3')*H* for epimer 2, C(4')*H* for epimer 2, C(1)H$_a$*H*$_b$ for both epimers, C(2)*H* for both epimers, C(4)*H* for both epimers, C(3)*H* for both epimers, 1 × PEG C*H*$_2$O), 4.17-4.21 (1H, stack), 4.24-4.31 (stack, 2H, A of AB, C(6')OC*H*$_a$H$_b$Ar for both epimers), 4.40-4.59 (stack, 2H), 4.64-4.76 (stack, 2H), 4.76-4.82 (stack, 2H, including C(1')*H*, for both epimers), 4.90-4.95 (stack, 1H, C(2'')*H* for both epimers), 4.99-5.06 (stack, 1H, N*H*Boc for both epimers), 5.25-5.39 (stack, 4H, 2 × C*H*=C*H*), 6.72-6.88 (stack, 8H, Ar), 7.11-7.19 (stack, 4H, Ar), 7.22-7.30 (stack, 4H, Ar), 7.66 (br s, 0.5H, C(1''')*H*) for epimer 1), 7.72 (br s, 0.5H, C(1''')*H*) for epimer 2), CON*H* resonance not observed; δ_C(125 MHz, $CDCl_3$) [14.0, 14.1 14.2 (CH_3, resonance overlap, C18, C20")], 22.5 (CH_2), 22.7 (CH_2), [25.6, 25.7 (CH_2, CH=CH*C*H$_2$CH=C)], [25.86, 25.89 CH_3, C(*C*H$_3$)$_a$(CH$_3$)$_b$], 26.5 (CH_2), [27.18, 27.20 (CH_2, *C*H$_2$CH=CHCH$_2$CH=CH*C*H$_2$)], 28.2 (CH_3, C(CH$_3$)$_a$(*C*H$_3$)$_b$, 28.4 (CH_3, C(*C*H$_3$)$_3$), 28.8 (CH_2), 29.0 (CH_2), [29.2, 29.31, 29.33, 29.4 (CH_2, resonance overlap)], [29.58, 29.63, 29.70 (CH_2, resonance overlap)], 31.5 (CH_2), 31.9 (CH_2), 33.1 (CH_2, C3''), 40.3 (CH_2, *C*H$_2$NHBoc), [49.4, 49.5 (CH, C2)], [55.21, 55.24 (CH_3, 4 × ArO*C*H$_3$, resonance overlap)], [64.3, 64.6 (CH, C2")], 64.7 (CH_2, C3'"), 68.2 (CH_2, C1), [69.1, 69.2 (CH_2, C6', resonance overlap), [70.0, 70.2, 70.4, 70.50, 70.52 (CH_2, 4 × CH_2O in PEG linker)], [72.6, 72.9 (CH_2, O*C*H$_2$Ar), [73.04, 73.12, 73.15 (CH_2, O*C*H$_2$Ar (resonance overlap))], [74.1, 74.2

(CH_2, OCH_2Ar (resonance overlap)), [74.4, 74.5 (CH, C4')], [75.1, 75.2 (CH, C3)], 76.2 (CH, C2' for both epimers (resonance overlap)), 77.6 (CH, C4, for both epimers (resonance overlap)], [78.8, 78.9 (CH, C3' for both epimers (resonance overlap)], 79.4 (CH, C3 *and* C, *C*$(CH_3)_3$) [98.9, 99.6 (CH, C1')], [107.87, 107.91 (C, $(CH_3)_2$*C*)], [113.6, 113.73, 113.75 113.77 (CH, Ar *ortho* to OMe)], [121.8, 122.1 (CH, C1'")], 127.9 (CH, *C*H=CH), 128.0 (CH, CH=*C*H), [129.0, 129.4, 129.5, 129.8, 129.9, (CH, Ar *meta* to OMe)], 130.0 (CH, *C*H=CH), 130.2 (CH, *C*H=CH), [130.6, 130.7, 130.9 (C, Ar *para* to OMe, some resonance overlap)], [145.4, 145.2 (C, C2'")], [159.1, 159.2, 159.3 (C, Ar *ipso* to OMe)], [167.31, 167,33 (C, CH_2*C*(O)NH)], [171.1 C of Boc]; MS (TOF ES+) *m/z* 1641.0 $[M + Na]^+$, 100%;

Alexa 594-labelled GalCer(C20:2) (109)

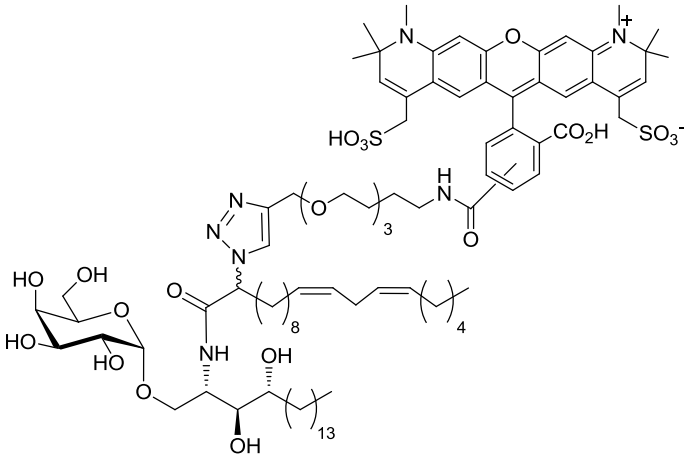

109

TFA (60 µL) was added dropwise over 1 min to a solution of Boc amide **142** (84 mg, 0.050 mmol) in CH_2Cl_2 / CH_3OH (2:1, 0.6 mL). After stirring overnight at r.t., the reaction mixture was concentrated under reduced pressure and the residual TFA was removed by co-evaporation with Et_2O (3 × 3 mL) to provide crude amine **143** as a white solid (49 mg, quant.), which was used in the step without further purification: selected data: MS (TOF ES+) *m/z* 1020.8 ($[M + Na]^+$, 100%);

NEt_3 (1 µL, 7.2 µmol) was added to a solution of crude amine **143** (2.3 mg, 2.3 µmol) in DMF (10 µL). After stirring for 1 h at r.t., Alexa Fluor® 594 carboxylic acid, succinimidyl ester **144** (1.0 mg, 1.2 µmol) was added. The reaction mixture was stirred for 12 h at r.t. and then the volatiles were removed under reduced pressure. Purification of the residue by flash column chromatography (eluent: gradient 0-50% CH_3OH in $CHCl_3$) afforded compound **109** as a dark blue solid (0.9 mg, 70%);

selected data: R_f = 0.3 for epimer A, R_f = 0.2 for epimer B in 65:35:4 $CHCl_3$ / MeOH / aq. NH_3.

Methyl 3',4'-*O*-isopropylidene-2'-*O*-(2,3,4,6-tetra-*O*-*p*-methoxybenzyl-D-galactopy-ranosyl)-(1→2)-L-threonate (155)

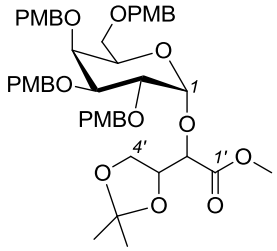

155

PPh_3 (1.46 g, 5.55 mmol) and CBr_4 (1.84 g, 5.55 mmol) were added sequentially to a solution of 2,3,4,6-tetra-*O*-*p*-methoxybenzyl-D-galactose **126** (1.22 g, 1.85 mmol) in CH_2Cl_2 (10 mL) at r.t. The reaction mixture was stirred for 3 h. In separate flasks, a solution of TMU (1.2 mL), DIPEA (1.6 mL) and Bu_4NBr (1.79 g, 5.55 mmol) in CH_2Cl_2 (5 mL), and a solution of methyl 3,4-*O*-isopropylidene-L-threonate **154** (493 mg, 2.59 mmol) in CH_2Cl_2 (5 mL) were stirred over activated 3 Å MS for 30 min, after which time, these solutions were added dropwise over 5 min, and sequentially (TMU/DIPEA/Bu_4NBr solution first), to the solution containing the glycosyl donor. The reaction mixture was stirred at r.t. for 2 d until there was no evidence by TLC that the donor was still being consumed. The reaction mixture

was then concentrated under reduced pressure, re-suspended in toluene (10 mL), filtered through a silica plug, washed with toluene (150 mL) and concentrated under reduced pressure to provide the crude product. Purification of the residue by flash column chromatography (20% EtOAc in hexane) afforded glycoside **153** as a colourless oil (693 mg, 45%, single α-anomer); R_f = 0.3 (20% EtOAc in hexane); $[\alpha]_D^{18}$ = + 11.2 (*c* 1, $CHCl_3$); ν_{max}(film) / cm^{-1}: 2935w, 2872w, 1739m (C=O), 1623m, 1581w, 1485m, 1415m, 1323s, 1128s, 1103s, 1064s, 883m, 843s, 736s, 697s; δ_H(500 MHz, $CDCl_3$) 1.30 (s, 3H, 1 × C(CH_3)$_2$), 1.35 (s, 3H, 1 × C(CH_3)$_2$), 3.40 (A of ABX, $J_{A\text{-}B}$ 8.9, $J_{A\text{-}X}$ 5.7, 1H, C(6)H_aH$_b$), 3.44-3.49 (m, 1H, C(6)H$_a$$H_b$), 3.72 (s, 3H, C(O)OC$H_3$), 3.76 (s, 3H, ArOC$H_3$), 3.775 (s, 3H, ArOC$H_3$), 3.778 (s, 3H, ArOC$H_3$), 3.79 (s, 3H, ArOC$H_3$), 3.90 (dd, *J* 8.9, 6.3, 1H, C(4')H_aH$_b$), 3.92-3.96 (stack, 2H, H3, H4), 4.00-4.06 (stack, 2H, H2, C(4')H$_a$$H_b$), 4.15 (app t, *J* 6.5, 1H, H5), 4.27 (d, *J* 7.0, 1H, H2'), 4.30 (A of AB, $J_{A\text{-}B}$ 11.4, 1H, C(6)OCH_aH$_b$Ar), 4.35 (B of AB, $J_{B\text{-}A}$ 11.4, 1H, C(6)OCH$_a$$H_b$Ar), 4.41 (app. q, *J* 6.6, 1H, H3'), 4.48 (A of AB, $J_{A\text{-}B}$ 11.2, 1H, C(4)OCH_aH$_b$Ar), 4.615 (A of AB, $J_{A\text{-}B}$ 11.2, 1H, C(3)OCH_aH$_b$Ar), 4.620 (A of AB, $J_{A\text{-}B}$ 11.4, 1H, C(2)OCH_aH$_b$Ar), 4.73 (B of AB, $J_{B\text{-}A}$ 11.4, 1H, C(2)OCH$_a$$H_b$Ar), 4.74 (A of AB, $J_{A\text{-}B}$ 11.2, 1H, C(3)OCH_aH$_b$Ar), 4.82 (B of AB, $J_{B\text{-}A}$ 11.2, 1H, C(4)OCH$_a$$H_b$Ar), 5.09 (d, *J* 3.7, 1H, H1), 6.73-6.87 (stack, 8H, Ar), 7.15-7.19 (stack, 4H, Ar), 7.23-7.33 (stack, 4H, Ar); δ_c(125 MHz, $CDCl_3$) 25.3 (CH_3, 1 × C(*C*H_3)$_2$), 26.1 (CH_3, 1 × C(*C*H_3)$_2$), 52.0 (CH_3, C(O)O*C*H_3), 55.2 (CH_3, 4 × ArO*C*H_3 resonance overlap), 66.1 (CH_2, C4'), 68.3 (CH_2, C6), 69.7 (CH, C5), 72.0 (CH_2, C(2)O*C*H_2Ar), 72.9 (CH_2, C(3)O*C*H_2Ar), 73.1 (CH_2, C(6)O*C*H_2Ar), 74.2 (CH_2, C(4)O*C*H_2Ar), 74.4 (CH, C4), 75.3 (CH, C3'), 75.4 (CH, C2'), 75.6 (CH, C2), 78.3 (CH, C3), 96.0 (CH, C1), 109.7 (C, (CH_3)$_2$*C*), [113.51, 113.54, 113.6, 113.7

(CH, Ar *ortho* to OMe)], [129.0, 129.5, 129.8 (CH, Ar *meta* to OMe, some resonance overlap)], 130.0 (C, Ar *para* to OMe), 130.8 (C, Ar *para* to OMe), 130.9 (C, Ar *para* to OMe), 131.2 (C, Ar *para* to OMe), 158.9 (C, Ar *ipso* to OMe), 159.0 (C, Ar *ipso* to OMe), 159.1 (C, Ar *ipso* to OMe), 159.2 (C, Ar *ipso* to OMe), 169.9 (C, *C*=O); MS (TOF ES+) *m/z* 855.2 ($[M + Na]^+$, 100%); HRMS (TOF ES+) calcd for $C_{46}H_{56}O_{14}Na$ ($[M + Na]^+$) 855.3568, found 855.3531.

This reaction was first performed without the addition of Hünig's base, which led to the formation of a mixture of two glycosyl products **155** and **156**. Selected data for **156**:

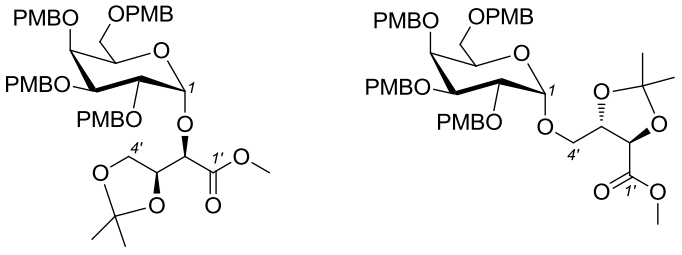

155, minor 1:3 **156**, major

δ_H(500 MHz, $CDCl_3$) selected data: 1.43 (s, 3H, 1 × C(CH_3)$_2$), 1.44 (s, 3H, 1 × C(CH_3)$_2$), 3.65 (dd, *J* 11.6, 5.0, 1H, C(4')H_aH$_b$), 3.73 (s, 3H, C(O)OCH_3), 3.78 (s, 3H, ArOCH_3), 3.79 (s, 6H, 2 × ArOCH_3), 3.80 (s, 3H, ArOCH_3), 4.42-4.44 (m, 1H, H2'), 4.90 (d, *J* 3.5, 1H, H1); δ_C(125 MHz, $CDCl_3$) selected data: 25.9 (CH_3, 1 × C(CH_3)$_2$), 26.8 (CH_3, 1 × C(CH_3)$_2$), 52.3 (CH_3, C(O)OCH_3), 55.2 (CH_3, 4 × ArOCH_3

resonance overlap), 67.5, 68.6, 69.5, 72.6, 72.7, 73.0, 74.2, 74.6, 75.54, 76.2, 78.4, 78.5, 98.2 (CH, C1), 111.5 (C, $(CH_3)_2C$), 170.9 (C, *C*=O).

3',4'-*O*-isopropylidene-2'-*O*-(2,3,4,6-tetra-*O*-*p*-methoxybenzyl-D-galactopyranosyl)-(1→2)-L-threitol (153)

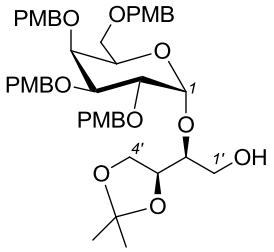

153

A solution of methyl ester **155** (200 mg, 0.24 mmol) in Et_2O (1 mL) was added over 5 min to a stirred suspension of $LiAlH_4$ (14 mg, 0.36 mmol) in Et_2O (2 mL). After an initial vigorous reaction had subsided, the mixture was heated at reflux for 3 h and then cooled to r.t., diluted with Et_2O (10 mL) and poured into NH_4Cl solution (5 mL). H_2O (5 mL) was added and the layers were separated. The aqueous phase was extracted with Et_2O (3 × 10 mL). The combined organic extracts were dried (Na_2SO_4) and concentrated under reduced pressure. Purification of the residue by flash column chromatography (30% EtOAc in hexane) afforded alcohol **153** as a colourless oil (183 mg, 95%). R_f = 0.3 (40% EtOAc in hexane); $[\alpha]_D^{18}$ = + 39.6 (*c* 1,

$CHCl_3$); ν_{max}(film) / cm^{-1}: 3465 br (O–H), 2920w, 2878w, 1497w, 1454m, 1370m, 1209m, 1078s, 1049s, 911m, 850m, 736s, 698s; δ_H(500 MHz, $CDCl_3$) 1.25 (s, 3H, 1 × C(CH_3)$_2$), 1.34 (s, 3H, 1 × C(CH_3)$_2$), 3.40-3.49 (stack, 2H, C(6)H_aH_b), 3.57-3.61 (stack, 2H, C(1')H_aH_b), 3.61-3.68 (m, 1H, H2'), 3.766 (s, 3H, ArOCH_3), 3.769 (s, 3H, ArOCH_3), 3.774 (s, 3H, ArOCH_3), 3.799 (s, 3H, ArOCH_3), 3.84 (dd, *J* 8.4, 5.8, 1H, C(4')H_aH$_b$), 3.89-3.95 (stack, 3H, C(4')H$_a$$H_b$, H3, H4), 4.01 (dd, *J* 9.9, 3.8, 1H, H2), 4.08-4.12 (m, 1H, H5), 4.16 (app. q, *J* 5.9, 1H, H3'), 4.33 (A of AB, J_{A-B} 11.7, 1H, C(6)OCH_aH$_b$Ar), 4.39 (B of AB, J_{B-A} 11.7, 1H, C(6)OCH$_a$$H_b$Ar), 4.48 (A of AB, J_{A-B} 11.3, 1H, C(4)OCH_aH$_b$Ar), 4.62 (A of AB, J_{A-B} 11.2, 1H, C(2)OCH_aH$_b$Ar), 4.65 (s, 2H, C(3)OCH_2Ar), 4.80 (B of AB, J_{B-A} 11.2, 1H, C(2)OCH$_a$$H_b$Ar), 4.82 (B of AB, 1H, J_{B-A} 11.3, C(4)OCH$_a$$H_b$Ar), 4.89 (d, *J* 3.9, 1H, H1), 6.78-6.91 (stack, 8H, Ar), 7.13-7.26 (stack, 6H, Ar), 7.27-7.32 (stack, 2H, Ar); δ_c(125 MHz, $CDCl_3$) 24.9 (CH_3, 1 × C(*C*H_3)$_2$), 26.3 (CH_3, 1 × C(*C*H_3)$_2$), 55.15 (CH_3, ArO*C*H_3), 55.19 (CH_3, 2 × ArO*C*H_3, resonance overlap), 55.22 (CH_3, ArO*C*H_3), 62.0 (CH_2, C1'), 65.4 (CH_2, C4'), 68.4 (CH_2, C6), 69.7 (CH, C5), 72.1 (CH_2, C(3)O*C*H_2Ar), 73.0 (CH_2, C(6)O*C*H_2Ar), 74.05 (CH, C4), 74.13 (CH_2, C(2)O*C*H_2Ar), 74.2 (CH_2, C(4)O*C*H_2Ph), 75.2 (CH, C3'), 75.8 (CH, C2), 79.3 (CH, C3), 81.9 (CH, C2'), 100.2 (CH, C1), 109.3 (C, (CH_3)$_2$*C*), [113.5, 113.69, 113.74, 113.8 (CH, Ar *ortho* to OMe)], [129.0, 129.4, 129.7, 130.0 (CH, Ar *meta* to OMe)], [130.6, 130.8 (C, Ar *para* to OMe, some resonance overlap)], [159.08, 159.11, 159.2, 159.3 (C, Ar *ipso* to OMe)]; MS (TOF ES+) *m/z* 827.1 ([M + Na]$^+$, 100%); HRMS (TOF ES+) calcd for $C_{45}H_{56}O_{13}Na$ ([M + Na]$^+$) 827.3619, found 827.3621.

Methyl 3',4'-*O*-isopropylidene-2-*O*-(2,3,4,6-tetra-*O*-benzyl-D-galactopyranosyl)-(1→2)-L-threonate (157)

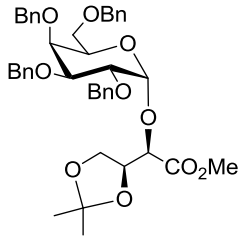

157

PPh_3 (1.46 g, 5.55 mmol) and CBr_4 (1.84 g, 5.55 mmol) were added sequentially to a solution of 2,3,4,6-tetra-*O*-benzyl-D-galactose **51** (1.00 g, 1.85 mmol) in CH_2Cl_2 (10 mL) at r.t. The reaction mixture was stirred for 3 h. In separate flasks, a solution of TMU (1.2 mL), DIPEA (1.6 mL) and Bu_4NBr (1.79 g, 5.55 mmol) in CH_2Cl_2 (5 mL), and a solution of methyl 3,4-*O*-isopropylidene-L-threonate **154** (493 mg, 2.59 mmol) in CH_2Cl_2 (5 mL) were stirred over activated 3 Å MS for 30 min, after which time, these solutions were added dropwise (over 5 min) and sequentially (TMU/DIPEA/Bu_4NBr solution first) to the solution containing the glycosyl donor. The reaction mixture was stirred at r.t. for 2 d until there was no evidence by TLC that the donor was still being consumed. The reaction mixture was then concentrated under reduced pressure, re-suspended in toluene (10 mL), filtered through a silica plug, washed with toluene (150 mL) and concentrated under reduced pressure to provide the crude product. Purification of the residue by flash column chromatography (10% EtOAc in hexane) afforded glycoside **157** as a colourless oil (593 mg, 45%, single α-anomer). R_f = 0.3 (15% EtOAc in hexane); $[\alpha]_D^{20}$ = + 50.0 (*c* 1, $CHCl_3$); ν_{max}(film) / cm^{-1}: 2991m, 2902m, 1742s

(C=O), 1613m, 1500w, 1455m, 1373m, 1266w, 1208m, 1101s, 1075s, 739m, 698m; δ_H(500 MHz, $CDCl_3$) 1.32 (s, 3H, 1 × C(CH_3)$_2$), 1.36 (s, 3H, 1 × C(CH_3)$_2$), 3.47 (A of ABX, J_{A-B} 9.0, J_{A-X} 5.8, 1H, C(6)H_aH$_b$), 3.53-3.56 (m, 1H, C(6)H$_a$$H_b$), 3.72 (s, 3H, OC$H_3$), 3.91 (dd, 1H, *J* 8.6, 6.3, C(4')H_aH$_b$), 3.99-4.03 (stack, 2H, H3, H4), 4.06 (dd, *J* 8.6, 6.6, 1H, C(4')H$_a$$H_b$), 4.09 (dd, *J* 10.1, 3.7, 1H, H2), 4.21 (app t, *J* 6.6, 1H, H5), 4.30 (d, *J* 7.0, 1H, H2'), 4.38 (A of AB, J_{A-B} 11.7, 1H, C(6)OCH_aH$_b$Ph), 4.40-4.46 [stack, 2H, (including 1H, B of AB, J_{B-A} 11.7, C(6)OCH$_a$$H_b$Ph), H3'], 4.57 (A of AB, J_{A-B} 11.5, 1H, C(4)OCH_aH$_b$Ph), 4.71 (A of AB, J_{A-B} 11.7, 1H, C(2)OCH_aH$_b$Ph), 4.72 (A of AB, J_{A-B} 11.7, 1H, C(3)OCH_aH$_b$Ph), 4.82 (B of AB, J_{B-A} 11.7, 1H, C(2)OCH$_a$$H_b$Ph), 4.85 (B of AB, J_{B-A} 11.7, 1H, C(3)OCH$_a$$H_b$Ph), 4.92 (B of AB, J_{B-A} 11.5, 1H, C(4)OCH$_a$$H_b$Ph), 5.16 (d, *J* 3.6, 1H, H1), 7.23-7.41 (stack, 20H, OCH$_2$*Ph*); δ_c(125 MHz, $CDCl_3$) 25.4 (CH_3, 1 × C(*C*H$_3$)$_2$), 26.1 (CH_3, 1 × C(*C*H$_3$)$_2$), 52.1 (CH_3, O*C*H$_3$), 66.2 (CH_2, C4'), 68.6 (CH_2, C6), 69.8 (CH, C5), 72.5 (CH_2, C(2)O*C*H$_2$Ph), 73.3 (CH_2, C(3)O*C*H$_2$Ph), 73.5 (CH_2, C(6)O*C*H$_2$Ph), 74.8 (CH_2, C(4)O*C*H$_2$Ph), 75.0 (CH, C4), 75.4 (CH, C3'), 75.6 (CH, C2'), 76.0 (CH, C2), 78.6 (CH, C3), 96.0 (CH, C1), 109.8 (C, (CH_3)$_2$*C*), [127.4, 127.5, 127.7, 127.8, 127.9, 128.2, 128.3, 128.4 (CH, Ph, some resonance overlap)], 137.9 (C, *ipso* Ph), 138.6 (C, *ipso* Ph), 138.7 (C, *ipso* Ph), 138.9 (C, *ipso* Ph), 169.9 (C, *C*=O); MS (TOF ES+) *m/z* 735.1 ([M + Na]$^+$, 100%); HRMS (TOF ES+) calcd for $C_{42}H_{48}O_{10}Na$ ([M + Na]$^+$) 735.3145, found 735.3148.

3',4'-*O*-isopropylidene-2'-*O*-(2,3,4,6-tetra-*O*-benzyl-D-galactopyranosyl)-(1→2)-L-threitol (158)

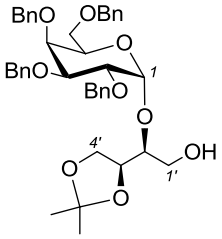

158

A solution of methyl ester **157** (350 mg, 0.49 mmol) in Et_2O (2 mL) was added over 5 min to a stirred suspension of $LiAlH_4$ (28 mg, 0.74 mmol) in Et_2O (3 mL). After an initial vigorous reaction had subsided, the mixture was heated at reflux for 3 h and then cooled to r.t., poured into NH_4Cl solution (5 mL) and H_2O (5 mL). The layers were separated and the aqueous phase was extracted with Et_2O (3 × 10 mL). The organic layer and the ethereal extracts were combined and the mixture was dried (Na_2SO_4) and concentrated under reduced pressure. The residue was purified by flash column chromatography (10% EtOAc in hexane) to afford alcohol **158** as a colourless oil (320 mg, 95%). R_f = 0.3 (25% EtOAc in hexane); $[\alpha]_D^{21}$ = + 33.6 (*c* 1, $CHCl_3$); ν_{max}(film) / cm^{-1}: 3471 br (O–H), 2933w, 2870w, 1497w, 1454m, 1370m, 1253w, 1210m, 1155m, 1132m, 1077s, 1046s, 910m, 889w, 850m, 733s, 696s; δ_H(500 MHz, $CDCl_3$) 1.26 (s, 3H, 1 × C(CH_3)$_2$), 1.36 (s, 3H, 1 × C(CH_3)$_2$), 3.45-3.57 (stack, 2H, C(6)H_2), 3.58-3.64 (stack, 2H, C(1')H_2), 3.65-3.70 (m, 1H, H2'), 3.85 (dd, *J* 8.4, 5.8, 1H, C(4')H_aH$_b$), 3.92-3.96 (m, 1H, C(4')H$_a$$H_b$), 4.00 (dd, *J* 10.0, 2.6, 1H, H3), 4.02-4.04 (m, 1H, H4), 4.09 (dd, *J* 9.9, 3.7, 1H, H2), 4.16-4.21

(stack, 2H, H3', H5), 4.42 (A of AB, $J_{A\text{-}B}$ 11.8, 1H, C(6)OCH_aH$_b$Ph), 4.46 (B of AB, $J_{B\text{-}A}$ 11.8, 1H, C(6)OCH$_a$$H_b$Ph), 4.58 (A of AB, $J_{A\text{-}B}$ 11.4, 1H, C(4)OCH_aH$_b$Ph), 4.71 (A of AB, $J_{A\text{-}B}$ 11.6, 1H, C(2)OCH_aH$_b$Ph), 4.76 (s, 2H, C(3)OCH_2Ph), 4.89 (B of AB, $J_{B\text{-}A}$ 11.6, 1H, C(2)OCH$_a$$H_b$Ph), 4.93 (B of AB, $J_{B\text{-}A}$ 11.4, 1H, C(4)OCH$_a$$H_b$Ph), 4.96 (d, *J* 3.7, 1H, H1), 7.23-7.40 (stack, 20H, OCH$_2$*Ph*), O*H* resonance not observed; δ_c(125 MHz, $CDCl_3$) 24.9 (CH_3, 1 × C(*C*H$_3$)$_2$), 26.3 (CH_3, 1 × C(*C*H$_3$)$_2$), 62.0 (CH_2, C1'), 65.5 (CH_2, C4'), 68.7 (CH_2, C6), 69.8 (CH, C5), 72.5 (CH_2, C(3)O*C*H$_2$Ph), 73.4 (CH_2, C(6)O*C*H$_2$Ph), 74.6 [(CH, C4) and (CH_2, C(2)O*C*H$_2$Ph) resonance overlap], 74.7 (CH_2, C(4)O*C*H$_2$Ph), 75.3 (CH, C3'), 76.2 (CH, C2), 79.5 (CH, C3), 81.9 (CH, C2'), 100.0 (CH, C1), 109.3 (C, (CH$_3$)$_2$*C*), [127.4, 127.6, 127.7, 128.0, 128.1, 128.2, 128.3, 128.4, 128.5 (CH, Ph, some resonance overlap)], 137.6 (C, *ipso* Ph on C(2)OBn), 138.0 (C, *ipso* Ph on C(6)OBn), 138.4 (C, *ipso* Ph on C(3)OBn), 138.6 (C, *ipso* Ph on C(4)OBn); MS (TOF ES+) *m/z* 707.1 ([M + Na]$^+$, 100%); HRMS (TOF ES+) calcd for $C_{41}H_{48}O_9Na$ ([M+Na]$^+$) 707.3196, found 707.3231.

(2''*S*,3''*S*,4''*R*)-2''-Azido-1-*O*-[3',4'-*O*-isopropylidene-2'-*O*-(2,3,4,6-tetra-*O*-benzyl-D-galactopyranosyl)-(1→2)-L-threitol]-3'',4''-*O*-isopropylidene-octadecane-1'',3'',4''-triol (160)

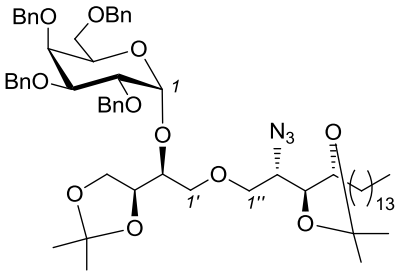

160

Tf_2O (80 µL, 0.49 mmol) was added dropwise over 2 min to a solution of alcohol **158** (320 mg, 0.47 mmol) and 2,6-di-*tert*-butylpyridine (120 µL, 0.52 mmol) in CH_2Cl_2 (5 mL) at 0 °C. After 30 min, the reaction mixture was diluted with CH_2Cl_2 (15 mL) and the resulting solution washed sequentially with H_2O (2 × 30 mL) and brine (10 mL), dried (Na_2SO_4) and filtered. Removal of the solvent under reduced pressure provided crude triflate **159** as a colourless oil [R_f = 0.7 (25% EtOAc in hexane)], which was used immediately in the next etherification step. A solution of alcohol **78** (180 mg, 0.47 mmol) in DMF (3 mL) was treated with NaH (60% dispersion in mineral oil, 40.0 mg, 1.00 mmol) at 0 ºC. After 20 min, a solution of triflate **159** (assuming 100% conversion, 0.47 mmol) in THF (2 mL) was added dropwise over 2 min. The resulting solution was stirred at this temperature for 1 h and then at r.t. for 12 h. The reaction was then quenched by the addition of MeOH (1 mL) followed by $NaHCO_3$ solution (5 mL) and extraction with Et_2O (3 × 10 mL). The combined organic fractions were washed with brine (10 mL) and dried

(Na_2SO_4), filtered and the solvent was removed under reduced pressure. The residue was purified by flash column chromatography (eluent: 10% EtOAc in hexane) to provide ether **160** as a colourless oil (355 mg, 72%); R_f = 0.3 (10% EtOAc in hexane); $[\alpha]_D^{20}$ = + 14.0 (*c* 1, $CHCl_3$); ν_{max}(film) / cm^{-1}: 2923s, 2854m, 2098m (N_3), 1497w, 1454m, 1369m, 1249m, 1216m, 1097s, 1058s, 859w, 736m, 698s; δ_H(500 MHz, $CDCl_3$) 0.86 (t, *J* 6.8, 3H, CH_2CH_3), 1.21-1.29 (stack, 30H, alkyl chain methylenes, 2 × $C(CH_3)_2$), 1.33 (s, 3H, 1 × $C(CH_3)_2$), 1.35 (s, 3H, 1 × $C(CH_3)_2$), 1.39-1.55 (stack, 2H), 3.40 (ddd, *J* 9.7, 7.3, 2.5, 1H, H2"), 3.45-3.50 (m, 1H, C(6)H_aH_b), 3.51-3.63 (stack, 4H, C(6)H_aH_b, C(1')H_aH_b, C(1")H_aH_b), 3.76-3.86 (stack, 4H, C(1")H_aH_b, C(4')H_aH_b, H3" or H4", H2'), 3.95 (dd, *J* 10.1, 2.7, 1H, H3), 3.97 (dd, *J* 8.4, 6.6, 1H, C(4')H_aH_b), 3.99-4.01 (m, 1H, H4), 4.02-4.07 (stack, 2H, H2, H3" or H4"), 4.22-4.28 (stack, 2H, H5, H3'), 4.38 (A of AB, J_{A-B} 11.8, 1H, C(6)OCH_aH_bPh), 4.42 (B of AB, J_{B-A} 11.8, 1H, C(6)OCH_aH_bPh), 4.56 (A of AB, J_{A-B} 11.5, 1H, C(4)OCH_aH_bPh), 4.71(A of AB, J_{A-B} 11.7, 1H, C(3)OCH_aH_bPh), 4.72 (A of AB, J_{A-B} 12.1, 1H, C(2)OCH_aH_bPh)], 4.76 (B of AB, J_{B-A} 12.1, 1H, C(2)OCH_aH_bPh), 4.78 (B of AB, J_{B-A} 11.7, 1H, C(3)OCH_aH_bPh), 4.91 (B of AB, J_{B-A} 11.5, 1H, C(4)OCH_aH_bPh), 5.11 (d, *J* 3.7, 1H, H1), 7.19-7.31 (stack, 18H, OCH_2Ph), 7.32-7.36 (stack, 2H, OCH_2Ph); δ_C(125 MHz, $CDCl_3$) 14.1 (CH_3, CH_2CH_3), 22.7 (CH_2), 25.4 (CH_3, 1 × $C(CH_3)_2$), 25.7 (CH_3, 1 × $C(CH_3)_2$), 26.3 (CH_3, 1 × $C(CH_3)_2$), 26.4 (CH_2), 28.2 (CH_3, 1 × $C(CH_3)_2$), 29.4 (CH_2), 29.5 (CH_2), [29.6, 29.6, 29.7, 29.7 (CH_2, alkyl chain, resonance overlap)], 31.9 (CH_2), 59.9 (CH, C2"), 65.9 (CH_2, C4'), 68.8 (CH_2, C6), 69.3 (CH, C5), 71.1 (CH_2, C1'), 72.5 (CH_2, C1"), 72.9 (CH_2, C(3)OCH_2Ph), 73.0 (CH_2, C(2)OCH_2Ph), 73.5 (CH_2, C(6)OCH_2Ph), 74.7 (CH_2, C(4)OCH_2Ph), 75.0 (CH, C4), 75.5 (CH, C3" or C4"), 76.0 (CH, C3'), 76.4 (CH,

C2), 76.7 (CH, C2'), 77.7 (CH, C4" or C3"), 78.9 (CH, C3), 97.0 (CH, C1), 108.3 (C, $(CH_3)_2C$ of 1,2-*anti* diol), 109.1 (C, $(CH_3)_2C$ of 1,2-*syn* diol), [127.39, 127.41, 127.49, 127.51, 127.7, 127.8, 127.9, 128.19, 128.22, 128.3, 128.4 (CH, Ph, some resonance overlap)], 138.1 (C, *ipso* Ph), 138.78 (C, *ipso* Ph), 138.82 (C, *ipso* Ph), 138.9 (C, *ipso* Ph); *m/z* (TOF ES+) 1072.8 ($[M + Na]^+$, 100%); HRMS *m/z* (TOF ES+) calcd for $C_{62}H_{87}N_3O_{11}Na$ ($[M + Na]^+$) 1072.6238, found 1072.6246.

(2''*S*,3''*S*,4''*R*)-2''-Amino-1-*O*-[3',4'-*O*-isopropylidene-2'-*O*-(2,3,4,6-tetra-*O*-benzyl-D-galactopyranosyl)-(1→2)-L-threitol]-3'',4''-*O*-isopropylidene-octadecane-1'',3'',4''-triol (161)

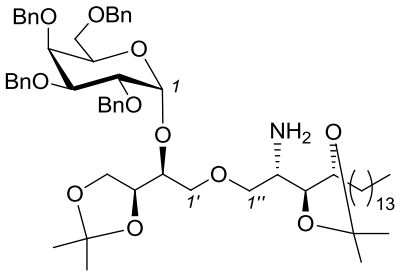

161

PMe_3 (240 µL of a 1.0 M soln in THF, 0.240 mmol) was added dropwise over 5 min to a solution of azide **160** (200 mg, 0.194 mmol) in THF / H_2O (2 mL, 15:1). The reaction mixture was stirred at r.t. for 2 h and then concentrated under reduced pressure. The residual H_2O was removed by co-evaporation with toluene (3 × 3 mL) to provide the crude amine product. Purification of the residue by flash

column chromatography (40% EtOAc in hexane) afforded amine **161** as a colourless oil (175 mg, 88%); R_f = 0.3 (40% EtOAc in hexane); $[\alpha]_D^{22}$ = + 8.0 (*c* 1, $CHCl_3$); ν_{max}(film) / cm^{-1}: 3032 br (N–H), 2922s, 2853m, 1497w, 1454m, 1369m, 1246m, 1214m, 1095s, 1054s, 856m, 734s, 697s; δ_H(500 MHz, $CDCl_3$) 0.88 (t, *J* 7.1, 3H, CH_2CH_3), 1.22-1.31 (stack, 30H, alkyl chain methylenes, 1 × $C(CH_3)_2$ from each acetal), 1.33 (s, 3H, 1 × $C(CH_3)_2$ from acetal protecting C(3'')OH and C(4'')OH), 1.39 (s, 3H, 1 × $C(CH_3)_2$ from acetal protecting C(3')OH and C(4')OH), 1.46-1.60 (stack, 2H), 3.40 (dd, *J* 9.5, 5.9, 1H, C(6)H_aH_b), 3.47-3.57 (stack, 3H, [including 3.50 (dd, *J* 9.5, 6.7, 1H, C(6)H_aH_b)], H2", C(1")H_aH_b, C(6)H_aH_b)), 3.62 (A of ABX, J_{A-B} 11.6, J_{A-X} 2.8, 1H, C(1')H_aH_b), 3.68 (B of ABX, J_{B-A} 11.4, J_{B-X} 4.7, 1H, C(1')H_aH_b), 3.75-3.79 (m, 1H, H2'), 3.82-3.88 (stack, 2H, C(4')H_aH_b, C(1")H_aH_b), 3.94-4.01 (stack, 3H, H3, H4, C(4')H_aH_b), 4.05-4.11 (stack, 2H, H2, H5), 4.16-4.21 (m, 1H, H4"), 4.34-4.41 (stack, 3H, [including 4.40 (A of AB, J_{A-B} 11.8, 1H, C(6)OCH_aH_bPh)], H3", H3', C(6)OCH_aH_bPh)), 4.46 (B of AB, J_{B-A} 11.8, 1H, C(6)OCH_aH_bPh), 4.53 (A of AB, J_{A-B} 11.4, 1H, C(4)OCH_aH_bPh), 4.76 (A of AB, J_{A-B} 11.7, 1H, C(2)OCH_aH_bPh), 4.77 (A of AB, J_{A-B} 11.6, 1H, C(3)OCH_aH_bPh), 4.85 (B of AB, J_{B-A} 11.6, 1H, C(3)OCH_aH_bPh), 4.90 (B of AB, J_{B-A} 11.4, 1H, C(4)OCH_aH_bPh), 4.92 (B of AB, J_{B-A} 11.7, 1H, C(2)OCH_aH_bPh), 4.97 (d, *J* 3.7, 1H, H1), 7.22-7.38 (stack, 18H, OCH_2Ph), 7.43 (br d, 2H, OCH_2Ph), NH_2 resonance not observed; δ_c(125 MHz, $CDCl_3$) 14.1 (CH_3, CH_2CH_3), 22.7 (CH_2), 24.5 (CH_3, 1 × $C(CH_3)_2$), 24.7 (CH_3, 1 × $C(CH_3)_2$), 26.1 (CH_3, 1 × $C(CH_3)_2$), 26.5 (CH_3, 1 × $C(CH_3)_2$), 26.9 (CH_2), [29.3, 29.4, 29.53, 29.6, 29.67, 29.70 (CH_2, alkyl chain, resonance overlap)], 31.9 (CH_2), 52.1 (CH, C2"), 65.7 (CH_2, C4'), 69.2 (CH_2, C6), 69.6 (CH_2, C1"), 70.1 (CH, C5), 70.5 (CH_2, C1'), 72.7 (CH_2, C(3)OCH_2Ph), 73.5

(CH_2, C(6)O*C*H_2Ph), 73.9 (CH_2, C(2)O*C*H_2Ph), 74.7 (CH, C4), 74.8 (CH_2, C(4)O*C*H_2Ph), 75.00 (CH, C3'), 75.04 (CH, C3"), 75.4 (CH, C2), 76.7 (CH, C4"), 77.7 (CH, C2'), 79.1 (CH, C3), 97.6 (CH, C1), 108.7 (C, $(CH_3)_2C$ for acetal protecting C(3'')OH and C(4'')OH), 109.7 (C, $(CH_3)_2C$ for acetal protecting C(3')OH and C(4')OH), [127.6, 127.7, 127.8, (CH, Ph, some resonance overlap)], [128.2, 128.3, 128.4 (CH, Ph, some resonance overlap)], 128.7 (CH, Ph), 137.7 (C, *ipso* Ph), 137.8 (C, *ipso* Ph), 138.4 (C, *ipso* Ph), 138.5 (C, *ipso* Ph); MS (TOF ES+) *m/z* 1046.5 ($[M + Na]^+$, 100%), 1024.5 ($[M + H]^+$, 80); HRMS (TOF ES+) *m/z* 1024.6521 ($[M + H]^+$). $C_{62}H_{90}NO_{11}$ requires 1024.6514; 1046.6349 ($[M + Na]^+$). $C_{62}H_{89}NO_{11}Na$ requires 1046.6333.

(2''*S*,3''*S*,4''*R*)-2''-Hexacosanoylamino-3'',4''-*O*-isopropylidene-1-*O*[3',4'-*O*-isopropylidene-2'-*O*-(2,3,4,6-tetra-*O*-benzyl-D-galactopyranosyl)-(1→2)-L-threitol]octadecane-1'',3'',4''-triol (162)

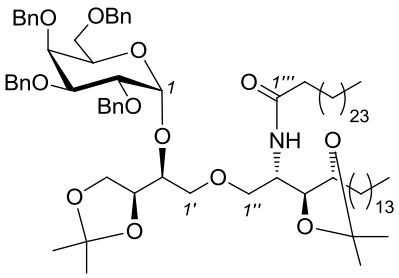

162

A screw-capped glass tube containing a solution of hexacosanoic acid (91 mg, 0.23 mmol) in oxalyl chloride (2.0 mL, 23 mmol) was closed tightly and heated at 70 ºC for 2 h. The volatiles were then evaporated under a stream of argon and the tube then placed on a high vacuum line for at least 2 h to remove the residual volatiles. The resulting acid chloride was used directly without further purification. A solution of freshly prepared acid chloride **47** (105 mg, 0.23 mmol) in CH_2Cl_2 (0.5 mL) was added dropwise over 2 min to a solution of amine **161** (154 mg, 0.15 mmol) and NEt_3 (42 µL, 0.30 mmol) in CH_2Cl_2 (1.0 mL) at 0 ºC. The reaction mixture was stirred at r.t. for 12 h and then diluted with CH_2Cl_2 (10 mL), washed sequentially with $NaHCO_3$ solution (10 mL), brine (2 mL) and then dried over Na_2SO_4. The drying agent was removed by filtration and the filtrate concentrated under reduced pressure. Purification of the residue by flash column chromatography provided amide **162** as a white solid (179 mg, 85%). R_f = 0.3 (15% EtOAc in hexane); mp 69-70 ºC; $[\alpha]_D^{20}$ = + 41.6 (*c* 1, $CHCl_3$); ν_{max}(film) / cm^{-1}:

3283 br (N-H), 2919s, 2851s, 1641m (C=O), 1543w, 1497w, 1468m, 1455m, 1369m, 1246m, 1216m, 1157m, 1098s, 1064s, 860w, 735m, 698m; δ_H(500 MHz, $CDCl_3$) 0.86 (t, *J* 6.8, 6H, × CH_2CH_3), 1.18-1.30 (stack, 73H, alkyl chain methylenes, 1 × $C(CH_3)_2$ from acetal protecting C(3')OH and C(4')OH, 1 × $C(CH_3)_2$ from acetal protecting C(3'')OH and C(4'')OH), 1.34 (s, 3H, 1 × $C(CH_3)_2$ from acetal protecting C(3')OH and C(4')OH), 1.37 (s, 3H, 1 × $C(CH_3)_2$ from acetal protecting C(3'')OH and C(4'')OH), 1.40-1.66 (stack, 5H, alkyl chain methylenes), 2.00-2.14 (stack, 2H, C(2''')H_aH_b), 3.41 (dd, *J* 9.5, 2.6, 1H, C(1")H_aH_b), 3.45-3.55 (stack, 4H, C(6)H_aH_b, C(1')H_aH_b), 3.67 (dd, *J* 9.5, 3.7, 1H, C(1")H_aH_b), 3.75-3.81 (stack, 2H, H2', C(4')H_aH_b), 3.92-3.98 (stack, 4H, H3, C(4')H_aH_b, H3", H4"), 4.00-4.02 (m, 1H, H4), 4.05 (dd, *J* 10.1, 3.7, 1H, H2), 4.08-4.16 (m, 1H, H2"), 4.20-4.26 (stack, 2H, H5, H3'), 4.39 (A of AB, J_{A-B} 11.8, 1H, C(6)OC$H_a$$H_b$Ph), 4.42 (B of AB, J_{B-A} 11.8, 1H, C(6)OC$H_a$$H_b$Ph), 4.55 (d, *J* 11.5, 1H, C(4)OC$H_a$$H_b$Ph), 4.70 (A of AB, J_{A-B} 12.0, 1H, C(2)OC$H_a$$H_b$Ph), 4.72 (A of AB, J_{A-B} 11.7, 1H, C(3)OC$H_a$$H_b$Ph), 4.77 (B of AB, J_{B-A} 11.7, 1H, C(3)OC$H_a$$H_b$Ph), 4.78 (B of AB, J_{B-A} 12.0, 1H, C(2)OC$H_a$$H_b$Ph), 4.91 (d, *J* 11.5, 1H, C(4)OC$H_a$$H_b$Ph), 5.05 (d, *J* 3.7, 1H, H1), 5.74 (br d, *J* 9.3, 1H, N-H), 7.20-7.36 (stack, 20H, OCH_2Ph); δ_C(125 MHz, $CDCl_3$) 14.1 (CH_3, 2 × CH_2CH_3), 22.7 (CH_2), 25.3 (CH_3, 1 × $C(CH_3)_2$), 25.7(CH_2), 25.8 (CH_3, 1 × $C(CH_3)_2$), 26.3 (CH_3, 1 × $C(CH_3)_2$), 26.5 (CH_2), 28.0 (CH_3, 1 × $C(CH_3)_2$), 29.0 (CH_2), [29.3, 29.4, 29.5, 29.6, 29.7 (CH_2, alkyl chain, resonance overlap)], 31.9 (CH_2), 36.8 (CH_2, C2'''), 48.1 (CH, C2"), 65.8 (CH_2, C4'), 68.8 (CH_2, C6), 69.3 (CH, C5), 70.5 (CH_2, C1'), 71.3 (CH_2, C1"), 72.8 (CH_2, C(3)OCH_2Ph), 73.2 (CH_2, C(2)OCH_2Ph), 73.5 (CH_2, C(6)OCH_2Ph), 74.7 (CH_2, C(4)OCH_2Ph), 74.8 (CH, C4), 76.0 (CH, C3'), 76.15 (CH, C3" or C4"), 76.20 (CH, C2), 76.3 (CH, C2'), 77.8 (CH,

C4" or C3"), 79.0 (CH, C3), 96.5 (CH, C1), 107.8 (C, $(CH_3)_2C$ of acetal protecting C(3'')OH and C(4'')OH), 109.1 (C, $(CH_3)_2C$ of acetal protecting C(3')OH and C(4')OH), [127.3, 127.4, 127.5, 127.6, 127.70, 127.75, 127.8 (CH, Ph, some resonance overlap)], [128.1, 128.2, 128.3, 128.4 (CH, Ph, some resonance overlap)], 137.9 (C, *ipso* Ph), 138.6 (C, *ipso* Ph), 138.7 (C, 2 × *ipso* Ph), 172.4 (C, *C*=O); MS (TOF ES+) *m/z* 1425.0 ($[M + Na]^+$, 100%); HRMS (TOF ES+) calcd for $C_{88}H_{139}NO_{12}Na$ ($[M+Na]^+$) 1425.0195, found 1425.0200.

Gal*p*-α-(1→2)-ThrCer (149)

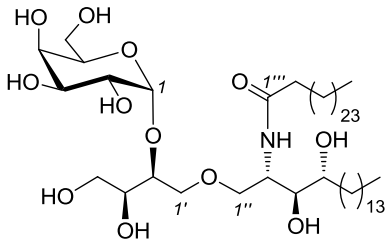

149

TFA (150 µL) was added dropwise over 1 min to a solution of diacetal **162** (50 mg, 0.036 mmol) in CH_2Cl_2 / H_2O (10:1, 0.6 mL). After stirring for 2 h at r.t., the reaction mixture was concentrated under reduced pressure and the residual TFA was removed by co-evaporation with Et_2O (3 × 3 mL) to provide crude tetraol as a white solid (48 mg, quant.), which was used in the next step without further purification. $Pd(OH)_2/C$ (20 mg, 0.014 mmol, 10% wet) was added to a solution of the crude benzylated compound (48 mg, 0.036 mmol) in THF/CH_3OH (3:1, 5 mL).

H_2 gas was bubbled through the stirred suspension for 8 h. The reaction mixture was then filtered, washed with $CHCl_3/CH_3OH$ (8:2, 100 mL) and concentrated under reduced pressure to provide the crude product, which was purified by flash column chromatography (15% CH_3OH in $CHCl_3$) to afford the fully deprotected compound **149** as a white solid (26 mg, 75%). R_f = 0.4 (15% CH_3OH in chloroform); mp 84-85 ºC; $[\alpha]_D^{20}$ = + 56 (*c* 0.1, 2:1 $CHCl_3/CH_3OH$); ν_{max}(film) / cm^{-1} 3303 v br (OH), 2944m, 2833m, 1677w (C=O), 1450w, 1217m, 1031s, 762s, 667m; δ_H(400 MHz, 2:1 $CDCl_3/CD_3OD$) 0.84 (t, *J* 6.7, 6H, 2 × CH_2CH_3), 1.15-1.33 (stack, 67H, alkyl chain methylenes), 1.34-1.65 (stack, 5H, alkyl chain methylenes), 2.20 (t, *J* 7.6, 2H), 3.52-3.76 (stack, 9H), 3.77-3.90 (stack, 6H), 3.92 (br d, *J* 3.0, 1H), 4.03-4.07 (m, 1H), 4.12-4.19 (m, 1H), 5.15 (d, *J* 4.1, 1H), O*H* resonances not observed; δ_C(100 MHz, 2:1 $CDCl_3/CD_3OD$) 14.1 (CH_3, 2 × CH_2CH_3), 23.1 (CH_2), 26.25 (CH_2), 26.28 (CH_2), [29.8, 29.9, 30.03, 30.06, 30.12 (CH_2, alkyl chain, resonance overlap)], 32.3 (CH_2), 32.8 (CH_2), 36.7 (CH_2), 49.8 (CH), 62.3 (CH_2), 62.9 (CH_2), 69.5 (CH), 70.1 (CH), 70.5 (CH), 71.1 (CH_2), 72.2 (CH_2), 72.3 (CH), 72.7 (CH), 73.3 (CH), 74.6 (CH), 78.1 (CH), 96.2 (CH), 175.2 (C, *C*=O); MS (TOF ES+) *m/z* 984.9 ($[M + Na]^+$, 100%); HRMS (TOF ES+) calcd for $C_{54}H_{107}NO_{12}Na$ ($[M+Na]^+$) 984.7691, found 984.7701.

Chapter 6

References

6. References

(1) Sompayrac, L. *How the Immune system works*; 3rd ed. ed., 2008.

(2) Janeway, C. A.; Medzhitov, R. *Annu. Rev. Immunol.* **2002**, *20*, 197-216.

(3) Venkataswamy, M. M.; Porcelli, S. A. *Semin. Immunol.* **2010**, *22*, 68-78.

(4) Giabbai, B.; Sidobre, S.; Crispin, M. D.; Sanchez-Ruíz, Y.; Bachi, A.; Kronenberg, M.; Wilson, I. A.; Degano, M. *J. Immunol.* **2005**, *175*, 977-984.

(5) Van Kaer, L. *Nat. Rev. Immunol.* **2005**, *5*, 31-42.

(6) Lantz, O.; Bendelac, A. *J. Exp. Med.* **1994**, *180*, 1097-1106.

(7) Benlagha, K.; Kyin, T.; Beavis, A.; Teyton, L.; Bendelac, A. *Science* **2002**, *296*, 553-555.

(8) Pellicci, D. G.; Hammond, K. J.; Uldrich, A. P.; Baxter, A. G.; Smyth, M. J.; Godfrey, D. I. *J. Exp. Med.* **2002**, *195*, 835-844.

(9) Kronenberg, M.; Gapin, L. *Nat. Rev. Immunol.* **2002**, *2*, 557-568.

(10) Metelitsa, L. S.; Naidenko, O. V.; Kant, A.; Wu, H. W.; Loza, M. J.; Perussia, B.; Kronenberg, M.; Seeger, R. C. *J. Immunol.* **2001**, *167*, 3114-3122.

(11) Kawano, T.; Nakayama, T.; Kamada, N.; Kaneko, Y.; Harada, M.; Ogura, N.; Akutsu, Y.; Motohashi, S.; Iizasa, T.; Endo, H.; Fujisawa, T.; Shinkai, H.; Taniguchi, M. *Cancer Res.* **1999**, *59*, 5102-5105.

(12) Carnaud, C.; Lee, D.; Donnars, O.; Park, S. H.; Beavis, A.; Koezuka, Y.; Bendelac, A. *J. Immunol.* **1999**, *163*, 4647-4650.

(13) Eberl, G.; MacDonald, H. R. *Eur. J. Immunol.* **2000**, *30*, 985-992.

(14) Nishimura, T.; Kitamura, H.; Iwakabe, K.; Yahata, T.; Ohta, A.; Sato, M.; Takeda, K.; Okumura, K.; Van Kaer, L.; Kawano, T.; Taniguchi, M.; Nakui, M.; Sekimoto, M.; Koda, T. *Int. Immunol.* **2000**, *12*, 987-994.

(15) Nakagawa, R.; Serizawa, I.; Motoki, K.; Sato, M.; Ueno, H.; Iijima, R.; Nakamura, H.; Shimosaka, A.; Koezuka, Y. *Oncol. Res.* **2000**, *12*, 51-58.

(16) Burdin, N.; Brossay, L.; Kronenberg, M. *Eur. J. Immunol.* **1999**, *29*, 2014-2025.

(17) Naumov, Y. N.; Bahjat, K. S.; Gausling, R.; Abraham, R.; Exley, M. A.; Koezuka, Y.; Balk, S. B.; Strominger, J. L.; Clare-Salzer, M.; Wilson, S. B. *Proc. Natl. Acad. Sci. USA* **2001**, *98*, 13838-13843.

(18) Exley, M.; Garcia, J.; Balk, S. P.; Porcelli, S. *J. Exp. Med.* **1997**, *186*, 109-120.

(19) Joyce, S.; Van Kaer, L. *Curr. Opin. Immunol.* **2003**, *15*, 95-104.

(20) Calabi, F.; Jarvis, J. M.; Martin, L.; Milstein, C. *Eur. J. Immunol.* **1989**, *19*, 285-292.

(21) Calabi, F.; Milstein, C. *Nature* **1986**, *323*, 540-543.

(22) Dascher, C. C.; Brenner, M. B. *Trends Immunol.* **2003**, *24*, 412-418.

(23) Vincent, M. S.; Gumperz, J. E.; Brenner, M. B. *Nat. Immunol.* **2003**, *4*, 517-523.

(24) Moody, D. B.; Besra, G. S.; Wilson, I. A.; Porcelli, S. A. *Immunol. Rev.* **1999**, *172*, 285-296.

(25) Jahng, A.; Maricic, I.; Aguilera, C.; Cardell, S.; Halder, R. C.; Kumar, V. *J. Exp. Med.* **2004**, *199*, 947-957.

(26) Moody, D. B.; Briken, V.; Cheng, T. Y.; Roura-Mir, C.; Guy, M. R.; Geho, D. H.; Tykocinski, M. L.; Besra, G. S.; Porcelli, S. A. *Nat. Immunol.* **2002**, *3*, 435-442.

(27) Moody, D. B.; Young, D. C.; Cheng, T. Y.; Rosat, J. P.; Roura-Mir, C.; O'Connor, P. B.; Zajonc, D. M.; Walz, A.; Miller, M. J.; Levery, S. B.; Wilson, I. A.; Costello, C. E.; Brenner, M. B. *Science* **2004**, *303*, 527-531.

(28) Moody, D. B.; Ulrichs, T.; Mühlecker, W.; Young, D. C.; Gurcha, S. S.; Grant, E.; Rosat, J. P.; Brenner, M. B.; Costello, C. E.; Besra, G. S.; Porcelli, S. A. *Nature* **2000**, *404*, 884-888.

(29) Maître, B.; Angénieux, C.; Wurtz, V.; Layre, E.; Gilleron, M.; Collmann, A.; Mariotti, S.; Mori, L.; Fricker, D.; Cazenave, J. P.; van Dorsselaer, A.; Gachet, C.; de Libero, G.; Puzo, G.; Hanau, D.; de la Salle, H. *Biochem. J.* **2009**, *419*, 661-668.

(30) de la Salle, H.; Mariotti, S.; Angénieux, C.; Gilleron, M.; Garcia-Alles, L. F.; Malm, D.; Berg, T.; Paoletti, S.; Maître, B.; Mourey, L.; Salamero, J.; Cazenave, J. P.; Hanau, D.; Mori, L.; Puzo, G.; De Libero, G. *Science* **2005**, *310*, 1321-1324.

(31) Bendelac, A.; Savage, P. B.; Teyton, L. *Annu. Rev. Immunol.* **2007**, *25*, 297-336.

(32) Gumperz, J. E. *Traffic* **2006**, *7*, 2-13.

(33) Kang, S. J.; Cresswell, P. *EMBO J.* **2002**, *21*, 1650-1660.

(34) Natori, T.; Koezuka, Y.; Higa, T. *Tetrahedron Lett.* **1993**, *34*, 5591-5592.

(35) Naidenko, O. V.; Maher, J. K.; Ernst, W. A.; Sakai, T.; Modlin, R. L.; Kronenberg, M. *J. Exp. Med.* **1999**, *190*, 1069-1079.

(36) McCarthy, C.; Shepherd, D.; Fleire, S.; Stronge, V. S.; Koch, M.; Illarionov, P. A.; Bossi, G.; Salio, M.; Denkberg, G.; Reddington, F.; Tarlton, A.; Reddy, B. G.; Schmidt, R. R.; Reiter, Y.; Griffiths, G. M.; van der Merwe, P. A.; Besra, G. S.; Jones, E. Y.; Batista, F. D.; Cerundolo, V. *J. Exp. Med.* **2007**, *204*, 1131-1144.

(37) Berkers, C. R.; Ovaa, H. *Trends Pharmacol. Sci.* **2005**, *26*, 252-257.

(38) Crowe, N. Y.; Uldrich, A. P.; Kyparissoudis, K.; Hammond, K. J.; Hayakawa, Y.; Sidobre, S.; Keating, R.; Kronenberg, M.; Smyth, M. J.; Godfrey, D. I. *J. Immunol.* **2003**, *171*, 4020-4027.

(39) Giaccone, G.; Punt, C. J.; Ando, Y.; Ruijter, R.; Nishi, N.; Peters, M.; von Blomberg, B. M.; Scheper, R. J.; van der Vliet, H. J.; van den Eertwegh, A. J.; Roelvink, M.; Beijnen, J.; Zwierzina, H.; Pinedo, H. M. *Clin. Cancer Res.* **2002**, *8*, 3702-3709.

(40) Seino, K.; Motohashi, S.; Fujisawa, T.; Nakayama, T.; Taniguchi, M. *Cancer Sci.* **2006**, *97*, 807-812.

(41) Nieda, M.; Okai, M.; Tazbirkova, A.; Lin, H.; Yamaura, A.; Ide, K.; Abraham, R.; Juji, T.; Macfarlane, D. J.; Nicol, A. J. *Blood* **2004**, *103*, 383-389.

(42) Ishikawa, A.; Motohashi, S.; Ishikawa, E.; Fuchida, H.; Higashino, K.; Otsuji, M.; Iizasa, T.; Nakayama, T.; Taniguchi, M.; Fujisawa, T. *Clin. Cancer Res.* **2005**, *11*, 1910-1917.

(43) Uchida, T.; Horiguchi, S.; Tanaka Y.; Yamamoto, H.; Kunii, N.; Motohashi, S.; Taniguchi, M.; Nakayama, T.; Okamoto, Y. *Cancer Immunol. Immunother.* **2008**, *57*, 337–345.

(44) Zajonc, D. M.; Cantu, C.; Mattner, J.; Zhou, D.; Savage, P. B.; Bendelac, A.; Wilson, I. A.; Teyton, L. *Nat. Immunol.* **2005**, *6*, 810-818.

(45) Koch, M.; Stronge, V. S.; Shepherd, D.; Gadola, S. D.; Mathew, B.; Ritter, G.; Fersht, A. R.; Besra, G. S.; Schmidt, R. R.; Jones, E. Y.; Cerundolo, V. *Nat. Immunol.* **2005**, *6*, 819-826.

(46) Borg, N. A.; Wun, K. S.; Kjer-Nielsen, L.; Wilce, M. C.; Pellicci, D. G.; Koh, R.; Besra, G. S.; Bharadwaj, M.; Godfrey, D. I.; McCluskey, J.; Rossjohn, J. *Nature* **2007**, *448*, 44-49.

(47) Sidobre, S.; Hammond, K. J.; Bénazet-Sidobre, L.; Maltsev, S. D.; Richardson, S. K.; Ndonye, R. M.; Howell, A. R.; Sakai, T.; Besra, G. S.; Porcelli, S. A.; Kronenberg, M. *Proc. Natl. Acad. Sci. USA* **2004**, *101*, 12254-12259.

(48) Parekh, V. V.; Singh, A. K.; Wilson, M. T.; Olivares-Villagomez, D.; Bezbradica, J. S.; Inazawa, H.; Ehara, H.; Sakai, T.; Serizawa, I.; Wu, L.; Wang, C. R.; Joyce, S.; Van Kaer, L. *J. Immunol.* **2004**, *173*, 3693-3706.

(49) Zhou, D.; Mattner, J.; Cantu, C.; Schrantz, N.; Yin, N.; Gao, Y.; Sagiv, Y.; Hudspeth, K.; Wu, Y. P.; Yamashita, T.; Teneberg, S.; Wang, D.; Proia, R. L.; Levery, S. B.; Savage, P. B.; Teyton, L.; Bendelac, A. *Science* **2004**, *306*, 1786-1789.

(50) Kang, S. J.; Cresswell, P. *Nat. Immunol.* **2004**, *5*, 175-181.

(51) Chen, X.; Wang, X.; Keaton, J. M.; Reddington, F.; Illarionov, P. A.; Besra, G. S.; Gumperz, J. E. *J. Immunol.* **2007**, *178*, 6181-6190.

(52) Christiansen, D.; Milland, J.; Mouhtouris, E.; Vaughan, H.; Pellicci, D. G.; McConville, M. J.; Godfrey, D. I.; Sandrin, M. S. *PLoS Biol.* **2008**, *6*, 1527-1538.

(53) Gumperz, J. E.; Roy, C.; Makowska, A.; Lum, D.; Sugita, M.; Podrebarac, T.; Koezuka, Y.; Porcelli, S. A.; Cardell, S.; Brenner, M. B.; Behar, S. M. *Immunity* **2000**, *12*, 211-221.

(54) Cox, D.; Fox, L.; Tian, R.; Bardet, W.; Skaley, M.; Mojsilovic, D.; Gumperz, J.; Hildebrand, W. *PLoS ONE* **2009**, *4*, 5325-5329.

(55) Fan, Q. H.; Ni, N. T.; Li, Q.; Zhang, L. H.; Ye, X. S. *Org. Lett.* **2006**, *8*, 1007-1009.

(56) Yuan, W.; Kang, S. J.; Evans, J. E.; Cresswell, P. *J. Immunol.* **2009**, *182*, 4784-4791.

(57) Park, J. J.; Kang, S. J.; De Silva, A. D.; Stanic, A. K.; Casorati, G.; Hachey, D. L.; Cresswell, P.; Joyce, S. *Proc. Natl. Acad. Sci. USA* **2004**, *101*, 1022-1026.

(58) Fox, L. M.; Cox, D. G.; Lockridge, J. L.; Wang, X.; Chen, X.; Scharf, L.; Trott, D. L.; Ndonye, R. M.; Veerapen, N.; Besra, G. S.; Howell, A. R.; Cook, M. E.; Adams, E. J.; Hildebrand, W. H.; Gumperz, J. E. *PLoS Biol.* **2009**, *7*, 1-15.

(59) Chang, D. H.; Deng, H.; Matthews, P.; Krasovsky, J.; Ragupathi, G.; Spisek, R.; Mazumder, A.; Vesole, D. H.; Jagannath, S.; Dhodapkar, M. V. *Blood,* **2008**, *112*, 1308-1316.

(60) Ito, Y.; Tamiya-Koizumi, K.; Koide, Y.; Nakagawa, M.; Kawade, T.; Nishida, A.; Murate, T.; Takemura, M.; Suzuki, M.; Yoshida, S. *Biochemistry* **2001**, *40*, 11571-11577.

(61) Brossay, L.; Naidenko, O.; Burdin, N.; Matsuda, J.; Sakai, T.; Kronenberg, M. *J. Immunol.* **1998**, *161*, 5124-5128.

(62) Miyamoto, K.; Miyake, S.; Yamamura, T. *Nature* **2001**, *413*, 531-534.

(63) Veerapen, N.; Reddington, F.; Salio, M.; Cerundolo, V.; Besra, G. S. *Bioorg. Med. Chem.* **2011**, *19*, 221-228.

(64) Chang, Y. J.; Huang, J. R.; Tsai, Y. C.; Hung, J. T.; Wu, D.; Fujio, M.; Wong, C.; Yu, A. L. *Proc. Natl. Acad. Sci. USA* **2007**, *104*, 10299-10304.

(65) Goff, R. D.; Gao, Y.; Mattner, J.; Zhou, D.; Yin, N.; Cantu, C.; Teyton, L.; Bendelac, A.; Savage, P. B. *J. Am. Chem. Soc.* **2004**, *126*, 13602-13603.

(66) Forestier, C.; Takaki, T.; Molano, A.; Im, J. S.; Baine, I.; Jerud, E. S.; Illarionov, P. A.; Ndonye, R.; Howell, A. R.; Santamaria, P.; Besra, G. S.; Dilorenzo, T. P.; Porcelli, S. A. *J. Immunol.* **2007**, *178*, 1415-1425.

(67) Yu, K. O.; Im, J. S.; Molano, A.; Dutronc, Y.; Illarionov, P. A.; Forestier, C.; Fujiwara, N.; Arias, I.; Miyake, S.; Yamamura, T.; Chang, Y. T.; Besra, G. S.; Porcelli, S. A. *Proc. Natl. Acad. Sci. USA* **2005**, *102*, 3383-3388.

(68) Kawano, T.; Cui, J.; Koezuka, Y.; Toura, I.; Kaneko, Y.; Motoki, K.; Ueno, H.; Nakagawa, R.; Sato, H.; Kondo, E.; Koseki, H.; Taniguchi, M. *Science* **1997**, *278*, 1626-1629.

(69) Trappeniers, M.; Van Beneden, K.; Decruy, T.; Hillaert, U.; Linclau, B.; Elewaut, D.; Van Calenbergh, S. *J. Am. Chem. Soc.* **2008**, *130*, 16468-16469.

(70) Reddy, B. G.; Silk, J. D.; Salio, M.; Balamurugan, R.; Shepherd, D.; Ritter, G.; Cerundolo, V.; Schmidt, R. R. *ChemMedChem* **2009**, *4*, 171-175.

(71) Schmieg, J.; Yang, G.; Franck, R. W.; Tsuji, M. *J. Exp. Med.* **2003**, *198*, 1631-1641.

(72) Yang, G.; Schmieg, J.; Tsuji, M.; Franck, R. W. *Angew. Chem., Int. Ed.* **2004**, *43*, 3818-3822.

(73) Li, X.; Chen, G.; Garcia-Navarro, R.; Franck, R. W.; Tsuji, M. *Immunology* **2009**, *127*, 216-225.

(74) Pellicci, D. G.; Patel, O.; Kjer-Nielsen, L.; Pang, S. S.; Sullivan, L. C.; Kyparissoudis, K.; Brooks, A. G.; Reid, H. H.; Gras, S.; Lucet, I. S.; Koh, R.; Smyth, M. J.; Mallevaey, T.; Matsuda, J. L.; Gapin, L.; McCluskey, J.; Godfrey, D. I.; Rossjohn, J. *Immunity* **2009**, *31*, 47-59.

(75) Lee, T.; Cho, M.; Ko, S. Y.; Youn, H. J.; Baek, D. J.; Cho, W. J.; Kang, C. Y.; Kim, S. *J. Med. Chem.* **2007**, *50*, 585-589.

(76) Bock, V. D.; Hiemstra, H.; van Maarseveen, J. H. *Eur. J. Org. Chem.* **2006**, 51-68.

(77) Kolb, H. C.; Sharpless, K. B. *Drug Discov. Today* **2003**, *8*, 1128-1137.

(78) Shiozaki, M.; Tashiro, T.; Koshino, H.; Nakagawa, R.; Inoue, S.; Shigeura, T.; Watarai, H.; Taniguchi, M.; Mori, K. *Carbohydr. Res.* **2010**, *345*, 1663-1684.

(79) Maziak, L.; Lajoie, G.; Belleau, B. *J. Am. Chem. Soc.* **1986**, *108*, 182-183.

(80) Myers, A. C.; Kowalski, J. A.; Lipton, M. A.-. *Bioorg. Med. Chem. Lett.* **2004**, *14*, 5219-5222.

(81) Cho, C. Y.; Moran, E. J.; Cherry, S. R.; Stephans, J. C.; Fodor, S. P.; Adams, C. L.; Sundaram, A.; Jacobs, J. W.; Schultz, P. G. *Science* **1993**, *261*, 1303-1305.

(82) Bordwell, F. G.; Fried, H. E. *J. Org. Chem.* **1991**, *56*, 4218-4225.

(83) Bordwell, F. G.; Ji, G. Z. *J. Am. Chem. Soc.* **1991**, *113*, 8398-8401.

(84) Mathew, T.; Billich, A.; Cavallari, M.; Bornancin, F.; Nussbaumer, P.; De Libero, G.; Vasella, A. *Chem. Biodiversity* **2009**, *6*, 705-724.

(85) Rajan, R.; Wallimann, K.; Vasella, A.; Pace, D.; Genazzani, A. A.; Canonico, P. L.; Condorelli, F. *Chem. Biodiversity* **2004**, *1*, 1785-1799.

(86) Mathew, T.; Billaud, C.; Billich, A.; Cavallari, M.; Nussbaumer, P.; De Libero, G.; Vasella, A. *Chem. Biodiversity* **2009**, *6*, 725-738.

(87) Mathew, T.; Cavallari, M.; Billich, A.; Bornancin, F.; Nussbaumer, P.; De Libero, G.; Vasella, A. *Chem. Biodiversity* **2009**, *6*, 1688-1715.

(88) Wilstermann, M.; Balogh, J.; Magnusson, G. *J. Org. Chem.* **1997**, *62*, 3659-3665.

(89) Marco-Contelles, J.; Gallego, P.; Rodriguez-Fernandez, M.; Khiar, N.; Destabel, C.; Bernabe, M.; Martinez-Grau, A.; Chiara, J. L. *J. Org. Chem.* **1997**, *62*, 7397-7412.

(90) Goddard-Borger, E. D.; Stick, R. V. *Org. Lett.* **2007**, *9*, 3797-800.

(91) Cavender, C. J.; Shiner, V. J. *J. Org. Chem.* **1972**, *37*, 3567-3569.

(92) Vasella, A.; Witzig, C.; Chiara, J. L.; Martinlomas, M. *Helv. Chim. Acta* **1991**, *74*, 2073-2077.

(93) Alper, P. B.; Hung, S. C.; Wong, C. H. *Tetrahedron Lett.* **1996**, *37*, 6029-6032.

(94) Nyffeler, P. T.; Liang, C. H.; Koeller, K. M.; Wong, C. H. *J. Am. Chem. Soc.* **2002**, *124*, 10773-10778.

(95) Lundquist, J. T. t.; Pelletier, J. C. *Org. Lett.* **2001**, *3*, 781-783.

(96) Kratzer, B.; Mayer, T. G.; Schmidt, R. R. *Eur. J. Org. Chem.* **1998**, 291-298.

(97) Lemieux, R. U.; Driguez, H. *J. Am. Chem. Soc.* **1975**, *97*, 4069-4075.

(98) Lemieux, R. U.; Bundle, D. R.; Baker, D. A. *J. Am. Chem. Soc.* **1975**, *97*, 4076-4083.

(99) Lemieux, R. U.; Hendriks, K. B.; Stick, R. V.; James, K. *J. Am. Chem. Soc.* **1975**, *97*, 4056-4062.

(100) Nishida, Y.; Shingu, Y.; Dohi, H.; Kobayashi, K. *Org. Lett.* **2003**, *5*, 2377-2380.

(101) Shingu, Y.; Nishida, Y.; Dohi, H.; Kobayashi, K. *Org. Biomol. Chem.* **2003**, *1*, 2518-2521.

(102) Appel, R. *Angew. Chem., Int. Ed.* **1975**, *14*, 801-811.

(103) Verheyden, J. P.; Moffatt, J. G. *J. Org. Chem.* **1972**, *37*, 2289-2299.

(104) Matto, P.; Modica, E.; Franchini, L.; Facciotti, F.; Mori, L.; de Libero, G.; Lombardi, G.; Fallarini, S.; Panza, L.; Compostella, F.; Ronchetti, F. *J. Org. Chem.* **2007**, *72*, 7757-7760.

(105) Staudinger, H.; Meyer, J. *Helv. Chim. Acta* **1919**, *2*, 635-646.

(106) Fan, G. T.; Pan, Y. S.; Lu, K. C.; Cheng, Y. P.; Lin, W. C.; Lin, S.; Lin, C. H.; Wong, C. H.; Fang, J. M.; Lin, C. C. *Tetrahedron* **2005**, *61*, 1855-1862.

(107) Tian, W. Q.; Wang, Y. A. *J. Org. Chem.* **2004**, *69*, 4299-4308.

(108) Klein, H. F.; Schmidt, A.; Florke, U.; Haupt, H. J. *Inorg. Chim. Acta* **2003**, *342*, 171-178.

(109) Pedersen, B. S.; Scheibye, S.; Nilsson, N. H.; Lawesson, S. O. *Bull. Soc. Chim. Belg.* **1978**, *87*, 223-228.

(110) Cava, M. P.; Levinson, M. I. *Tetrahedron* **1985**, *41*, 5061-5087.

(111) Jesberger, M.; Davis, T. P.; Barner, L. *Synthesis* **2003**, 1929-1958.

(112) Jones, B. A.; Bradshaw, J. S. *Chem. Rev.* **1984**, *84*, 17-30.

(113) Nishio, T.; Ori, M. *Helv. Chim. Acta* **2001**, *84*, 2347-2354.

(114) Nishio, T. *Tetrahedron Lett.* **1995**, *36*, 6113-6116.

(115) Nishio, T.; Sekiguchi, H. *Tetrahedron* **1999**, *55*, 5017-5026.

(116) Cherkasov, R. A.; Kutyrev, G. A.; Pudovik, A. N. *Tetrahedron* **1985**, *41*, 2567-2624.

(117) Smith, P. A. S. *Org. React.* **1946**, *3*, 337-449.

(118) Saunders, J. H.; Slocombe, R. J. *Chem. Rev.* **1948**, *43*, 203-218.

(119) Cao, Z.; Yuan, Y.; Jeyabalan, G.; Du, Q.; Tsung, A.; Geller, D. A.; Billiar, T. R. *Am J Physiol Gastrointest Liver Physiol* **2009**, *297*, G249-G258.

(120) Adams, R.; Ulich, L. H. *J. Am. Chem. Soc.* **1920**, *42*, 599-611.

(121) Holas, T.; Vávrová, K.; Šíma, M.; Klimentová, J.; Hrabálek, A. *Bioorg. Med. Chem.* **2006**, *14*, 7671-7680.

(122) Ghosh, A. K.; Duong, T. T.; McKee, S. P.; Thompson, W. J. *Tetrahedron Lett.* **1992**, *33*, 2781-2784.

(123) Silk, J. D.; Salio, M.; Reddy, B. G.; Shepherd, D.; Gileadi, U.; Brown, J.; Masri, S. H.; Polzella, P.; Ritter, G.; Besra, G. S.; Jones, E. Y.; Schmidt, R. R.; Cerundolo, V. *J. Immunol.* **2008**, *180*, 6452-6456.

(124) Garcia Diaz, Y. R.; Wojno, J.; Cox, L. R.; Besra, G. S. *Tetrahedron-Asymmetry* **2009**, *20*, 747-753.

(125) Oki, S.; Tomi, C.; Yamamura, T.; Miyake, S. *Int. Immunol.* **2005**, *17*, 1619-1629.

(126) Karadimitris, A.; Gadola, S.; Altamirano, M.; Brown, D.; Woolfson, A.; Klenerman, P.; Chen, J. L.; Koezuka, Y.; Roberts, I. A.; Price, D. A.; Dusheiko, G.; Milstein, C.; Fersht, A.; Luzzatto, L.; Cerundolo, V. *Proc. Natl. Acad. Sci. USA* **2001**, *98*, 3294-3298.

(127) Sullivan, B. A.; Nagarajan, N. A.; Wingender, G.; Wang, J.; Scott, I.; Tsuji, M.; Franck, R. W.; Porcelli, S. A.; Zajonc, D. M.; Kronenberg, M. *J. Immunol.* **2010**, *184*, 141-153.

(128) Tashiro, T.; Sekine-Kondo, E.; Shigeura, T.; Nakagawa, R.; Inoue, S.; Omori-Miyake, M.; Chiba, T.; Hongo, N.; Fujii, S.; Shimizu, K.; Yoshiga, Y.; Sumida, T.; Mori, K.; Watarai, H.; Taniguchi, M. *Int. Immunol.* **2010**, *22*, 319-328.

(129) Im, J. S.; Arora, P.; Bricard, G.; Molano, A.; Venkataswamy, M. M.; Baine, I.; Jerud, E. S.; Goldberg, M. F.; Baena, A.; Yu, K. O.; Ndonye, R. M.; Howell, A. R.; Yuan, W.; Cresswell, P.; Chang, Y. T.; Illarionov, P. A.; Besra, G. S.; Porcelli, S. A. *Immunity* **2009**, *30*, 888-898.

(130) van den Elzen, P.; Garg, S.; Leon, L.; Brigl, M.; Leadbetter, E. A.; Gumperz, J. E.; Dascher, C. C.; Cheng, T. Y.; Sacks, F. M.; Illarionov, P. A.; Besra, G. S.; Kent, S. C.; Moody, D. B.; Brenner, M. B. *Nature* **2005**, *437*, 906-910.

(131) Yuan, W.; Qi, X.; Tsang, P.; Kang, S. J.; Illaniorov, P. A.; Besra, G. S.; Gumperz, J.; Cresswell, P. *Proc. Natl. Acad. Sci. USA* **2007**, *104*, 5551-5556.

(132) Zhou, D.; Cantu, C., 3rd; Sagiv, Y.; Schrantz, N.; Kulkarni, A. B.; Qi, X.; Mahuran, D. J.; Morales, C. R.; Grabowski, G. A.; Benlagha, K.; Savage, P.; Bendelac, A.; Teyton, L. *Science* **2004**, *303*, 523-527.

(133) Panchuk-Voloshina, N.; Haugland, R. P.; Bishop-Stewart, J.; Bhalgat, M. K.; Millard, P. J.; Mao, F.; Leung, W. Y.; Haugland, R. P. *J. Histochem. Cytochem.* **1999**, *47*, 1179-1188.

(134) Berlier, J. E.; Rothe, A.; Buller, G.; Bradford, J.; Gray, D. R.; Filanoski, B. J.; Telford, W. G.; Yue, S.; Liu, J. X.; Cheung, C. Y.; Chang, W.; Hirsch, J. D.; Beechem, J. M.; Haugland, R. P.; Haugland, R. P. *J. Histochem. Cytochem.* **2003**, *51*, 1699-1712.

(135) Sakai, T.; Ehara, H.; Koezuka, Y. *Org. Lett.* **1999**, *1*, 359-361.

(136) Sakai, T.; Naidenko, O. V.; Iijima, H.; Kronenberg, M.; Koezuka, Y. *J. Med. Chem.* **1999**, *42*, 1836-1841.

(137) Vo-Hoang, Y.; Micouin, L.; Ronet, C.; Gachelin, G.; Bonin, M. *ChemBioChem* **2003**, *4*, 27-33.

(138) Xia, C.; Zhang, W.; Zhang, Y.; Woodward, R. L.; Wang, J.; Wang, P. G. *Tetrahedron* **2009**, *65*, 6390-6395.

(139) Zhou, X. T.; Forestier, C.; Goff, R. D.; Li, C.; Teyton, L.; Bendelac, A.; Savage, P. B. *Org. Lett.* **2002**, *4*, 1267-1270.

(140) Schiefner, A.; Fujio, M.; Wu, D.; Wong, C. H.; Wilson, I. A. *J. Mol. Biol.* **2009**, *394*, 71-82.

(141) Wu, D.; Zajonc, D. M.; Fujio, M.; Sullivan, B. A.; Kinjo, Y.; Kronenberg, M.; Wilson, I. A.; Wong, C. H. *Proc. Natl. Acad. Sci. USA* **2006**, *103*, 3972-3977.

(142) Wun, K. S.; Cameron, G.; Patel, O.; Pang, S. S.; Pellicci, D. G.; Sullivan, L. C.; Keshipeddy, S.; Young, M. H.; Uldrich, A. P.; Thakur, M. S.; Richardson, S. K.; Howell, A. R.; Illarionov, P. A.; Brooks, A. G.; Besra, G. S.; McCluskey, J.; Gapin, L.; Porcelli, S. A.; Godfrey, D. I.; Rossjohn, J. *Immunity* **2011**, *34*, 327-339.

(143) Morita, M.; Motoki, K.; Akimoto, K.; Natori, T.; Sakai, T.; Sawa, E.; Yamaji, K.; Koezuka, Y.; Kobayashi, E.; Fukushima, H. *J. Med. Chem.* **1995**, *38*, 2176-2187.

(144) Natarajan, A.; Du, W.; Xiong, C. Y.; DeNardo, G. L.; DeNardo, S. J.; Gervay-Hague, J. *Chem. Commun. (Camb)* **2007**, 695-697.

(145) Hansen, T. M.; Engler, M. M.; Forsyth, C. J. *Bioorg. Med. Chem. Lett.* **2003**, *13*, 2127-2130.

(146) Lin, S. N.; Fang, K.; Hashimoto, M.; Nakanishi, K.; Ojima, I. *Tetrahedron Lett.* **2000**, *41*, 4287-4290.

(147) Veronese, F. M.; Pasut, G. *Drug Discov. Today* **2005**, *10*, 1451-1458.

(148) Zalipsky, S.; Mullah, N.; Harding, J. A.; Gittelman, J.; Guo, L.; DeFrees, S. A. *Bioconjug. Chem.* **1997**, *8*, 111-118.

(149) Garcia Diaz, Y. R. *PhD Thesis*, University of Birmingham (Birmingham, UK).

(150) Masuda, Y.; Mori, K. *Eur. J. Org. Chem.* **2005**, 4789-4800.

(151) Auberson, Y.; Vogel, P. *Angewandte Chemie-International Edition in English* **1989**, *28*, 1498-1499.

(152) Rostovtsev, V. V.; Green, L. G.; Fokin, V. V.; Sharpless, K. B. *Angew. Chem., Int. Ed.* **2002**, *41*, 2596-2599.

(153) Kolb, H. C.; Finn, M. G.; Sharpless, K. B. *Angew. Chem., Int. Ed.* **2001**, *40*, 2004-2008.

(154) Booth, C.; Bushby, R. J.; Cheng, Y. L.; Evans, S. D.; Liu, Q. Y.; Zhang, H. L. *Tetrahedron* **2001**, *57*, 9859-9866.

(155) *Carbohydrate Chemistry*; Boons, G.-J., Ed.; Blackie Academic & Professional, Thomson Science, London, New York, 1998.

(156) Zhai, D.; Zhai, W.; Williams, R. M. *J. Am. Chem. Soc.* **1988**, *110*, 2501-2505.

(157) Nicotra, F.; Panza, L.; Russo, G. *J. Org. Chem.* **1987**, *52*, 5627-5630.

(158) Whalen, L. J.; Halcomb, R. L. *Org. Lett.* **2004**, *6*, 3221-3224.

(159) Strecker, A. *Justus Liebigs Ann. Chem.* **1850**, *75*, 27-45.

(160) Strecker, A. *Justus Liebigs Ann. Chem.* **1854**, *91*, 349-351.

(161) Davis, F. A.; Reddy, R. E.; Portonovo, P. S. *Tetrahedron Lett.* **1994**, *35*, 9351-9354.

(162) Davis, F. A.; Reddy, R. E.; Szewczyk, J. M. *J. Org. Chem.* **1995**, *60*, 7037-7039.

(163) Abell, J. P.; Yamamoto, H. *J. Am. Chem. Soc.* **2009**, *131*, 15118-15119.

(164) Seayad, A. M.; Ramalingam, B.; Yushinaga, K.; Nagata, T.; Chai, C. L. L. *Org. Lett.* **2010**, *12*, 264-267.

(165) Kling, M. R.; Easton, C. J.; Poulos, A. *J. Chem. Soc., Perkin Trans. 1* **1993**, 1183-1189.

(166) Mori, K. *Tetrahedron* **1972**, *28*, 3747-3756.

(167) Takahashi, S.; Kubota, A.; Nakata, T. *Tetrahedron* **2003**, *59*, 1627-1638.

(168) Pirrung, M. C.; Pei, T. *J. Org. Chem.* **2000**, *65*, 2229-2230.

(169) Berdeaux, O.; Vatele, J. M.; Eynard, T.; Nour, M.; Poullain, D.; Noel, J. P.; Sebedio, J. L. *Chem. Phys. Lipids* **1995**, *78*, 71-80.

(170) Bach, T.; Kruger, L. *Eur. J. Org. Chem.* **1999**, 2045-2057.

(171) Mahmudi-Azer, S.; Lacy, P.; Bablitz, B.; Moqbel, R. *J. Immunol. Methods* **1998**, *217*, 113-119.

(172) Prigozy, T. I.; Naidenko, O.; Qasba, P.; Elewaut, D.; Brossay, L.; Khurana, A.; Natori, T.; Koezuka, Y.; Kulkarni, A.; Kronenberg, M. *Science* **2001**, *291*, 664-667.

(173) Gadola, S. D.; Silk, J. D.; Jeans, A.; Illarionov, P. A.; Salio, M.; Besra, G. S.; Dwek, R.; Butters, T. D.; Platt, F. M.; Cerundolo, V. *J. Exp. Med.* **2006**, *203*, 2293-2303.

(174) Darmoise, A.; Maschmeyer, P.; Winau, F. *Adv. Immunol.* **2010**, *105*, 25-62.

(175) Veerapen, N.; Brigl, M.; Garg, S.; Cerundolo, V.; Cox, L. R.; Brenner, M. B.; Besra, G. S. *Bioorg. Med. Chem. Lett.* **2009**, *19*, 4288-4291.

(176) Figueroa-Pérez, S.; Schmidt, R. R. *Carbohydr. Res.* **2000**, *328*, 95-102.

(177) Maier, T.; Schmidt, R. R. *Carbohydr. Res.* **1991**, *216*, 483-494.

(178) Graziani, A.; Passacantilli, P.; Piancatelli, G.; Tani, S. *Tetrahedron: Asymmetry* **2000**, *11*, 3921-3937.

(179) Morita, M.; Sawa, E.; Yamaji, K.; Sakai, T.; Natori, T.; Koezuka, Y.; Fukushima, H.; Akimoto, K. *Biosci. Biotechnol., Biochem.* **1996**, *60*, 288-292.

(180) Michieletti, M.; Bracci, A.; Compostella, F.; De Libero, G.; Mori, L.; Fallarini, S.; Lombardi, G.; Panza, L. *J. Org. Chem.* **2008**, *73*, 9192-9195.

(181) Gensler, W. J.; Alam, I.; Prasad, R. S.; Radhakrishna, A. I.; Chaudhuri, A. P. *Tetrahedron* **1979**, *35*, 2595-2600.

(182) Al Dulayymi, J. R.; Baird, M. S.; Roberts, E. *Tetrahedron* **2005**, *61*, 11939-11951.

(183) Nicolaou, K. C.; Mitchell, H. J.; Fylaktakidou, K. C.; Rodriguez, R. M.; Suzuki, H. *Chem. Eur. J.* **2000**, *6*, 3116-3148.

(184) Martin, S. F.; Chen, H. J.; Yang, C. P. *J. Org. Chem.* **1993**, *58*, 2867-2873.